People's Democratic Republic of Algeria

Ministry of Higher Education and Scientific Research

University of Mohamed Boudiaf - M'sila

FACULTY OF SCIENCES

DEPARTMENT OF BIOCHEMISTRY AND MICROBIOLOGY

Series Number: ……

Inscription Number: ……

Thesis

Presented in order to obtain a diploma of

3rd CYCLE DOCTORATE

Specialty: Biological Sciences
Option: Applied Biochemistry

THEME

Formulation, Characterization and Evaluation of the Biological Effects of Selenium Nanoparticles and *Sonchus maritimus* Aqueous Extract Nanoforme in Animal Model of Experimental Metabolic Syndrome

Presented by
CHETEHOUNA Sara

Thesis defense: ……/……/ 2024

Examining Committee:

Familly & First Name	Grade	Establishment	Quality
BOUDJELAL Amel	Professor	Univ. of M'sila	President
RÉGGAMI Yassine	M.C.A	Univ. of Skikda	Supervisor
DEROUICHE Samir	Professor	Univ. of El-Oued	Co-Supervisor
BENKHALED Abderrahim	M.C.A	Univ. of M'sila	Examinator
KHENICHE Abdelhakim	M.C.A	Univ. of M'sila.	Examinator
DAHDOUH Faouzi	M.C.A	HNSTE of Skikda	Examinator.

Academic year: 2023/2024

إهـــــــــــداء

*لحظة لطالما انتظرتها كثيراً... أن أعيش واقعا بات حلمًا بعيدًا بالأمس...متشبثًا بأعماق نفسي... ألا و هو أن اتوج مسيرة دراستي و أكون ممن أضافوا رُبَّ قَطرة نافعة في بحر العلم الواسع...فلك الحمد **"ربّي"** على ما أودعتني...و لك الحمد أن وفقتني على رفع هذا التحدي و أكرمتني بالصبر والثبات و سخرت لي من أجل هذا السبيل أحبتي...من عجزتْ أمامهم كل عبارات الشكر و الثناء و الاحترام...*

لهذا ازجُ أسمى و أرقى تحياتي الخالصة

*الى الشمس التي أضاءت ظلام عقلي، و حَملت وتحمَّلت كل لحظات فرحي وهمي...**نبع الحنان" أمي"***

*الى الذي كان و لازال يعلمني بأن الصدق منجاة و أن العبر بالنهايات...**سندي الثابت" أبي"***

*إلى يدي اليمنى ومُتكَئي...**رِفعتي وعِزوَتي " أخويّ "***

*إلى حكايتي التي لا تصفها الحروف، صوت حكمتي، بيت سري و النور الذي يضيء حياتي...**مرآة شخصي "أختي"***

*الى التي أضافت بوجودها بريقاً أخر لحياتي، مؤنسة وحدتي، رفيقتي وأختي التي لم تلدها أمي...**غاليتي "زوجة أخي"***

*إلى الضياء الذي أنار عائلتنا بقدومه وبث فيها عبق روحه و طاهرة براءته...**حبايب قلبي "بنات أخي وأختي"***

*إلى ذاك الذي لا يوزن بميزان و لا يقدر بأثمان، الذي علمني أن للنجاح أسرار، و أن المستحيل يتحقق بالإصرار...**أستاذي، معلمي و أبي الثاني "درويش سمير"***

*إلى من رزعت في أعماقها الصفاء وسقتها بماء الود والعطاء، رفيقتي التي أبت إلاأن نكون معاً رغم كل شيء... **عزيزتي "إسلام"***

*الى التي لن يعيدها الزمان، من كانت ثمار شجرة جذورها الوفاء وأغصانها الإخاء، التي لا يخفت بريقها عني لحظة...**غاليتي "وِداد"***

*و الى كل من رافقني وشجعني للتفوق في مشوار دراستي... **"أحبتي" و "أساتذتي" الأفاضل***

ســـــــاره

Acknowledgement

*T*he patience, the strength, the courage, the good health and the good people that I met is the best gift from **Allah** to me, my first thank and love is always to him.

I would like to express my honest gratitude to my supervisor **Dr. REGGAMI Yassine** for his precious advices and his constant confidence in me to be able to shed new light in this topic.

I would like to express my honest gratitude to my co-supervisor **Pr. DEROUICHE Samir** for agreeing to supervise me, for his dynamism, his help and motivation that allowed me to go further in my research, I also, so grateful to him for all the experience that I gained it in my carrier.

I thank **Pr. BOUDJELAL Amel** who has given me the honor to accept the presidency of this thesis. Respectful tribute.

I thank **Dr. BENKHALED Abderrahim**, **Dr. KHENICHE Abdelhakim** and **Dr. DAHDOUH Faouzi** for having agreed to examine my thesis and the honor for thier presence. Permit me to express to them my deep respect.

I am grateful to **Pr. BENSACI Tayeb** dean of Faculty of Sciences in Mohamed Boudiaf-M'sila University.

I am grateful to **Pr. BOUDJELAL Amel** and **Research Teams** of the Laboratory of Biology: Applications in Health and Environment in Faculty of Sciences, Mohamed Boudiaf-M'sila University.

I am so grateful to **Ms. BOULAARES Islam, Ms. ATOUSSI Ouidad, Mrs. FRAHTIA Ahlem, Dr. DEROUICHE Manel, Dr. BRIK Hakima** and **Research Team** of the Laboratory of Biodiversity and Application of Biotechnology in the Agricultural Field in Faculty of Natural Sciences and Life, Echahid Hamma Lakhdar University of El Oued.

I do not forget to express my thanks to my big sister **Ms. GOBI Sana** head of pedagogic laboratories in Faculty of Nature and Life Sciences in El Oued University, thanks for your encouragement and your honest work.

I am grateful to **Pr. DEBOUBA Mohamed** director of Higher Institute of Applied Biology of Medenine in Gabès University, Tunisia.

I also thank the members of Dr. Kelif Amar's medical laboratory, Ben Amor Djilani Hospital in El-Oued, Slimane Amirat Hospital in Touggourt, Chemistry laboratory in Faculty of Exact Sciences in El-Oued University, Laboratory of Valorisation and Technology of Sahara Resources (VTRS) in El-Oued University, Scientific and Technical Research Center in Physico-Chemical Analysis (CRAPC) in Biskra, Institute of Arid Regions (IRA) in Medenine, Tunisia, Electron Microscope Laboratory of Health Sciences Faculty in UiTM University, Malaysia, Department of Food Technology of Plant Origin in Faculty of Food Science and Nutrition in Poznań University of Life Sciences, Poland.

*W*ith all love and sincere to everyone who contributed to this work.

Abstract

This investigation aimed to study the biosynthesis and characterization of selenium nanoparticles using *Sonchus maritimus* extract (SmE-SeNPs) and *Sonchus maritimus* extract-loaded niosomes (SmE-N) and their impact on experimental metabolic syndrome (MetS) in rats. *S. maritimus* extract, niosomes and SeNPs were characterized using standard techniques including LC-MS, GC, SEM and TEM analysis. Further, *in-vitro* biological activities of *S. maritimus* extract and SeNPs were assessed. In the *in-vivo* study, thirty-six males' albino Wistar rats were randomly divided into 6 groups (n=6); healthy rats (Control), untreated MetS rats received high fructose diet (HFD), MetS rats treated with *S. maritimus* extract-loaded niosomes (SmE-N), MetS rats treated with selenium nanoparticles (SeNPs), MetS rats treated with SeNPs and *S. maritimus* extract-loaded niosomes (SeNPs-SmE-N), MetS rats treated with metformin (Met). MetS was induced by oral administration of diet contain 35% fructose for 13 weeks. The rats were received treatments via intraperitoneal route for four weeks. Phytochemical and chromatographic findings revealed that *S. maritimus* contains the majority of the main active compounds, including, flavonoids, phenolic acids and volatile compounds of various kinds. Our characterization results of SmE-SeNPs showed a spherical shape with very small size (7.154±0.47 nm), with high antioxidant, anti-inflammatory, hypoglycemic, antibacterial and anticancer properieties without any toxicity in rats. Niosomes that encapsulate *S. maritimus* extract appeared with a diameter around 208.04±9.74 nm. *In vivo* results, experimental MetS group (HFD) showed important alterations in the most of biochemical markers and lipid profile with very significant decrease ($P<0.001$) in hepatic glycogen. The behavior of rats and brain AChE activity were significantly modified ($P<0.001$). Additionally, the hematological analysis revealed that high fructose diet induced perturbation in erythrogram profile by significant decline ($P<0.001$). While, the protein levels were significantly increased ($P<0.01$) in different organs, compared to control rats. Furthermore, the oxidative stress balance in the liver, brain, heart, kidney, and testiculs was adversely affected by an increase in MDA and a decrease in GSH levels, GPx and SOD activities compared to control group. On the other hand, the histological investigation revealed some abnormalities in the mentioned tissue of HFD group, as compared with the control. Treating animals by SmE-N and SeNPs provided partial improvement and restoration of the previous parameters. The combination of the both nanotherapies has proven highly effectiveness. We conclude that SmE-SeNPs have a big *in vitro* pharmacological action and *in vivo* combined with niosomes a high powerful against MetS induced by high fructose diet, which opening the new opportunities for the application of nanotherapy in this field.

Key words: Metabolic syndrome, Oxidative stress, *Sonchus maritimus*, Niosomes, SmE-SeNPs, Characterization, Phytochemicals, Biological activities.

الملخص

يهدف هذا العمل إلى دراسة تأثير جسيمات السيلينيوم النانوية المصنعة حيويا بمستخلص نبات *Sonchus maritimus* (SmE-SeNPs) والنيوزومات المحملة بمستخلص *Sonchus maritimus* على المتلازمة الأيضية التجريبية لدى الجرذان. تم توصيف المستخلص النباتي، النيوزومات و جسيمات السيلينيوم النانوية باستخدام التقنيات القياسية بما في ذلك تحاليل LC-MS، GC، SEM وTEM . كذلك تم إجراء تقييم مختبري، خارج الجسم الحي، للأنشطة البيولوجية لمستخلص *S. maritimus* وجسيمات السيلينيوم النانوية. في دراسة أخرى، داخل الجسم الحي، تم تقسيم ستة وثلاثين ذكرًا من جرذان ويستار البيضاء بشكل عشوائي إلى 6 مجموعات (العدد = 6) ؛ جرذان سليمة (الشاهد)، جرذان مصابة بالمتلازمة الأيضية غير معالجة تلقت نظامًا غذائيًا عالي الفركتوز(HFD) ، جرذان مصابة بالمتلازمة الأيضية معالجة بالنيوزومات المحملة بمستخلص *S. maritimus* (SmE-N)، جرذان مصابة بالمتلازمة الأيضية معالجة بجسيمات السيلينيوم النانوية (SeNPs)، جرذان مصابة بالمتلازمة الأيضية معالجة بالنيوزومات المحملة بمستخلص نبات *S. maritimus* وجسيمات السيلينيوم النانوية (SeNPs-SmE-N) ، و جرذان مصابة بالمتلازمة الأيضية معالجة بالميتفورمين (Met). تم إحداث المتلازمة الأيضية عن طريق تناول نظام غذائي يحتوي على 35٪ من الفركتوز عن طريق الفم لمدة 13 أسبوعًا. تلقت الجرذان هاته العلاجات داخل الصفاق لمدة أربعة أسابيع. النتائج الكيميائية النباتية والكروماتوغرافية أظهرت أن *S. maritimus* يحتوي على غالبية المركبات النشطة الرئيسية، بما في ذلك مركبات الفلافونويد والأحماض الفينولية والمركبات المتطايرة بمختلف أنواعها. أبدت نتائج توصيف جسيمات السيلينيوم النانوية المُصنَّعة حيويًا باستخدام مستخلص *S. maritimus* شكلًا كرويًا ذو حجم صغير جدًا (7.154 ± 0.47 نانومتر، مع خصائص عالية مضادة للأكسدة، مضادة للالتهابات، خافضة لسكر الدم، مضادة للبكتيريا، مضادة للسرطان دون أي سمية لدى الجرذان. ظهرت النيوزومات التي تحتوي على مستخلص *S. maritimus* بقطر حوالي 208.04 ± 9.74 نانومتر. أبدت مجموعة الجرذان المصابة بالمتلازمة الأيضية التجريبية (HFD) تغيرات مهمة في معظم المؤشرات البيوكيميائية ومستوى الدهون مع انخفاض معنوي جداً ($P<0.001$) في الجليكوجين الكبدي. كما تم ملاحظة إضطراب سلوك الجرذان ونشاط انزيم الاسيتيل كولين استيراز في الدماغ بشكل ملحوظ جداً ($P<0.001$). بالإضافة إلى ذلك، أظهر تحاليل مكونات الدم أن النظام الغذائي عالي الفركتوز أدى إلى حدوث تغيرت معنوية، بما في ذلك انخفاض معنوي لعدد كريات الدم الحمراء ($P<0.001$). في حين ارتفعت مستويات البروتين معنوياً ($P<0.01$) في مختلف الأعضاء مقارنة بالجرذان السليمة. علاوة على ذلك، فقد أظهرت النتائج تأثر نظام الدفاع المضاد للأكسدة سلباً في الكبد، الدماغ، القلب، الكلى والخصيتين من خلال زيادة مستوى بيروكسيد الدهون (MDA) وانخفاض مستويات الجلوتاثيون (GSH) بالتوازي مع إنخفاض أنشطة كل من إنريم الجلوتاثيون بيروكسيديز(GPx وانزيم ديسميتاز عالي الاكسدة (SOD) مقارنة بالمجموعة الشاهدة. من ناحية أخرى، أظهر الفحص النسيجي وجود بعض التشوهات في الأنسجة المذكورة سابقاً في المجموعة المصابة بالمتلازمة الأيضية (HFD) مقارنة مع المجموعة الشاهدة. علاج الحيوانات بواسطة النيوزمات المحملة بمستخلص نبات *S. maritimus* وجسيمات السيلنيوم النانوية أدى الى تحسن جزئي لمعظم المعايير البيولوجية والنسيجية المذكورة سالفاً. الجمع بين العلاجين النانويين أثبت فعاليته العالية. نستنتج من ذلك أن السيلينيوم له تأثير دوائي كبير في الدراسة المخبرية وفي الجسم الحي بالاضافة الى النيوسومات لهم فاعلية كبيرة ضد المتلازمة الأيضية الناجمة عن اتباع نظام غذائي عالي الفركتوز، مما يفتح فرصًا جديدة لتطبيق العلاج النانوي في هذا المجال.

الكلمات المفتاحية: المتلازمة الأيضية، الإجهاد التأكسدي، نبات *Sonchus maritimus* ، النيوزومات ، جسيمات السيلنيوم النانوية ، التوصيف، المركبات الكيميائية النباتية، الأنشطة البيولوجية

Abbreviations List

Ach: Acetylcholine

AChE: Acetylcholine Esterase

ALAT: Alanine Amino-Transferase

ASAT: Aspartate Amino-Transferase

ASCh: Acetylthiocholine

Aβ: Amyloid beta

BHT: Butylated Hydroxytoluene

BSA: Bovine Serum Albumin

CD 68: Cluster of Differentiation 68

CKD: Chronic Kidney Disease

Conc: Concentration

Creat: Creatinine

CRP: C-Reactive Protein

CVD: Cardiovascular Disease

DMSO: Dimethyl Sulfoxide

DNA: Deoxyribonucleic Acid

DPPH: 1,1-Diphenyl-2-(2,4,6-Trinitrophenyl) Hydrazine

DTNB: 5,5'-Dithiobis(2-Nitrobenzoic Acid)

EDTA: Ethylenediamine Tetraacetic Acid

EDX: Energy Dispersive X-ray

EE: Encapsulation Efficiency

FCR: Folin-Ciocalteu's Reagent

FRAP: Ferric Reducing Ability Power

FT-IR: Fourier Transform Infrared Spectrophotomety

GC: Gas Chromatography

GFB: Glomerular Filtration Barrier

GFR: Glomerular Filtration Rate

GLUT 2: Glucose Transporter 2

GLUT 5: Glucose Transporter 5

GOT: Glutamate Oxaloacetate Transaminase

GPT: Glutamate Pyruvate Transaminase

GPx: Glutathione Peroxidase

GSH: Reduced Glutathione

GSSG: Oxidized Glutathione

HbA1c: Hemoglobin A1C

HDL: High-Density Lipoproteins

HFD: High Fructose Diet

HMG-CoA: 3-Hydroxy-3-methylglutaryl-coenzyme A

HMGR: 3-Hydroxy-3-methylglutaryl-coenzyme A Reductase

HPLC: High-Performance Liquid Chromatography

IC_{50}: Inhibition Concentration of 50%

IDF: International Diabetes Federation

IL-1: Interleukin 1

IL-12 p70: Interleukin 12p70

IL-1β: Interleukin 1β

IL-6: Interleukin 6

IR: Insulin Resistance

LC/MS: Liquid Chromatography-Mass Spectrometry

LDL: Low-Density Lipoproteins

MCF-7: Michigan Cancer Foundation-7

MCI: Moderate Cognitive Impairment

MDA: Malondialdehyde

Met: Metformin

MetS: Metabolic Syndrome

NAFLD: Non-Alcoholic Fatty Liver Disease

NBT: Nitro-Blue Tetrazolium chloride

NF-κB: Nuclear Factor kappa B

NIST: National Institute of Standards and Technology

NO: Nitric Oxide

NOX: NADPH Oxidase
NPs: Nanoparticles
OD: Optic density
pSTAT1: phospho-Signal Transducers and Activators of Transcription 1
pSTAT3: phospho-Signal Transducers and Activators of Transcription 3
p-tau: phosphorylated tau protein
RAAS: Renin-Angiotensin-Aldosterone System
RBC: Red Blood Cell
RNA: Ribonucleic Acid
RNS: Reactive Nitrogen Species
ROS: Reactive Oxygen Species
RPMI: Roswell Park Memorial Institute
SCh: Thiocholine
SEM: Scanning Electronic Microscope
SeNPs: Selenium Nanoparticles
SeNPs-SmE-N: Selenium nanoparticles and *Sonchus maritimus* extract -loaded niosomes
siRNA: Small Interfering Ribonucleic Acid
SmE: *Sonchus maritimus* extract
SmE-N: *Sonchus maritimus* extract-loaded niosomes
SmE-SeNPs: Selenium Nanoparticles biosynthesized using *Sonchus maritimus* extract
SOD: Superoxide Dismutase
SPME: Solid-Phase Micro-Extraction
T2DM: Type 2 Diabetes Mellitus
TBA: Thiobarbituric Acid
TBARS: Thiobarbituric Acid Reactive Substances
TC: Total Cholesterol
TCA: Trichloroacetic Acid
TEM: Transmission Electron Microscopy
TG: Triglycerides
TNF-α: Tumor Necrosis Factor alpha
TPC: Total Phenol Contents
TrxR: Thioredoxin Reductase
UA: Uric Acid
USA: United States of America
UV-Vis: Ultraviolet-Visible spectrophotometry
VLDL: Very Low-Density Lipoproteins
WBC: White Blood Cells
WHO: World Health Organization

Figures List

Figure 01: Pathophysiological mechanisms of MetS and its main complications 12
Figure 02: *Sonchus maritimus* 15
Figure 03: Multi-directional applications in nanomedicine 17
Figure 04: Biosynthesis of selenium nanoparticles 21
Figure 05: leaves of *Sonchus maritimus* 25
Figure 06: *In vivo* Experimental design of study 29
Figure 07: Preparation method of *S. maritimus* aqueous extract 30
Figure 08: Preparation method of *S. maritimus* extract-loaded niosomes 31
Figure 09: Green synthesis of SmE-SeNPs 32
Figure 10: Chromatogram of HPLC analysis of *S. maritimus* leaves aqueous extract 52
Figure 11: LC-MS analysis of leaves aqueous extract of *Sonchus maritimus* 53
Figure 12: Chromatogram of GC analysis of *S. maritimus* leaves aqueous extract 54
Figure 13: Optical micrographs of SmE-loaded niosomes at magnification ×400 61
Figure 14: SEM micrograph of SmE-loaded niosomes(A) and their distribution frequency(B) .. 62
Figure 15: Physical stability of SmE-loaded niosomes at 4 °C 63
Figure 16: UV-visible spectrum and reaction color changes of green synthesized SmE-SeNPs 63
Figure 17: FT-IR spectrum of functional groups exist in *S. maritimus* and SmE-SeNPs 64
Figure 18: Chemical composition and morphology of SmE-SeNPs based on SEM micrograph and EDX spectra 65
Figure 19: Shape and size of SmE-SeNPs based on TEM micrograph (A) and their distribution frequency (B) 65
Figure 20: DPPH scavenging ability of *S. maritimus* aqueous extract and SmE-SeNPs compared to ascorbic acid 66
Figure 21: Ferric reducing ability of *S. maritimus* aqueous extract and SmE-SeNPs compared to ascorbic acid 67
Figure 22: IC_{50} values of inhibition of albumin denaturation ability of *S. maritimus* aqueous extract and SmE-SeNPs compared to diclofenac 67
Figure 23: IC_{50} leveles of anti-hemolysis ability of *S. maritimus* aqueous extract and SmE-SeNPs compared to diclofenac 68
Figure 24: In vitro α-amylase inhibition activity of *S. maritimus* aqueous extract and SmE-SeNPs compared to acarbose standard 69
Figure 25: Effect of *S. maritimus* aqueous extract and SmE-SeNPs compared to metformin standard on glucose uptake by yeast cells 69

Figure 26: Glucose-binding capacity of of *S. maritimus* aqueous extract and SmE-SeNPs compared to metformin at different glucose concentrations 70
Figure 27: Antibacterial activity of SmE-SeNPs against *Escherichia coli* (a), *Pseudomonas aeruginosa* (b) and *Staphylococcus aureus* (c) 71
Figure 28: Antibacterial activity of *S. maritimus* aqueous extract against *Escherichia coli* (a), *Pseudomonas aeruginosa* (b) and *Staphylococcus aureus* (c) 71
Figure 29: Determination of cytotoxic percentage (A) and microscopic analysis of anti-proliferative property of SmE-SeNPs (B_1) against the MCF-7 breast cancer cell line (B_2) 73
Figure 30: Macroscopic visualization of SmE-SeNPs' suppression of the MCF-7 breast cancer cell line's capacity to form colonies through the use of crystal violet staining 73
Figure 31: Liver glycogen levels in control, HFD and treated groups 76
Figure 32: Biochemical markers in control, HFD and treated groups 77
Figure 33: Lipid profile levels in control, HFD and treated groups 79
Figure 34: Acetylcholine esterase activity in control, HFD and treated groups 79
Figure 35: Clinical score of rat's behaviors in control, HFD and treated groups 80
Figure 36: Liver, brain, heart, kidneys and testicles protein levels in control, HFD and treated groups 81
Figure 37: MDA levels of liver, brain, heart, kidneys and testicles in control, HFD and treated groups 83
Figure 38: Total thiol levels of liver, brain, heart, kidneys and testicles in control, HFD and treated groups 85
Figure 39: GSH levels of liver, brain, heart, kidneys and testicles in control, HFD and treated groups 86
Figure 40: SOD activity of liver, brain, heart, kidneys and testicles in control, HFD and treated groups 87
Figure 41: GPx activity of liver, brain, heart, kidneys and testicles in control, HFD and treated groups 89
Figure 42: GPx/GSH report of liver, brain, heart, kidneys and testicles in control, HFD and treated groups 90
Figure 43: GSH/Total thiol rate of liver, brain, heart, kidneys and testicles in control, HFD and treated groups 91
Figure 44: Total antioxidant capacity of liver, brain, heart, kidneys and testicles in control, HFD and treated groups 93
Figure 45: Histological micrographs of liver section in control, HFD and treated groups with hematoxylin and eosin (H&E) at magnification ×400. 94

Figure 46: Histological micrographs of brain section in control, HFD and treated groups with hematoxylin and eosin (H&E) at magnification ×400. 95
Figure 47: Histological micrographs of heart tissue (A) and collagen (B) in control, HFD and treated groups with hematoxylin and eosin (H&E) at magnification ×400. 97
Figure 48: Histological micrographs of kidney section in control, HFD and treated groups with hematoxylin and eosin (H&E) at magnification ×400. 98
Figure 49: Histological micrographs of testiculs section in control, HFD and treated groups with hematoxylin and eosin (H&E) at magnification ×400. 100

Tables List

Table 01: Standard and high fructose diet composition 26
Table 02: Clinical grading scores of rat's behaviors 43
Table 03: Phytochemical analysis of *Sonchus maritimus* aqueous extract 50
Table 04: Yield rate and content of total phenols, flavonoids and condensed tannins in *Sonchus maritimus* aqueous extract 51
Table 05: Content of mineral elements in dry leaves of *Sonchus maritimus* 51
Table 06: Chemical structure of identified biocompounds by HPLC analysis in *S. maritimus* leaves aqueous extract 52
Table 07: Retention time of detected phytochemical compounds by LC-MS analysis in leaves aqueous extract of *Sonchus maritimus* 53
Table 08: The detected phytocompounds using GC analysis of *S. maritimus* aqueous extract 54
Table 09: Total phenol contents (TPC) and encapsulation efficiency of niosomes 62
Table 10: α-amylase inhibition activity of *S.maritimus* aqueous extract, selenium nanoparticles and acarbose (standard) at different concentrations 69
Table 11: Diameter of inhibition zone of antibiotics against *E. coli*, *P. aeruginosa* and *S. aureus* 72
Table 12: Intraperitoneally acute toxicity test of *S. maritimus* aqueous extract and SmE-SeNPs on physiological parameters of albino Wistar rats 74
Table 13: Growth parameters of control, HFD and treated groups 75
Table 14: Blood erythrocyte and leukocyte lines in control and experimental groups of control, HFD and treated groups 82
Table 15: Grading of histological modifications in liver section in control, HFD and treated groups 94
Table 16: Grading of histological modifications in brain section in control, HFD and treated groups 96
Table 17: Grading of histological modifications in heart section of control, HFD and treated groups 97
Table 18: Grading of histological modifications in kidney section in control, HFD and treated groups 99
Table 19: Grading of histological modifications in testiculs section in control, HFD and treated groups 100

Summary

Dedicace .....

Acknowledgement .....

Abstract .....

الملخص .....

Abbreviations List .....

Figures List .....

Tables List .....

Introduction **1**

First part: Bibliographic synthesis

I. Metabolic syndrome 5

1. Definition and clinical diagnosis 5

2. Epidemiology and prevalence 5

3. Pathophysiology 6

3.1. Genetic mechanisms 6

3.2. Environmental mechanisms 6

3.3. Insulin resistance 6

3.4. Dyslipidemia 7

3.5. Arterial hypertension 7

3.6. Oxidative stress 8

3.7. Chronic inflammation 8

4. Complications 9

4.1. Type 2 diabetes mellitus 9

4.2. Cardiovascular diseases 9

4.3. Nonalcoholic fatty liver disease 10

4.4. Hepatic encephalopathy 10

4.5. Genito-urinary disorders 11

5. Therapeutic and preventive approach 12

6. Experimental metabolic syndrome 13

II. *Sonchus maritimus* 14

1. Definition and localization 14

2. Botanical description and scientific classification 14

2.1. Botanical description 14

2.2. Taxonomy 14

3. Chemical composition 15

4. Pharmacological propriety....15
III. Nanotechnology....17
1. Definition....17
2. Nanomedcine....17
3. Niosomes....18
4. Selenium nanoparticles (SeNPs)....18
4.1. Green synthesis of selenium nanoparticles....19
4.1.1. Synthesis of SeNPs using plant extract....19
4.1.2. Synthesis of SeNPs using microorganisms....20
4.2. Biomedical potential of selenium nanoparticles....21

Second part: Experimental part

Material and Methods

I. Material....25
I.1. Plant material....25
I.2. Animals....25
I.2.1. Experimental metabolic syndrome induction....26
I.2.2. Experimental design....26
I.2.3. Sacrifice, blood sampling and tissue collection....27
I.3. Cells and Reagents....27
II. Methods....30
1. *In vitro* study....30
1.1. Aqueous extract preparation and yield rate determination....30
1.2. Preparation of niosomes....31
1.3. Green synthesis of selenium nanoparticles using *Sonchus maritimus* extract (SmE-SeNPs)....32
1.4. Qualitative phytochemical analysis....32
1.4.1. Phenols....33
1.4.2. Flavonoids....33
1.4.3. Alkaloids....33
1.4.4. Tannins....33
1.4.5. Terpenoids....33
II.4.6. Reducing compound....33
1.4.7. Saponins....33
1.4.8. Unsaturated steroids....34
1.4.9. Derived steroids....34
1.5. Quantitative phytochemical analysis....34

1.5.1. Total phenols....34
1.5.2. Total flavonoids....34
1.5.3. Condensed tannins....35
1.5.4. Content of mineral element....35
1.6. Chromatographic analysis....35
1.6.1. High-performance liquid chromatography (HPLC) analysis....35
1.6.2. Liquid chromatography and mass spectrometry (LC/MS) analysis....35
1.6.3. Gas chromatography (GC) analysis....36
1.7. Characterization of niosomes....36
1.7.1. Morphological characterization of niosomes....36
1.7.2. Encapsulation efficiency of niosomes....37
1.7.3. Physical stability of niosomes....37
1.8. Physical characterization of selenium nanoparticles....37
1.9. Antioxidant activities....38
1.9.1. DPPH radical scavenging ability test....38
1.9.2. Ferric reducing ability test "FRAP"....38
1.10. Anti-inflammatory activities....39
1.10.1. Inhibition of protein denaturation ability test....39
1.10.2. Anti-hemolytic ability test....39
1.11. Hypoglycemic activities....40
1.11.1. α-amylase inhibition activity test....40
1.11.2. Glucose uptake in yeast cells test....40
1.11.3. Glucose adsorption test....41
1.12. Antibacterial activity....41
1.13. Anticancer activity test....42
1.13.1. Culturing of cell lines....42
1.13.2. MTT assay....42
2. *In vivo* study....42
2.1. Acute toxicity test....42
2.2. Clinical grading scores of rat's behaviors....43
2.3. Hematological parameters....43
2.4. Biochemical parameters....43
2.5. Homogenates preparation....44
2.6. Determination of tissue protein....44
2.7. Determination of liver glycogen....44
2.8. Determination of acetylcholinesterase (AChE) activity....44

2.9. Estimation of oxidative stress parameters 45
2.9.1. Determination of malondialdehyde (MDA) level 45
2.9.2. Determination of total thiol 45
2.9.3. Determination of reduced glutathione (GSH) level 46
2.9.4. Determination of superoxide dismutase (SOD) activity 46
2.9.5. Determination of glutathione peroxidase (GPx) activity 46
2.9.6. Determination of total antioxidant capacity 47
2.10. Histopathological analysis 47
2.11. Statistical analysis 48

Results48

I. *In vitro* assays 50
1. Phytochemical analysis 50
1.1. Qualitative and quantitative phytochemical analysis of *Sonchus maritimus* 50
1.1.1. Qualitative phytochemicals analysis 50
1.1.2. Quantitative phytochemicals analysis 50
1.1.3. Content of mineral elements analysis 51
1.2. Chromatographic analysis 51
1.2.1. HPLC analysis of *Sonchus maritimus* aqueous extract 51
1.2.2. LC/MS analysis of *Sonchus maritimus* aqueous extract 52
1.2.3. GC analysis of *Sonchus maritimus* aqueous extract 53
2. Characterization of SmE-loaded niosomes 61
2.1. Morphological characterization 61
2.1.1. Optic microscopy analysis 61
2.1.2. Scanning electron microscopy analysis 62
2.2. Encapsulation efficiency of SmE-loaded niosomes 62
2.3. Physical stabilization of SmE-loaded niosomes 62
3. Characterization of selenium nanoparticles (SmE-SeNPs) 63
3.1. UV-visible spectroscopy 63
3.2. FT-IR spectroscopy 64
3.3. SEM with EDX analysis 64
3.4. TEM analysis 65
4. Biological activities 66
4.1. Antioxidant activity 66
4.1.1. DPPH radical scavenging ability 66
4.1.2. Ferric reducing ability “FRAP” 66
4.2. Anti-inflammatory activity 67

4.2.1. Inhibition of protein denaturation ability....67
4.2.2. Anti-hemolysis ability....68
4.3. Hypoglycemic activity....68
4.3.1. α-amylase inhibition activity....68
4.3.2. Glucose uptake by yeast cells ability....69
4.3.3. Glucose adsorption capacity....70
4.4. Antibacterial activity....70
4.5. Anticancer activity....72
II. *In vivo* assays....73
1. Acute toxicity study....73
2. Growth parameters....74
3. Liver glycogen level....75
4. Biochemical parameters....76
5. Lipid profile....78
6. Acetylcholine esterase activity....79
7. Clinical grading scores of rat's behaviors....80
8. Protein level....80
9. Hematological parameters....82
10. Oxidative stress parameters....82
10.1. Malondialdehyde (MDA) level....82
10.2. Total thiol level....84
10.3. Reduced glutathione (GSH) level....85
10.4. Superoxide dismutase (SOD) activity....86
10.5. Glutathione peroxidase (GPx) activity....88
10.6. GPx/GSH report....89
10.7. GSH/Total thiol rate....90
10.8. Total antioxidant capacity....92
11. Histopathological analysis....93
11.1. Histology of liver tissue section....93
11.2. Histology of brain tissue section....95
11.3. Histology of heart section....96
11.4. Histology of kidney tissue section....98
11.5. Histology of testicle tissue section....99

Discussion

I. *In vitro* study....102
1. Qualitative and quantitative phytochemical analysis of *Sonchus maritimus*....102

2. Characterization of SmE-loaded niosomes 104
3. Characterization of selenium nanoparticles 105
3. Biological activities 106
II. *In vivo* study 109
1. Acute toxicity study 111
2. Growth parameters 112
3. Liver glycogen level 113
4. Biochemical parameters and lipid profile 113
5. Acetyl cholinesterase activity and clinical grading scores of rat's behaviors 116
6. Protein levels 116
7. Hematological parameters 118
8. Oxidative stress markers 119
9. Histological analysis 122
Conclusion & Perspective
Conclusion 126
Perspective 127
Bibliographical references
Annex

Introduction

Introduction

The metabolic syndrome (MetS) is a complex condition constructed from a number of interconnected factors including insulin resistance, dyslipidemia, central adiposity, atherosclerotic disease, endothelial dysfunction, low grade inflammation, and low testosterone levels for males (Gorbachinsky et al., 2022). MetS increases the risk of type 2 diabetes mellitus, hypertension, cardiovascular complications, non-alcoholic fatty liver diseases and even mortality (Shen et al., 2022). Where the clinical signs of metabolic syndrome such as diabetes mellitus, non-alcoholic fatty liver disease and cirrhosis are characterized by a pro-inflammatory condition and may be related by cognitive impairment with subtle changes in attention, memory, psychomotor speed, coordination and executive decision making, which represent the main symptoms of hepatic encephalopathy (Ballester et al., 2022). The oxidative stress and the intracellular redox imbalance, which caused by the persistence of the inflammatory conditions that distinguish the MetS, serve as a link between the MetS and the mentioned related disorders; the increase of oxidant species formation in MetS has been recognized as a main underlying mechanism for impairment of the antioxidant systems, mitochondrial dysfunction, accumulation of lipid and and protein oxidation products (Vona et al., 2019).There is no effective treatment for MetS, and there is ongoing discussion over the underlying cause of MetS while some people think that insulin resistance is the metabolic cause whereas others think that obesity is the cause (Kamenova, 2020).

Phytotherapy may be helpful for treating or avoiding metabolic syndrome because herbal medicines frequently include a variety of biologically active compounds that can interact to increase one another's effectiveness or have a synergistic impact, providing more benefit than a single chemical ingredient (Sabarathinam et al., 2022). In recent decades, due to pathomechanism complication of MetS, the reseachers focus a light on therapeutic effect of secondary metabolites, specially the polyphenols and discuss their therapeutic implications on MetS for apply this evidence in future directions (Zamani-Garmsiri et al., 2022). *Sonchus maritimus* is one of specie belonging to Asteraceae family which is one of the largest families has medicinal effect and economic importance (Saed et al., 2019). The genus Sonchus is classied as one of edible wild plants that are extensively distributed in Africa, Europe and Asia; whereas Sonchus species contain many bioactive components such as phenols, flavonoids, coumarins, fatty acids, steroids, tocopherols, saccharides (Elhady et al., 2022). *Sonchus maritimus* has demonstrated effectiveness against infections and pathogenic bacteria as well as antioxidant and anticancer properties (Hameed et al., 2021).

There has been a great deal of interest in the use of natural compounds as medications, particularly polyunsaturated fatty acids like linoleic acid, which are useful as functional dietary "bioactive lipids" (Hegazy et al., 2019). It targets the liver to control energy metabolism as well as maintain metabolic balance (Yustisia et al., 2022).

Nanotechnology is one of the most interesting 21st-century technologies. It involves the ability to observe, quantify, manipulate, assemble, and create materials at the nanoscale level, which is frequently between 1 and 100 nm (Bayda et al., 2020). The commercial demand for nanoparticles has grown recently due to the variety of uses for them in industries like medical, chemistry, catalysis, electronics and energy (Singh & Dhaliwal, 2015).

Among the key functions of nanotechnology in the pharmaceutical industry is to create it possible to ameliorate the drug delivery systems and design intelligent nanocarriers which not only have the capacity to deliver particular biosubstances to target the treatment site, while can enhance the solubility of medications, protect medicinal molecules from harmful enzymes and control medicine in the circulatory system (Khodabakhsh et al., 2022). Niosomes are vesicular nanocarriers which used as drug delivery system, can include both hydrophilic and hydrophobic substances, allowing them to target diseased tissue with preserving the healthy tissue adjacent (Witika et al., 2022).

Metallic nanoparticles are receiving great attention due to the unique characteristic of nanoparticles such as the greater surface area to volume ratio, small size and biosafity which make them to have a wide range of potential biomedical applications (Yao et al., 2019). Metal nanoparticles have been produced using different methods, including traditional chemical synthesis and eco-friendly synthesis (El Shafey, 2020). Plant extracts, which contain bioactive components that can serve as significant biocatalysts in the synthesis of nanoparticles as well as natural nanoparticle stabilizers, are used in the green synthesis of nanoparticles (Fritea et al., 2017). Selenium is a vital trace element for human health, where the body requires between 40 and 300 micrograms per day of selenium, it plays a significant part in the regulation of human metabolism. It was recorded that the elemental selenium nanoparticles have remarkable biological activities, involved the ability to modulate the immune system and stimulate bone growth, in addition to antioxidant activity (Rajeshkumar et al., 2018; Xia et al., 2022).

Due to the complexity of MetS and researchers' failure to find an adequate and effective treatment. For these purpose, the aim of this study is to prepare selenium nanoparticles by biological method using aqueous extract of *Sonchus maritimus*, as well as to formulate niosomes loaded *Sonchus maritimus* extract. On the other hand, studying the pharmaceutical effectiveness

of these materials in order to alleviate the symptoms and effects of biochemical and physiological changes resulting from high fructose diet.

In order to achieve Our objective, we divided this work into two parts as follows:

- **The first part:** based on *in-vitro* study; *Sonchus maritimus* extraction, niosomes preparation, green synthesis of selenium nanoparticles, quantitative and qualitative characterization of prepared compounds and evaluation of their biological properties.
- **The second part:** based on *in-vivo* study for assessment of the nano-phytotherapy efficiency of *S. maritimus* leave aqueous extract, biosynthesized SeNPs and a novel niosomal approach against metabolic, physiological and histological modifications induced by the experimental metabolic syndrome in rats.

First part

Bibliographic synthesis

I. Metabolic syndrome

1. Definition and clinical diagnosis

Metabolic syndrome (MetS) is not a disease but it is clustering of a complicated metabolic disorder, its major clinical symptoms are hyperglycemia, hyperlipidemia, obesity and hypertension. It has been hypothesized that the onset and development of MetS is associated with pathophysiological processes such insulin resistance, dysfunction of adipose tissue, low-grade inflammation and endothelial dysfunction. However, there are still no effective therapeutic preventative or treatment options for metabolic syndrome (Gorbachinsky et al., 2022; M. Yang et al., 2023). The significance of metabolic syndrome has increased recently since it raises the risk of hypertension, non-alcoholic fatty liver disease, type 2 diabetes mellitus, cardiovascular complications, cognitive impairment and death (Shen et al., 2022). The oxidative stress and the intracellular redox imbalance, serve as a link between the MetS and the mentioned related disorders (Vona et al., 2019). Contrasting conceptual models were used by the researchers to build their diagnostic strategy due to several definitions that were provided for identification of MetS, such as the International Diabetes Federation (IDF) definition is focused on central obesity, while the World Health Organization (WHO) definition is focused on insulin resistance. Multiple MetS definitions resulted in conflicting findings and confusion. These determined clinical constructs have been applied as a diagnosis criterion (Aguilar-Salinas & Viveros-Ruiz, 2019).

2. Epidemiology and prevalence

Socioeconomic status and lifestyle habits significantly influence on the prevalence rates of the MetS (Wang et al., 2020). MetS affects about 20–30% of the adult population in a majority of countries. The incidence is depending on age, sex, race and diagnostic criteria. The prevalence of MetS is anticipated to rise to nearly 53 % at 2035 (Belhayara et al., 2020). In according of the Center of Disease Control and Prevention (CDC), The incidence of MetS increased by 35% in the United States since the appearance of the MetS term in the 1980s until 2012. The prevalence of MetS is comparable to that of T2DM and obesity. Around 85% of people with T2DM also have MetS, increasing their risk of CVDs (Fahed et al., 2022). The metabolic syndrome is highly prevalent not only in the USA, Europe, and Asia, but is also becoming more prevalent throughout most of Africa (Faijer-Westerink et al., 2020; Wang et al., 2020). An epidemiological study carried out in Algeria about the prevalence of MetS from 2016-2017 confirmed that one of each three Algerian adults had MetS (Ngwasiri et al., 2023).

3. Pathophysiology

The interaction of environmental, dietary, and genetic variables results in the multifactorial etiology of MetS. The chronic low-grade inflammation, oxidative stress, insulin resistance and adipocyte dysfunction all contribute to MetS progression the impairment of lipid and glucose homeostasis in insulin-sensitive organs such the liver, adipocytes and muscle (Mendrick et al., 2018; Zafar et al., 2018).

3.1. Genetic mechanisms

Numerous studies have found a link between MetS and associated characteristics with single-nucleotide polymorphisms in various susceptibility genes. Modification of cytokine levels, pro-oxidants, and interrupted energy homeostasis are in response to the genetic changes. In addition, if MetS imbalances are left unchecked, they can become self-perpetuating causing further susceptibility to various complications. A patient's family history and genetic background also affect how well they respond to treatment. Insulin resistance and associated features are more likely to occur in first-degree relatives of type 2 diabetics. Numerous genome-wide association studies have discovered genes linked to obesity, lipid levels and lipoprotein levels as well as genes linked to hypertension (Zafar et al., 2018).

3.2. Environmental mechanisms

New branch of science called epigenetics has recently developed in the area of the development of lifestyle disorders, and it offers a much more comprehensive explanation for the global growth in MetS than a purely hereditary perspective. Impaired energy balance, excessive calorie supply, and poor energy expenditure from inactivity are among the factors that contribute to obesity which are directly linked to metabolic syndrome (Safi-Stibler & Gabory, 2020). Environmental factors including lifestyle factors like food habits, addictive substances, sleeping pattern, psychosocial stress and socioeconomic status as well as both external and physical and factors like hazardous environmental pollutants and prescribed medicines afect both epigenetic and genetic machinery (involving DNA methylation, covalent alteration of histone proteins and higher-order chromatin structures) altering health status and puts people at risk for developing the MetS (Ghosh et al., 2023).

3.3. Insulin resistance

Hyperinsulinemia was found to be the strongest predictor of the onset of type 2 diabetes in non-diabetics and that insulin resistance was predominant in type 2 diabetes. Reaven (1992) is

first used the name "Syndrome X," which was later changed by others to "metabolic syndrome," to highlight how IR (also known as hyperinsulinemia or low glucose tolerance) is the primary cause of type 2 diabetes, atherosclerotic dyslipidemia, and hypertension. The progression of these metabolic disorders was found to potentially be preceded by increases in insulin concentration, and the involvement of insulin resistance in the metabolic syndrome was linked with decreases in insulin sensitivity. When an elevation in insulin and fasting glucose levels, there are rising in the severity of metabolic syndrome components, and the ensuing response involves glucose intolerance, dyslipidemia (high triglycerides, LDL and low HDL) and hypertension which represent the metabolic syndrome's pathophysiological construct (Nylén et al., 2019).

3.4. Dyslipidemia

Dyslipidemia which is marked by high levels of triglycerides (TG) and LDL cholesterol and low levels of HDL cholesterol, is an identifiable feature of the MetS (Reilly & Rader, 2003). The release of more free fatty acids, primarily from visceral depots, as a consequence of insulin-resistant in metabolic syndrome leads to increased liver VLDL synthesis, higher triglycerides and LDL, and enhanced HDL clearance. Hyperglycemia and enhanced gluconeogenesis is brought on by increased free fatty acid release, which also induces insulin resistance in the liver. These metabolic processes cause adipocyte fuel dysfunction, which is shown by adipocyte enlargement and ectopic lipid accumulation in crucial organs such the liver, heart, muscle and pancreas. Excessive lipid production in the pancreas can result in lipotoxicity, which may stimulate endoplasmic reticulum stress-induced cell death (Nylén et al., 2019). Among the contributory factor in the alterations of HDL that occur during inflammation, the rise in the production of lipases which act on HDL phospholipids, lowering their lipid content and stimulating HDL catabolism (Vyletelová et al., 2022).

3.5. Arterial hypertension

Another crucial element of MetS, which can be found in up to one-third of MetS patients, is high blood pressure. There is evidence that even in the absence of T2DM, MetS increases a patient's risk of cardiovascular morbidity and mortality (Mulè et al., 2014). Numerous factors effect on the hypertension development as a component of MetS, including, oxidative stress and endothelial dysfunction, in addition to irregularities in inflammatory mediators have also been described to be involved with the development of hypertension. In turn, this results in a high level of interaction between the MetS components. The development of atherosclerosis and the

high blood pressure are two significant consequences of the MetS, and they are significantly influenced by two main MetS components, IR and obesity (Aboonabi et al., 2019).

3.6. Oxidative stress

The occurrence of oxidative stress is brought on by an excess of harmful reactive oxygen (ROS) and nitrogen species (RNS) that outpace the ability of cellular antioxidant defense, the significance of oxidative stress in many MetS components, such as insulin resistance, obesity, hypertension and others, is being supported by new research findings (Tain & Hsu, 2022). Obesity can cause systemic oxidative stress because of enhanced NADPH oxidase (NOX) activity in adipocytes ROS production, chronic inflammation and reduced antioxidant defenses. In addition, Inflammation and oxidative stress are intimately related to obesity, where the obese people have activated pro-inflammatory transcription factors in their adipocytes, these redox-sensitive transcription factors cause the release of inflammatory cytokines, which in fact increases the production of ROS. Oxidative stress disrupts insulin signaling and promotes insulin resistance through decreasing of peripheral insulin sensitivity due to mitochondrial H_2O_2 and reactive oxygen species production and NOX activation. Furthermore, the oxidative stress is related to endothelial damage, vascular dysfunction, systemic inflammation, renal dysfunction and sympathetic nervous system excitation that lead to hypertension (high blood pressure) (Masenga et al., 2023). Excessive ROS induce the damage of protein, lipid, nucleic acid, and carbohydrate. Which leads to a proinflammatory cytokine production increase that persists over time and causes cellular inflammation. Oxidative stress is believed to cause -cell dysfunction, increase leptin release by adipocytes, lower insulin signaling and glucose tolerance, and ultimately result in the development of insulin resistance (H. Lee & Jose, 2021).

3.7. Chronic inflammation

C-reactive protein (CRP) and Proinflammatory cytokines, including interleukin-6, tumour necrosis factor-a, and several others, have been linked to the metabolic syndrome in numerous studies. Adipokines are thought to have a direct connection to obesity-related diseases, including insulin resistance and the metabolic syndrome (Buchmann et al., 2022). Through the secretion of proinflammatory adipokines like leptin and chemerin as well as the dysregulation of the anti-inflammatory protein adiponectin, adipose tissue plays a role in the inflammatory pathways. Inflammatory biomarkers that are present in the circulatory system, including as CRP, fibrinogen, cytokines and chemokines produced by monocytes, are also changed and promote the inflammation and insulin resistance. The extent to which inflammatory indicators and the metabolic syndrome are related is currently unknown (Nilsson et al., 2019).

4. Complications

4.1. Type 2 diabetes mellitus

The primary complication of MetS is type 2 diabetes, which is highly prevalent globally due to its association with both an increase in obesity and a lack of physical activity. According to several studies, type 2 diabetes is five times more probable to develop in people with MetS. The incidence of type 2 diabetes is on the rise worldwide. Due to hyperglycemia and specific aspects of insulin resistance, people with type 2 diabetes are more susceptible to develop microvascular complications (such as nephropathy, retinopathy, and neuropathy) and macrovascular problems (such as cardiovascular diseases and other comorbidities). The numerous physiopathological abnormalities that cause the decline in homeostasis of glucose in type 2 diabetes are also influenced by environmental variables (Regufe et al., 2020). Notably, patients with MetS have remarkably elevated risk for type 2 diabetes mellitus, independent of numerous other risk factors. MetS is influenced by insulin resistance, meaning the failure of insulin to optimally promote glucose uptake into the body's cells, and hyperinsulinemia. According to the current theory, insulin resistance leads to an increase in blood glucose levels, which increases the need for pancreatic cells to generate and secrete more insulin. Initially restoring euglycemia in the prediabetic individuals condition, this compensating hyperinsulinemic response by the beta cells is complex. However, prolonged exposure to excess lipids and glucose causes beta cell malfunction and/or cell death which lead to overt diabetes (Hudish et al., 2019).

4.2. Cardiovascular diseases

The syndrome metabolic includes a number of metabolic conditions including hypertension, dyslipidemia and IR, which are frequently linked to the accumulation of central fat and form a combination of cardiovascular risk factors that are indicative of the development of cardiovascular diseases (Bovolini et al., 2021). Compared with individuals without the syndrome, persons with MetS had a 2-fold increased risk for developing CVD during the following 5 to 10 years, a 2- to 4-fold increased risk for stroke, a 3- to 4-fold increased risk of myocardial infarction and a 2-fold increased chance of dying from such an event (Lopez-candales et al., 2017). CVD could not only be caused by risk factors of classic metabolic; other factors include inflammatory cytokines and reactive oxygen species (ROS), which cause oxidative stress and chronic inflammation, both of which significantly raise the risk of CVD. Those who are metabolically healthy but normal weight or those who are metabolically healthy

but overweight both have higher levels of TNFα and IL-12 p70 ,which develop the CVD for individual with MetS (Ghosh et al., 2023)

4.3. Nonalcoholic fatty liver disease

The hepatic manifestation of MetS, is the non-alcoholic fatty liver disease (NAFLD), was once thought. New information, on the other hand, suggests that NAFLD is a systemic condition that is directly linked to MetS and that it is both a consequence and a cause of MetS. Non-alcoholic fatty liver disease frequently coexists with other metabolic syndrome complications. Its relation to these conditions is in fact more complicated (Lim et al., 2021). The chronic low-grade inflammation seen in metabolic disorders may be related to extra-hepatic signs associated with NAFLD. Prolonged inflammation in NAFLD is caused by modifications to the gastrointestinal microbiota and the excessive accumulation of visceral adipose tissue, due to unhealthy diet, which is in charge of raising the secretion of both classical cytokines and adipocytokines. New research reveals that the cytokines of the interleukin-1 family, which have both pro- and anti-inflammatory actions, are the key mediators in the phenomenon known as adipose tissue-liver crosstalk (Milovanovic et al., 2021).

4.4. Hepatic encephalopathy

The metabolic syndrome is a significant problem for public health, it starts in middle age and develops with time, eventually leading to serious conditions, MetS lead to hepatic encephalopathy which is neurological disorder that develops as a result of a chronic liver disease complication that causes brain inflammation and, in more severe cases, behavioral abnormalities, cerebral edema, and mental confusion. Non-alcoholic fatty liver disease is one of the most common causes of chronic liver disease and among the main complication of MetS that has been associated to mild cerebral dysfunction and cognitive deterioration (Hadjihambi et al., 2022; Mikkelsen et al., 2022). MetS is considered as risk factor for dementia, and it frequently coexists with dementia in a single person, MetS itself potentially influencing on the progression and development of dementia. Clinical and epidemiological data strongly support the hypothesis that metabolic syndrome and dementia are interacted, especially moderate cognitive impairment (MCI), where, the Individuals who have metabolic syndrome are more probable to suffer from progression of cognitive loss in old age. Studies using animal models of advanced dementia fed a high-fat diet have produced experimental data showing decreased cognitive function and enhanced the pathology, which include neuroinflammation (Ivanova et al., 2020).

4.5. Genito-urinary disorders

It has been suggested that MetS can result in modifications in renal function and structure, including a decreased glomerular filtration rate (GFR) and an increase in urine microalbumin through a complex pathogenesis. MetS and chronic kidney disease (CKD) are causative and impact one another (Yanai et al., 2021). An important contributing factor to MetS is insulin resistance, which can cause sodium retention and vascular endothelium vasoconstriction by antinatriuresis, which induces the RAAS activation and accumulation of lipid in renal tubular through deposition of droplet in tubular cells and in interstitial extracellular, causing the interstitial fibrosis and tubular atrophy, furthermore, it leading to loss of the renal podocyte foot, which causes macromolecular leakage and proteinuria through partial shedding of the glomerular filtration barrier (GFB) (Lin et al., 2022). Ischemia carried on by hypertension, which is the primarily damages of the kidneys, including, injuries of glomerular, Nephro tubular and renal vascular, that are all brought on by ischemia, with renal damage to the tubular system being the most common type (Simeoni et al., 2021). During MetS, leptin, adiponectin, chemerin, pro-inflammatory cytokine and another adipokines are strangely secreted by adipose tissue, encourages the oxidative stress, inflammatory effects, endothelial dysfunction, and increased sympathetic activity, which induce alteration of renal structure and function including augmented renal volume weight and hyperfiltration, with damaging the GFB (basement membrane and endothelial cells) (Lin et al., 2022). Hypogonadism in among the complication of MetS in males, it has been proven that MetS features such as hyperinsulinemia, hyperglycemia (with elevated HbA1c), obesity, hypertriglyceridemia and elevated CRP, as well as low HDL are linked to decrease of serum testosterone levels. Also, weight loss may reverse these trends. In Addition, it may be associated with low-grade inflammatory state, which known to occur in MetS; where in Leydig cells, TNF-α and IL-1 have been shown to block steroidogenesis and to prevent cleaving cholesterol side chains using cytochrome P450, respectively. This is thought to reduce the production of testosterone (Gorbachinsky et al., 2022). Physiological communication and common etiological factors of both the reproductive system and the kidneys are the main factor in the occurrence of genetic urological complications in individuals with MetS.

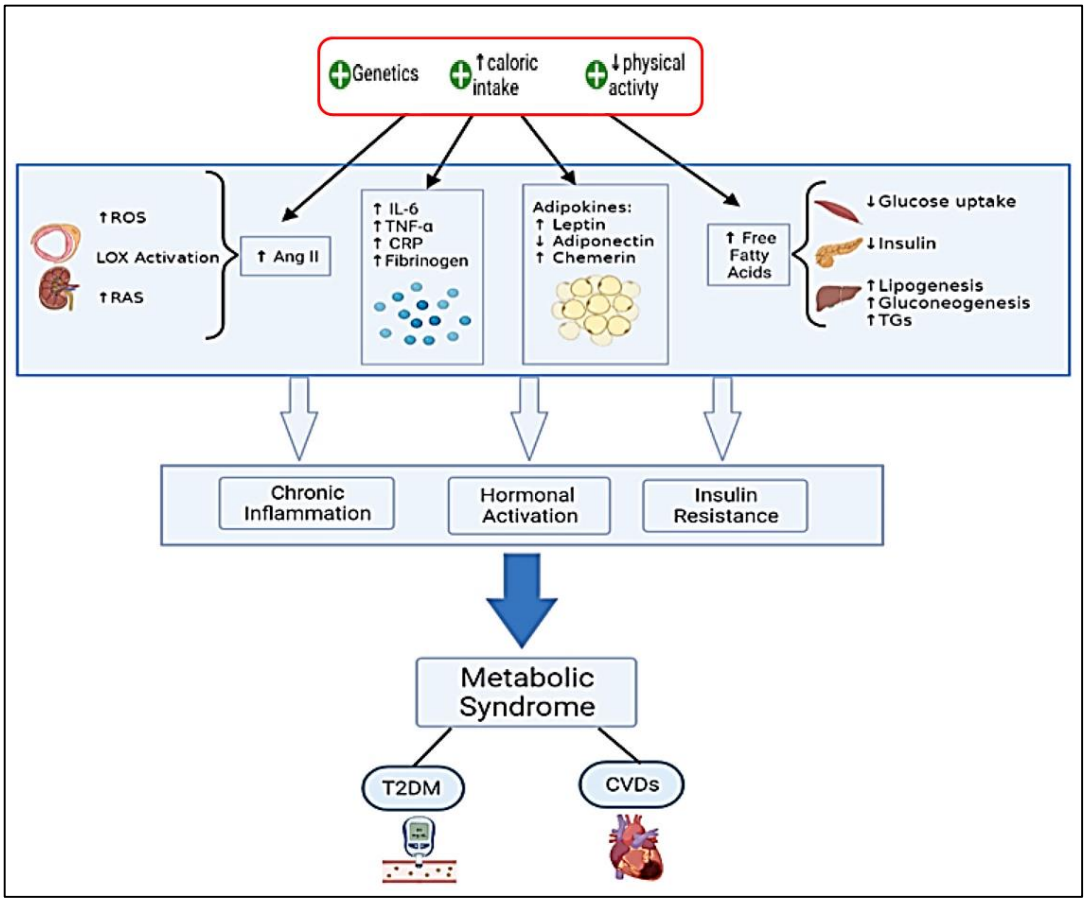

Figure 01: Pathophysiological mechanisms of MetS and its main complications (Fahed et al., 2022)

5. Therapeutic and preventive approach

There are actually no specific recommendations or guidelines available for therapy of metabolic syndrome because there are no published papers on the medical management of the MetS (Wang et al., 2020). Additionally, as a result of the incomplete understanding of the cellular and molecular mechanisms underlying the pathophysiology of the metabolic syndrome, the treatment alternatives have not yet been identified (Mottillo et al., 2010). The current therapeutic approaches mainly concentrate on treating the specific components of the MetS, with the general objectives of minimizing the risk of type 2 diabetes and cardiovascular disease or preventing them through lifestyle changes include increasing physical exercise, eating nutritious food with the optimum number of calories overall, and maintaining a healthy weight. Furthermore, some therapy approaches may significantly affect two or more metabolic syndrome components. However, numerous therapy initiatives aimed at treating visceral fat and insulin resistance linked to the metabolic syndrome may have the most overall effectiveness in accomplishing these objectives (Wang et al., 2020). Metformin is the systemic medication which is used in individuals with type 2 diabetes mellitus associated with MetS. It is a glucophage drug,

decreases blood glucose level, ameliorates body mass index, which is closely connected to drops in IL-6 plasma levels (Ranchoux et al., 2019).

6. Experimental metabolic syndrome

According to experimental studies, the metabolic syndrome can be induced in animal model by intake and consumption of a high caloric diet, including high fat, high carbohydrates, high fructose and others, to develop different components of MetS which consists of hyperglycemia, insulin resistance, atherogenic dyslipidemia, high blood pressure, central obesity, oxidative stress and pro-inflammatory state (Lasker et al., 2019). Previous study used the high-caloric diet based on high-fat for 12 weeks to create the similar physiological condition of MetS in human, the diet was include for each 2400 g of dietary contained 1518 g the standard food powder mixed with 480 g of lard (fat), 360 g of sucrose, 360 g of starch and 24 g cholesterol (Nakhaei et al., 2019). Due to the importance of fructose and its role for inducing the symptoms of metabolic syndrome, some research papers used it in rats as solution in drinking water (10%) for nine week (Réggami et al., 2021) and others as diet where the fructose was mixed with fat (60% fructose and 60% fat) for seventy days (Derouiche et al., 2019). Russa *et al. (2019)* depended on cafeteria diet with mean of 75 kcal/rat/day for ninety-five day, embodied the unhealthy food in our daily life style, the diet was consist of cookies (briny or sweet), cereals, milk chocolate, processed meats, potato chips, high-fat cheese, condensed milk with sugar.

II. *Sonchus maritimus*

1. Definition and localization

Sonchus maritimus is annual or perennial herb, a class of nutritious wild plants that are extensively distributed in Africa, Asia, and Europe (Fouad et al., 2020). It is one of Asteraceae family's species which have a largest and economically importance and medicinal impact (Saed et al., 2019). Sonchus species are eatable to humans as a leafy green vegetable. They used as a potherb in folk medicine's Chinese, which is popular as a traditional medicine for the therapy of various diseases since ancient times (Fouad et al., 2020). They are known to contain several bioactive compounds, are also regarded as sources of numerous dietary supplements. These species have a potential pharmacological effects, including antioxidant, hepatoprotective, anti-inflammatory, anticancer, cardioprotective and antimicrobial proprieties (Elhady et al., 2022).

2. Botanical description and scientific classification

2.1. Botanical description

Sonchus maritimus is simple or branched herb with 40 cm tall and have glandular hairs on cylindrical or ribbed stem. Leaves of this species are 10 x 4.5 cm^2, pinnatifid, slightly lanceolate, glabrous without margins or weakly spinulose rather denticulate. Companulate head is axillary and terminal with 1.4 x 0.9cm^2, involve ventrally glandular hairs and glabrous above. Flowers ligulate, consist of ligules yellow. Elliptic achenes with 0.3 x 0.1 cm^2. Pappus of this plant have 0.5 cm long, and they are deciduous, slender, whitish, without neck (Qureshi et al., 2002).

2.2. Taxonomy

Sonchus maritimus is a member of the subgenus Sonchus and genus Sonchus which include in subtribe Crepidinae of Lactuceae tribe, that belongs to Asteraceae family, one of the largest in the world. It has a widespread distribution, with more than 1100 genus and 2500 species (Giner et al., 1993; Kim & Chunghee, 2007; Saed et al., 2019).

Kingdom: Plantae
Family: Asteraceae
Tribe: Lactuceae
Subtribe: Crepidinae
Genus: Sonchus
Subgenus: Sonchus
Species: *Sonchus maritimus*

Figure 02: *Sonchus maritimus*
(Original photo)

3. Chemical composition

Sonchus maritimus have gained value as nutritional supplements due to their richness in phytochemicals compounds and mineral contents. A relative good content of dietary mineral elements such as phosphorus (P), manganese (Mn), magnesium (Mg), calcium (Ca), sodium (Na), potassium (K) are detected in *S. maritimus*. (Hameed et al., 2021). The bioactive substances that contained in Sonchus species are phenols, flavonoids, flavanols, alkaloids, proanthocyanins, phytate, saponins and sesquiterpene lactones of the guaianolide and eudismanolide structures, also high amount of ascorbic acid (vitamin C), fatty acids, oxalic acid, carotenoids and mineral contents (Mohasib et al., 2020), tannins, anthraquinones,coumarins and hydroxy-coumarins, quercetin, rutin,, myrecetin, catechin, kaempferol and apigenin, which have been isolated and characterized from their different parts. On the other hand, quarantined nine sesquiterpene glycosides from the elevated parts of one of Sonchus species, these were named as following sonchusides-A, sonchusides-B, sonchusides-C, sonchusides--D glucozaluzanin-C, crepidiaside-A, macrocliniside-A, picrisides-B and picrisides-C. These contribute to make Sonchus species valuable nutritional and pharmacological profile (Asif & Saeed, 2020).

4. Pharmacological propriety

Sonchus species have a notable antioxidant capacity due to high content of ascorbic acid along with numerous phenolic acids, as well as flavonoids, tannins and fatty acids through the direct free radical scavenging ability and reducing power (Hameed et al., 2021) by decreasing the reactive oxygen species (ROS) Malondialdehyde (MDA) levels, and enhancing the activity of antioxidant enzymes such as superoxide dismutase (SOD), glutathione peroxidase (GPx) (Yang et al., 2023).

Anti-inflammatory activity of Sonchus species is shown by reducing the secretions of inflammatory mediators (NO) and pro-inflammatory cytokines including the tumour necrosis factor (TNF)-α, interleukin (IL)-6 and IL-1β, and inhibiting the gene expression of nuclear factor-κB (NF-κB) and signal transducers and activators of transcription (pSTAT1 and pSTAT3). The phytocomponents such as ferulaic acid, villosol, ursolic acid, β-sitosterol and rutin may are the pharmacological agents against inflammatory diseases (Li et al., 2017).

The possible antimtabolic disorder, antihyperglycemic and antihyperlipidimic impacts of these plants could be related to secondary metabolite content (flavonoids, terpenoids, carotenoids, glycosides), they may be an effective agent for the treatment of MetS which related to oxidative stress and inflammation states (Dutta et al., 2020).

Previous studies have indicated that mentioned phytocompounds possess other pharmacological activities, including antibacterial motion, neuroprotective, hepatoprotective, cardiovascular therapy, antitumor effect, rheumatism and general pain, even as a general tonic, headaches, antinociceptive as well as anti-ageing properties (Mohasib et al., 2020).

III. Nanotechnology

1. Definition

Nanotechnology is one of the most attractive XXI century technologies. It involves the ability to observe, quantify, manipulate, assemble, and create materials at the nanoscale level, which is frequently between 1 and 100 nm. It allows the transformation or self-assembly of individual atoms, molecules, or molecular clusters into specific configurations to create materials with novel and notably distinct characteristics (Bayda et al., 2020). The applications of nanotechnology are among the most innovative and promising technology in wide industries including food packaging and safety, medicine, drug delivery, healthcare, cosmetics, chemical industries, energy science, environment management and optoelectronics; these uses are based on the special magnetic, chemical, optical and structural characteristics of nanosized particles that are not showed by bulk substance (Deepasree & Venugopal, 2022).

2. Nanomedcine

The word "nanomedicine" is used to describe the use of nanotechnologies in healthcare and medicine. nanomedicine uses the nanoscale technologies to diagnose, prevent, treat and monitor diseases (Sim & Wong, 2021). The medical fields have a lot of promise for using nanotechnologies, including the diagnostic tools such as imaging techniques, drug delivery systems, implants, tissue-engineered constructs and pharmaceutical therapies; due to their remarkable effectiveness in binding, absorbing, and transporting small-molecule drug, RNA, DNA and proteins (Ahmed et al., 2021). It has advanced therapies of various diseases, including cardiovascular diseases, diabetes, psychiatric and neurodegenerative diseases, cancer, musculoskeletal conditions, bacterial and viral infections (Sim & Wong, 2021).

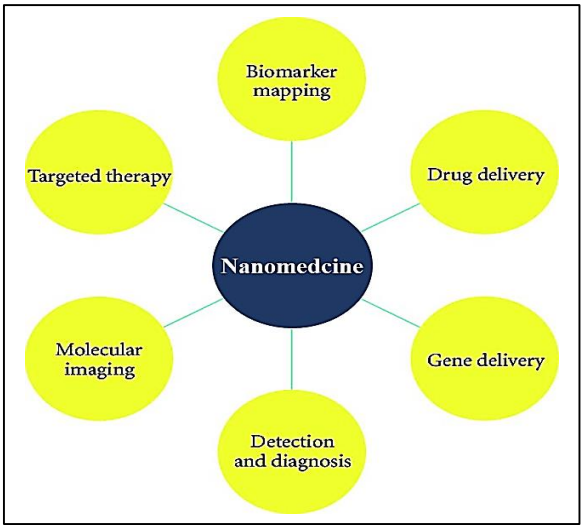

Figure 03: Multi-directional applications in nanomedicine (Liu et al., 2010)

3. Niosomes

Niosomes are vesicular nanoformulations serve as drug delivery system, characterize by the adaptability for drug delivery and the capability to entrap both hydrophilic and hydrophobic substances, distributing them using a variety of delivery methods, including oral, ophthalmic, pulmonary, topical and parenteral, allowing them to target the affected tissue while protecting the nearby healthy tissue (Witika et al., 2022). Smart nanostructured deliver the medications to the target locations in a (temporal/spatial) regulated way with lower dose frequency, reducing the adverse effects and addressing the most serious problems associated with conventional pharmaceutical therapies, including rapid clearance, nonspecific distribution, unpredictable drug release, and low bioavailability (Lombardo et al., 2019). For biotechnology applications, these nanoformulations are designed using nanocarrier systems engineering in complex environment through multiform interactions within specific biological medium (Werner et al., 2018). Niosomes prepared using various methods depending on the desired size of vesicle, number of bilayers, size distribution, required vesicle membrane permeability and aqueous phase entrapment efficiency. Generally, niosomes are produced by hydration of a surfactant and lipid mixture in an aqueous media leads to the creation of a colloidal dispersion (Bagheri et al., 2014).

4. Selenium nanoparticles (SeNPs)

Selenium is a crucial trace element that supports healthy immune and antioxidant systems and protects against a number of deadly or degenerative diseases. it is an essential element acts as cofactor and coenzyme of various selenoproteins and enzymes in the body and provides protection to cells and tissues from oxidative injuries and stress because it has an important role in peroxides and iodine metabolism, regulates the free radicals' and iodine's levels (Ikram et al., 2021). The biological effects of selenium are mostly caused by the presence of the selenocysteine amino acid in proteins. About 100 selenoproteins were found in mammals, among these, selenoprotein-P and antioxidant enzymes including thioredoxin reductase and glutathione peroxidase, which made it as an antioxidant to diseases related to oxidative stress, such as fatty liver, diabetes and atherosclerosis (Guan et al., 2018). A low level of selenium in the body may result in problems with the immune system, the heart, the skeleton, and the muscles. Selenium supplements are also known to protect against a wide range of harmful factors, including physical ones like magnetic fields or heat stress and chemical ones like medicines with serious side effects, pesticides, carcinogens, heavy metals and mycotoxins (Fan et al., 2020). Therefore, selenium nanoparticles (SeNPs) produced using several biocompatible materials are a safer source of selenium delivery with lower toxic impact, greater bioavailability, higher biological

propriety and better absorption capacity compared to elemental selenium such as disodium selenite and sodium selenite (Lin et al., 2023). Thus, SeNPs hold a distinctive place in the field of nanotechnology and can be used as a therapeutic agent or an approach to delivering medication (Alhazza et al., 2022), since they present an exceptional chance not only as theranostic agents but also have enormous potential as transporters for proteins, siRNA, chemotherapeutics, and other substances (Khurana et al., 2019). In addition, SeNPs are widely used as antioxidant, anticancer and antibacterial agents due to evidence suggesting that they are superior to organic and inorganic selenocompounds in scavenging free radicals, preventing oxidative damage to deoxyribonucleic acid and increasing the expression of selenoproteins (Jha et al., 2022).

4.1. Green synthesis of selenium nanoparticles

Biogenic nanoparticle (NP) synthesis is currently receiving a lot of attention due to its eco-friendly method with low cost, and relative ease of synthesis when it can be finished in a few minutes to a few hours at room temperature, it also benefits from ease of characterization (Gour & Jain, 2019). The physical and chemical approaches are no longer preferred because they take a lot of time and need the use of chemical products that are harmful to both environment and human health. Additionally, current technologies are expensive and produce toxic waste, which has prompted the development of new and better methods for synthesizing SeNPs (Ndwandwe et al., 2021). The green synthesis not only eliminates the use of hazardous and poisonous chemicals that are used in the other methods, but also lowering energy consumption due to the availability of local resources, it uses natural and environmentally acceptable materials that act as reducing, end-capping and dispersants agents. Presently, green synthesis method basically uses the extracts of various plant parts or the microorganisms such as bacteria, algae and fungi, which contain the polyphenols and proteins that replace the chemicals and act as reducing agents to convert metal ions into lower valence state (Ying et al., 2022).

4.1.1. Synthesis of SeNPs using plant extract

The use of plant extracts for SeNPs synthesis has gained popularity and has more advantages than the use of microorganisms due to its simplicity (a single-step approach), high yielding capacity and inexpensive, as well as the fact that it is nonpathogenic and economical (Korde et al., 2020; Salem & Fouda, 2021). The phytosynthesis of SeNPs has benefits over more conventional techniques due to their biocompatibility and *in vivo* effects (Ikram et al., 2021). Plant extracts involve a wide range of bioactive substances, including polyphenols, flavonoids, alkaloids, tannins, triterpenoids, carbohydrates and proteins, that participate in the capping and

reduction process of the metal salt precursors for the SeNPs synthesis. Additionally, the use of plant extracts allows to produce NPs with different nanoscale average size (Dikshit et al., 2021; Djouadi & Derouiche, 2021).

4.1.2. Synthesis of SeNPs using microorganisms

Microorganisms like bacteria, algae, fungi and yeast are utilized to produce selenium nanoparticles with different nanosize because they are simple to cultivate and have a rapid growth rate under ambient condition of pH, temperature and pressure (Saravanan et al., 2021). Extracellular and intracellular mechanisms are the main pathways for the synthesis of SeNPs (Murugesan et al., 2019) through bioaccumulation, precipitation, biomineralization and biosorption to reduce metal ions to NPs where cellular biomolecules are existed using distinct metabolic pathways, enzymes and proteins, which are involved in the reduction process of elementary selenium to SeNPs (Annamalai et al., 2021; Ranjitha & Rai, 2021a). In the extracellular mechanism, the introduced metal salts are converted into NP in the culture broth or affixed to the cell membrane. On the other hand, in the intracellular mechanism, the added metal ions are converted into NPs inside the cell after being transported by internalization across the cellular membrane, afterward, various techniques such as cell lysis and others are used to free the internally synthesized NPs into the supernatant where they can then be recovered and purified (Zambonino et al., 2021).

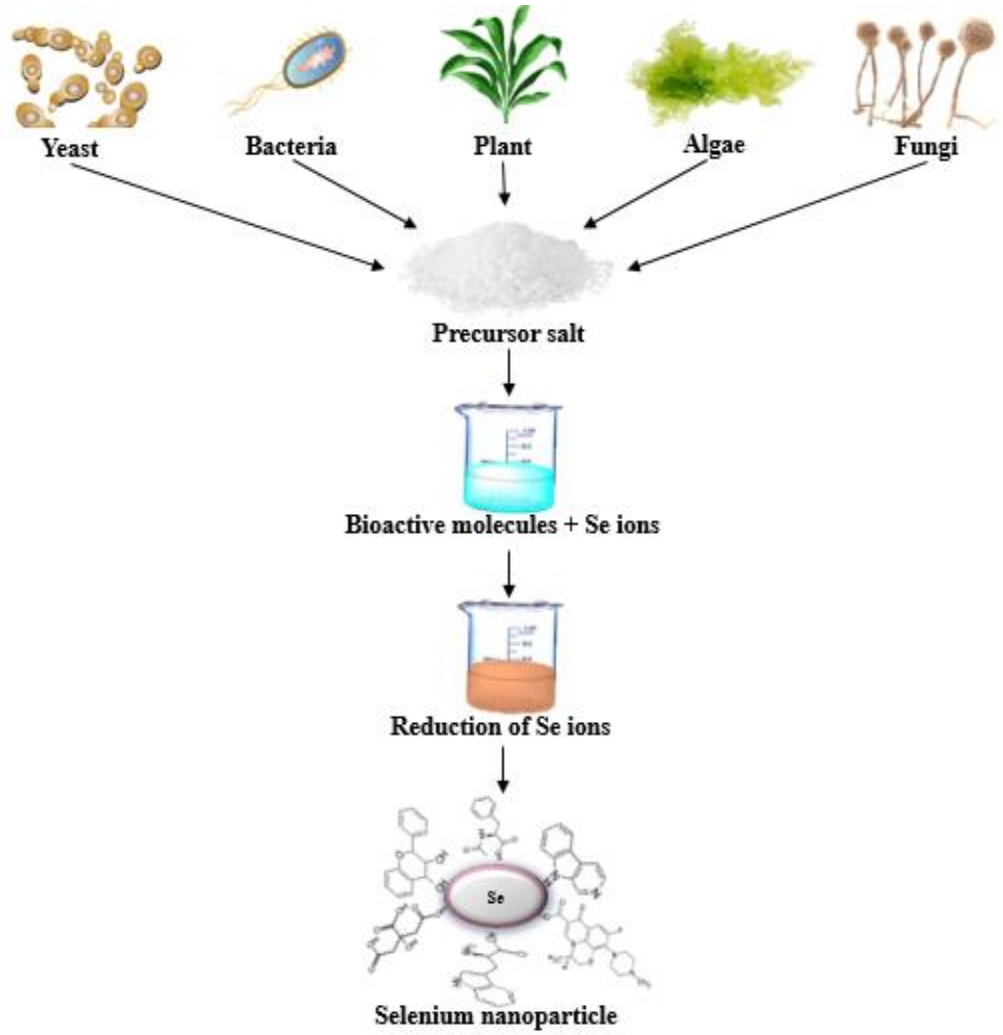

Figure 04: Biosynthesis of selenium nanoparticles (Derouiche et al., 2022).

4.2. Biomedical potential of selenium nanoparticles

SeNPs received attention as a result of their widespread application in pharmacotherapy fields. SeNPs are more effective at fighting free radical species and have an acceptable bioavailability, biocompatibility, smaller size and lower toxic impact when compared to inorganic selenium element, including selenate, selenite and selenomethionine based on experimental findings. SeNPs have significant physiological and metabolic functions, including the regulation of the immune system and the antioxidant defense system (Ashraf et al., 2023). SeNPs include outstanding functionalities to assist a variety of biomedical applications, including diabetes and associated complications treatments, cancer therapy, treatment of microbial infections, gene delivery, bioimaging and biosensing, this attracting carrier enables the delivery of treatments to distinct areas of disease or infection, reducing off-target medication toxicity and thereby limiting adverse effects, depending on the synthesis procedure carried out at a particular condition (Deepasree & Venugopal, 2022).

The attractive antioxidant capacity of SeNPs appears *in vivo* due to the importance of selenium containing in selenoproteins structure and their critical role in antioxidant enzymes involved in redox state regulation, through increased activities of glutathione peroxidase (GPx), superoxide dismutase (SOD) and thioredoxin. shorthand (TrxR) (Qiao et al., 2020). It proved that SeNPs have a synergic antioxidant effects through reducing power and free radical scavenging ability due to biosubstances involved in their construction (Kumar et al., 2020). According to previous research, SeNPs play an advantageous role in antioxidant defense and enhance the immune system's ability to protect cells from free radical attack (Kojouri et al., 2020).

SeNPs perform their anti-inflammatory effects, in particular when SeNPs are green synthesized and coated with natural bioactive compounds, by ameliorating macrophage infiltration through the decline in of cluster of differentiation 68 (CD68) levels in affected tissue, modulating the secretion of TNF-α and IL-6 by preventing nuclear factor kappa B (NF-κB) which results in transcription of these pro-inflammatory cytokines (Zhu et al., 2017).

SeNPs, as a potential anticancer medicine and drug carrier, has considerable significance in lowering the risk of getting cancer since it can address the problems with standard medications' inadequate action and instability in target organs. SeNPs can stop the growth of malignancies By encouraging tumor cells to undergo apoptosis, the major mechanisms of this action being after activating the appropriate signaling pathways by triggering apoptosis, creating excessive reactive oxygen species (ROS), and inducing mitochondrial damage (Lin et al., 2023).

As reported in the various literature, the therapeutic effect of selenium nanoparticles against diabetes, fatty liver, atherosclerosis and associated complications are related to regulation of biochemical markers, oxidative stress markers, reduced inflammation, and pancreatic apoptosis (Guan et al., 2018; Martínez-Esquivias et al., 2021).

Using biosynthesis method, nanotechnology has offered the great safety technique for lowering selenium's toxicity, enhancing its biological functionality, replacing the antibotics which have side effects due to their superior biocompatibility and antibacterial capabilities. The excellent antimicrobial activity of SeNPs may be due to their spherical shape and smaller size which helps to penetrate the cellular membrane of the microorganisms and induced the cell death by different mechanisms (Ikram et al., 2021).

Second part

Experimental part

Material and Methods

I. Material

I.1. Plant material

Sonchus maritimus were collected in November from a village in Djamaa of El Oued state, Algeria. The leaves were dried at room temperature after being washed with distilled water. The totally dried leaves were ground using a mechanical grinder. Then the powder stored in the airtight containers until the use at room temperature.

Figure 05: leaves of *Sonchus maritimus* (original photo)

I.2. Animals

From the Institute Pasteur of Algiers, thirty-six males of albino Wistar rats were obtained (weighing 173.08± 3.48 g and aging 7–8 weeks old). The rats were kept in plastic cages at the animal house of Natural and Life Sciences Faculty, in University of Echahid Hamma Lakhdar-El Oued, Algeria. The animals were housed under standard conditions (12/12 h dark/light cycle with temperature 25 ± 2 °C,). During the study, the animals were acclimatized with this condition and were given a standard food (Table 01) and free access of water which were provided ad libitum. All experimental processes used, as well as the care and handling of rats, were according to international guidelines confirmed by referenced local Ethics Committee (06 EC/DCMB/FNSL/EU2021) of the Department of Cellular and Molecular Biology, Faculty of Natural Sciences and Life, University of El-Oued, Algeria.The rats were weekly weighted, and their food and water intakes were daily measured.

Table 01: Standard and high fructose diet composition (Southon et al., 1984)

Raw materials	Standard diet		High Fructose diet	
	Quantity (g/kg)	Percentage (%)	Quantity (g/kg)	Percentage (%)
Maize	326	32.6	211.9	21.19
Cellulose	326	32.6	211.9	21.19
Protein	168	16.8	109.2	10.92
Sacrose	60	6	39	3.9
Vitamin	40	4	26	2.6
Minerals	40	4	26	2.6
Oil	40	4	26	2.6
Fructose	-	-	350	35

The standerd diet was prepared by manifactore of Souf Nutrition Animal, Eloued.

I.2.1. Experimental metabolic syndrome induction

All animals were kept on a specially prepared high fructose diet (HFD) designed to induce metabolic syndrome, with the exception of the normal control group. Every three to four days, a freshly prepared diet containing 35% fructose was given (Table 01). This diet was administrated for 13 weeks according to Hu *et al.* (2012). Therefore, consumption of a high-fructose diet by normal rats usually induced a metabolic syndrome model with histological and biochemical alterations (Yahya et al., 2023).

I.2.2. Experimental design

After two weeks of acclimatization, the thirty-six rats were randomly divided into six groups of six (06) rats in each one as following:

Group 01 (Control): normal control group standard diet;
Group 02 (HFD): High-fructose diet group;
Group 03 (HFD+ SmE-N): High-fructose diet group treated by *S. maritimus* extract-loaded niosomes;
Group 04 (HFD+SeNPs): High-fructose diet group treated by green synthesized selenium nanoparticles using *Sonchus maritimus* extract (SmE-SeNPs);
Group 05 (HFD+SeNPs-SmE-N): High-fructose diet group treated by *S. maritimus* extract-loaded niosomes and SmE-SeNPs;
Group 06 (HFD + Met): High-fructose diet group treated by metformin;

Metabolic syndrome was induced by consumption of diet contain 35% fructose for 13 weeks. After that and for four weeks, the animals treated orally by metformin (50 mg/Kg

b.w/day) (Hassan et al., 2020), by SmE-N (50 mg/Kg b.w/day) (AlAmri et al., 2020), SmE-SeNPs (0.5 mg/Kg b.w/day) (Othman et al., 2022) and SeNPs- SmE-N through intraperitoneally injection. The control, HFD, and Met groups were received via intraperitoneal injection with physiological water in order to expose to the same experimental conditions as the other treated groups.

I.2.3. Sacrifice, blood sampling and tissue collection

After 12 hours of fasting and at the end of the treatment period, the rats were sacrificed while being a little anesthetized with chloroform (94%) delivered by inhalation. Blood samples were taken during the decapitation and placed in EDTA tubes that were identified for each rat to carried the hematological, the plasma had been separated by centrifugation for 10 minutes at 1500 rpm, the plasma samples were kept at -20 °C until the determination of lipid profile and other biochemical parameters, each rat's fasting blood glucose level was measured using a glucometer (Vital Chek®, China). Brain, heart, liver, kidneys and testicles were carefully removed and washed in sodium chloride (0.9% of NaCl) and weighed; the organs then stored in the freezer at -20 °C until the homogenates preparation for assume the glycogen, acetylcholinesterase activity, protein, total thiol, lipid peroxidation and oxidative stress parameters.

I.3. Cells and Reagents

MCF-7 (epithelial cell line was collected from as collected from someone's breast tissue suffering from metastatic cancer). Reagents were of analytical grade from Sigma-Aldrich including Hydrogen chloride (HCl), Methanol (CH_4O), Ethanol (C_2H_6O), Chloroform ($CHCl_3$), Wagner reagent, Ammoniac, Nitric acid (HNO_3), Sulfuric acid (H_2SO_4), Phosphoric acid (H_3PO_4), Fehling solution, Folin-Ciocalteu reagent (FCR), Sodium carbonate (Na_2CO_3), Aluminum trichloride ($AlCl_3$), Gallic acid ($C_7H_8O_6$), Quercetin ($C_{15}H_{10}O_7$), Catechin ($C_{15}H_{14}O_6$), Vanillin ($C_8H_8O_3$), Ferric chloride ($FeCl_3$), Potassium ferricyanide ($K_3[Fe(CN)_6]$), Ethanol, Linoleic acid($C_{18}H_{32}O_2$), Tween 80 ($C_{64}H_{124}O_{26}$), Cholesterol ($C_{27}H_{46}O$), Sodium selenite (Na_2SeO_3), Ascorbic acid ($C_6H_8O_6$), Diclofenac ($C_{14}H_{11}Cl_2NO_2$), Metformin ($C_4H_{11}N_5$), Acarbose ($C_{25}H_{43}NO_{18}$), Fructose ($C_6H_{12}O_6$), Glucose ($C_6H_{12}O_6$), α-amylase, Yeast (*Saccharomyces cerevisiae*), 3,5-Dinitrosalicylic acid ($C_7H_4N_2O_7$), Potassium sodium tartrate tetrahydrate ($C_4H_{12}KNaO_{10}$), Potassium phosphate buffer (Dipotassium phosphate (K_2HPO_4) & Potassium dihydrogen phosphate (KH_2PO_4)), sodium phosphate buffer (Sodium phosphate dibasic (Na_2HPO_4) & Sodium phosphate monobasic (NaH_2PO_4)), bovine serum albumin (BSA), 1,1-diphenyl-2-(2,4,6-trinitrophenyl)hydrazine (DPPH) ($C_{18}H_{12}N_5O_6$), Tris ($C_4H_{11}NO_3$), Sodium

chloride (NaCl) , Salicylic acid ($C_7H_6O_3$), Coomassie brilliant blue ($C_4H_4O_6KNa.4H_2O$), Trichloroacetic acid (TCA)($C_2HCl_3O_2$), Thiobarbituric acid (TBA)($C_4H_4N_2O_2S$), Butylated hydroxytoluene (BHT)($C_{15}H_{24}O$), 5,5'-dithiobis(2-nitrobenzoic acid) (DTNB)($C_{14}H_8N_2O_8S_2$), Reduced glutathione (GSH)($C_{10}H_{17}N_3O_6S$), Sodium hydroxide (NAOH), Ethylenediaminetetra-acetic Acid (EDTA)($C_{10}H_{16}N_2O_8$), Methionine ($C_5H_{11}NO_2S$), Nitro-blue tetrazolium chloride (NBT)($C_{40}H_{30}Cl_2N_{10}O_6$), Riboflavin ($C_{17}H_{20}N_4O_6$), Anthrone ($C_{14}H_{10}O$), Acetylcholine (Ach) ($C_7NH_{16}O_2^+$).

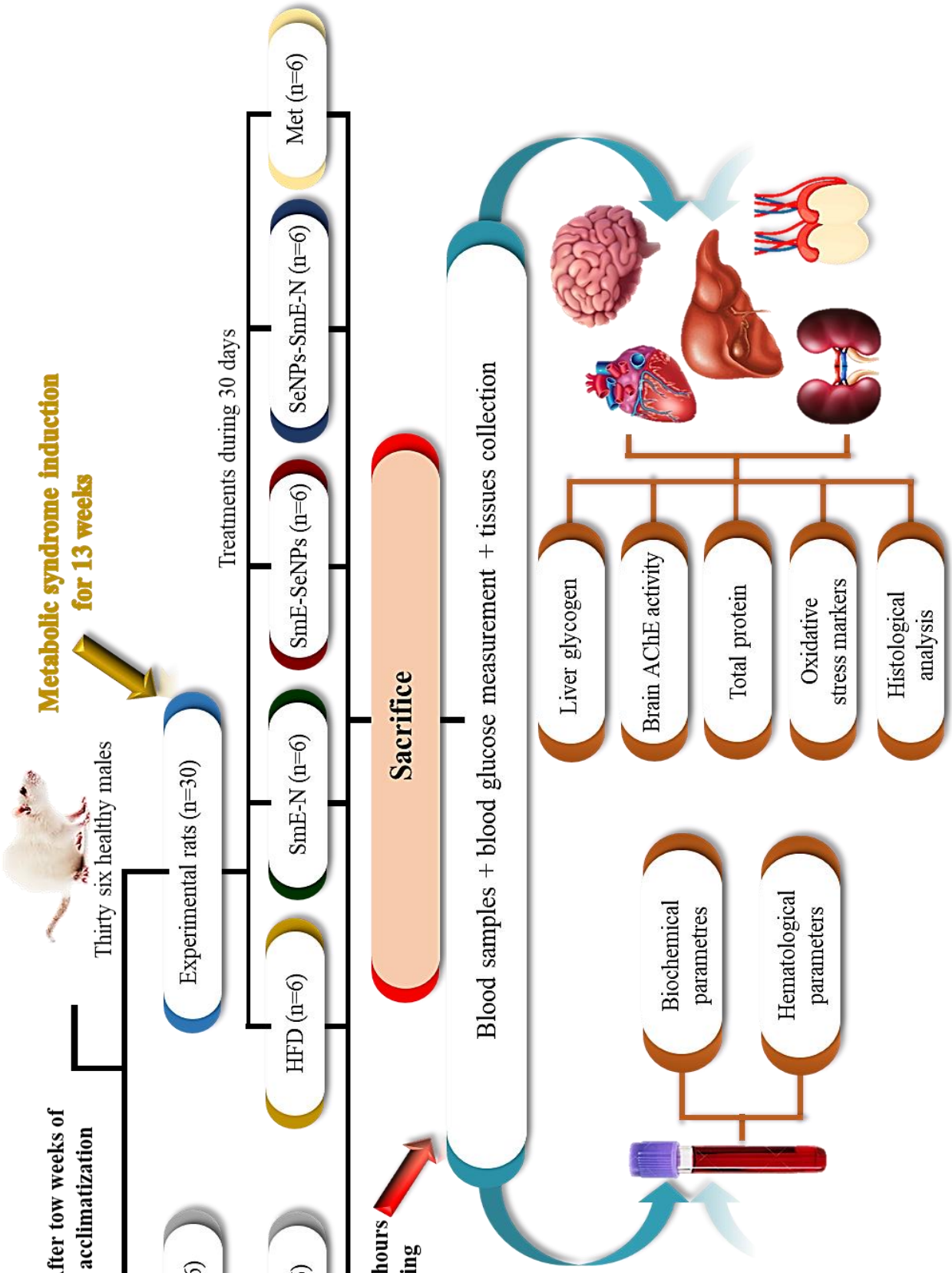

Figure 06: *In vivo* Experimental design of study

II. Methods

1. *In vitro* study

1.1. Aqueous extract preparation and yield rate determination

The leaves aqueous extract of *Sonchus maritimus* was prepared according to Derouiche *et al.* (2017); 10 g of *Sonchus maritimus* dry leaves powder was mixed with 100 mL of distilled water at 50°C for 2 hours. The mixture was next macerated for 24 hours at ambient temperature before being filtered using Whatman filter paper N°1 and then drying in an oven **(Figure 07)**.

For determining the yield rate, the freshly prepared leaves aqueous extract of *S. maritimus* was keeped for an overnight in oven-drying till geting a constant weight of dried extract (Chetehouna et al., 2022). The yield rate calculated using the following equation:

$$\text{Yield rate (\%)} = 100 \times \frac{\text{Weight of dried leaves extract}}{\text{Amount of dry leaves}}$$

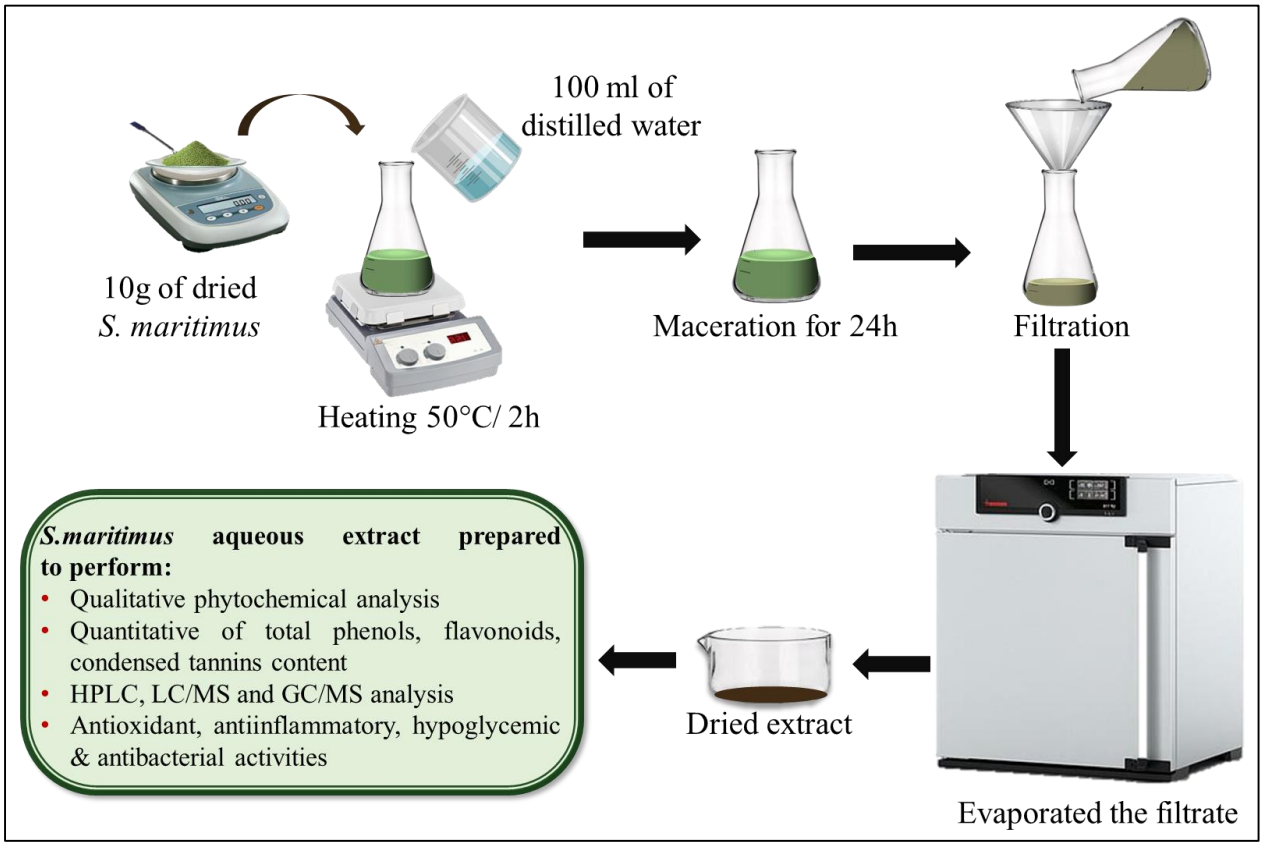

Figure 07: Preparation method of *S. maritimus* aqueous extract

1.2. Preparation of niosomes

The niosomes preparation method were described by Mohamad & Fahmy (2020); in a round-bottom flask, 100 µg of non-ionic surfactant including tween 80, 30 mg of cholesterol and 50 µg of linoleic acid to biocongugate as stabilizer, were dissolved in 100 mL ethanol: chloroform with 2:1 ratio. Then the rotary evaporator (BUCHI R-210 Rotavapor®, Switzerland) were used to eliminate the organic solvents under vacuum to form a thin layer on the wall of the flask. Residual solvents were evaporated in oven at 30 °C for 12 h. After that, the layer was sonicated in an ultrasonic bath (DIGITAL ULTRASONIC CLEANER UC-230D, Spain) at 50 °C for 60 min while being mixed with 10 mL of aqueous extract solution to produce an aqueous niosomal suspension containing *Sonchus maritimus* extract. The phytoniosome suspension was left at room temperature during overnight and then stored in refrigerator for further studies, (Figure 08).

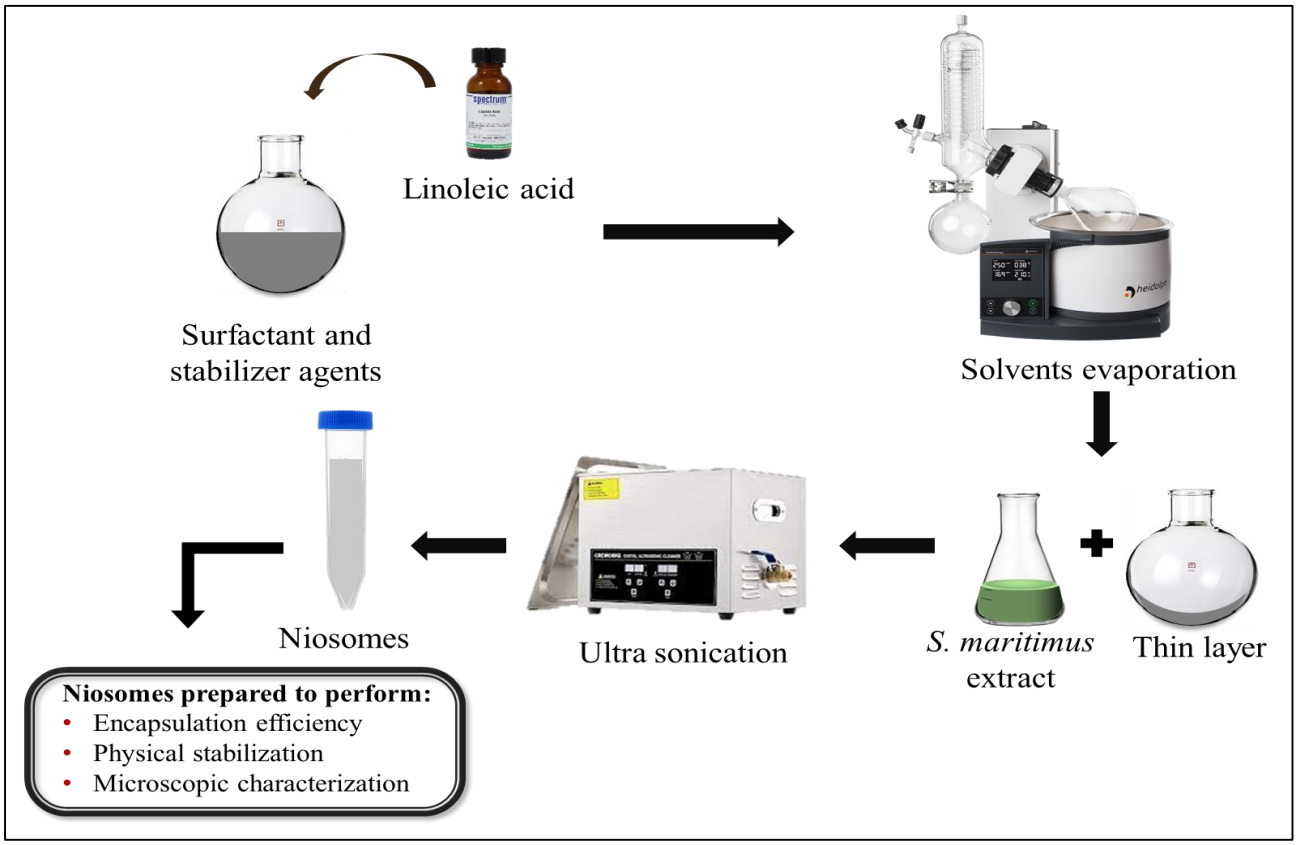

Figure 08: Preparation method of S. maritimus extract-loaded niosomes

1.3. Green synthesis of selenium nanoparticles using *Sonchus maritimus* extract (SmE-SeNPs)

Selenium nanoparticles were prepared by mixing 20 mL of leaves aqueous extract of *Sonchus maritimus* and 100 mL of sodium selenite (0.1 M), then dropwise of ascorbic acid solution (80 mM) were added until a slightly yellow color was obtained. After changing of the color, the reaction mixture was incubated in the dark under constant heating and stirring at 72°C/130 rpm to prevent photo-catalysis. SmE-SeNPs samples were obtained by centrifugation of mixture solution after being changed to red color, SmE-SeNPs have been washed twice with distilled water and ethanol, then dried and stored in an opaque closed flask until use (Khandsuren & Prokisch, 2021), (Figure 09).

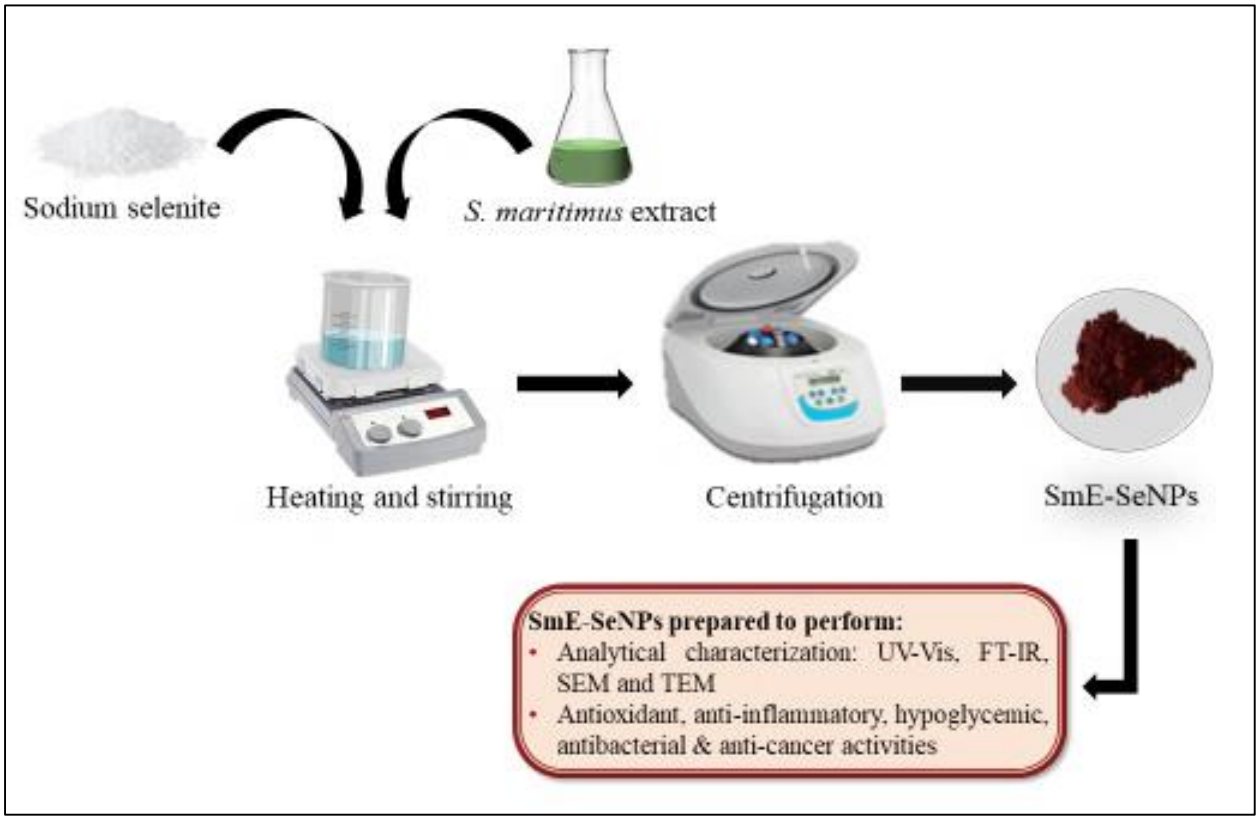

Figure 09: Green synthesis of SmE-SeNPs

1.4. Qualitative phytochemical analysis

The methods of Evans (2009), Harborne (1998), Wadood *et al.* (2013) and Harborne, (1973) were described for qualitative phytochemical screening to identify the phytochemicals compound that present in the aqueous extract of *Sonchus maritimus*.

1.4.1. Phenols

In a test tube, a few drops of a 5% ferric chloride solution were introduced into 5 mL of aqueous extract; the presence of phenolic compounds is detected by the appearance of a dark green color.

1.4.2. Flavonoids

In a test tube, 1 mL of sulfuric acid and 5 mL of diluted ammoniac were introduced into 5 mL of aqueous extract; the presence of flavonoids is detected by the appearance of a yellow color.

1.4.3. Alkaloids

In a test tube, a few drops of hydrochloric acid then a few drops (1to3) of Wagner reagent were introduced into 1 mL of aqueous extract; the presence of alkaloids is indicated by the appearance of brown precipitation.

1.4.4. Tannins

In a test tube, 1 mL of a 2% ferric chloride solution was introduced into 5 mL of aqueous extract; the appearance of greenish or bluish-blackish color is indicated the presence of tannins.

1.4.5. Terpenoids

In a test tube, 2 mL of chloroform and 3 mL of concentrated sulfuric acid were introduced into 5 mL of aqueous extract; the presence of terpenoids is detected by the appearance of reddish brown color.

II.4.6. Reducing compound

In a test tube, 2 mL of Fehling's liquor including reagent A (1 mL) and reagent B (1 mL) were introduced into a volume of aqueous extract then the reaction mixture incubated in a boiling water bath; the presence of reducing sugars is detected by the appearance of brick-red precipitate.

1.4.7. Saponins

In a test tube, 5 mL of distilled water was added to 5mL of extract, then mixed with vigurious manual agitation, the presence of saponins is detected by the formation of a steady foam.

1.4.8. Unsaturated steroids

In a test tube, 0.5 mL of acetic acid then 0.5 mL of concentrated sulfuric acid were introduced into aqueous extract; the presence of unsaturated steroids is detected if the solution does not give any green color.

1.4.9. Derived steroids

In a test tube, 0.5 mL of sulfuric acid was added to the aqueous extract, the presence of steroid derivatives is detected by the appearance of red color.

1.5. Quantitative phytochemical analysis

1.5.1. Total phenols

The quantitative analysis of total phenols in *S. maritimus* aqueous extract carried out according to the method of Slinkard & Singleton (1977); 125 µL of *S. maritimus* aqueous extract were added to 500 µL of distilled water, the solution was introduced into test tubes, then 125 µL of Folin-Ciocalteu's reagent (FCR) was added. After 5 min, 1250 µL of sodium carbonate (7.5 g/L) was added to accelerate the medium to trigger the redox reaction, after that the volume of the reaction mixture completed with distilled water to 03 mL and stirred, then the solution was incubated for 2 h at room temperature in a dark condition. The absorbance of each solution was measured at 765 nm using a UV-VIS spectrophotometer (Jenwey). A standard calibration curve was obtained from different concentrations of Gallic acid solution (10 -100 µg/mL), and performed under the same assay procedure conditions. The results were expressed on mg of Gallic acid per g of *S. maritimus* aqueous extract. All measurements were repeated 03 times.

1.5.2. Total flavonoids

The total flavonoids content in *S. maritimus* aqueous extract was carried out according to the method described by Ahn *et al.* (2007); 1000 µL of *S. maritimus* aqueous extract was mixed with 1000 µL of aluminum chloride (2%). After 10 min of incubation at room temperature, the absorbance of each solution was measured at 430 nm using a UV-VIS spectrophotometer (Jenwey). A standard calibration curve was obtained from different concentrations of quercetin solution (10 - 100 µg/mL), and performed under the same assay procedure assay procedure. The results were expressed on mg of Quercetin per g of *S. maritimus* aqueous extract. All measurements are repeated 03 times.

1.5.3. Condensed tannins

The condensed tannins content in *S. maritimus* aqueous extract was determined using spectrophotometry method and carried out according to the described method of Broadhurst and Jones (1978). 500 µL of *S. maritimus* aqueous extract was mixed with 3 mL of vanillin reagent (4%), freshly prepared in methanol, then 1500 µl of concentrated hydrochloric acid were added to reaction mixture and stirred thoroughly. After 15 min of reaction at temperature between 20 and 2°C, the different assay steps were in the dark condition, the absorbance of each solution was measured at 500 nm against water. A standard calibration curve was obtained from different concentrations of Catechin solution (10 - 1000 µg/mL), and performed under the same assay procedure. The results were expressed on mg of Catechine per g of *S. maritimus* aqueous extract. All measurements are repeated 03 times.

1.5.4. Content of mineral element

Dried leaves of *Sonchus maritimus* were heated in silica crucibles of muffle furnace (Nabertherm, Germany) at 600°C for 4 hours, the ash was dissolved in 3 mL of hot concentrated nitric acid. After filtration using Whatman filter paper, the volume was completed to 10 mL. The metals contents of sodium, potassium, calcium, magnesium, copper, zinc, iron and manganese were measured using atomic absorption spectrophotometer auto sampler (Shimadzu AA-6800). The results were expressed on µg per g of dry leaves of *Sonchus maritimus*.

1.6. Chromatographic analysis

1.6.1. High-performance liquid chromatography (HPLC) analysis

S. maritimus aqueous extract were filtered before the injection in the apparatus. The experimental conditions had being used were as following: Injection volume: 20µL; Temperature: 30 ˚C; the column: stationary phase C18 (length: 150 mm, diameter: 4.6 mm); Mobile phase: A: acetonitrile; B: 2 % glacial acetic acid solution (pH = 2.6); Gradient: 0-5 min: 5 % A; 25-30 min: 35% A; 35-45 min: 70% A. Debit: 0.5 mL/min; The HPLC equipment were connected to a detector that reads polyphenols at λ= 280 nm and flavonoids at λ = 360 nm.

1.6.2. Liquid chromatography and mass spectrometry (LC/MS) analysis

The LC-MS-2020 (Shimadzu, Kyoto, Japan) coupled with an electro-nebulization ionizing source in the negative mode, a quadrupole mass spectrometer was used to evaluate phenolic components from 5 µl of sample (*S. maritimus* extract). An ultra-fast liquid chromatography system (Shimadzu, Kyoto, Japan) including the autosampler (SIL-20AC XR),

the binary pump system n (LC-20AD XR), the column oven (CTO-20AC), and the the degasser (DGU-20A 3R), which was connected in parallel to the mass spectrometry analyzer. InertSustain C18 analytical column (GL Sciences Japan) with dimensions of 150 millimeters x 3 millimeters and 3 milcrometers, was utilized for the analysis. the mobile phase constitued from acetic acid (0,02%) mixed with H2O/ACN (1/1 ; v/v), elution by linear isocratic mode, with 10-minute acquisition time. The flow rate of mobile phase was 0.4 mL/min, the column's temperature was kept at 40 °C. The sample injection volume was 20 µL. Spectra were captured in selected ion monitoring (SIM) mode, and software of Shimadzu Lab Solutions LC-MS was used for analysis. High-pure nitrogen was used as a nebulizer and supplemental gas. By comparing the obtained mass spectrum and retention time, phenolic substances were identified using the standards (>98% pure) that provided by Sigma Chemical Co. (St Louis, MO, USA).

1.6.3. Gas chromatography (GC) analysis

Volatiles were extracted from headspace using solid-phase micro-extraction (SPME) by DVB/CAR/PDMS fiber. Initially, the fiber in the GC injection point needed to be conditioned at 270°C. After that, the fiber was inserted via an adaptor into the vial holding the sample and allowed to sit at room temperature for 15 minutes. The fiber was then inserted via the injection port of a gas chromatograph to begin the desorption process. In the splitless mode, desorption took place over 10 minutes at 260°C. Agilent Technologies' 5975C VL Triple-Axis, paired with a 7890A GC system, was used for the analysis, which was conducted in Santa Clara, California. Helium served as the carrier gas for the separation process, which was carried out on a DB-5MS capillary column (25 m × 0.2 mm; layer thickness of 0.33 µm; produced by J&W, Folsom, California) at an average flow rate of 0.6 mL/min. The injector and transfer line had temperatures of 260°C and 280°C, respectively. In the oven, the temperature was programmed to start at 40°C and stay there for three minutes. After that, it grew at a rate of 4°C per minute to 160°C and then at a rate of 10°C per minute to 280°C, with a final temperature hold of three minutes. The mass range that was scanned was 33–333 Da. The ionization energy was determined to be 70 eV. Volatiles were identified using the NIST (National Institute of Standards and Technology) 05 library.

1.7. Characterization of niosomes

1.7.1. Morphological characterization of niosomes

The formulated niosomes were examined using optical microscopy at magnification ×400 using an optical microscope (Optika B-293, Italy) which equipped with camera (Optika C-B5,

Italy). just a little of diluted vesicular mixture was put on a glass slide before being covered by lamella; to evaluate the shape consistency and the size of niosomes. In addition, the phytoniosomes were identified under a scanning electronic microscope (SEM) after centrifugation of the niosomes suspension which was followed by three washes to obtain the encapsulated *S. maritimus* extract in niosomes.

1.7.2. Encapsulation efficiency of niosomes

Encapsulation efficiency of encapsulated *S. maritimus* in niosomes was determined according to Raeiszadeh *et al.* (2018). 100 mg of S. maritimus aqueous extract was used for preparing niosomes (SmE-N). The encapsulated *S. maritimus* extract were separated from the non-encapsulated *S. maritimus* extract using centrifugation of the prepared niosomes at 4°C for 30 min at 15700g. The supernatant was recuperated and the capsules were dissolved by isopropyl alcohol. The amount of free bioactive compounds present in the supernatant as well as encapsulated bioactive compounds were measured using Follin-Ciocalteu method (Slinkard and Singleton, 1977). The analysis was performed and repeated three times. Encapsulation efficiency (EE%) was estimated as following:

$$\text{EE}\ (\%) = 100 \times \frac{\text{amount of encapsulated compound}}{\text{Initial amount of compound}}$$

1.7.3. Physical stability of niosomes

Physical stability of niosomes was investigated according to Raeiszadeh *et al.* (2018), which was evaluated in term of encapsulation efficiency (EE%) of *S. maritimus* extract-loaded niosomesthat was estimated during 1 day, 7 days, 30 days, 60 days and 90 days from niosomes preparation after they were kept under especial condition at 4°C with relative humidity of 25%. Results are represented by mean±SD (n=3).

1.8. Physical characterization of selenium nanoparticles

Selenium nanoparticles have been characterized using various analytical techniques; ultraviolet-visible spectrophotometry (UV-Vis) using Jenwey apparatus to indicate the synthesize of SmE-SeNPs, the absorbance peaks were recorded in the range between 200 and 800 nm; Fourier Transform Infrared Spectrophotomety (FT-IR) using Thermo Scientific iS5 apparatus to detect the functional groups that found in the sample and confirm the presence of Se-O bound; Scanning Electron Microscopy (SEM) and Energy Dispersive X-ray (EDX) were performed to exanimate the morphological surface, to determine the average size of the particles

and to identify the purity and the elements that present in the sample; Transmission Electron Microscopy (TEM) was carried out using TECNAI apparatus to determine more exactly the size and the shape of nanoparticles.

1.9. Antioxidant activities

1.9.1. DPPH radical scavenging ability test

The relative antioxidant capacity of *S. maritimus* extract and SmE-SeNPs was evaluated using a DPPH (2,2- Diphenyl-1-picrylhydrazyl) radical scavenging assay, according to Nwidu *et al.* (2017). Different concentrations (200, 175, 150, 125, 100, 75, 50, 25, 10 and 5 µg/mL) of *S. maritimus* extract solution and SeNPs colloidal solution were prepared in distilled water. 20 µL of the sample, or standard was mixed with 160 µL of DPPH (0.1 Mm) in ethanol before being mixed with 20 µL of distilled water. Various concentrations of ascorbic acid (standard) were performed under the same experimental processed conditions of the samples. The mixtures reactions were incubated in the dark condition at 37°C for 40 min, the sample absorbance (A_1) was measured at λ= 517 nm using UV-Vis spectrophotometre (Jenwey). The negative control was a blank (A_0). The results express using IC_{50} values which was determined by inhibition percentage:

$$\text{Inhibition percentage (\%)} = \frac{A0 - A1}{A0} \times 100$$

1.9.2. Ferric reducing ability test "FRAP"

FRAP assay assess the antioxidant activity of sample through reduction of ferric ion (Fe^{3+}) to ferrous ion (Fe^{2+}) by antioxidants present in sample. According to Oyaizu (1986), 1000 µL of different concentrations (200, 175, 150, 125, 100, 75, 50, 25, 10 and 5 µg/mL) of *S. maritimus* extract or of SmE-SeNPs was mixed with 2500 µL of phosphate buffer solution (pH 6.6; 0.2 M), then 2500 µL of potassium ferricyanide (1%) was added. The mixtures solutions were incubated in water bath for 20 minutes at 50°C, the reaction was stopped by adding 2500 µL of trichloroacetic acid (10%). The mixtures reactions were centrifuged at 3000 rpm for 10 min, then 2500 µL of the supernatant, 2500 µL of distilled water, and 500 µL of ferric chloride (0.1 %) were mixed. The sample absorbance (A_1) was measured at λ= 700 nm. Various concentrations of ascorbic acid (standard) were performed under the same experimental processed conditions of the samples. The negative control was a blank (A_0). The results express using IC_{50} values which was estimated using the regression line equation against different

concentrations of samples using FRAP values which calculated according to Yazdani *et al.* (2019):

$$\text{FRAP}\ (\%) = \frac{\text{A1} - \text{A0}}{\text{A1}} \times 100$$

1.10. Anti-inflammatory activities

1.10.1. Inhibition of protein denaturation ability test

In vitro anti-inflammatory activity of *Sonchus maritimus* extract and SmE-SeNPs were studied using inhibition of protein denaturation assay according to Vennila *et al.* (2018). Various concentrations (10–100 µg/mL) of *S. maritimus* extract or SmE-SeNPs was mixed with serum albumin solution (1%), the mixture solutions were incubated during 30 min at ambient temperature. After that, the reaction solution's pH was adjusted to 2 using a few drops of concentrated hydrochloric acid solution; then, the mixture solutions were exposed to heating in 72 °C during 30 min; after the incubation, the tubes were cooled for 10 min in ice bath. Finally, the sample absorbance (A_1) was measured at λ= 660 nm. The diclofenac (Standard) were exposed to the same experimental condition of the sample. The blank was used as negative control (A_0). The results were expressed as IC_{50} which calculated using the line regression of inhibition percentage:

$$\text{Inhibition percentage}\ (\%) = \frac{\text{A0} - \text{A1}}{\text{A0}} \times 100$$

1.10.2. Anti-hemolytic ability test

Anti-hemolysis test was performed according to Vinjamuri *et al.* (2015) which assess the protective capacity of bioactive compounds in the sample against red blood cell (RBC) membrane lysis induced by 1X PBS. 5mL of blood was obtained from healthy volunteers was placed into EDTA tube to stop its coagulation, then the blood centrifuged at 4°C for 10 min at 1000 tour/min. the pipette was used with the utmost care to remove totally the plasma and white buffy layer. The erythrocytes were then washed three times with 1X PBS (0.1 M; pH 7.4) using centrifugation method for 5 minutes. Erythrocytes that had been washed were kept at 4°C and used within 6 hours for the test. 50 µL of diluted erythrocytes suspension 10% were mixed with 100 µL of various concentration (10-100 µg/mL) of *S. maritimus* extract or SmE-SeNPs, a positive control was 100 µL of different concentrations of diclofenac and a negative control was 100 µL of 1XPBS. After that, the reaction solutions were incubated during one hour at 37°C in

water bath. The volume of reaction mixtures was completed to 1 mL by adding 1X PBS, then centrifuged at 300 rpm for 3 minutes. The hemoglobin amount in the supernatant of samples (A_0) were subsequently determined using a spectrophotometer (Jenwey) at λ= 540 nm. The results were expressed by IC_{50} which were calculated using the percentage of hemolysis as following:

$$\text{Hemolysis inhibition (\%)} = \frac{\text{A0} - \text{A1}}{\text{A0}} \times 100$$

1.11. Hypoglycemic activities

1.11.1. α-amylase inhibition activity test

The α-amylase inhibition activity of *S. maritimus* extract and SmE-SeNPs were carried out according to Bauer *et al.* (2023); 50 µL of different concentrations (10 µg/mL to 5000 µg/mL) of *S. maritimus* aqueous extract or SmE-SeNPs solutions were mixed with 50 µL of α-amylase (0.5 mg/mL) prepared in sodium phosphate buffer (20 mM, pH 6.9), the solutions were pre-incubated for 10 min at 25ºC, 50 µL of starch solution (1%) that had been cooked for 15 min prepared in the same buffer solution was then added. The reaction mixtures were incubated for 10 min at 25ºC. Afterward, 100 µL of 3,5-dinitrosalicylic acid (1%) prepared in sodium potassium tartrate (30%) dissolved in 0.4 M sodium hydroxide were added. The mixtures were incubated for 5 min at 100ºC then cooled at room temperature. Absorbance of samples (A_1) was assessed at 540 nm by a microplate reader (BioTek). The buffer sample which substitute the extract or nanoparticles was used as control (A_0). Acarbose was used as standard. The inhibition percentage of α-amylase enzyme was determined using the following equation:

$$\alpha - \text{amylase inhibiton (\%)} = \frac{\text{A0} - \text{A1}}{\text{A0}} \times 100$$

1.11.2. Glucose uptake in yeast cells test

Assay of glucose uptake in yeast cells was carried according to Cirillo *et al.* (1963). Yeast suspension of *Saccharomyces cerevisiae* in distilled water was exposed to repeated centrifugation at 3000 rpm for 5 min until clear supernatant liquid was get to prepare diluted suspension 10% (v/v) in distilled water. Different concentrations (50 to 250 µg/mL) of *S. maritimus* extract or SmE-SeNPs were added to 1000 µL of glucose solution (5 mM), the mixtures were incubated at 37 °C for 10 min. 100 µL of diluted yeast suspension was added to start the reaction followed by vortexing and then incubation for 1 h at 37 °C. Afterward, the

reaction solutions were centrifuged for 5 min at 2500 rpm. Absorbance of glucose amount of the sample (A_1) was measured in the supernatant using a microplate reader (BioTek) at 520 nm. The blank was used as negative control (A_0). Metformin was used as standard. The following formula was used to determine the percentage of glucose uptake by yeast cells:

$$\text{Glucose uptake}(\%) = \frac{\text{A0} - \text{A1}}{\text{A0}} \times 100$$

1.11.3. Glucose adsorption test

The glucose adsorption ability of *S. maritimus* extract and SmE-SeNPs were performed using the method of Rehman *et al.* (2018); 100 mL of glucose solution of five various concentrations (3-5 mM) were mixed well with 1 g of sample and stirred. Then, the solutions were incubated during 6 h at 37°C in a water bath. After incubation, the reaction solutions were centrifuged 20 min at 4800 rpm. The glucose amount was measured in the supernatant using glucose oxidase peroxidase. The amount of bound glucose was assessed using following formula:

$$\text{Glucose bound} = \frac{\text{G1} - \text{G6}}{\text{weight of sample}} \times \text{volume of sample}$$

where, G_1 indicates the concentration of glucose in original solution, indicates the concentration of glucose in solution after 6 hours.

1.12. Antibacterial activity

The disc diffusion method was used to carry out the antibacterial activity according to Mwitari *et al.* (2013). The assay was performed on Mueller Hinton agar plates to assess the antibacterial properties of *S. maritimus* extract and SmE- SeNPs against common Gram-negative bacteria (*Escherichia coli* ATCC 25922 and *Pseudomonas aeruginosa* ATCC 27853) and Gram-positive bacteria (*Staphylococcus aureus* ATCC 25923). which were conserved at 4°C on nutrient agar plates. Activation of bacteria was carried out in the incubator at 37 °C for 24 h. Sterile physiological water was used to prepare bacterial solution. The bacterial suspension was evenly distributed by streaking of the swab three times on dry surface of Mueller Hinton agar. Afterward, sterile discs' paper (Whatman N°.3) of 6 mm were impregnate with 20 µL of various concentration (10, 20 and 30 mg/mL) of *S. maritimus* aqueous extract and SmE-SeNPs solutions, discs were left to dry on a clean workstation and were then put on inoculated agar surface. Negative control was impregnated discs with sterile distilled water. The all Petri plates were

incubated during 24 h at 37°C. The standard antibiotics used as positive control against all pathogens were amoxicillin, gentamicin, ceftazidime, ciprofloxacin and cotrimoxazole. The inhibition zone of each disc were assessed in millimeters unit (mm) after the incubation. Experiments were carried out in triplicate.

1.13. Anticancer activity test

1.13.1. Culturing of cell lines

RPMI-1640 (Sigma, USA) medium containing 10% fetal bovine serum, 100 units/mL penicillin, and 100 g/mL streptomycin (Capricorn Scientifc GmbH, Ebsdorfergrund, Germany) was used for growing all cell lines. Trypsin-EDTA (Capricorn Scientifc GmbH, Ebsdorfergrund, Germany) was utilized in order to trypsinize the cell lines at a short duration of time while they were adherent monolayers cultured at 37 degrees Celsius and humid atmosphere in incubator with 5% of CO2. These cells are regularly examined and verified.

1.13.2. MTT assay

The cytotoxicity test was carried out using a previous investigation (Mahmood et al., 2022).The test involved seeding 96-well plates with cells and letting them sit for an entire day. After that, for 24, 48, and 72 hours, those cells had been treated with a range of SmE-SeNPs concentrations (v/v) (3.125%, 6.25%, 12.5%, 25%, and 50%). After the cells had been incubated for the specified duration of time, 50µL of MTT solution was added. A microplate equipment was used to measure the absorbance (492 nm) after medium aspiration and DMSO addition, and the experiment was incubated for a period of four hours. After the formazan formed, it was dissolved in dimethyl sulfoxide and its absorbance at 520 nm was obtained using a micro titer plate reader.

2. *In vivo* study

2.1. Acute toxicity test

Acute toxicity assay of *S. maritimus* aqueous extract and SmE-SeNPs were performed according to the method described of Lorke (1983). From Pasteur Institute of Algeria stat, twenty-five (25) males of albino Wistar rats weighing 141.38 ± 3.85 g and being eight weeks' old were obtained. The animals were housed in plastic cages at the Animal room of Natural and Life Sciences Faculty, in University of Echahid Hamma Lakhdar-El Oued, Algeria. The rats were separated into five groups, five rats in each cage (n = 5). After 12 h of fasting; the rats of each group were given by intraperitoneal injection a single dose of *S. maritimus* aqueous extract

(250 and 500 mg/kg b.w) and SmE-SeNPs (2.5 and 5 mg/kg b.w), then were kept under observation for 14 days to follow their behavior as well as the mortality and compared them with control group. All experimental processes used, as well as the care and handling of rats, were according to international guidelines confirmed by referenced local Ethics Committee (06 EC/DCMB/FNSL/EU2021) of the Department of Cellular and Molecular Biology, Faculty of Natural Sciences and Life, University of El-Oued, Algeria.

2.2. Clinical grading scores of rat's behaviors

During the treatment period, the clinical behavioral signs in the control and experimental groups were performed, the clinical grading scores of behaviors is according to Farjam *et al.* (2012) as following (Table 02):

Table 02: Clinical grading scores of rat's behaviors

Clinical grade	Behavior
0	Normal behavior
1	Mild lethargy
2	Decreased motor activity
3	Sever ataxia, no spontaneous righting reflex
4	No reaction to pain stimuli

2.3. Hematological parameters

The Hematological parameters were determined using Rayto Automatic Touch Screen Hematology Analyzer (RT-7600).

2.4. Biochemical parameters

Glutamate oxaloacetate transaminase(GOT), Glutamate pyruvate transaminase (GPT), Uric acid (UA), Urea, Creatinine (Creat) and lipid profile including total cholesterol (TC), triglyceride (TG) and high density lipoprotein cholesterol (HDL-c) in the plasma were determined using (Mindray BS-200, China), Glycosylated Hemoglobin (Hb1c) using (Medcoon, Germany) and Testosterone using (Mindray BS-900i, Germany) by commercial reagent kits (Bio Lab, France and Spin, Spain). Low density lipoprotein cholesterol (LDL-c) and Very low density lipoprotein cholesterol (VLDL-c) levels were determined according to equation of Friedewald *et al.* (1972) :

$$LDLc = TC - VLDLc - HDLc$$

$$VLDLc = \frac{Triglyceride}{5}$$

2.5. Homogenates preparation

1g of liver, brain, heart, kidney or testicles tissues of the all experimental rats group was homogenized and grinding in 9 mL of Tris buffer saline solution (Tris (50 mM), NaCl (150m M), pH 7.4) in cold condition. The obtained homogenates were then centrifuged for 15 min at 5000 rpm at 4°C, after that the supernatants of each rat were stored at -20°C (Derouiche et al., 2017).

2.6. Determination of tissue protein

The determination of proteins amount in the tissue were assessed according to Bradford (1976) using a colorimetric method by a spectrophotometer (Jenwey) using Coomassie blue reagent. The intensity of blue color corresponds to proteins concentration in the sample. 1 ml of the homogenate were mixed with 5 mL of Coomassie blue, the reaction mixtures were then shaken. After 5 min, the absorption was measured at λ= 595 nm. The protein amount in tissues were determined using standard calibration curve of bovine serum albumin (BSA) (0.1-1 mg/mL) were previously performed under the same procedure assay conditions.

2.7. Determination of liver glycogen

Glycogen estimation in liver tissue were carried out according to Duvhåteau & Florkin (1959) using a colorimetric method. 1000 µL of anthrone reagent is added to 25 µL of homogenate, the mixture was then incubated at 80 °C for 10 min in a water bath. The intensity of a green color is proportional to the quantity of carbohydrates present in the sample. Optical density was read at λ= 620 nm against a reagent blank containing distilled water. The carbohydrate concentration was calculated using standard calibration curve of glucose (0.1-1 mg/mL), performed under the same experimental conditions.

2.8. Determination of acetylcholinesterase (AChE) activity

AChE activity was carried out according to method of Ellman *et al.* (1961). An incubation solution containing 50 µL of acetylcholine (0.8 mM), 1000 µL of phosphate buffer (100 mM, pH 7.5), and 50 µL of DTNB (1.0 mM) was used to evaluate the rate of cholinergic hydrolysis. 50 µL of homogenate were added to reaction solution which pre incubated at 25 °C

for 3 min after being shaken. The acetylcholinesterase contained in the tissue fraction will react with acetylthiocholine (ASCh) to release acetate and thiocholine (SCh) which reacts with 5-5'-Dithio-bis (2-nitrobenzoate) (DTNB) giving the yellow TNB product. The hydrolysis was measured at λ= 412 nm each 3 min at 25 °C. The results were expressed on µmol /min/ mg of protein according to fallowing equation:

$$\text{AChE (nmol/min/mg prot)} = \frac{\Delta\,\text{DO} / \Delta\,\text{t} \times 1691.18}{\text{Prot}}$$

2.9. Estimation of oxidative stress parameters

2.9.1. Determination of malondialdehyde (MDA) level

The estimation of MDA in the samples was carried out in accordance with Yagi (1976) based on a colorimetric method which measures the optical density of a pink complex of thiobarbituric acid reactive substances which formed from the condensation MDA in acid medium and under heating in the presence of thiobarbituric acid. 200 µl of homogenates samples were Introduced into a glass test tube with vise, mixed with 800 µl of TBA reagent and then hermetically closed. The mixtures were heated in a water bath for 15 min at 100 °C. Then, they were cooled for 30 min in a cold water bath, the tubes were opened to let the gases produced during the reaction get out. After incubation, the solutions were centrifuged for 5 min at 3000 rpm and the supernatant optic density (OD) was read at λ= 532 nm using a spectrophotometer (Jenwey). The concentration of thiobarbituric acid (TBARS) was assessed using molecular extinction coefficient of MDA using a following equation:

$$\text{MDA (nmol /mg of prot)} = \frac{\text{OD sample}}{1.53 \text{ x } 10 \text{ ^ } 5 \times \text{mg of prot}}$$

2.9.2. Determination of total thiol

Total thiol (-SH) groups in samples were measured according to Ellman (1959) using DTNB reagent which reacted with the SH groups to create a complex with a yellow color which had a maximum absorption peak at λ = 412 nm. 1 mL of Tris-EDTA buffer (0.25 M; 20 mM) was added to 50 µL of homogenate, the absorbance was read against Tris-EDTA buffer alone (A_1) at λ = 412 nm. After that, 20 µL DTNB (10 Mm) prepared in methanol were added to the reaction mixture, after 10 min, the sample absorbance was read (A_2) again. The DTNB

absorbance was also read as a blank (B). The concentration of total thiol (mM) in sample was calculated using the following equation:

$$\text{Total thiol (mM/mg of prot)} = (A2 - A1 - B) \times \frac{1.07}{0.05 \times 13.6 \times \text{mg of prot}}$$

2.9.3. Determination of reduced glutathione (GSH) level

The GSH levels in different homogenate samples were determined in accordance with method of Weckbecker and Cory (1988), briefly, based on measurement of optic density of TNB (2-nitro-5-mercocapturic acid) formed from reduction of Elman reagent (DTNB) in presence of SH groups exist in GSH. 800µL of samples were added to 200µL of salicylic acid (0.25%). Then, the mixture solutions were centrifuged for 5 min at 1000 rpm. 500 mL of supernatant were mixed with 25 µl of DTNB (0.01 mol/L) and 1000µL of tris buffer solution (Tris 0.4mol; NaCl 0.02mol; pH = 8.9 after 5 min, the optic density of sample (OD) was read at λ= 412 nm. The GSH concentrations were expressed on (nmol/mg of protein) according to following equation:

$$\text{GSH (nmol/mg of prot)} = \frac{(OD \times 1 \times 1.525)}{13133 \times 0.8 \times 0.5 \times \text{mg of prot}}$$

2.9.4. Determination of superoxide dismutase (SOD) activity

The estimation of SOD activity in samples were according to Beauchamp and Fridovich (1971) using a colorimetric method. 50 µL of sample was introduced into test tubes and mixed with 1000 µL (0,1 mM, 13 mM), 1800µL phosphate buffer solution (50 mM; pH 7.8) and 100 µL of NBT (75 µM). The tubes were incubated for 5 min at 25°C. 50 µL of riboflavin (2 µM) were then added and incubated in a light box for 20 min. The optic density was read at 560 nm. The SOD activity was expressed on Unit/mg of protein, the inhibition percentage of NBT reduction by SOD was according to following equation:

$$\text{Inhibition percentage (\%)} = \frac{\text{OD blanc} - \text{OD sample}}{\text{OD blanc}} \times 100$$

Where 1 Unit of SOD is equal to 50% inhibition.

2.9.5. Determination of glutathione peroxidase (GPx) activity

The glutathione peroxidase (GPx) activity was estimated according to Flohé & Günzler (1984). This method is based on hydrogen peroxide (H_2O_2) reduction in reduced glutathione

presence (GSH) which transformed into (GSSG) under activity of GPx activity. 200 µL of homogenate were mixed with 400 µL of GSH (0.1 mM) and 200 µL of TBS buffer solution (Tris 50 mM; NaCl 150 mM; pH 7.4); the mixture was incubated for 5 min at 25 °C in a water bath. After that, 200 µL of hydrogen peroxide (1.3 mM) were added to initiate reaction and left to act for 10 min, 1000 µL of TCA (1%) were then added to stop the reaction and putted to incubate for 30 min. Therefore, the mixture reactions were centrifuged for 10 min at 3000 rpm, and 480 µL of supernatant were mixed with 2200 µL of TBS buffer solution and 320 µL of DTNB (1 mM). After 5 min of incubation the optical densities (OD) was read at λ= 412 nm. The enzymatic activity of GPx was expressed on µmol GSH/mg of protein and determined using the following equation:

$$\text{GPx (µmol GSH/mg of prot)} = \left[\left(\frac{\text{OD sample} - \text{OD blanc}}{\text{OD blanc}}\right) \times 0.4\right] \times 5/\text{mg of prot})$$

2.9.6. Determination of total antioxidant capacity

Total antioxidant capacity was estimated according to Oyaizu (1986), 1000 µL of homogenate was mixed with 2500 µL of phosphate buffer solution (pH 6.6; 0.2 M), then 2500 µL of potassium ferricyanide (1%) was added. The mixtures solutions were incubated in water bath for 20 minutes at 50°C, the reaction was stopped by adding 2500 µL of trichloroacetic acid (10%). The mixtures reactions were centrifuged at 3000 rpm for 10 min, then 2500 µL of the supernatant, 2500 µL of distilled water, and 500 µL of ferric chloride (0.1 %) were mixed. The sample absorbance (A_1) was measured at λ= 700 nm. The absorbance of blank (A_0) was also measured. The results expressed as total antioxidant capacity values which calculated according to Yazdani *et al.* (2019) equation:

$$\text{Total antioxidant capacity (\%)} = \frac{\text{A1} - \text{A0}}{\text{A1}} \times 100$$

2.10. Histopathological analysis

The liver, brain, heart, kidney and testiculs were removed and washed with 0.9% of sodium chloride after the sacrifice and immersed in formaldehyde (10 %) and phosphate buffer solution (pH 7.6) as a fixative solution for 48 h, dehydrated in ascending ethanol grades, cleaned by toluene, submerged in blocks of paraffin. Using a rotator microtome, the specimens were submerged, then cut into sections with a thickness of 5 µm and colored by hematoxylin-eosin. The histopathological study was carried out using an optical microscope (Optika B-293, Italy)

equipped with camera (Optika C-B5, Italy). The photomicrographs analysis was done by image processing software, Optika.

2.11. Statistical analysis

The data were represented in the form of graphs and histograms using office EXCEL 2019. Results are represented as means ± standard deviations (Mean ± SD). ANOVA test are performed to indicate statistically significant differences. The results of the invivo tests were expressed as Mean ± Standard Error of Mean (Mean ± SEM) and compared between the groups studied using the Student's t-test. The MINITAB version 19 data processing and analysis program has been used for all calculations.

Results

I. *In vitro* assays

1. Phytochemical analysis

1.1. Qualitative and quantitative phytochemical analysis of *Sonchus maritimus*

1.1.1. Qualitative phytochemicals analysis

The qualitative analysis revealed presence of different phyto-compounds in aqueous extract of *Sonchus maritimus* including phenols, flavonoids, terpenoids, tannins, unsaturated steroids, derived steroids and sponins, However, absence reducing compoundsand of alkaloids and was observed (Table 03).

Table 03: Phytochemical analysis of *Sonchus maritimus* aqueous extract

Phytochemicals	***Sonchus maritimus***
Phenols	+
Flavonoids	+
Alkaloids	-
Tannins	+
Terpenoids	+
Reducing compounds	-
Saponins	+
Unsaturated steroids	+
Derived steroids	+

(+) presence; (-) absence

1.1.2. Quantitative phytochemicals analysis

The quantitative phytochemical results presented in table 04 demonstrated an important yield rate with richness of *Sonchus maritimus* aqueous extract on a reasonable amount of total phenols, flavonoids and condensed tannins.

Table 04: Yield rate and content of total phenols, flavonoids and condensed tannins in *Sonchus maritimus* aqueous extract

Parameters	Aqueous extract of *Sonchus maritimus*
Yield rate (%)	26.650 ± 0.173
Total phenols (mg EGA/g of extract)	23.190 ± 0.781
Total Flavonoids (mg EQer/g of extract)	12.906 ± 0.154
Condensed Tannins (mg ECat/g of extract)	2.890 ± 0.474

1.1.3. Content of mineral elements analysis

Results in table 05 showed a richness of dry leaves of *Sonchus maritimus* with different mineral nutrients, including major elements such as sodium, potassium, calcium and magnesium, and minor elements such as copper, zinc, iron and manganese.

Table 05: Content of mineral elements in dry leaves of *Sonchus maritimus*

Mineral Elements		*Sonchus maritimus* (µg/g of dry leaves)
Major Elements	**Na**	13188 ± 659.4
	K	35716 ± 1785.8
	Ca	10508 ± 525.4
	Mg	3992 ± 199.6
	Fe	154 ± 7.7
Minor Elements	**Cu**	0.52 ± 0.026
	Zn	0.41 ± 0.0205
	Mn	0.45 ± 0.0225

1.2. Chromatographic analysis

1.2.1. HPLC analysis of *Sonchus maritimus* aqueous extract

Chromatographic results revealed an abundance of polyphenols in leaves aqueous extract of *Sonchus maritimus* as indicated in figure 10 through appearance of peaks in chromatogram of various phenolic acids, including vanillic acid, gallic acid, caffiec acid and chlorogenic acid, as well as different flavonoids, including, rutin, quercetin and naringin as what shown in table 06.

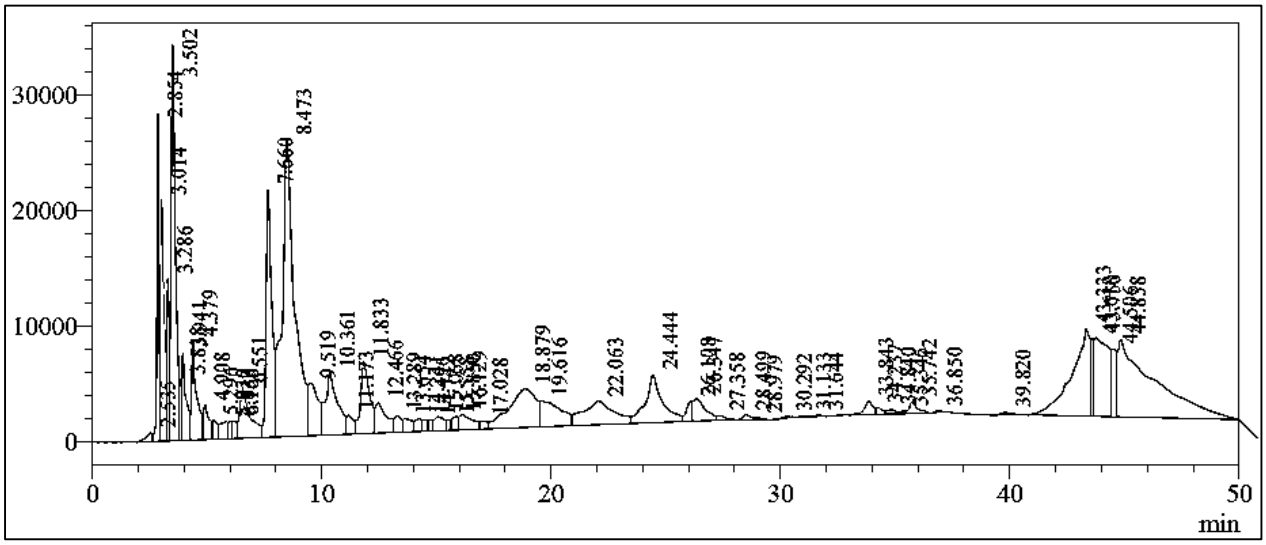

Figure 10: Chromatogram of HPLC analysis of *S. maritimus* leaves aqueous extract

Table 06: Chemical structure of identified biocompounds by HPLC analysis in *S. maritimus* leaves aqueous extract

N^{br}	Name	Formula	Ret. Time (min)	Area	Height
1	Gallic acid	$C_7H_6O_5$	5.296	22785	1632
2	Chlorogenic Acid	$C_{16}H_{18}O_9$	13.289	30467	1435
3	Vanillic Acid	$C_8H_8O_4$	15.558	11524	933
4	Caffeic Acid	$C_9H_8O_4$	16.129	53432	1346
5	Rutin	$C_{27}H_{30}O_{16}$	28.499	9261	424
6	Naringin	$C_{27}H_{32}O_{14}$	34.840	10463	369
7	Quercetin	$C_{15}H_{10}O_7$	44.838	738821	6678

1.2.2. LC/MS analysis of *Sonchus maritimus* aqueous extract

LC/MS results were presented in figure 11 and table 07. This method performed to determine the concentrations of some phenolic acids and flavonoids in *S. maritimus* extract based on retention time, which included quercetin (36,420 ppm), apigenin-7-o-glucoside (4,995 ppm), luteolin (130,638 ppm), trans cinnamic (13,170 ppm), o-coumaric acid (5,148 ppm), trans ferulic acid (47,428 ppm) and protocatechuic acid (115,159 ppm).

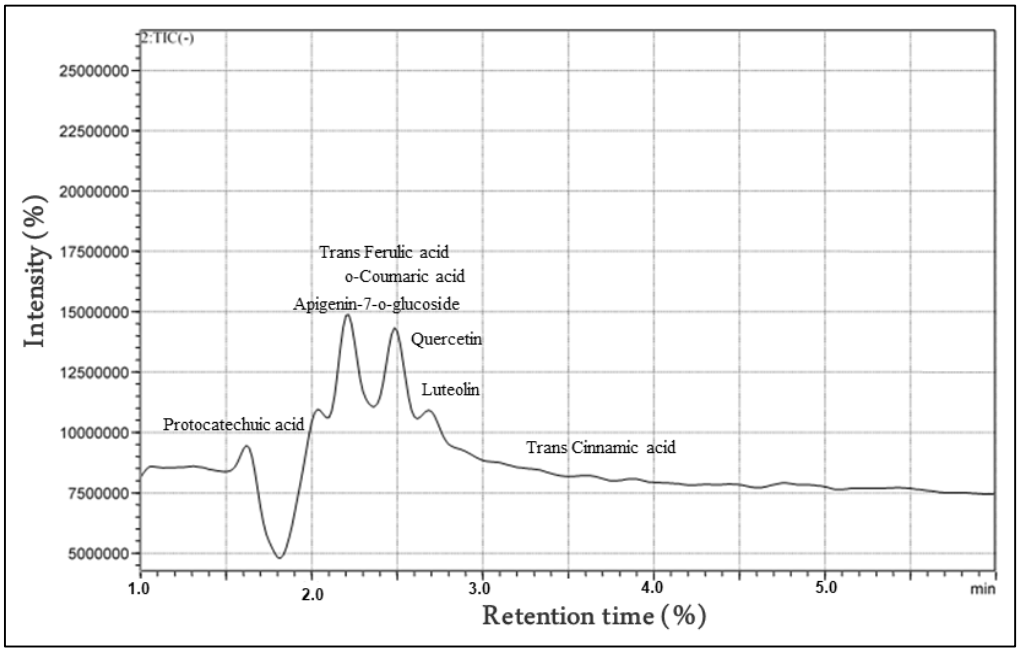

Figure 11: LC-MS analysis of leaves aqueous extract of *Sonchus maritimus*

Table 07: Retention time of detected phytochemical compounds by LC-MS analysis in leaves aqueous extract of *Sonchus maritimus*

N^{br}	Name	Chemical formula	Ret. Time (min)	m/z	Conc. (ppm)
1	Protocatechuic acid	$C_7H_6O_4$	1.608	153.00	115.159
2	Trans Ferulic acid	$C_{10}H_{10}O_4$	2.494	193.00	47.428
3	o-Coumaric acid	$C_9H_8O_3$	2.488	163.00	5.148
4	Apigenin-7-o-glucoside	$C_{21}H_{20}O_{10}$	2.438	431.00	4.995
5	Quercetin	$C_{15}H_{10}O_7$	2.572	301.00	36.420
6	Trans Cinnamic acid	$C_9H_8O_2$	3.594	147.00	13.170
7	Luteolin	$C_{15}H_{10}O_6$	2.757	285.00	130.638

1.2.3. GC analysis of *Sonchus maritimus* aqueous extract

The results of GC analysis of *S. maritimus* leaves aqueous extract presented in figure 12 and table 08, the analysis was revealed 283 volatile compounds. The identification of volatile biocompound was performed using the comparison with NIST standards 05 library. Determinition of the phytochemicals is based on elution and availability over a correspond retention time such as 1-Hexanol, 2-ethyl-, Ethylene glycol - Adipate - Diethylene glycol, Cyclotrisiloxane, hexamethyl-, Cyclopentasiloxane, decamethyl-, 1-[2,4-

Bis(trimethylsiloxy)phenyl]-2-[(4-trimethylsiloxy) phenyl]propan-1-one, Cyclopentasiloxane, decamethyl-, Cyclotetrasiloxane, octamethyl-, 6-Chloro-2,3-quinoxalinediol, O, O', di-TMS, 1,1,3,3,5,5,7,7-Octamethyl-7-(2-methylpropoxy)tetrasiloxan-1-ol, Dibutyl phthalate, Pentanoic acid, 2,2,4-trimethyl-3-carboxyisopropyl, isobutyl ester, Phloroglucinaldehyde, tris(tert-butyldimethylsilyl) ether, ,3,5-Triethoxy-1,1,1,7,7,7-hexamethyl-5-(trimethylsilyloxy)tetrasiloxane, Heptasiloxane, 1,1,3,3,5,5,7,7,9,9,11,11,13,13-tetradecamethyl-, Pentadecane, Heptasiloxane, 1,1,3,3,5,5,7,7,9,9,11,11,13,13-tetradecamethyl-, Hexadecane, Oxime-, methoxy-phenyl-_, Eicosane, and Methyl Alcohol.

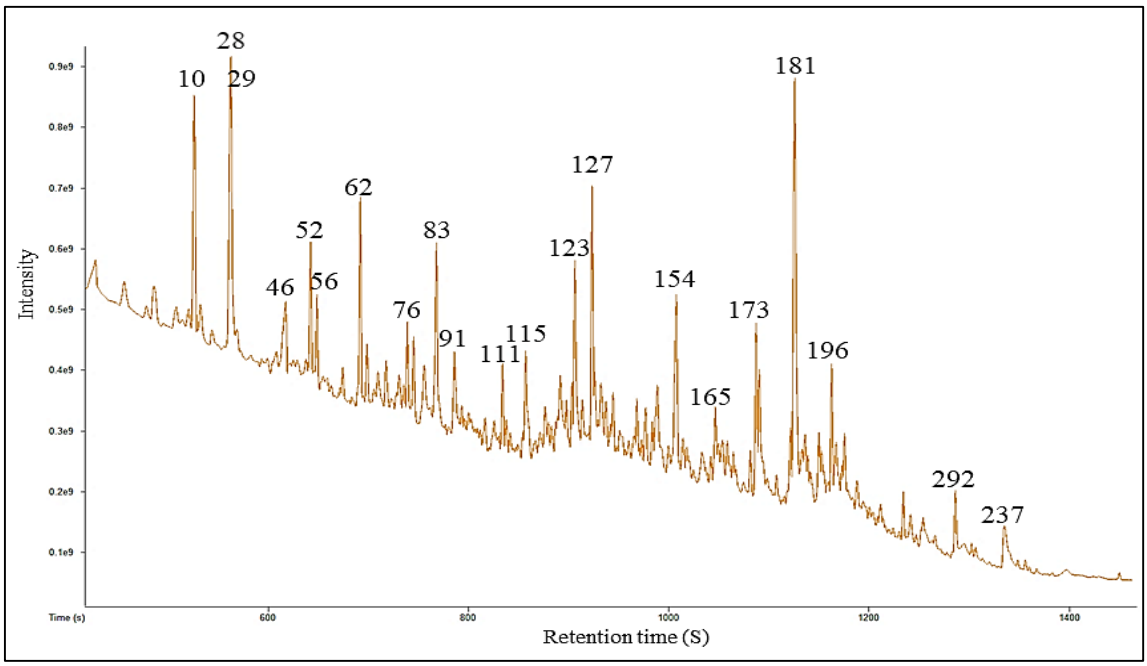

Figure 12: Chromatogram of GC analysis of *S. maritimus* leaves aqueous extract

Table 08: The detected phytocompounds using GC analysis of *S. maritimus* aqueous extract

Peak	Name	Formula	Ret. Time (s)
1	Pentanoic acid	$C_5H_{10}O_2$	303.431
2	Isocrotonic acid	$C_4H_6O_2$	306.021
3	Silane, ethoxytriethyl-	$C_8H_{20}OSi$	339.988
4	Dimethyl Sulfoxide	C_2H_6OS	348.768
5	Butanoic acid, 2-methyl-	$C_5H_{10}O_2$	367.487
6	Benzeneethanol, α,β-dimethyl-	$C_{10}H_{14}O$	380.592
7	Cyclobutane, 1,1,2,3,3-pentamethyl-	C_9H_{18}	388.367
8	2-Butanone, 3-chloro-	$C_4H_7C_lO$	399.417
9	Heptanal	$C_7H_{14}O$	415.563
10	Oxime-, methoxy-phenyl-_	$C_8H_9NO_2$	428.032
11	1,3,5,7-Tetroxane	$C_4H_8O_4$	432.062
12	Dimethyl sulfone	$C_2H_6O_2S$	436.428
13	Hexanoic acid, methyl ester	$C_7H_{14}O_2$	443.312

14	1-Methoxy-2-propyl acetate	$C_6H_{12}O_3$	455.864
15	α-Pinene	$C_{10}H_{16}$	456.918
16	2-Propanol, 1-butoxy-	$C_7H_{16}O_2$	463.176
17	1-Pentanone, 1-(2-thienyl)-	$C_9H_{12}OS$	477.443
18	p-Aminotoluene	C_7H_9N	484.372
19	Cyclopropane, butyl-	C_7H_{14}	495.389
20	Benzene, 1-methyl-3-(1-methylethyl)-	$C_{10}H_{14}$	499.065
21	β-Phellandrene	$C_{10}H_{16}$	502.242
22	β-Pinene	$C_{10}H_{16}$	507.091
23	Benzene, 1,1'-(1-ethenyl-1,3-propanediyl)bis-	$C_{17}H_{18}$	510.877
24	5-Hepten-2-one, 6-methyl-	$C_8H_{14}O$	514.91
25	2-Octanone	$C_8H_{16}O$	519.123
26	Furan, 2-pentyl-	$C_9H_{14}O$	520.74
27	2-(2-tert-Butyldimethylsilyloxy-5-methylphenyl)benzotriazole	$C_{19}H_{25}N_3OSi$	525.212
28	1-[2,4-Bis(trimethylsiloxy)phenyl]-2-[(4-trimethylsiloxy)phenyl]propan-1-one	$C_{24}H_{38}O_4Si_3$	525.986
29	Cyclotetrasiloxane, octamethyl-	$C_8H_{24}O_4Si_4$	526.236
30	5-Hydroxy-7-methoxy-2-methyl-3-phenyl-4-chromenone	$C_{17}H_{14}O_4$	527.309
31	Octanal	$C_8H_{16}O$	532.469
32	2-Propanol, 1-(2-ethoxypropoxy)-	$C_8H_{18}O_3$	535.324
33	2-Propanone, 1-hydroxy-	$C_3H_6O_2$	535.705
34	3-Carene	$C_{10}H_{16}$	544.039
35	Propane-1,2,3-triamine	$C_3H_{11}N_3$	547.372
36	Oxirane, [[(2-ethylhexyl)oxy]methyl]-	$C_{11}H_{22}O_2$	556.323
37	1-Hexanol, 2-ethyl-	$C_8H_{18}O$	561.763
38	Butanedioic acid, dimethyl ester	$C_6H_{10}O_4$	565.005
39	Benzyl alcohol	C_7H_8O	569.147
40	2(3H)-Furanone, 5-ethenyldihydro-5-methyl-	$C_7H_{10}O_2$	575.793
41	2(3H)-Furanone, 5-ethyldihydro-	$C_6H_{10}O_2$	589.535
42	Undecane, 2,2-dimethyl-	$C_{13}H_{28}$	590.839
43	Phenylglyoxal	$C_8H_6O_2$	603.872
44	Acetophenone	C_8H_8O	604.578
45	2-Hexene, 3,5-dimethyl-	C_8H_{16}	611.733
46	Cyclotrisiloxane, hexamethyl-	$C_6H_{18}O_3Si_3$	618.049
47	Benzenemethanol, α,α-dimethyl-	$C_9H_{12}O$	624.96
48	1-[4-(2-Hydroxy-3-morpholin-4-ylpropoxy)phenoxy]-3-morpholin-4-ylpropan-2-ol	$C_{20}H_{32}N_2O_6$	631.295
49	Undecane, 2-methyl-	$C_{12}H_{26}$	633.22
50	Octane, 6-ethyl-2-methyl-	$C_{11}H_{24}$	633.957
51	Undecane	$C_{11}H_{24}$	637.62
52	Nonanal	$C_9H_{18}O$	642.495
53	Benzeneacetic acid, 10-undecenyl ester	$C_{19}H_{28}O_2$	654.744
54	Triethyl phosphate	$C_6H_{15}O_4P$	667.3
55	Methyl Alcohol	CH_4O	673.197
56	Pentanedioic acid, dimethyl ester	$C_7H_{12}O_4$	674.851
57	Cyclopentanone	C_5H_8O	677.151
58	Bicyclo[3.1.1]heptan-2-one, 6,6-dimethyl-	$C_9H_{14}O$	683.021

59	(6,6-Dimethylbicyclo[3.1.1]hept-2-en-2-yl)methyl ethyl carbonate	$C_{13}H_{20}O_3$	685.067
60	1-Heptene, 6-methyl-	C_8H_{16}	689.576
61	(+)-2-Bornanone	$C_{10}H_{16}O$	690.859
62	Cyclopentasiloxane, decamethyl-	$C_{10}H_{30}O_5Si_5$	692.043
63	Cyclohexanone, 5-methyl-2-(1-methylethyl)-	$C_{10}H_{18}O$	698.618
64	Octane, 3-ethyl-2,7-dimethyl-	$C_{12}H_{26}$	699.297
65	Acetic acid, phenylmethyl ester	$C_9H_{10}O_2$	705.371
66	Decane, 1,1'-oxybis-	$C_{20}H_{42}O$	710.088
67	endo-Borneol	$C_{10}H_{18}O$	713.844
68	Cyclohexanol, 1-methyl-4-(1-methylethyl)-	$C_{10}H_{20}O$	717.525
69	1-(1-Methoxypropan-2-yloxy)propan-2-yl acetate	$C_9H_{18}O_4$	718.842
70	Benzeneethanol, α,α-dimethyl-, acetate	$C_{12}H_{16}O_2$	724.549
71	Cyclohexane, (1,3-dimethylbutyl)-	$C_{12}H_{24}$	727.801
72	3-Cyclohexen-1-ol, 5-methylene-6-(1-methylethenyl)-, acetate	$C_{12}H_{16}O_2$	728.323
73	Ethanol, 2-(2-butoxyethoxy)-	$C_8H_{18}O_3$	729.914
74	Naphthalene	$C_{10}H_8$	730.904
75	1,5,5-Trimethyl-6-methylene-cyclohexene	$C_{10}H_{16}$	735.553
76	Dodecane	$C_{12}H_{26}$	739.046
77	Decanal	$C_{10}H_{20}O$	745.303
78	Undecane, 2,5-dimethyl-	$C_{13}H_{28}$	752.875
79	Bicyclo[3.1.1]hept-2-en-6-one, 2,7,7-trimethyl-	$C_{10}H_{14}O$	756.042
80	2-ethenyl-3-ethylpyrazine	$C_8H_{10}N_2$	760.039
81	Nonane, 3-methyl-5-propyl-	$C_{13}H_{28}$	760.577
82	Benzaldehyde, 4-(1-methylethyl)-	$C_{10}H_{12}O$	765.985
83	1,1,3,3,5,5,7,7-Octamethyl-7-(2-methylpropoxy)tetrasiloxan-1-ol	$C_{12}H_{34}O_5Si_4$	768.21
84	1-Methyl-4-isopropyl-cyclohexyl 2-hydroperfluorobutanoate	$C_{14}H_{20}F_6O_2$	769.023
85	1,2-Benzisothiazole	C_7H_5NS	770.734
86	Carbonic acid, propargyl 2-ethylhexyl ester	$C_{12}H_{20}O_3$	777.058
87	Hexanedioic acid, dimethyl ester	$C_8H_{14}O_4$	780.042
88	Piperazine, 1,4-dinitro-	$C_4H_8N_4O_4$	782.373
89	2,4,6-Tris(trimethylsilyl)cyclohexane-1,3,5-trione	$C_{15}H_{30}O_3Si_3$	783.594
90	HEX-5-EN-3-OL	$C_6H_{12}O$	785.063
91	Phloroglucinaldehyde, tris(tert-butyldimethylsilyl) ether	$C_{25}H_{48}O_4Si_3$	785.987
92	(-)-Carvone	$C_{10}H_{14}O$	787.461
93	Dodecane, 5-methyl-	$C_{13}H_{28}$	791.487
94	3-Cyclohexene-1-carboxaldehyde, 1,3,4-trimethyl-	$C_{10}H_{16}O$	793.356
95	3,3,5-Triethoxy-1,1,1,7,7,7-hexamethyl-5-(trimethylsilyloxy)tetrasiloxane	$C_{15}H_{42}O_7Si_5$	799.349
96	Benzene, hexyl-	$C_{12}H_{18}$	800.539
97	1,2-Hydrazinedicarboxaldehyde	$C_2H_4N_2O_2$	801.92
98	Nonanoic acid	$C_9H_{18}O_2$	803.047
99	Tetradecane, 2,5-dimethyl-	$C_{16}H_{34}$	806.778
100	2,6-Dimethyldecane	$C_{12}H_{26}$	809.003
101	2-Bromo dodecane	$C_{12}H_{25}Br$	811.751
102	1H-Indol-3-amine	$C_8H_8N_2$	812.029

103	Heptadecane, 2,6,10,15-tetramethyl-	$C_{21}H_{44}$	816.697
104	Butanenitrile, 2,3-bis(benzoyloxyimino)-	$C_{18}H_{13}N_3O_4$	823.456
105	Dodecane, 2,6,10-trimethyl-	$C_{15}H_{32}$	824.478
106	Anethole	$C_{10}H_{12}O$	825.795
107	1H-Pyrazole, 1-methyl-	$C_4H_6N_2$	827.232
108	3-Aminopyrazine 1-oxide	$C_4H_5N_3O$	834.369
109	Decan-2-ol, dimethylpentafluorophenylsilyl ether	$C_{18}H_{27}F_5OSi$	836.85
110	Dodecane, 2,7,10-trimethyl-	$C_{15}H_{32}$	837.313
111	Naphthalene, 1-methyl-	$C_{11}H_{10}$	837.933
112	Oxirane, dodecyl-	$C_{14}H_{28}O$	841.676
113	Dodecane, 2,5-dimethyl-	$C_{14}H_{30}$	850.963
114	Benzene, (2-methyl-1-propenyl)-	$C_{10}H_{12}$	856.793
115	6-Chloro-2,3-quinoxalinediol, O, O', di-TMS	$C_{14}H_{21}ClN_2O_2Si_2$	857.169
116	Dodecane, 2,6,11-trimethyl-	$C_{15}H_{32}$	867.006
117	2,6,10-Trimethyltridecane	$C_{16}H_{34}$	873.8
118	Glycerol 1,2-diacetate	$C_7H_{12}O_5$	876.002
120	Tridecane, 6-methyl-	$C_{14}H_{30}$	879.865
121	Cyclohexene, 1-methyl-5-(1-methylethenyl)-, (R)-	$C_{10}H_{16}$	884.01
122	Tridecane, 4-methyl-	$C_{14}H_{30}$	887.032
123	Tridecane, 2-methyl-	$C_{14}H_{30}$	891.458
124	Ethanol, 2-(2-butoxyethoxy)-, acetate	$C_{10}H_{20}O_4$	892.152
125	Perhydrophenalene, (3aα, 6aα, 9aα, 9bβ)-	$C_{13}H_{22}$	895.964
126	Tridecane, 3-methyl-	$C_{14}H_{30}$	897.849
127	Hexadecane, 2,6,10,14-tetramethyl-	$C_{20}H_{42}$	903.359
128	1,2,4-Metheno-1H-indene, octahydro-1,7a-dimethyl-5-(1-methylethyl)-, [1S-(1α,2α,3aβ,4α,5α,7aβ,8S*)]-	$C_{15}H_{24}$	912.973
129	Nonane, 4,5-dimethyl-	$C_{11}H_{24}$	916.766
130	Ethanone, 1-(1-methylcyclohexyl)-	$C_9H_{16}O$	920.409
131	Tridecane, 4,8-dimethyl-	$C_{15}H_{32}$	927.099
132	Novaluron, N,N'-dimethyl-	$C_{19}H_{13}ClF_8N_2O_4$	927.52
133	Naphthalene, 1-ethyl-	$C_{12}H_{12}$	927.784
134	3-Amino-N-(4-fluoro-2-methylphenyl)propanamide	$C_{10}H_{13}FN_2O$	930.333
135	Diphenyl ether	$C_{12}H_{10}O$	933.289
136	Tetrasiloxane, 3,5-diethoxy-1,1,1,7,7,7-hexamethyl-3,5-bis(trimethylsiloxy)-	$C_{16}H_{46}O_7Si_6$	934.879
137	2-Thiopheneacetic acid, 3-tetradecyl ester	$C_{20}H_{34}O_2S$	940.293
138	1H-2-Indenone,2,4,5,6,7,7a-hexahydro-3-(1-methylethyl)-7a-methyl	$C_{13}H_{20}O$	941.794
139	Longifolene	$C_{15}H_{24}$	944.356
140	Tetracontane, 3,5,24-trimethyl-	$C_{43}H_{88}$	948.071
141	Tetracyclo[5.2.1.0(2,6).0(3,5)]non-8-ene, 4-methyl-4-phenyl-, endo-	$C_{17}H_{18}$	950.852
142	5,5-Dibutylnonane	$C_{17}H_{36}$	952.328
143	Pentadecane, 4-methyl-	$C_{16}H_{34}$	956.12
144	2(1H)-Naphthalenone, 3,4,4a,5,6,7-hexahydro-1,1,4a-trimethyl-	$C_{13}H_{20}O$	960.078
145	Tetradecane, 5-methyl-	$C_{15}H_{32}$	968.318
146	5,9-Undecadien-2-one, 6,10-dimethyl-	$C_{13}H_{22}O$	970.596
147	Tetradecane, 3-methyl-	$C_{15}H_{32}$	983.51

148	1-Dodecanol	$C_{12}H_{26}O$	986.695
149	2,5-Cyclohexadiene-1,4-dione, 2,6-bis(1,1-dimethylethyl)-	$C_{14}H_{20}O_2$	988.698
150	Anthracene, tetradecahydro-	$C_{14}H_{24}$	996.455
151	(2R,3R,3aR,6R,8aS)-3,7,7-Trimethyl-8-methyleneoctahydro-1H-3a,6-methanoazulen-2-ol	$C_{15}H_{24}O$	999.562
152	3-Buten-2-one, 4-(2,6,6-trimethyl-1-cyclohexen-1-yl)-	$C_{13}H_{20}O$	1003.65
153	Cycloheptasiloxane, tetradecamethyl-	$C_{14}H_{42}O_7Si_7$	1005.93
154	Pentadecane	$C_{15}H_{32}$	1007.54
155	Hordenine	$C_{10}H_{15}NO$	1011.59
155	Decyl octyl ether	$C_{18}H_{38}O$	1014.12
156	Naphthalene, 1,2,4a,5,6,8a-hexahydro-4,7-dimethyl-1-(1-methylethyl)-, (1α,4aα,8aα)-	$C_{15}H_{24}$	1018.22
157	Nonane, 5-methyl-5-propyl-	$C_{13}H_{28}$	1018.82
158	Carbonic acid, octadecyl prop-1-en-2-yl ester	$C_{22}H_{42}O_3$	1029.05
159	Dibenzofuran	$C_{12}H_8O$	1033.1
160	Dichlorophen, O,O'-(2-trifluoromethylbenzoyl)-	$C_{29}H_{16}Cl_2F_6O_4$	1035.19
161	Bis(tert-butyldimethylsilyl) 2,3-bis((tert-butyldimethylsilyl)oxy)fumarate	$C_{28}H_{60}O_6Si_4$	1035.77
162	trans-Calamenene	$C_{15}H_{22}$	1037.67
163	Hexadecane, 1-chloro-	$C_{16}H_{33}Cl$	1041.97
164	Nonyl tetradecyl ether	$C_{23}H_{48}O$	1044.8
165	Heptasiloxane, 1,1,3,3,5,5,7,7,9,9,11,11,13,13-tetradecamethyl-	$C_{14}H_{44}O_6Si_7$	1046.1
166	Benzene, (1-propylheptyl)-	$C_{16}H_{26}$	1048.77
167	Tetradecane, 4-methyl-	$C_{15}H_{32}$	1049.66
168	3-Ethoxy-1,1,1,7,7,7-hexamethyl-3,5,5-tris(trimethylsiloxy)tetrasiloxane	$C_{17}H_{50}O_7Si_7$	1058.8
169	Hexane, 3,4-bis(1,1-dimethylethyl)-2,2,5,5-tetramethyl-	$C_{18}H_{38}$	1060.9
170	7-[3,5-Dihydroxy-4-(4-hydroxyphenyl)-2-methoxyphenyl]-3-methoxy-3,4-dihydrooxepine-2,5-dione, 3TMS	$C_{29}H_{42}O_8Si_3$	1062.51
171	Pentadecane, 3-methyl-	$C_{16}H_{34}$	1064.54
172	Hexadecane	$C_{16}H_{34}$	1087.13
173	Pentanoic acid, 2,2,4-trimethyl-3-carboxyisopropyl, isobutyl ester	$C_{16}H_{30}O_4$	1090.26
174	Dodecanoic acid, 1-methylethyl ester	$C_{15}H_{30}O_2$	1107.68
175	Undecane, 5-ethyl-	$C_{13}H_{28}$	1114.82
176	Benzene, (1-pentylhexyl)-	$C_{17}H_{28}$	1115.57
177	9H-Xanthene	$C_{13}H_{10}O$	1116.32
178	Benzene, (1-butylheptyl)-	$C_{17}H_{28}$	1118.18
179	2,6-Bis(1,1-dimethylethyl)-4-(1-oxopropyl)phenol	$C_{17}H_{26}O_2$	1121.34
180	Dodecane, 3-methyl-	$C_{13}H_{28}$	1121.99
181	Ethylene glycol - Adipate - Diethylene glycol	$C_{12}H_{22}O_7$	1125.71
182	1,4-Methanobenzocyclodecene, 1,2,3,4,4a,5,8,9,12,12a-decahydro-	$C_{15}H_{22}$	1127.85
183	Hexadecane, 4-methyl-	$C_{17}H_{36}$	1131.36
184	Octane, 1,1'-oxybis-	$C_{16}H_{34}O$	1136.1
185	Cyclooctasiloxane, hexadecamethyl-	$C_{16}H_{48}O_8Si_8$	1138.79

186	Hexadecane, 3-methyl-	$C_{17}H_{36}$	1141.27
187	Benzene, (1-ethylnonyl)-	$C_{17}H_{28}$	1142.15
188	Amberonne (isomer 1)	$C_{16}H_{26}O$	1149.84
189	1,1'-Biphenyl, 2,2',5,5'-tetramethyl-	$C_{16}H_{18}$	1157.97
190	2,6-Diisopropylnaphthalene	$C_{16}H_{20}$	1158.57
191	Eicosane	$C_{20}H_{42}$	1162.53
192	Pentadecane, 2,6,10,14-tetramethyl-	$C_{19}H_{40}$	1167.1
193	Benzene, (1-methyldecyl)-	$C_{17}H_{28}$	1169.64
194	3-Isopropoxy-1,1,1,7,7,7-hexamethyl-3,5,5-tris(trimethylsiloxy)tetrasiloxane	$C_{18}H_{52}O_7Si_7$	1170.26
195	Sulfurous acid, di(2-ethylhexyl) ester	$C_{16}H_{34}O_3S$	1172.2
196	2,4-Dihydroxybenzoic acid, 3TMS derivative	$C_{16}H_{30}O_4Si_3$	1175.45
197	Benzoic acid, 2-ethylhexyl ester	$C_{15}H_{22}O_2$	1176.2
198	Tetrafluoromethane	CF_4	1177.69
199	4-(2-(4-Fluorophenyl)-1-hydroxyethenyl)benzene-1,3-diol, tris(tert-butyldimethylsilyl) ether	$C_{32}H_{53}FO_3Si_3$	1178.86
200	2,4,2',4'-Tetramethyl-biphenyl	$C_{16}H_{18}$	1179.21
201	1-Cyclohexene-3,5-dione, hexakis(trimethylsilyloxy)-	$C_{24}H_{54}O_8Si_6$	1183.07
202	1H-Indene, 2,3-dihydro-1,1,3-trimethyl-3-phenyl-	$C_{18}H_{20}$	1188.74
200	Benzene, (1-butyloctyl)-	$C_{18}H_{30}$	1191.33
201	1,3-di-iso-propylnaphthalene	$C_{16}H_{20}$	1192.9
202	10-Methylnonadecane	$C_{20}H_{42}$	1194.08
203	Decane, 3,7-dimethyl-	$C_{12}H_{26}$	1203.81
204	Heptadecane, 9-hexyl-	$C_{23}H_{48}$	1208.18
205	Cyclohexane, undecyl-	$C_{17}H_{34}$	1210.25
206	Benzene, 1,1'-(1,2-cyclobutanediyl)bis-, trans-	$C_{16}H_{16}$	1211.71
207	Heptadecane, 3-methyl-	$C_{18}H_{38}$	1214.12
208	Benzene, (1-ethyldecyl)-	$C_{18}H_{30}$	1216.34
209	Octanoic acid, octyl ester	$C_{16}H_{32}O_2$	1219.73
210	Naphtho[2,1-b]furan, dodecahydro-3a,6,6,9a-tetramethyl-	$C_{16}H_{28}O$	1224.23
211	Naphthalene, 1,2,3,4-tetrahydro-1-phenyl-	$C_{16}H_{16}$	1227.49
212	2-Naphthalenol, 1,2-dihydro-, acetate	$C_{12}H_{12}O_2$	1230.17
213	Octadecane	$C_{18}H_{38}$	1234.15
214	Phenanthrene	$C_{14}H_{10}$	1236.64
215	1-Octanol, 2-butyl-	$C_{12}H_{26}O$	1237.58
216	(6-Chloro-2-methylhexan-2-yl)benzene	$C_{13}H_{19}Cl$	1239.85
217	Benzene, (1-methylundecyl)-	$C_{18}H_{30}$	1243.46
218	Salicylic acid, 1-methylpropyl ester	$C_{11}H_{14}O_3$	1246.15
219	13-Methyltetradecanal	$C_{15}H_{30}O$	1247.04
220	Isopropyl myristate	$C_{17}H_{34}O_2$	1251.76
221	Cyclononasiloxane, octadecamethyl-	$C_{18}H_{54}O_9Si_9$	1253.61
222	Benzene, (1-pentyloctyl)-	$C_{19}H_{32}$	1257.4
223	Benzene, (1-butylnonyl)-	$C_{19}H_{32}$	1262.08
224	Heptane, 3-ethyl-5-methylene-	$C_{10}H_{20}$	1265.39
225	Undecane, 4,4-dimethyl-	$C_{13}H_{28}$	1269.64
226	Octadecane, 4-methyl-	$C_{19}H_{40}$	1273.97
227	Octadecane, 2-methyl-	$C_{19}H_{40}$	1277.55

228	Pentacos-1-ene	$C_{25}H_{50}$	1279.75
229	Phthalic acid, hex-3-yl isobutyl ester	$C_{18}H_{26}O_4$	1286.04
230	2-Amino-4-(1-ethylpropyl)-4H-benzo[h]chromene-3-carbonitrile	$C_{19}H_{20}N_{2O}$	1289.32
231	1,3,4-Oxadiazole-2(3H)-thione, 3-(4-morpholylmethyl)-5-phenoxymethyl-	$C_{14}H_{17}N_3O_3S$	1294.9
232	2-Methyltetracosane	$C_{25}H_{52}$	1297.5
233	Nonadecane	$C_{19}H_{40}$	1302.31
234	1-Pentadecanamine, N,N-dimethyl-	$C_{17}H_{37}N$	1306.23
235	Benzene, (1-methyldodecyl)-	$C_{19}H_{32}$	1313.72
234	Phthalic acid, 2-chloropropyl isobutyl ester	$C_{15}H_{19}ClO_4$	1317.24
235	Pentadecanoic acid, 14-methyl-, methyl ester	$C_{17}H_{34}O_2$	1319.79
236	1-[6,8-Dichloro-2-phenyl-4-quinolyl]hexahydro-3H-oxazolo[3,4-a]pyridine	$C_{22}H_{20}Cl_2N_2O$	1322.43
237	Dibutyl phthalate	$C_{16}H_{22}O_4$	1334.86
238	n-Hexadecanoic acid	$C_{16}H_{32}O_2$	1340.33
239	Cyclohexane, hexyl-	$C_{12}H_{24}$	1351.3
240	Furan-3-carboxylic acid, 5-(adamantan-1-yl)-2-methyl-, (2,6-dimethylphenyl)amide	$C_{24}H_{29}NO_2$	1359.94
241	4-cyano-3-fluorophenyl 4-(4-ethylcyclohexyl)benzoate	$C_{22}H_{22}FNO_2$	1365.78
242	4b,8-Dimethyl-2-isopropylphenanthrene, 4b,5,6,7,8,8a,9,10-octahydro-	$C_{19}H_{28}$	1370.9
243	Isopropyl palmitate	$C_{19}H_{38}O_2$	1382.93
244	4,4'-(Hexafluoroisopropylidene)diphenol	$C_{15}H_{10}F_6O_2$	1398.25
245	10,18-Bisnorabieta-8,11,13-triene	$C_{18}H_{26}$	1409.86
246	1,4-Benzenedicarboxylic acid, bis(2-methylpropyl) ester	$C_{16}H_{22}O_4$	1412.58
247	7-Isopropyl-1,1,4a-trimethyl-1,2,3,4,4a,9,10,10a-octahydrophenanthrene	$C_{20}H_{30}$	1420.12
248	Cyclodecane, methyl-	$C_{11}H_{22}$	1423.81
249	(1R,2S)-1-{3,4-Bis[(trimethylsilyl)oxy]phenyl}-N-(1-methylethyl)-1-[(trimethylsilyl)oxy]butan-2-amine	$C_{22}H_{45}NO_3Si_3$	1428.35
250	6-Octadecenoic acid, methyl ester, (Z)-	$C_{19}H_{36}O_2$	1431.92
251	Isothiazole	C_3H_3NS	1433.49
252	Fluoranthene	$C_{16}H_{10}$	1436.62
253	o-Anisic acid, tridec-2-ynyl ester	$C_{21}H_{30}O_3$	1441.28
254	1-Propene-1,2,3-tricarboxylic acid, tributyl ester	$C_{18}H_{30}O_6$	1467.4
255	2-Propenoic acid, 3-(4-methoxyphenyl)-, 2-ethylhexyl ester	$C_{18}H_{26}O_3$	1472.3
256	4-Chlorobutyric acid, pentadecyl ester	$C_{19}H_{37}ClO_2$	1494.45
257	Oxirane, hexadecyl-	$C_{18}H_{36}O$	1504.69
258	Benzene, 1,1'-sulfonylbis[4-chloro-	$C_{12}H_8Cl_2O_2S$	1520.65
259	Tributyl acetylcitrate	$C_{20}H_{34}O_8$	1526.73
260	Phthalic acid, butyl 2-pentyl ester	$C_{17}H_{24}O_4$	1528.83
261	1-Decanol, 2-ethyl-	$C_{12}H_{26}O$	1531.23
262	Tritriacontane, 2-methyl-	$C_{34}H_{70}$	1545.95
263	4,9-Decadien-2-amine, N-butyl-	$C_{14}H_{27}N$	1550
264	Benzoic acid, tridecyl ester	$C_{20}H_{32}O_2$	1553.84
265	Octanoic acid, heptadecyl ester	$C_{25}H_{50}O_2$	1588.23

266	Hexanedioic acid, bis(2-ethylhexyl) ester	$C_{22}H_{42}O_4$	1601.98
267	Benzoic acid, tetradecyl ester	$C_{21}H_{34}O_2$	1610.94
268	Hexanoic acid, 2-ethyl-, hexadecyl ester	$C_{24}H_{48}O_2$	1641.77
269	4-Hydroxybenzyl alcohol, 2TBDMS derivative	$C_{19}H_{36}O_2Si_2$	1647.39
270	9,10-Anthracenedione, 3-(1,2-dihydroxypropyl)-1,6,8-trihydroxy-, 5TMS	$C_{32}H_{54}O_7Si_5$	1652.42
271	Octan-2-yl palmitate	$C_{24}H_{48}O_2$	1656.61
272	Benzoic acid, pentadecyl ester	$C_{22}H_{36}O_2$	1665.72
273	Benzyldiethyl-(2,6-xylylcarbamoylmethyl)-ammonium benzoate	$C_{28}H_{34}N_2O_3$	1680.79
274	(E)-7-Benzylidene-1-azabicyclo[3.2.1]octan-5-yl methanesulfonate	$C_{15}H_{19}NO_3S$	1682.33
275	Phthalic acid, 2-ethylhexyl tetradecyl ester	$C_{30}H_{50}O_4$	1682.92
276	3-Methylheptacosane	$C_{28}H_{58}$	1704.01
277	Hexanoic acid, 2-ethyl-, anhydride	$C_{16}H_{30}O_3$	1717.43
278	Benzene, 1,4-bis(phenylthio)-	$C_{18}H_{14}S_2$	1723.03
279	2-Ethylhexyl stearate	$C_{26}H_{52}O_2$	1758.57
280	1,3-Benzenedicarboxylic acid, bis(2-ethylhexyl) ester	$C_{24}H_{38}O_4$	1785.54
281	Borane, diethyl(decyloxy)-	$C_{14}H_{31}BO$	1811.7
282	Squalene	$C_{30}H_{50}$	1835.94
283	Cholesta-4,6-dien-3-ol, (3*β*)-	$C_{27}H_{44}O$	1887.41

2. Characterization of SmE-loaded niosomes

2.1. Morphological characterization

2.1.1. Optic microscopy analysis

Figure 13 showed micrographs of prepared SmE-loaded niosomes under optical microscope at magnification ×400, the niosomes appeared as small vesicles in size with spherical shape and some aggregation were observed.

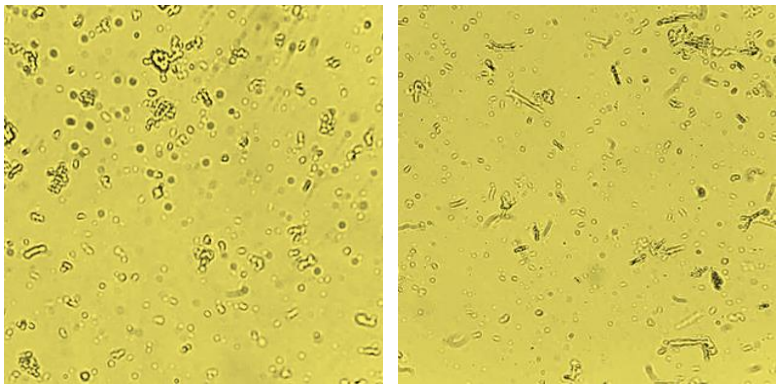

Figure 13: Optical micrographs of SmE-loaded niosomes at magnification ×400

2.1.2. Scanning electron microscopy analysis

The scanning electron microscopy analysis presented distribution of SmE-loaded niosomes that were observed to have like spherule structure with different sizes while more dispersed were averaging about 200 nm (Figure 14).

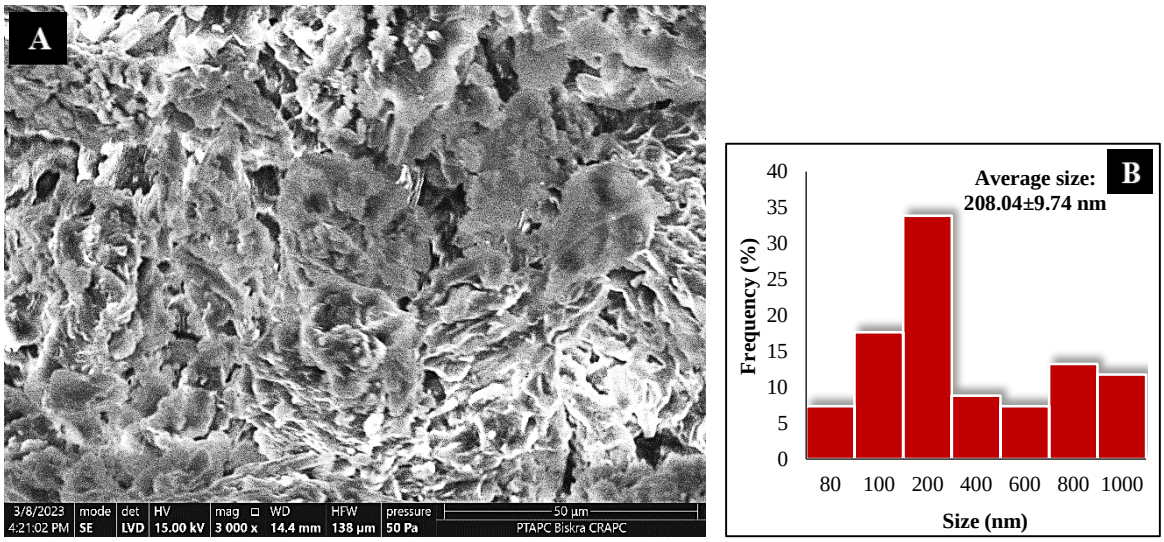

Figure 14: SEM micrograph of SmE-loaded niosomes (A) and their distribution frequency (B)

2.2. Encapsulation efficiency of SmE-loaded niosomes

Sonchus maritimus aqueous extract was loaded into niosomes without changing their morphology or structure, as shown in table 09, our prepared niosomes had a good encapsulation efficiency that could reach 61.4%.

Table 09: Total phenol contents (TPC) and encapsulation efficiency of niosomes

	TPC (mg)	**Percentage of TPC (%)**
***S.maritimus* extract**	3.0817±0.0241	100
Niosomes	1.8926±0.0374	61.41±1.21
Supernatant	1.189±0.0241	38.584± 0.831
Encapsulation Efficiency (%)	61.409 ± 0.924	

2.3. Physical stabilization of SmE-loaded niosomes

The results showed that our niosomal formulation of *Sonchus maritimus* presented a high physical stability over 60 days of sample storage at 4°C, no significant variation in encapsulation efficiency percentage shown in different storage periods including 1st, 7th, 30th and on the 60th

day, however, a significant reduction was observed to 54.71 % in encapsulation efficiency after 90 days as shown in figure 15, This confirmed that there was no leakage of *S. maritimus* extract from formulated niosomes within two months and that it was not affected by temperature.

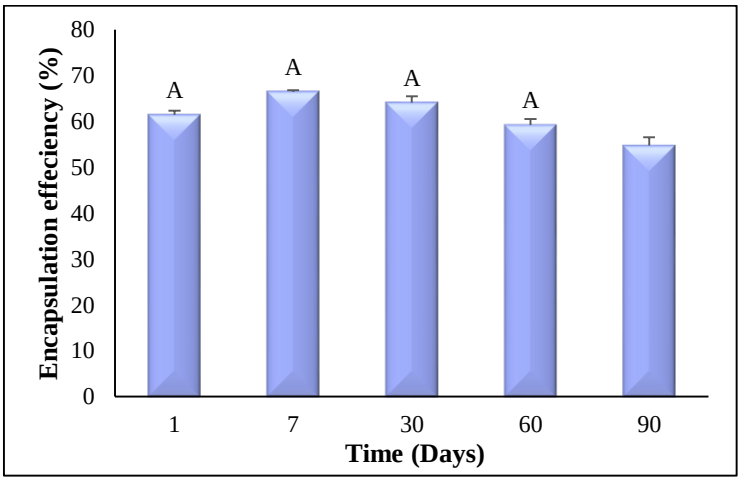

Figure 15: Physical stability of SmE-loaded niosomes at 4 °C

Mean EE % was studied as stability parameter. Mean not labeled with the letter A are significantly different from the control level mean

3. Characterization of selenium nanoparticles (SmE-SeNPs)

3.1. UV-visible spectroscopy

UV-visible spectrum revealed successful of green synthesis of SeNPs using leaves aqueous extract of *S. maritimus*, which was confirmed by the changes of reaction color from yellow to ruby red in function of time. Appearance of maximum absorption peak around λ=300 nm indicates the formulation of SmE-SeNPs in the samples in the different synthesis phases (Figure 16).

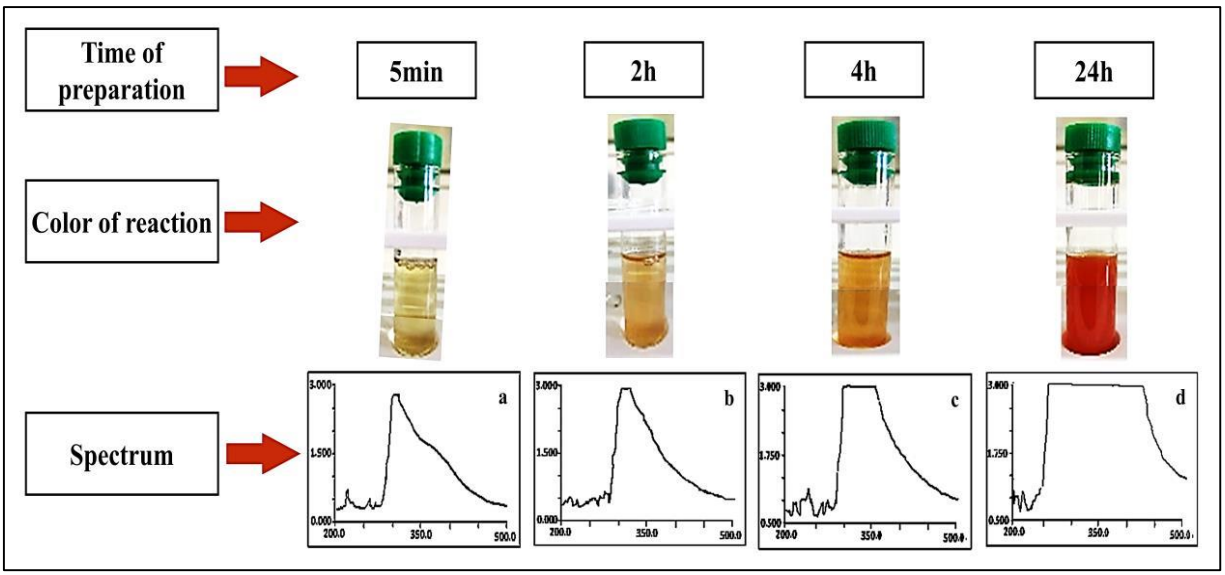

Figure 16: UV-visible spectrum and reaction color changes of green synthesized SmE-SeNPs

3.2. FT-IR spectroscopy

The FTIR spectrums of *S. maritimus* aqueous extract and SmE-SeNPs shown appearance of identified peaks of different functional groups in the both samples, including; a large band appeared at around 3400 cm^{-1}. Other peaks were about 1600 cm^{-1}. In addition to intense peaks at about 1400 cm^{-1} and 1200 cm^{-1}. Furthermore, strong intensity bending vibrations were related to the peaks seen around 824 cm^{-1}. However, a distinguished peak at 588 cm^{-1} appeared only in SmE-SeNPs spectrum, indicates the interaction Se-O, as presented in figure 17.

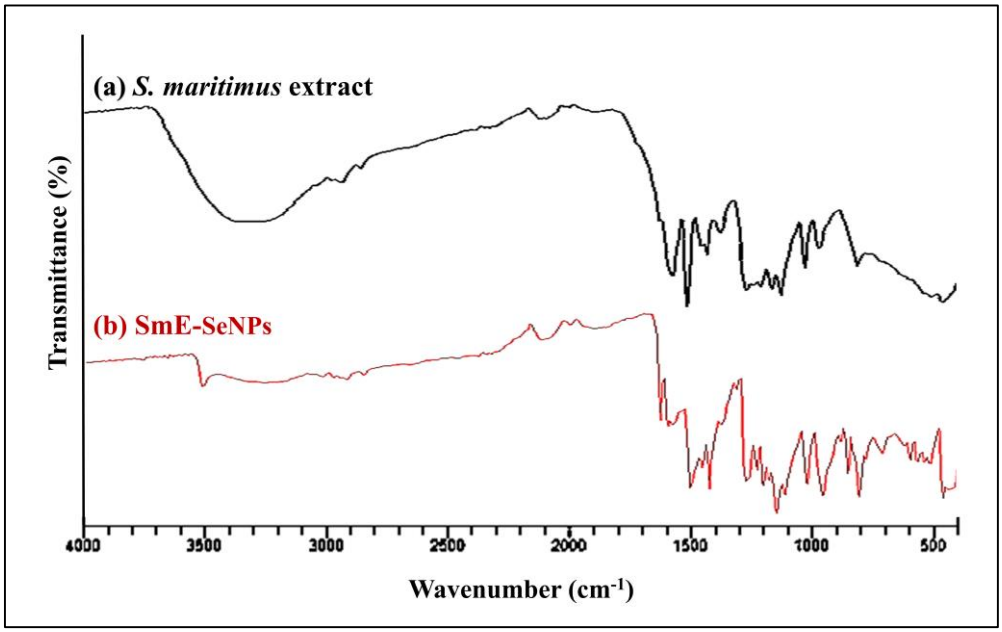

Figure 17: FT-IR spectrum of functional groups exist in *S. maritimus* and SmE-SeNPs

3.3. SEM with EDX analysis

Figure 18A showed the surface morphology and distribution of SmE-SeNPs under scanning electron microscope, which appeared to have a spherule-like shape. Figure 18B presented EDX spectra of SmE-SeNPs which demonstrated that Se and O were major elemental compositions in the sample, in addition to other minor elements, these indicate the purity of analyzed sample.

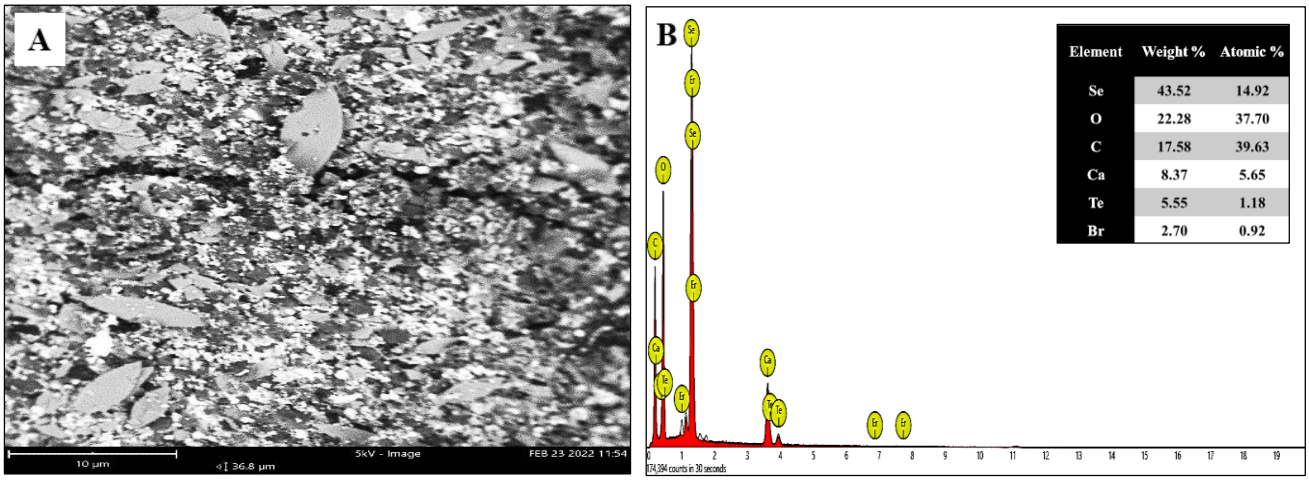

Figure 18: Chemical composition and morphology of SmE-SeNPs based on SEM micrograph and EDX spectra

3.4. TEM analysis

The shape and morphology of SmE-SeNPs was assessed under transmission electron microscope as presented in figure 19A, uniform spherical configuration and mono dispersing of the particles were clearly apparent in the image. Additionally, the results showed that SmE-SeNPs possess a very small size with average of 7.15±0.47 nm as presented in figure 19B.

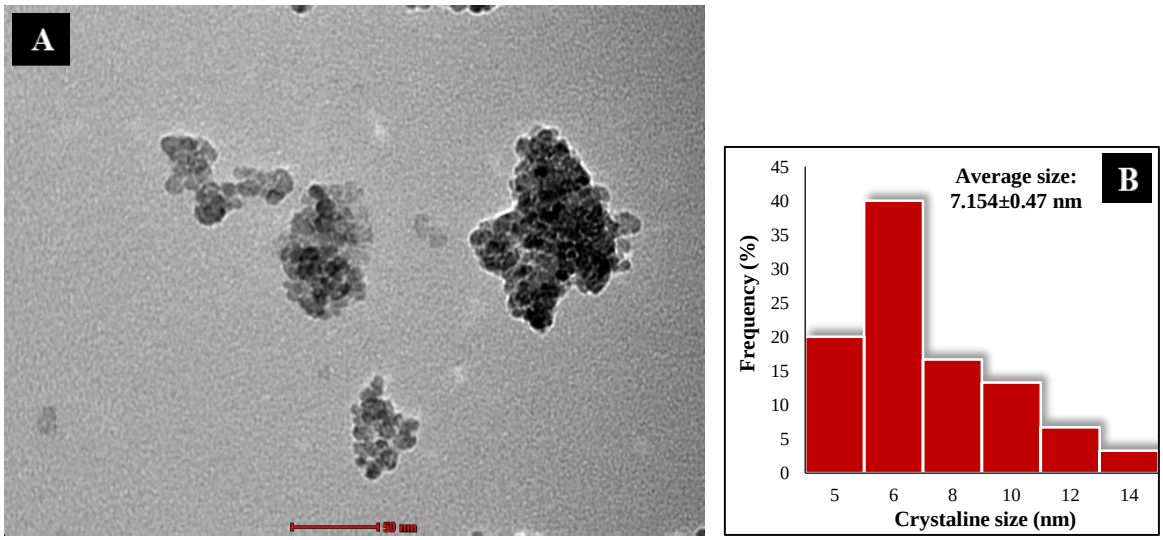

Figure 19: Shape and size of SmE-SeNPs based on TEM micrograph (A) and their distribution frequency (B)

4. Biological activities

4.1. Antioxidant activity

4.1.1. DPPH radical scavenging ability

Results in figure 20 demonstrated that biosynthesized selenium nanoparticles and *S. maritimus* aqueous extract had a moderate free radical scavenging activity compared to ascorbic acid (standard) with IC_{50} values 1511.31 ± 87.3 µg/mL, 1131.01 ± 65.3 µg/mL and 43.59 ± 10.1 µg/mL for SmE-SeNPs, *S. maritimus* extract and ascorbic acid respectively.

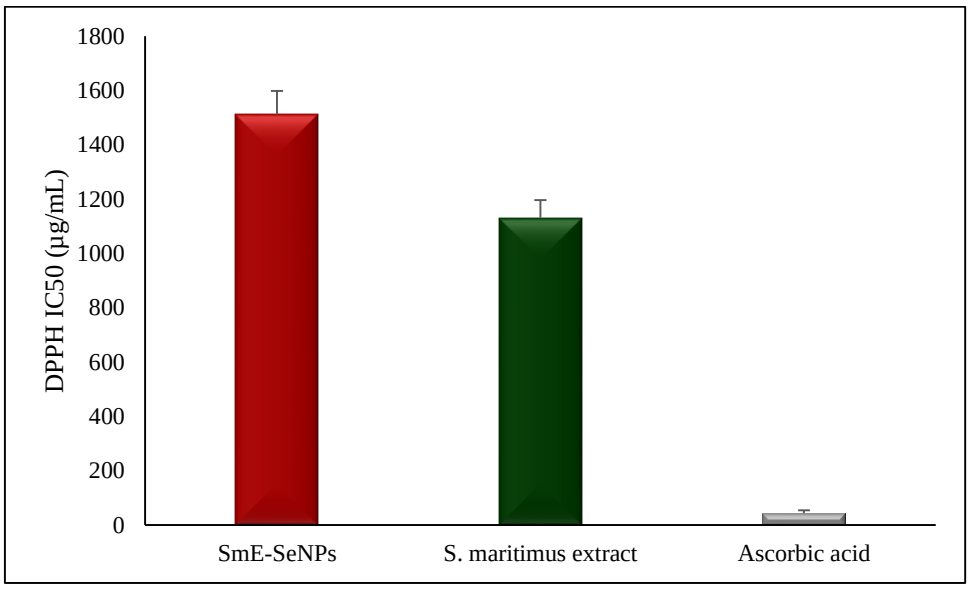

Figure 20: DPPH scavenging ability of *S. maritimus* aqueous extract and SmE-SeNPs compared to ascorbic acid

4.1.2. Ferric reducing ability "FRAP"

Figure 21 showed that SmE-SeNPs and *S. maritimus* aqueous extract exhibited FRAP activity less than standard (ascorbic acid), which expressed by IC_{50} values, 823.91 ± 47.7 µg/mL for SmE-SeNPs, 440.041 ± 25.4 µg/mL for *S. maritimus* aqueous extract and 39.28 ± 9.07 µg/mL for ascorbic acid.

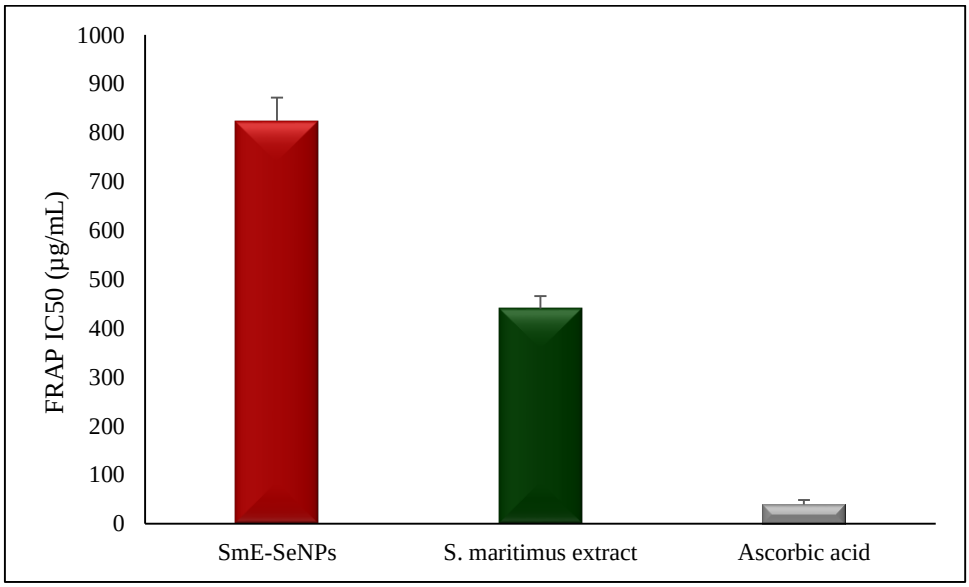

Figure 21: Ferric reducing ability of *S. maritimus* aqueous extract and SmE-SeNPs compared to ascorbic acid

4.2. Anti-inflammatory activity

4.2.1. Inhibition of protein denaturation ability

Obtained results in figure 22 showed that S. maritimus aqueous extract exhibited an inhibition of albumin denaturation better than SmE-SeNPs. In comparison with standard, the both samples demonstrated activities less than diclofenac with IC_{50} values 334.37 ± 29 µg/mL, 163.40 ± 14.1 µg/mL and 59.11 ± 5.12 µg/mL for *S. maritimus* extract, SmE-SeNPs and diclofenac respectively.

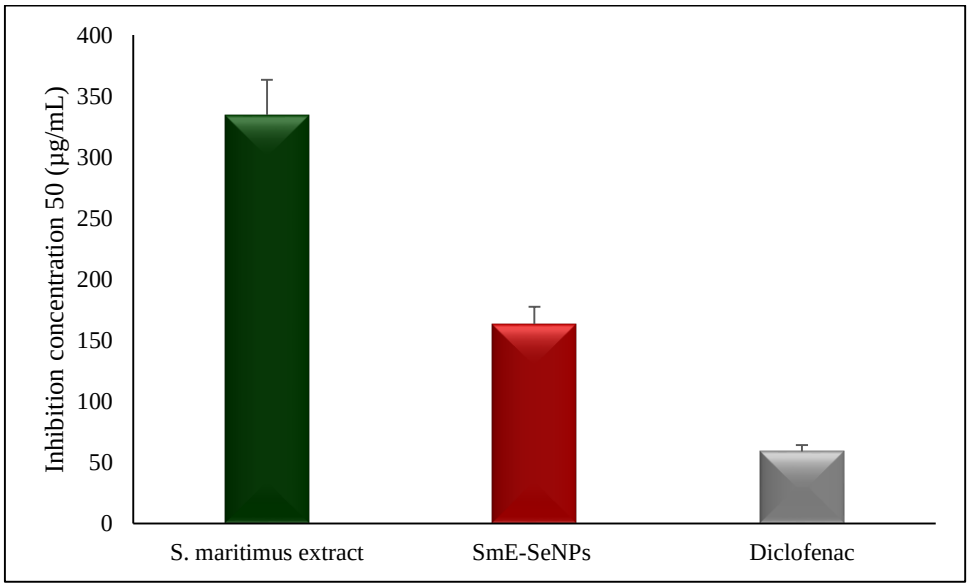

Figure 22: IC_{50} values of inhibition of albumin denaturation ability of *S. maritimus* aqueous extract and SmE-SeNPs compared to diclofenac

4.2.2. Anti-hemolysis ability

As shown in figure 23, the greater anti-hemolytic was showed in *S. maritimus* aqueous extract, then in SmE-SeNPs and better than a standard which expressed by IC_{50} values as following 53.54 ± 4.64 µg/mL for *S. maritimus* extract, 89.04 ± 4.11 µg/mL for SmE-SeNPs and 244.22 ± 14.1 µg/mL for standard.

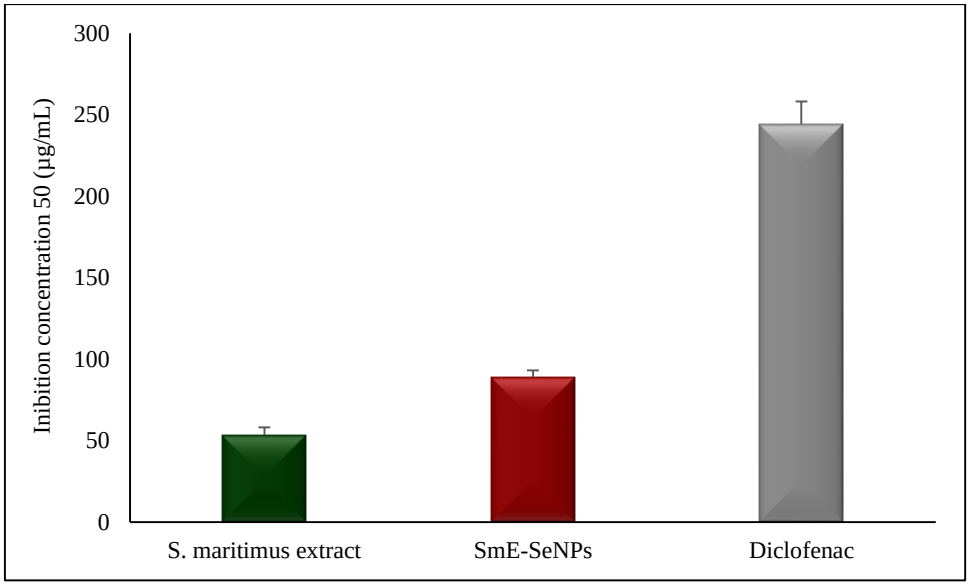

Figure 23: IC_{50} leveles of anti-hemolysis ability of *S. maritimus* aqueous extract and SmE-SeNPs compared to diclofenac

4.3. Hypoglycemic activity

4.3.1. α-amylase inhibition activity

In the present study, the in vitro α-amylase inhibition activity of *S. maritimus* aqueous extract and SmE-SeNPs was investigated using variable doses (0.01-1 mg/mL). SmE-SeNPs showed a good inhibition of α-amylase (carbohydrate-hydrolyzing enzymes) activity in a dose-dependent manner. As shown in table 10, inhibition percentage ranged from 5.08 ± 0.46 % to 67.61 ± 6.08 %and from 1.37 ± 0.12 % to 14.11 ± 1.27 % for *S. maritimus* aqueous extract and SmE-SeNPs respectively from the lowest to the highest concentration (0.01-1 mg/mL). However, the inhibition percentage of acarbose standard was from 0.28 ± 0.03 % to 3.55 ± 0.32 % from lowest to highest concentration. As shown in figure 24, IC_{50} of the *S. maritimus* extract and SmE-SeNPs were (0.72 ± 0.07 and 3.72 ± 0.45 mg/mL) while that of the acarbose standard was (IC_{50} = 14.82 ± 1.78 mg/mL).

Table 10: α-amylase inhibition activity of *S.maritimus* aqueous extract, selenium nanoparticles and acarbose (standard) at different concentrations

Conc. (mg/mL)	Inhibition percentage (%)		
	S.maritimus	**SmE-SeNPs**	**Acarbose**
0.01	5.08±0.46	1.37±0.12	0.28±0.03
0.025	5.81±0.52	1.42±0.13	0.33±0.03
0.05	7.39±0.67	1.51±0.14	0.41±0.04
0.075	9.19±0.83	1.60±0.14	0.50±0.04
0.1	10.77±0.97	1.69±0.15	0.58±0.05
0.25	19.12±1.72	2.23±0.20	1.07±0.10
0.5	36.03±3.24	7.24±0.65	1.90±0.17
0.75	51.82±4.66	10.49±0.94	2.72±0.25
1	67.61±6.08	14.11±1.27	3.55±0.32

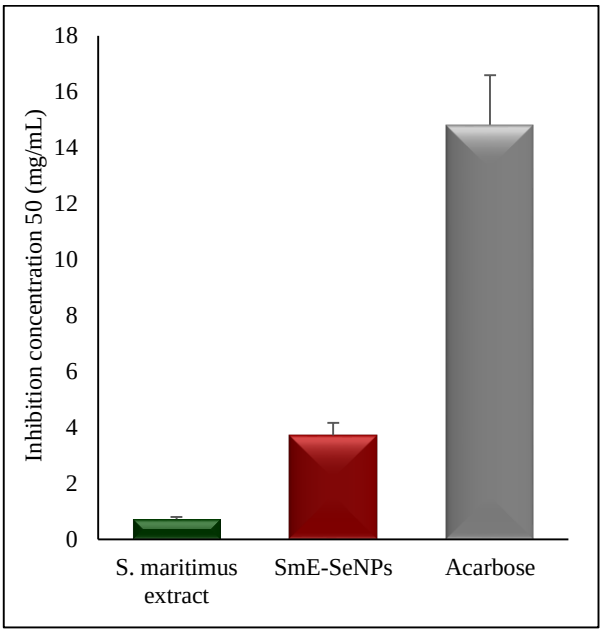

Figure 24: *In vitro* α-amylase inhibition activity of *S. maritimus* aqueous extract and SmE-SeNPs compared to acarbose standard

4.3.2. Glucose uptake by yeast cells ability

Figure 25 showed a linear uptake of glucose was observed for *S. maritimus* aqueous extract, SmE-SeNPs and metformin, where *S. maritimus* extract and SeNPs exhibited higher uptake activity compared to metformin standard. The glucose uptake by the yeast cells was found to be inversely proportional to glucose concentration.

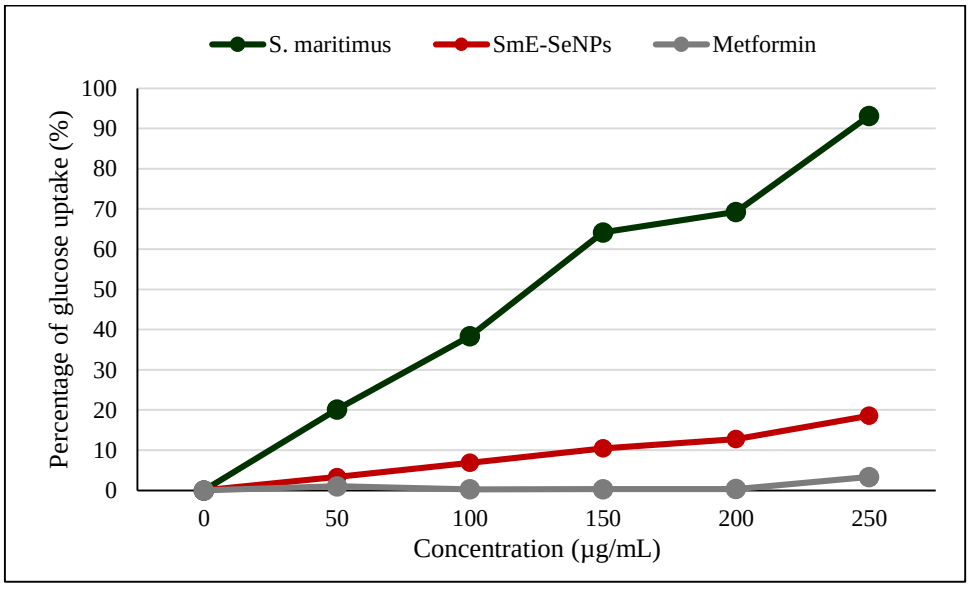

Figure 25: Effect of *S. maritimus* aqueous extract and SmE-SeNPs compared to metformin standard on glucose uptake by yeast cells

4.3.3. Glucose adsorption capacity

A directly proportional relationship between increase in bound glucose concentration and glucose concentration was established for *S. maritimus* aqueous extract, SmE-SeNPs and metformin, as presented in figure 26. Greater adsorption capacity was observed by SmE-SeNPs 3.89 ± 0.31 mM as compared to *S. maritimus* extract 0.63 ± 0.05 mM and metformin 0.11 ± 0.02 mM which was considered a positive control.

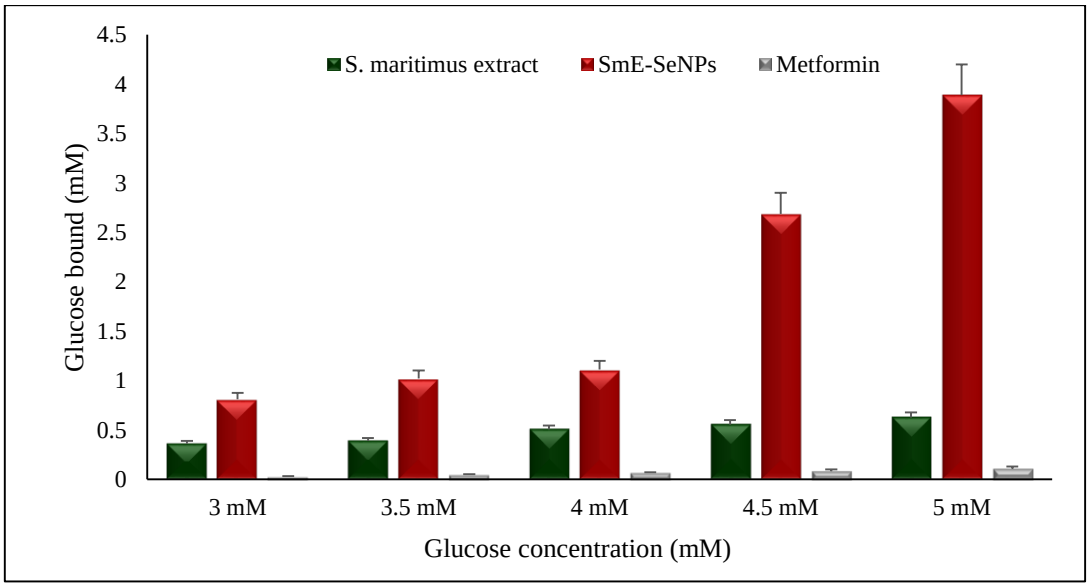

Figure 26: Glucose-binding capacity of of *S. maritimus* aqueous extract and SmE-SeNPs compared to metformin at different glucose concentrations

4.4. Antibacterial activity

The diameter of inhibition zone of SmE-SeNPs at concentration of 30 mg/mL against Gram-positive bacteria was observed reach up to 24.8 ± 1.72 mm for *E. coli* and 11 ± 1.91 mm against *S. aureus*; but, SmE-SeNPs didn't show any activity against *P. aeruginosa*, as presented in figure 27. However, *S. maritimus* demonstrated a low activity even at the highest concentration, where, 6.3 ± 0.73 mm, 6.2 ± 0.36 mm and 6.5 ± 0.75 mm against *E. coli*, *P. aeruginosa* and *S. aureus* respectively, as presented in figure 28. Furthermore, SmE-SeNPs exhibited a considerable antibacterial activity while *S. maritimus* aqueous extract did not provide an important activity against Gram-negative and Gram-positive bacteria when compered the inhibition zone of antibiotics as shown in table 11.

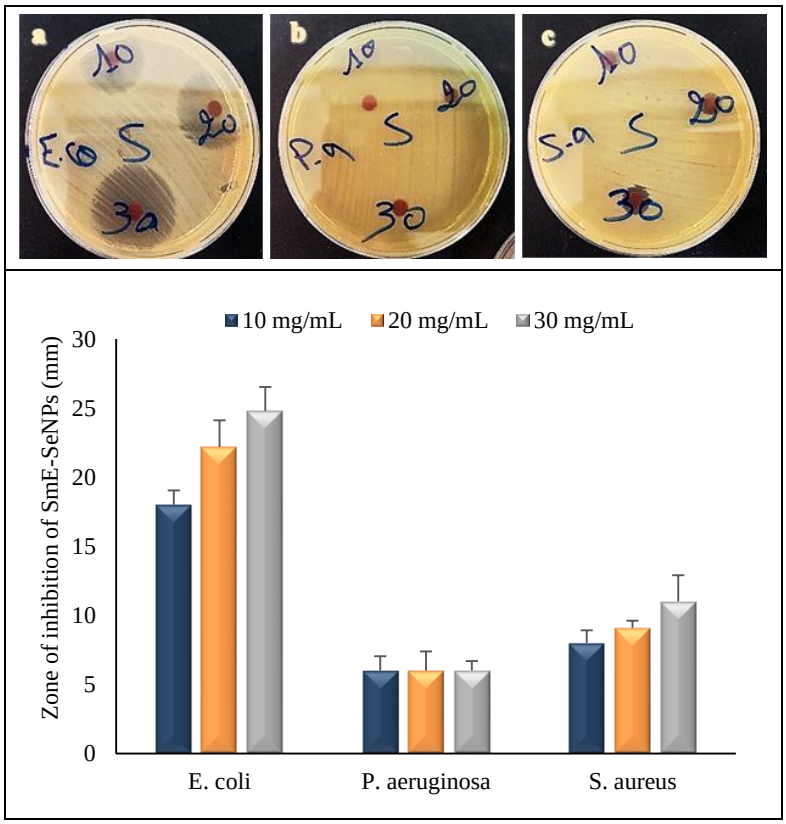

Figure 27: Antibacterial activity of SmE-SeNPs against *Escherichia coli* (a), *Pseudomonas aeruginosa* (b) and *Staphylococcus aureus* (c)

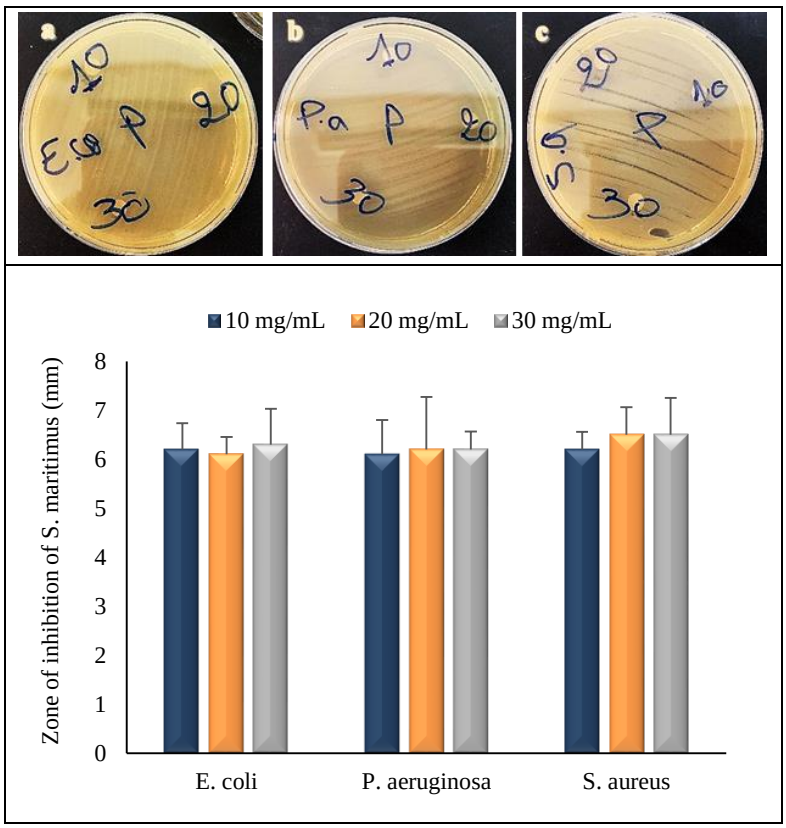

Figure 28: Antibacterial activity of *S. maritimus* aqueous extract against *Escherichia coli* (a), *Pseudomonas aeruginosa* (b) and *Staphylococcus aureus* (c)

Table 11: Diameter of inhibition zone of antibiotics against *E. coli*, *P. aeruginosa* and *S. aureus*

Antibiotics	*Escherichia coli* ATCC 25922	*Pseudomonas aeruginosa* ATCC 27853	*Staphylococcus aureus* ATCC 25923
Gentamicin	24 ± 0.96 mm	24 ± 1.2 mm	24 ± 0.72 mm
Amoxicillin	6 mm	6 mm	8 ± 0.33 mm
Ciprofloxacine	23 ± 0.92 mm	30 ± 0.9 mm	30 ± 1.2 mm
Cotrimosazole	23 ± 0.92 mm	6 mm	21 ± 0.84 mm
Ciftazidine	25 ± 0.75 mm	23 ± 1.15 mm	11 ± 0.44 mm

4.5. Anticancer activity

SmE-SeNPs' anticancer and cytotoxic properties were demonstrated via a dose-dependent effect on MCF-7 breast cancer cells. The results showed that SmE-SeNPs had a strong toxic effect on MCF-7 cells with IC_{50} (302.13±0.13 µg/mL) (Figure 29-A), as evidenced by microscopic observations that showed a decrease in cell amount and shrinkage along with a loss of cell-to-cell contact compared to untreated cells (Figure 29-B_1). The ability of the nanoparticles to slow down or stop the proliferation of cancer cells was used to identify the anticancer activity, which has been proven by the macroscopic crystal violet deterioration, as illustrated in Figure 30.

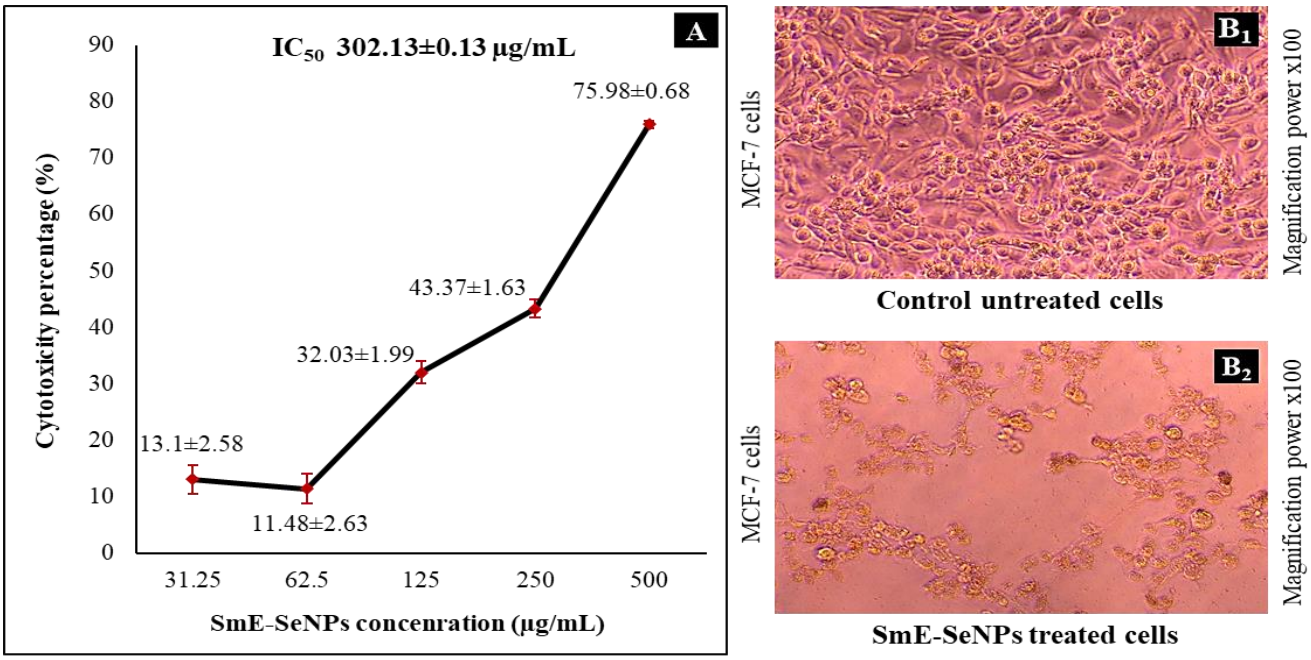

Figure 29: Determination of cytotoxic percentage (A) and microscopic analysis of antiproliferative property of SmE-SeNPs (B_1) against the MCF-7 breast cancer cell line (B_2)

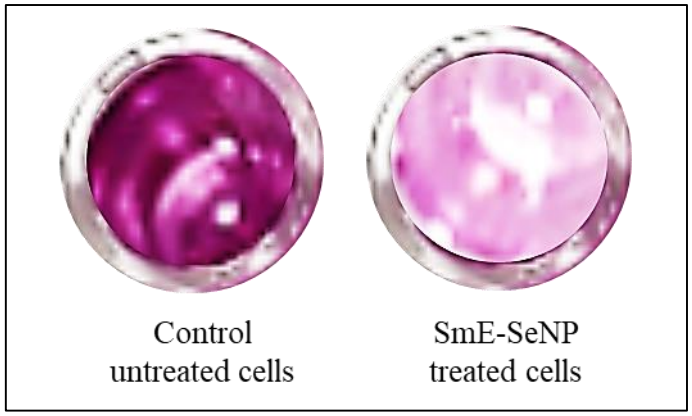

Figure 30: Macroscopic visualization of SmE-SeNPs' suppression of the MCF-7 breast cancer cell line's capacity to form colonies through the use of crystal violet staining

II. *In vivo* assays

1. Acute toxicity study

The results in table 12 showed that the physiological parameters including the case of eyes, sleep, movement and diarrhea were normal and didn't affect in the rats which were treated with different doses of *S. maritimus* aqueous extract (250 and 500 mg/kg b.w) and SmE-SeNPs (2.5 and 5 mg/kg b.w) compared to control animals which were injected with normal saline solution (0.9% NaCl). Additionally, no side effects or unusual symptoms were appeared, and no mortality cases were reported before 14 days.

Table 12: Intraperitoneally acute toxicity test of *S. maritimus* aqueous extract and SmE-SeNPs on physiological parameters of albino Wistar rats

Time	Test		Dead rats	Eyes	Sleep	Movement	Diarrhea
0 hour	*S. maritimus* extract	Control	0	N	N	N	N
		250 mg/kg b.w	0	N	N	N	N
		500 mg/kg b.w	0	N	N	N	N
	SmE-SeNPs	Control	0	N	N	N	N
		2.5 mg/kg b.w	0	N	N	N	N
		5 mg/kg b.w	0	N	N	N	N
3 hours	*S. maritimus* extract	Control	0	N	N	N	N
		250 mg/kg b.w	0	N	N	N	N
		500 mg/kg b.w	0	N	N	N	N
	SmE-SeNPs	Control	0	N	N	N	N
		2.5 mg/kg b.w	0	N	N	N	N
		5 mg/kg b.w	0	N	N	N	N
24 hours	*S. maritimus* extract	Control	0	N	N	N	N
		250 mg/kg b.w	0	N	N	N	N
		500 mg/kg b.w	0	N	N	N	N
	SmE-SeNPs	Control	0	N	N	N	N
		2.5 mg/kg b.w	0	N	N	N	N
		5 mg/kg b.w	0	N	N	N	N
7 days	*S. maritimus* extract	Control	0	N	N	N	N
		250 mg/kg b.w	0	N	N	N	N
		500 mg/kg b.w	0	N	N	N	N
	SmE-SeNPs	Control	0	N	N	N	N
		2.5 mg/kg b.w	0	N	N	N	N
		5 mg/kg b.w	0	N	N	N	N
14 Days	*S. maritimus* extract	Control	0	N	N	N	N
		250 mg/kg b.w	0	N	N	N	N
		500 mg/kg b.w	0	N	N	N	N
	SmE-SeNPs	Control	0	N	N	N	N
		2.5 mg/kg b.w	0	N	N	N	N
		5 mg/kg b.w	0	N	N	N	N

N: Normal

2. Growth parameters

The initial body weight of all groups was statistically similar. The results of final body weight, food intake, and water intake showed a very highly significant decrease ($P < 0.001$) in the all groups compared to the control; however, a significant increase ($P < 0.05$) in SmE-N, SeNPs, SeNPs-SmE-N and Metformin groups compared to the HFD, with exception SeNPs group for food intake and SmE-N group for water intake. The relative liver, heart, kidneys and testicles weight results demonstrate a very highly significant increase ($P < 0.001$) in HFG group

compared to the control; while there was a highly significant decrease (P<0.01) in SmE-N, SeNPs, SeNPs-SmE-N and Met groups compared to HFD group (Table 13).

Table 13: Growth parameters of control, HFD and treated groups

Parameters	Control (n=6)	HFD (n=6)	SmE-N (n=6)	SeNPs (n=6)	SeNPs-SmE-N (n=6)	Met (n=6)
Initial body weight (g)	179.17±4.72	173.33±6.38	171.67±7.24	171.17±7.08	171.2±3.19	172.00±7.18
Final Body Weight (g)	217.50±4.91	127.77±5.41***	153.5±3.67^{***c}	165.5±7.72^{***c}	155.25±1.44^{***c}	168.75±3.64^{***c}
Food intake (g/rat/day)	9.50±0.10	5.16±0.03***	6.16±0.032^{***c}	5.16±0.03***	5.33±0.07^{***a}	5.50±0.10^{***b}
Water intake (mL/rat/day)	20.82±0.004	8.25±0.21***	8.37±0.30***	9.53±0.50^{***a}	10.73±0.51^{***c}	9.31±0.38^{***a}
Relative liver Weight (g/100g b.w)	2.18±0.02	3.20±0.13***	2.64±0.03^{***c}	2.39±0.08^{*c}	2.56±0.10^{**c}	2.89±0.038^{***c}
Relative heart Weight (g/100g b.w)	0.25±0.005	0.33±0.005***	0.27±0.004^{***c}	0.25±0.007^{c}	0.26±0.01^{c}	0.27±0.006^{**c}
Relative kidneys Weight (g/100g b.w)	0.43±0.006	0.60±0.02***	0.50±0.007^{***c}	0.48±0.004^{***c}	0.45±0.005^{***c}	0.51±0.01^{***c}
Relative testicles Weight (g/100g b.w)	1.02±0.05	1.27±0.06***	0.89±0.05^{**c}	0.98±0.09^{b}	0.81±0.03^{***c}	1.11±0.04^{b}

Values are provided as (mean ± SEM): * *P*<0.05, ***P*<0.01, ****P*<0.001: comparison with control group; a *P*<0.05, b *P*<0.01, c *P*<0.001: comparison with HFD group.

3. Liver glycogen level

The results showed that hepatic glycogen levels were significantly decreased in HFD group (p<0.001) and treated groups (p<0.05), including, SeNPs, SeNPs-SmE-N and metformin groups, in comparison with control group. However, our treatment systems increased with very high significant (P<0.001) the liver glycogen levels of SmE-N, SeNPs-SmE-N and metformin groups and significantly increased in SeNPs groups (P<0.05) when compared to HFD group, as presented in figure 31.

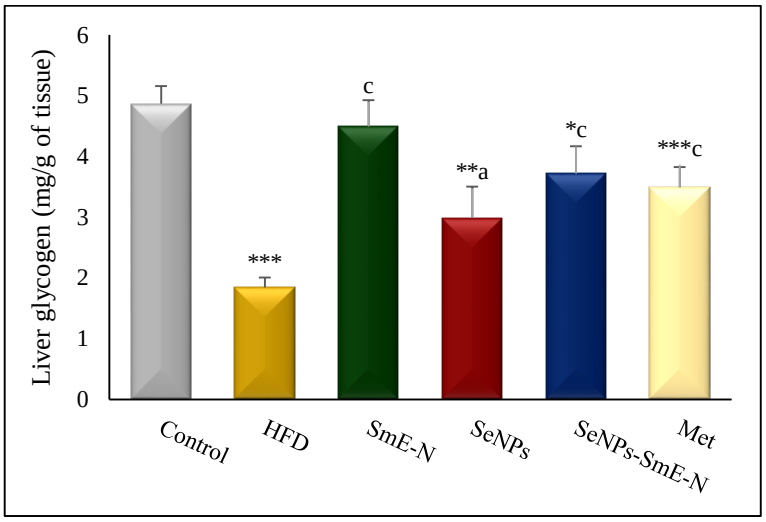

Figure 31: Liver glycogen levels in control, HFD and treated groups

Values are provided as (mean ± SEM): * $P<0.05$, ** $P<0.01$, *** $P<0.001$: comparison with control group; a $P<0.05$, b $P<0.01$, c $P<0.001$: comparison with HFD group.

4. Biochemical parameters

The obtained results presented in figure 32 showed a significant variation in biochemical results, where there were a significant increase ($P<0.05$) in blood glucose, glycated hemoglobin, urea, uric acid and creatinine levels, and transaminase enzymes activities (AST and ALT activities), while a significant decrease in testosterone level ($P<0.001$) of HFD group as compared to the control. Treatment by SmE-N, SeNPs, SeNPs-SmE-N and metformin exhibited a significant changes ($P<0.05$) in almost all of the mentioned parameters compared to HFD group and improved the biochemical disorders which induced by high fructose deit.

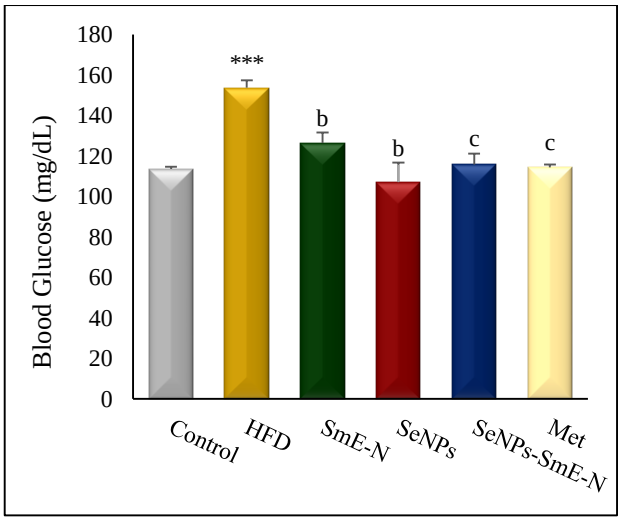

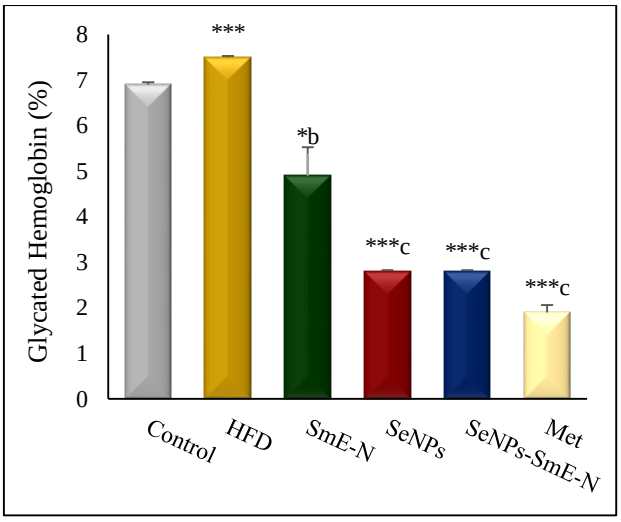

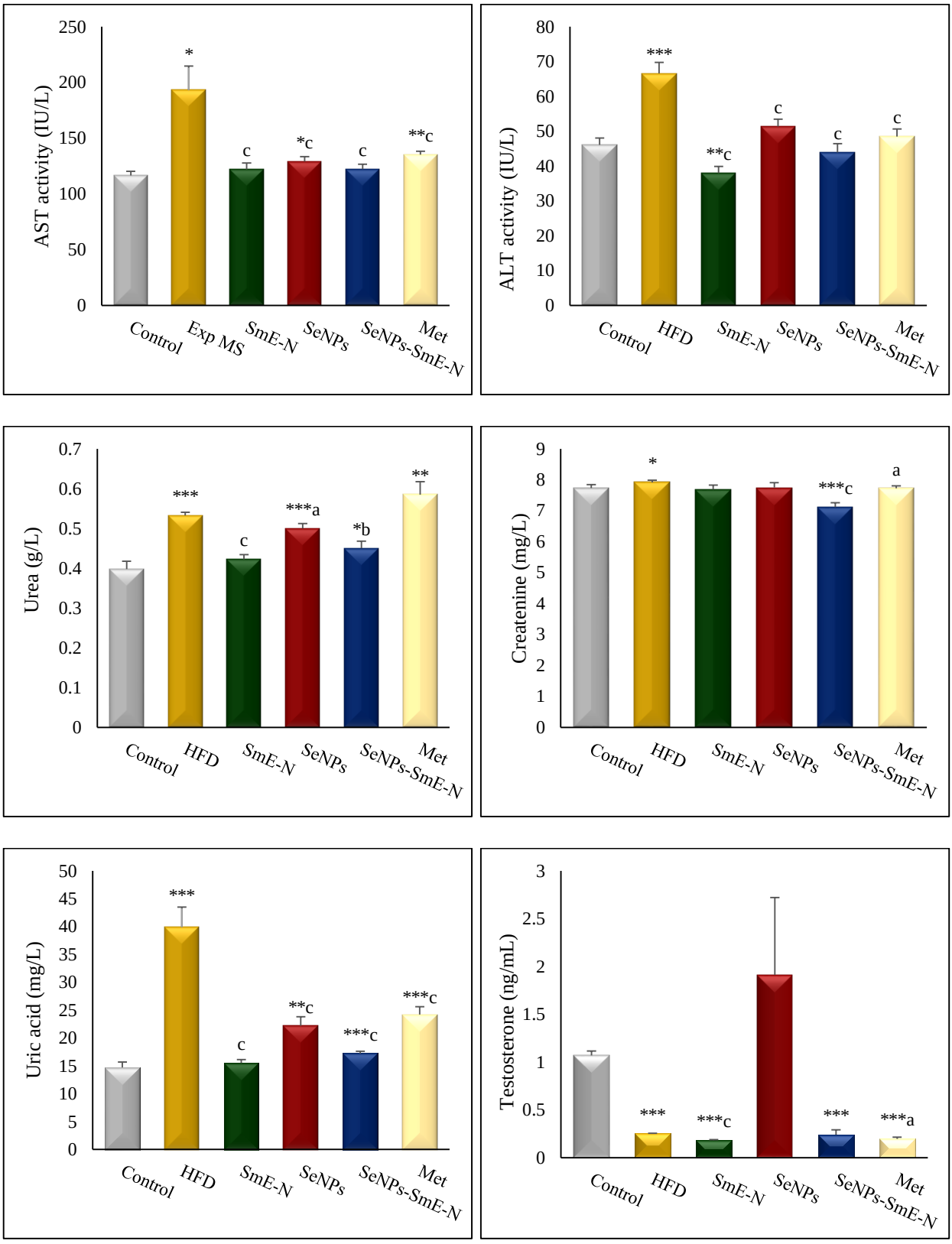

Figure 32: Biochemical markers in control, HFD and treated groups

Values are provided as (mean ± SEM): * P<0.05, ** P<0.01, *** P<0.001: comparison with control group; a P<0.05, b P<0.01, c P<0.001: comparison with HFD group.

5. Lipid profile

Our results of lipid profile (Figure 33) indicated that there were significant elevations in triglyceride, total cholesterol, LDL-C and VLDL-C levels in blood plasma of HFD ($P<0.001$) and treated ($P<0.01$) rats, with except SeNPs and Met rats for LDL-C level, when compared to the control rats. In comparison with HFD group, the results revealed that the using of various treatments induced a significantly decrease ($P<0.001$) in LDL-C level and significantly increase ($P<0.01$) in HDL-C level, in addition, SeNPs-SmE-N and Met were significantly reduced the total cholesterol level, while, there were some minor changes in triglyceride and VLDL-C and total cholesterol levels in SmE-N and SeNPs- SmE-N groups.

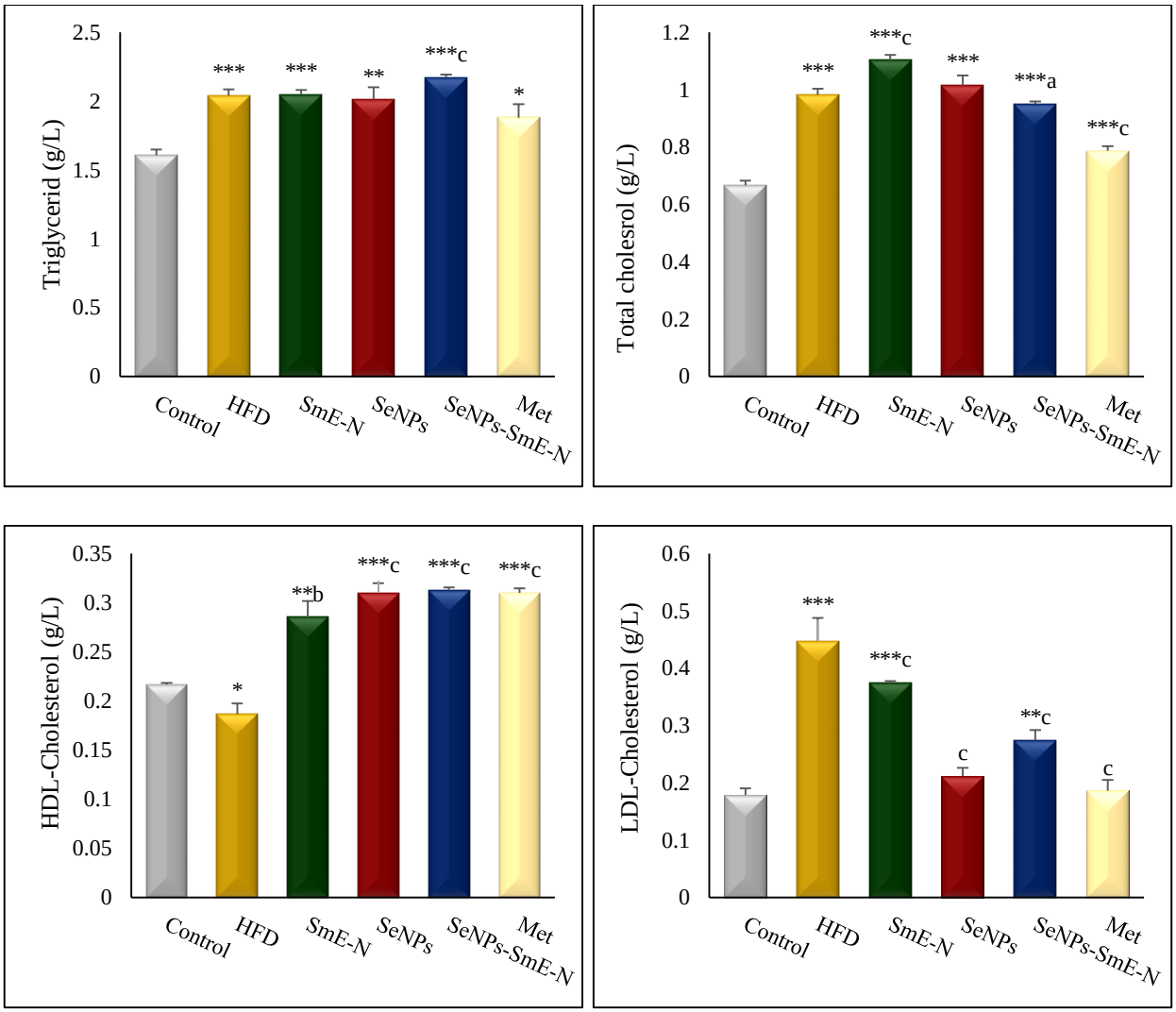

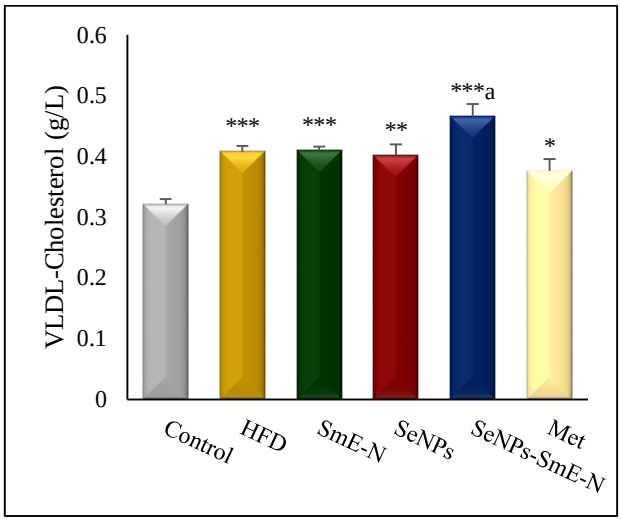

Figure 33: Lipid profile levels in control, HFD and treated groups

Values are provided as (mean ± SEM): * *P*<0.05, ***P*<0.01, ****P*<0.001: comparison with control group; a *P*<0.05, b *P*<0.01, c *P*<0.001: comparison with HFD group

6. Acetylcholine esterase activity

The acetylcholine esterase activity was significantly declined (P<0.001) in HFD, SmE-N and Met groups while significantly increased (P<0.01) in SeNPs-SmE-N group as compared to the control. Comparison with HFD groups demonstrated that there was a significant rising in the all treated groups (P<0.01) as shown in figure 34.

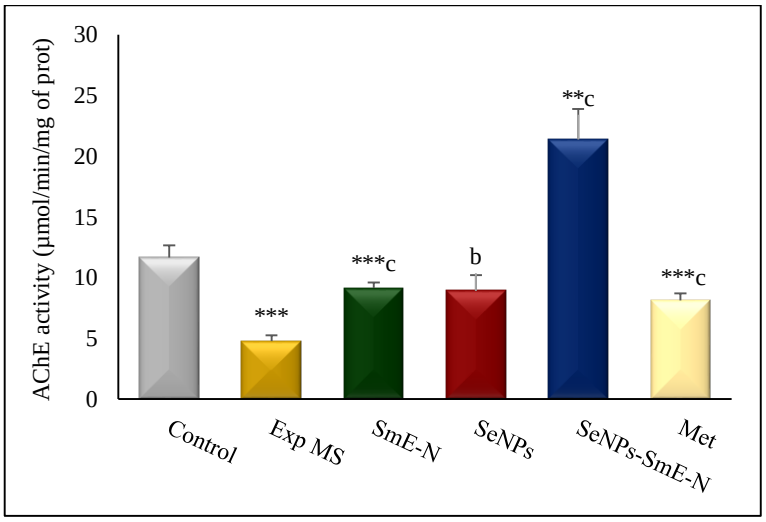

Figure 34: Acetylcholine esterase activity in control, HFD and treated groups

Values are provided as (mean ± SEM): * *P*<0.05, ***P*<0.01, ****P*<0.001: comparison with control group; a *P*<0.05, b *P*<0.01, c *P*<0.001: comparison with HFD group.

7. Clinical grading scores of rat's behaviors

The clinical score of rat's behaviors results illustrated in figure 35, which revealed that there was a significant increase in clinical score (P<0.001) of HFD group as compared to the control group. However, on comparison to HFD rats, it was observed a significantly decrease (P<0.05) of clinical score of rat's behaviors in the all treated groups by SmE-N, SeNPs, SeNPs-SmE-N and metformin.

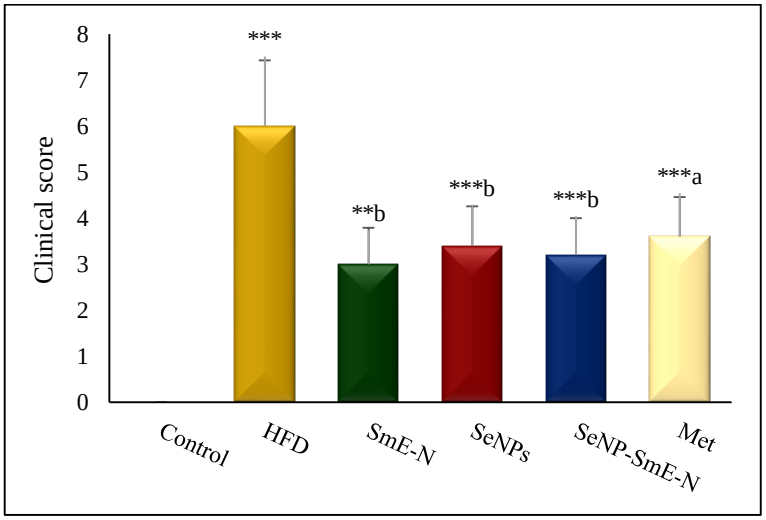

Figure 35: Clinical score of rat's behaviors in control, HFD and treated groups

Values are provided as (mean ± SEM): * *P*<0.05, ***P*<0.01, ****P*<0.001: comparison with control group; a *P*<0.05, b *P*<0.01, c *P*<0.001: comparison with HFD group.

8. Protein level

As shown in figure 36; the results demonstrated a significant increase in protein level of liver, brain, heart, kidneys and testicles in HFD group (P<0.01) and most of treated groups (P<0.05 .The treatment using SmE-N, SeNPs, SeNPs -SmE-N and metformin provided a high significant decrease (P<0.001) in protein levels of brain, heart, kidneys, testicles and liver, excluding liver protein level of SeNPs-SmE-N group which significantly increased (P<0.001), as compared to HFD group.

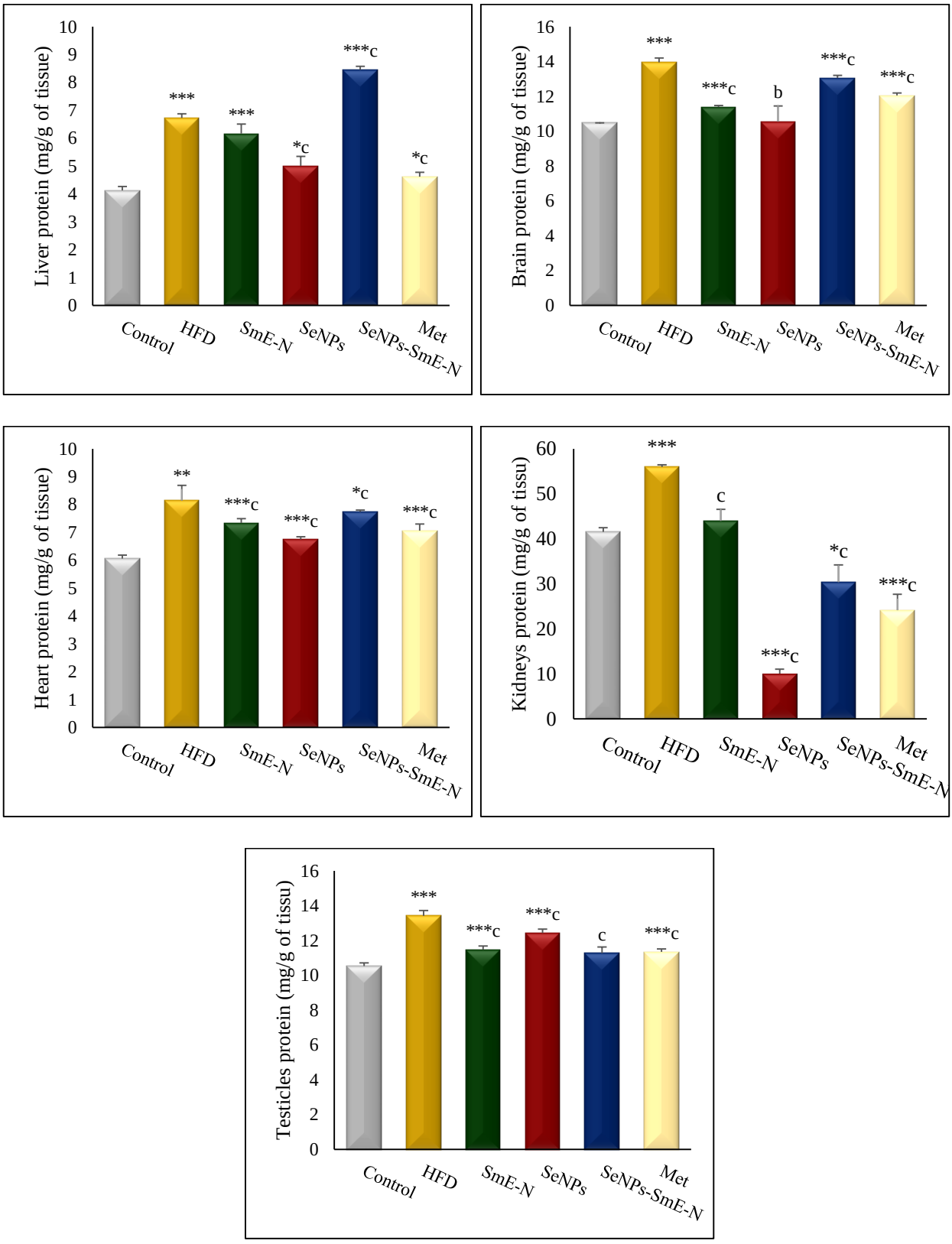

Figure 36: Liver, brain, heart, kidneys and testicles protein levels in control, HFD and treated groups

Values are provided as (mean ± SEM): * $P<0.05$, ** $P<0.01$, *** $P<0.001$: comparison with control group; a $P<0.05$, b $P<0.01$, c $P<0.001$: comparison with HFD group

9. Hematological parameters

Hematological parameters in table 14 demonstrated that, there were a significant decrease (P<0.01) of red blood cell (RBC), hemoglobin (HBG), hematocrit (HCT) and white blood cell (WBC) while a significant increase (P<0.01) of platelet in HFD group compared to the control. In the other hand, the all treated groups showed a significantly (P<0.05) rising of erythrogram parameters and enhanced the immune system by increasing in WBC, however, the platelet level was significantly reduced (P<0.05) by SmE-N and SeNPs treatment and did not affect by the metformin and SeNPs-SmE-N treatment when compared with HFD group.

Table 14: Blood erythrocyte and leukocyte lines in control and experimental groups of control, HFD and treated groups

Parameter	Control (n=6)	HFD (n=6)	SmE-N (n=6)	SeNPs (n=6)	SeNPs-SmE-N (n=6)	Met (n=6)
Red blood cell (10^{12}/L)	8.02±0.03	6.03±0.21***	7.59±0.13^{*c}	7.63±0.19^{c}	7.23±0.19^{**c}	7.12±0.18^{**b}
Hemoglobin (g/dL)	13.2±0.14	10.13±0.33***	12.22±0.30^{*c}	12.28±0.30^{c}	11.58±0.28^{**b}	12.38±0.21^{*c}
Hematocrit (%)	42.43±0.58	32.11±1.31***	39.98±0.74^{*c}	39.60±0.97^{*c}	37.90±0.755^{**c}	36.94±1.56^{*a}
Platelet (10^{9}/L)	808.3±14.6	1303±4.4***	1112.7±14.3^{***c}	1179.7±39.3^{***a}	1321±37.1***	1295.7±18.3***
White blood cell (10^{9}/L)	4.33±0.20	2.62±0.31**	4.12±0.19^{c}	4.59±0.36^{b}	3.93±0.23^{b}	4.36±0.28^{b}

Values are provided as (mean ± SEM): * *P*<0.05, ** *P*<0.01, *** *P*<0.001: comparison with control group; a *P*<0.05, b *P*<0.01, c *P*<0.001: comparison with HFD group.

10. Oxidative stress parameters

10.1. Malondialdehyde (MDA) level

In comparison to control group, the results showed that there were a significant elevations of MDA level in HFD group in liver (P<0.001), heart (P<0.001), kidneys (P<0.001), and testicles (P<0.01) organs. In addition, as compared to HFD rats, a significant decline (P<0.01) of MDA level in mentioned organs was observed in SmE-N, SeNPs, SeNPs- SmE-N and Met groups, while the results indicated a significant increase with a minor change in the SeNPs group in renal tissue (Figure 37).

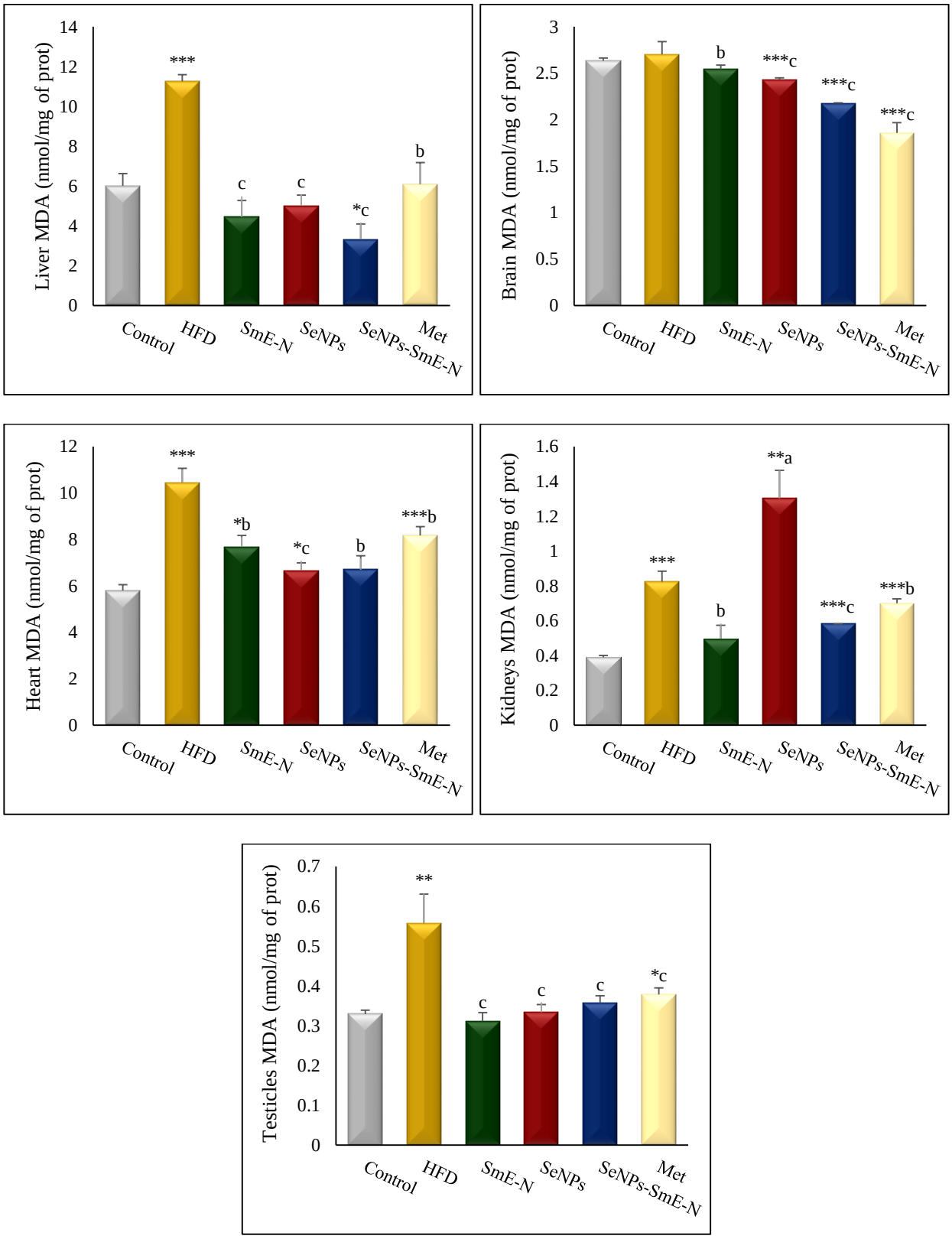

Figure 37: MDA levels of liver, brain, heart, kidneys and testicles in control, HFD and treated groups

Values are provided as (mean ± SEM): * $P<0.05$, ** $P<0.01$, *** $P<0.001$: comparison with control group; a $P<0.05$, b $P<0.01$, c $P<0.001$: comparison with HFD group

10.2. Total thiol level

Figure 38 showed the total thiol levels in liver, brain, heart, kidneys and testicles of rats, a significant decline in total thiol level of the different organs of HFD group ($P<0.01$), was observed. The drug delivery system using SmE-N, SeNPs and SeNPs -SmE-N in addition to metformin elevated significantly ($P<0.05$) the total thiol of brain, heart, kidneys and testicles, excluding total thiol of Met group, which significantly decreased in kidneys and no affected in heart as liver total thiol in SeNPs group, as compared to HFD group.

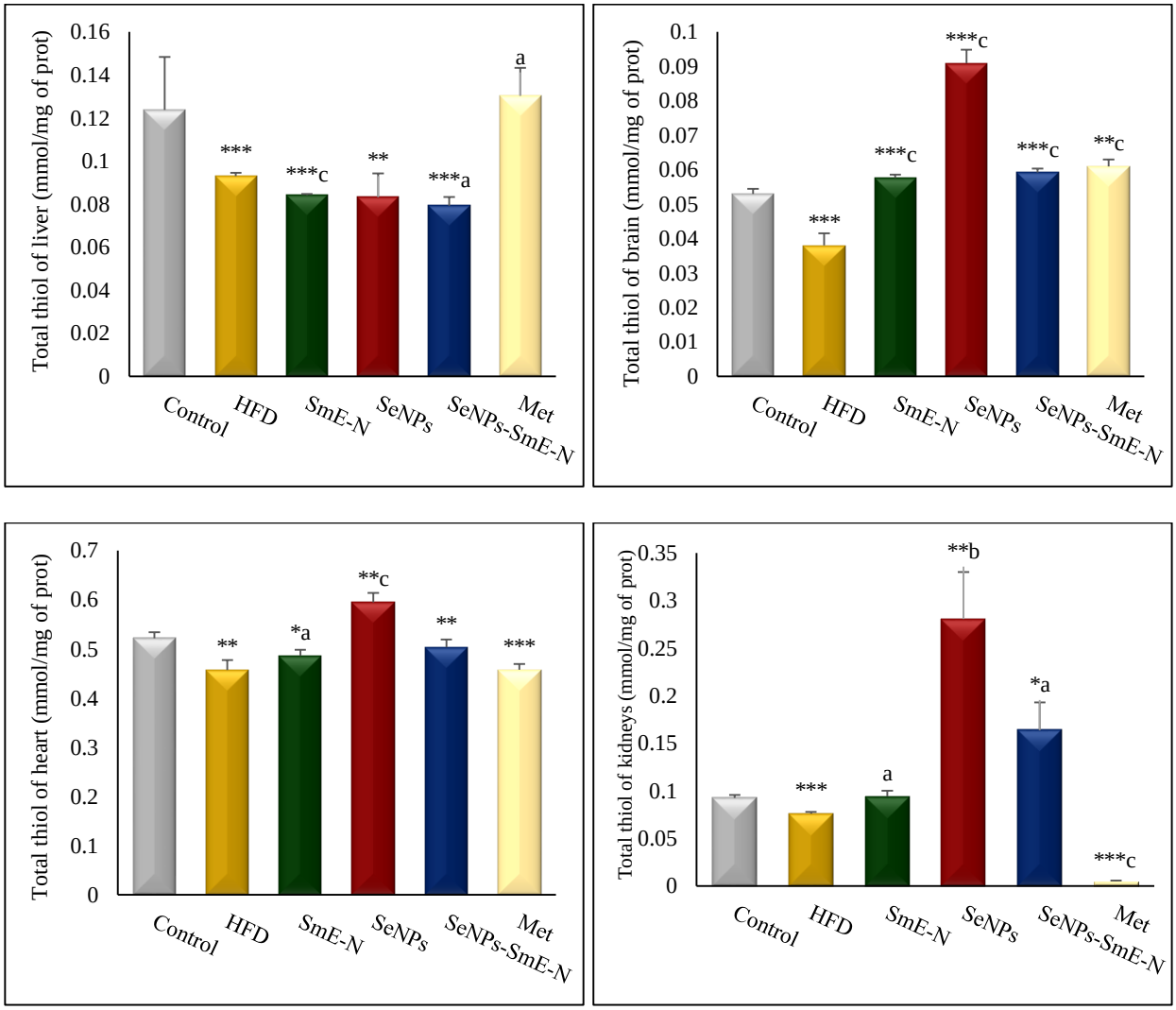

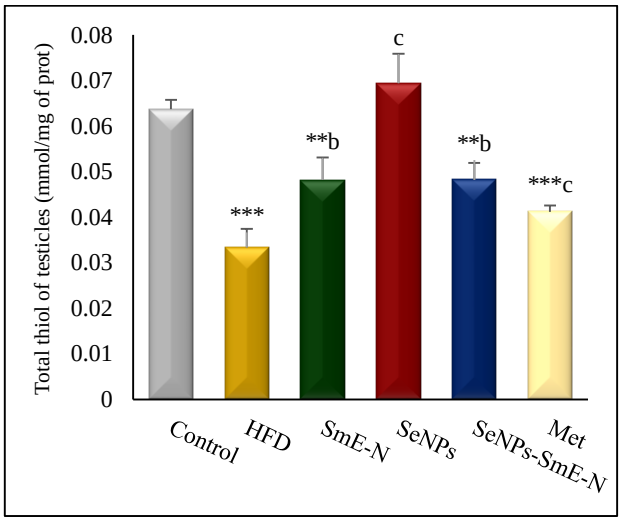

Figure 38: Total thiol levels of liver, brain, heart, kidneys and testicles in control, HFD and treated groups

Values are provided as (mean ± SEM): * *P*<0.05, ***P*<0.01, ****P*<0.001: comparison with control group; a *P*<0.05, b *P*<0.01, c *P*<0.001: comparison with HFD group

10.3. Reduced glutathione (GSH) level

Figure 39 presented the GSH concentration in various organs homogenate for the experimental group, when compared to the control there were a significant decrease of GSH level with (P<0.001) for liver, brain and testicles tissues, with (P<0.01) for heart tissue and with (P<0.05) for kidneys tissue in the HFD group. Furthermore, the GSH concentration in the all organs of different treated groups were significantly augmented as compared to the HFD rats, only SeNPs- SmE-N group was unaffected in liver homogenate.

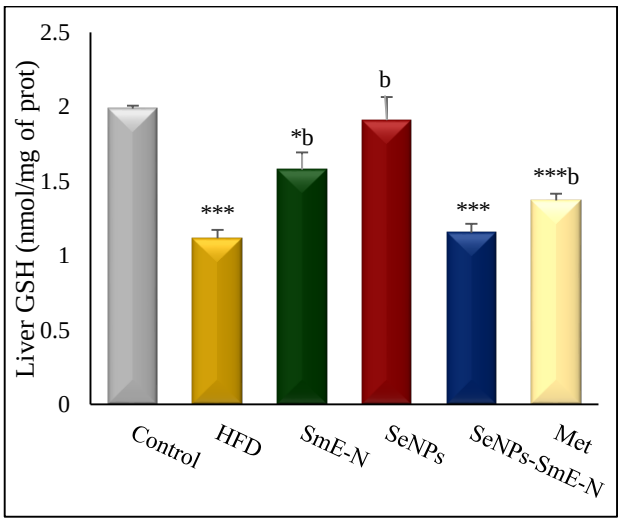

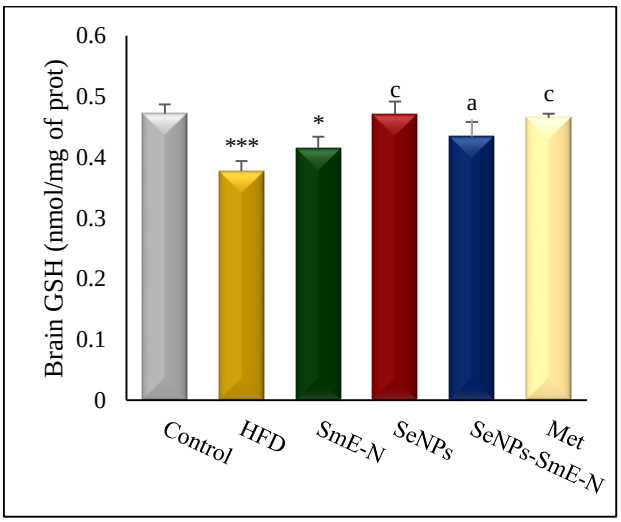

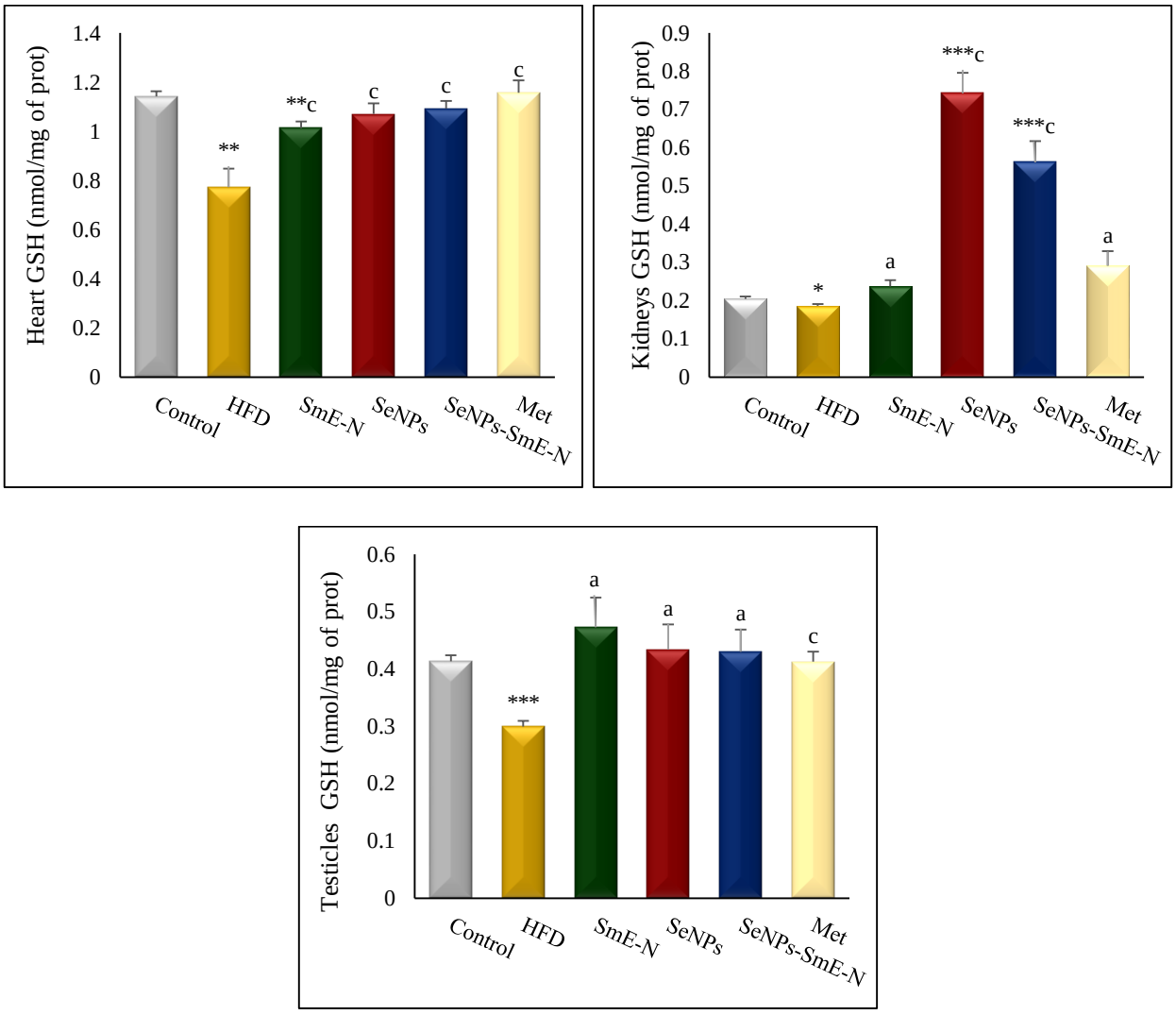

Figure 39: GSH levels of liver, brain, heart, kidneys and testicles in control, HFD and treated groups

Values are provided as (mean ± SEM): * $P<0.05$, ** $P<0.01$, *** $P<0.001$: comparison with control group; a $P<0.05$, b $P<0.01$, c $P<0.001$: comparison with HFD group

10.4. Superoxide dismutase (SOD) activity

The histograms presented results of SOD activities in different tissues of rats, a significant decrease were showed in liver, kidneys and testicles with ($P<0.001$), in brain and heart with ($P<0.01$) and ($P<0.05$) respectively, of the HFD animals when compared to the control. While, the treatment by niosomal delivery system using SmE-N and SeNPs-SmE-N with SeNPs and metformin induced a significant amelioration ($P<0.05$) in SOD activity in all of the mentioned organs in comparison to HFD rats (Figure 40).

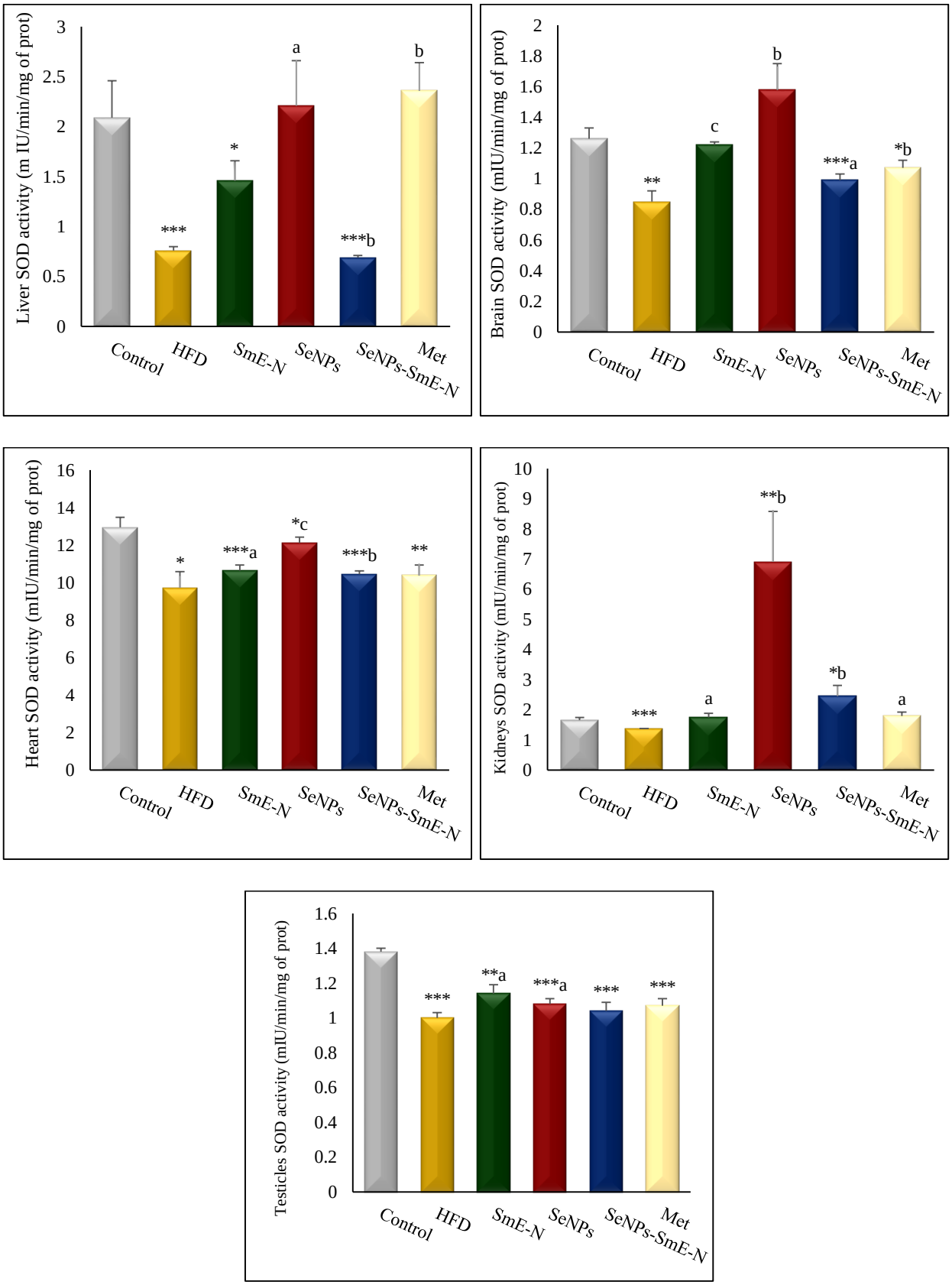

Figure 40: SOD activity of liver, brain, heart, kidneys and testicles in control, HFD and treated groups

Values are provided as (mean ± SEM): * $P<0.05$, ** $P<0.01$, *** $P<0.001$: comparison with control group; a $P<0.05$, b $P<0.01$, c $P<0.001$: comparison with HFD group

10.5. Glutathione peroxidase (GPx) activity

Hepatic, cerebral, cardiac, renal and testicular GPx activities were presented in figure 41. The results clarified that there was a significant reduction with ($P<0.001$) and ($P<0.01$) of GPx activities in the different tissues of HFD group compared to the control. Moreover, in comparison with HFD group, the data demonstrated a significant increase ($P<0.05$) of GPx activity in SmE-N, metformin, SeNPs and SeNPs-SmE-N treatment groups. The cerebral GPx activity was unaffected in SeNPs group while hepatic and cerebral GPx activities in SeNPs-SmE-N were significantly decreased and unaffected in heart tissue compared to HFD animals.

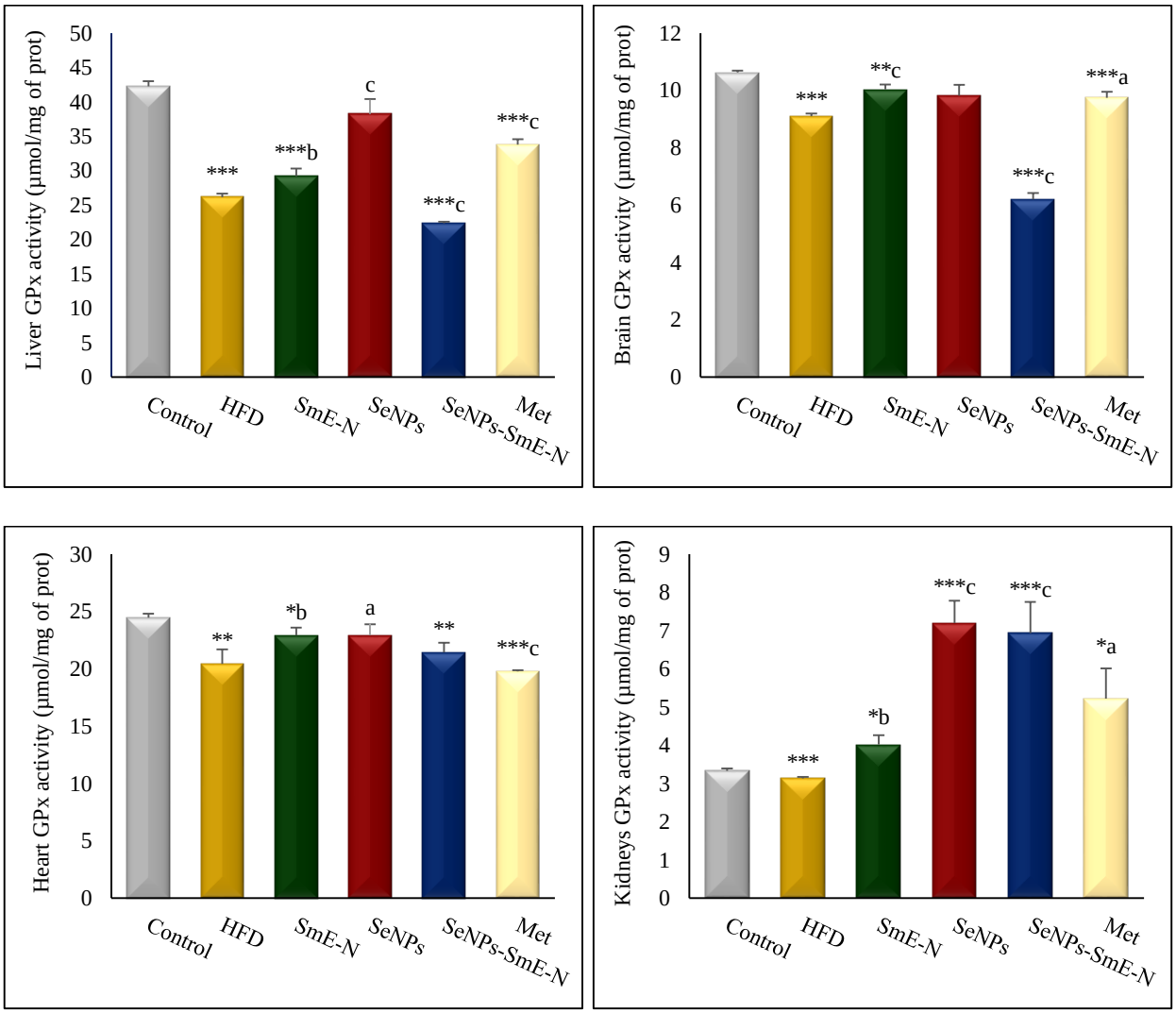

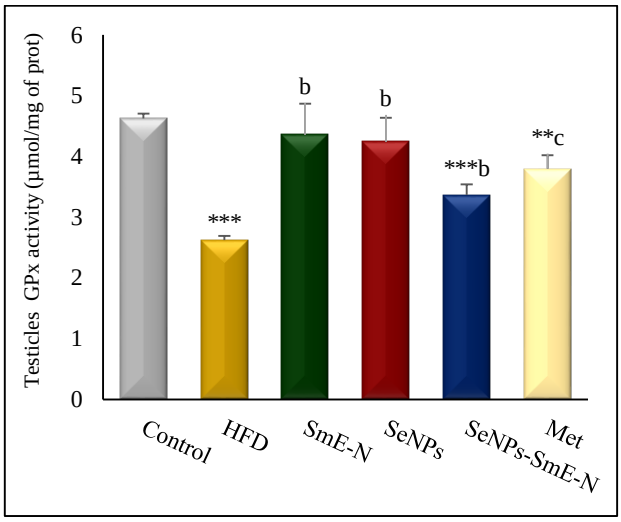

Figure 41: GPx activity of liver, brain, heart, kidneys and testicles in control, HFD and treated groups

Values are provided as (mean ± SEM): * *P*<0.05, ***P*<0.01, ****P*<0.001: comparison with control group; a *P*<0.05, b *P*<0.01, c *P*<0.001: comparison with HFD group

10.6. GPX/GSH report

The results of GPx/GSH report illustrated in figure 42. The comparison with control group revealed that there were very high significant declines (P<0.001) in GPx/GSH levels of liver, brain, kidneys, testicles, and a significant decline (P<0.05) in GPx/GSH level of heart in HFD group. However, a significant increase (P<0.001) in GPx/GSH level by SmE-N, SeNPs, SeNPs-SmE-N and metformin treatments were showed in all mentioned tissues, excluding the hepatic level of the SmE-N group which did not change significantly, when compared to the HFD group.

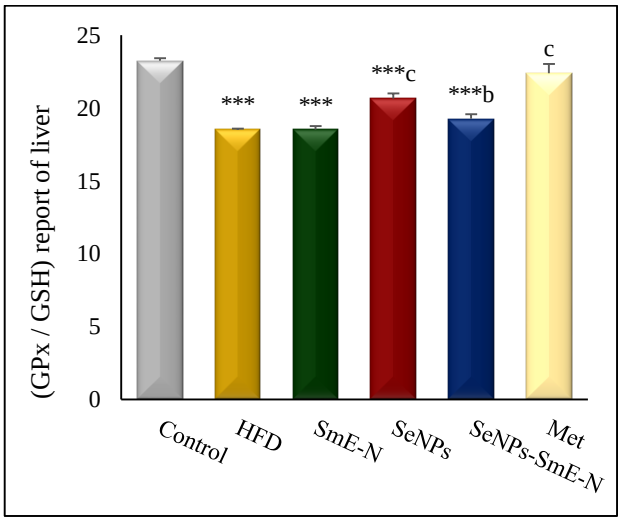

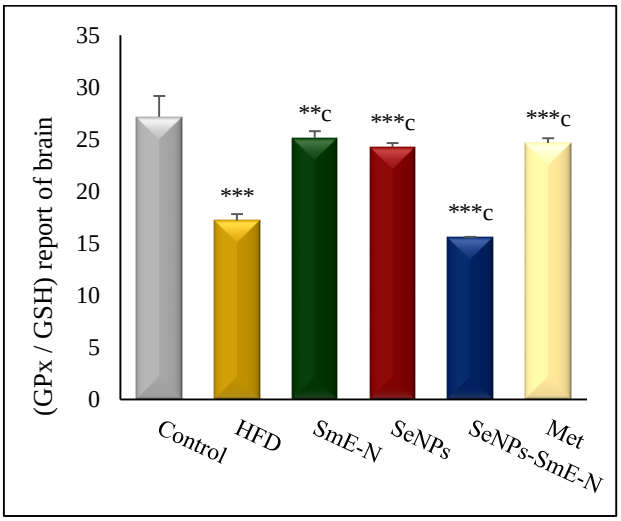

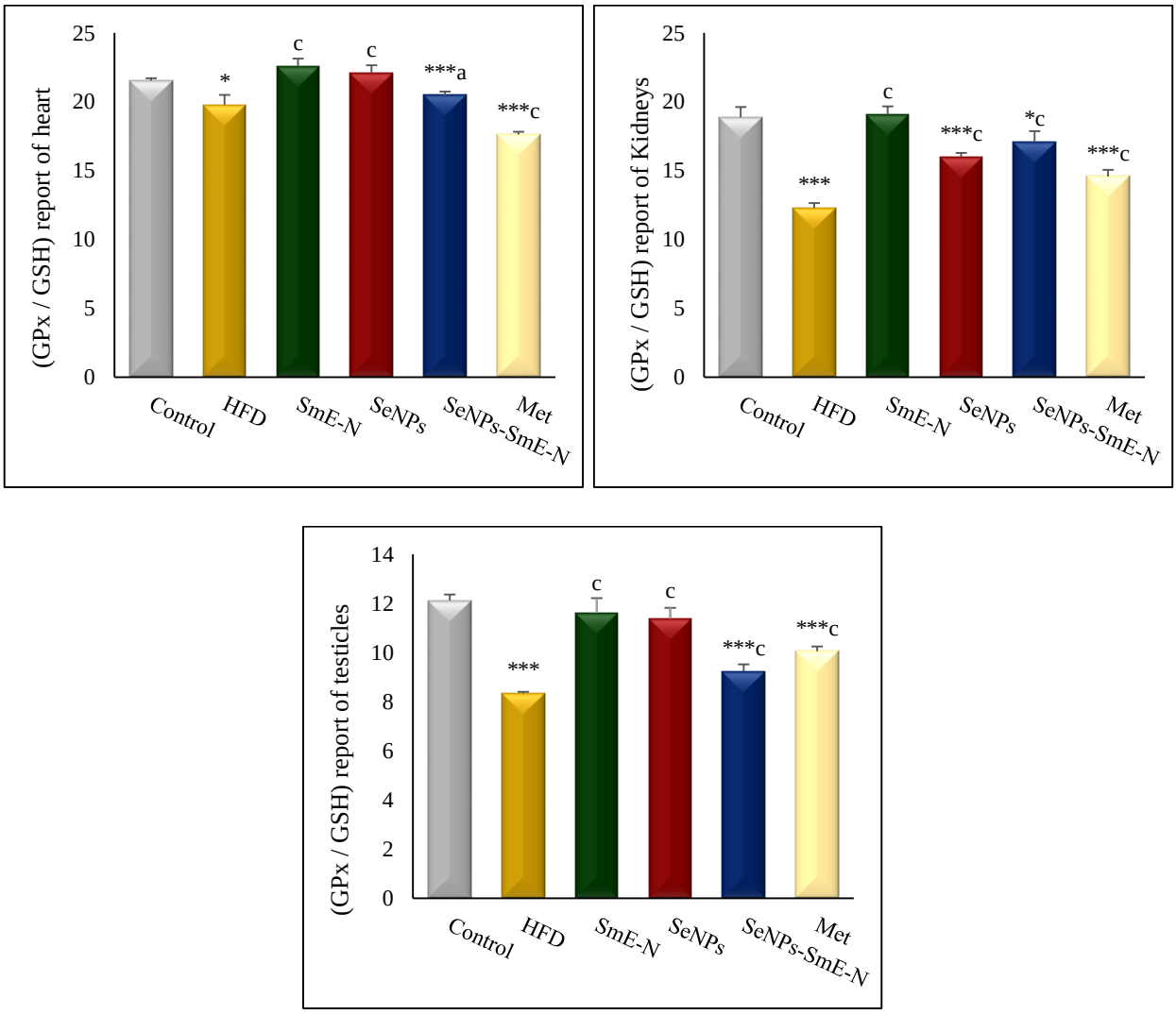

Figure 42: GPx/GSH report of liver, brain, heart, kidneys and testicles in control, HFD and treated groups

Values are provided as (mean ± SEM): * *P*<0.05, ***P*<0.01, ****P*<0.001: comparison with control group; a *P*<0.05, b *P*<0.01, c *P*<0.001: comparison with HFD group

10.7. GSH/Total thiol rate

Results in figure 43 showed that GSH/Total thiol levels in liver, brain, heart, kidneys and testicles were significantly decreased (P<0.01) in the HFD rats as compared to the control. In the other side, the comparison with HFD rats scored a significant increase (P<0.05) in the GSH/Total thiol levels for SmE-N, SeNPs, SeNPs-SmE-N, and Met groups in the all homogenates, with exception of cerebral level of SmE-N and metformin groups and renal level of SeNPs group, which did not change statistically.

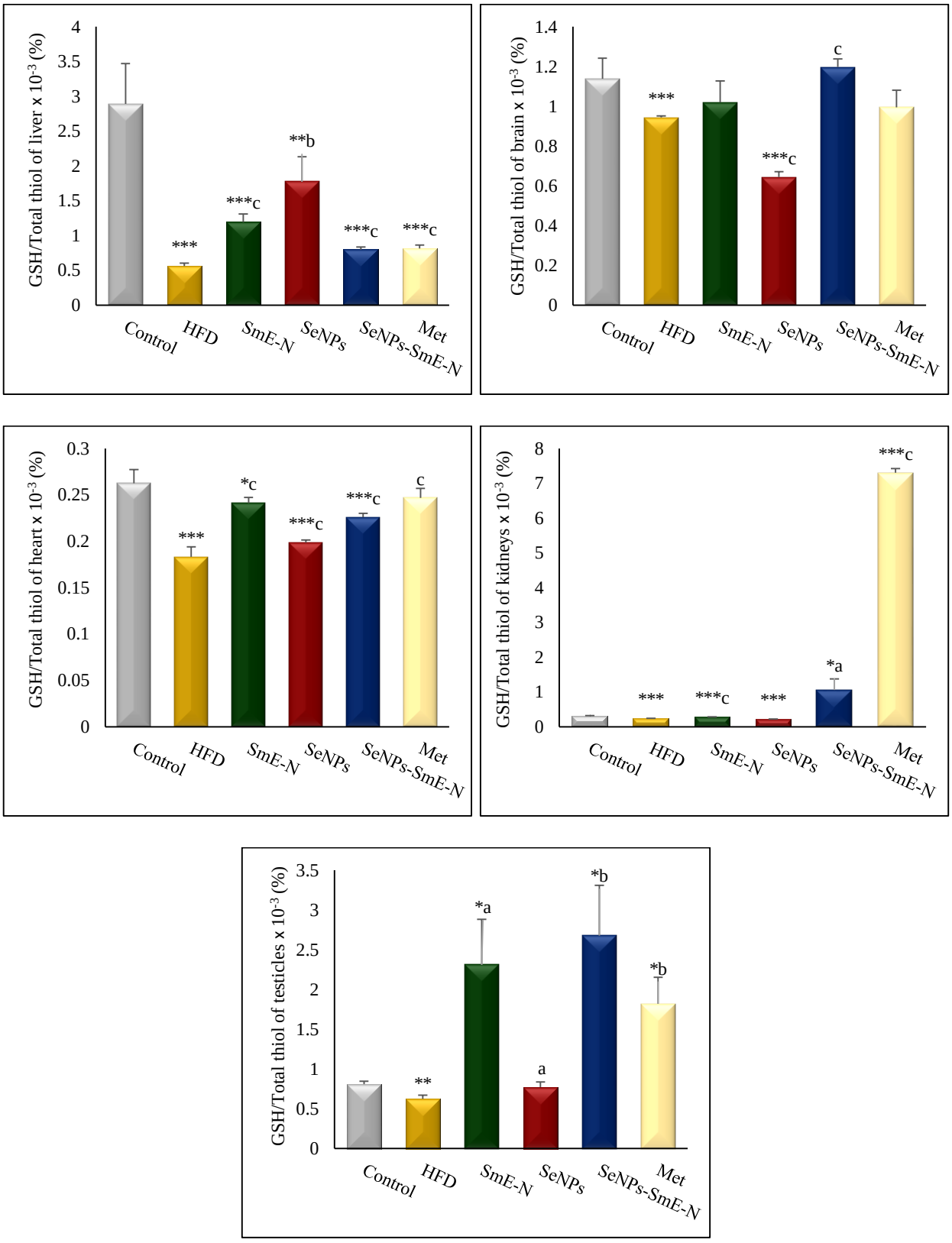

Figure 43: GSH/Total thiol rate of liver, brain, heart, kidneys and testicles in control, HFD and treated groups

Values are provided as (mean ± SEM): * P<0.05, ** P<0.01, *** P<0.001: comparison with control group; a P<0.05, b P<0.01, c P<0.001: comparison with HFD group

10.8. Total antioxidant capacity

The data presented in figure 44 demonstrated the total antioxidant capacity in hepatic, cerebral, cardiac, renal and testicular homogenates. The comparison with control group clarified that there was a significant decrease of total antioxidant capacities in liver, heart and testicles with ($P<0.001$) as well as in brain with ($P<0.05$) while did not change in kidneys of the HFD group. However, the data demonstrated a significant amelioration ($P<0.05$) of hepatic, cerebral, cardiac, and testicular total antioxidant capacities in SmE-N, SeNPs, SeNPs-SmE-N and Met treated groups, with except of the hepatic and testicular activities in SeNPs-SmE-N and SeNPs animals respectively, when compared with the HFD group.

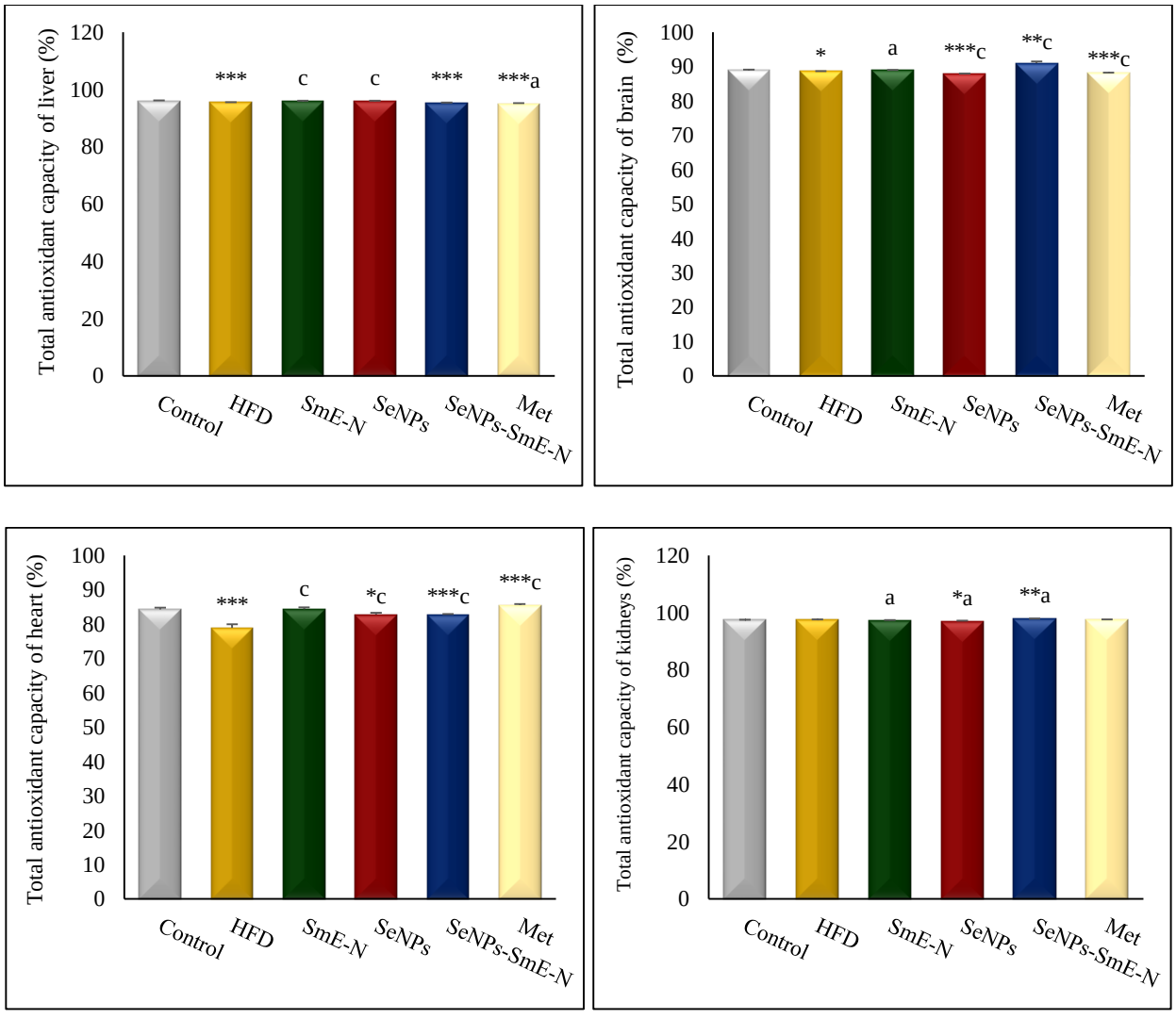

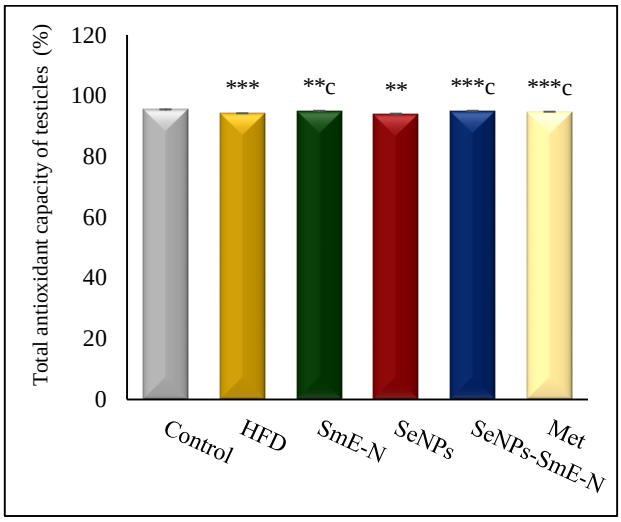

Figure 44: Total antioxidant capacity of liver, brain, heart, kidneys and testicles in control, HFD and treated groups

Values are provided as (mean ± SEM): * $P<0.05$, ** $P<0.01$, *** $P<0.001$: comparison with control group; a $P<0.05$, b $P<0.01$, c $P<0.001$: comparison with HFD group

11. Histopathological analysis

11.1. Histology of liver tissue section

Histological analysis of liver tissue section of control group appeared normal hepatocyte structure, however huge alterations including infiltration of inflammatory cells, hemorrhage, necrosis, vacuolization of cytoplasm and intracytoplasmic vacuoles were showed in liver tissue of HFD group. While, the drug delivery system using niosomes of SeNPs-SmE-N and SeNPs ameliorated the hepatocyte structure better than SmE-N and metformin treatment, which showed less necrosis and inflammatory cells infiltration compared to HFD section. Whereas liver section of Met group was distinguished by a large number of intracytoplasmic lipid droplet vacuoles when we compared them to the HFD group, as presented in figure 45 and table 15.

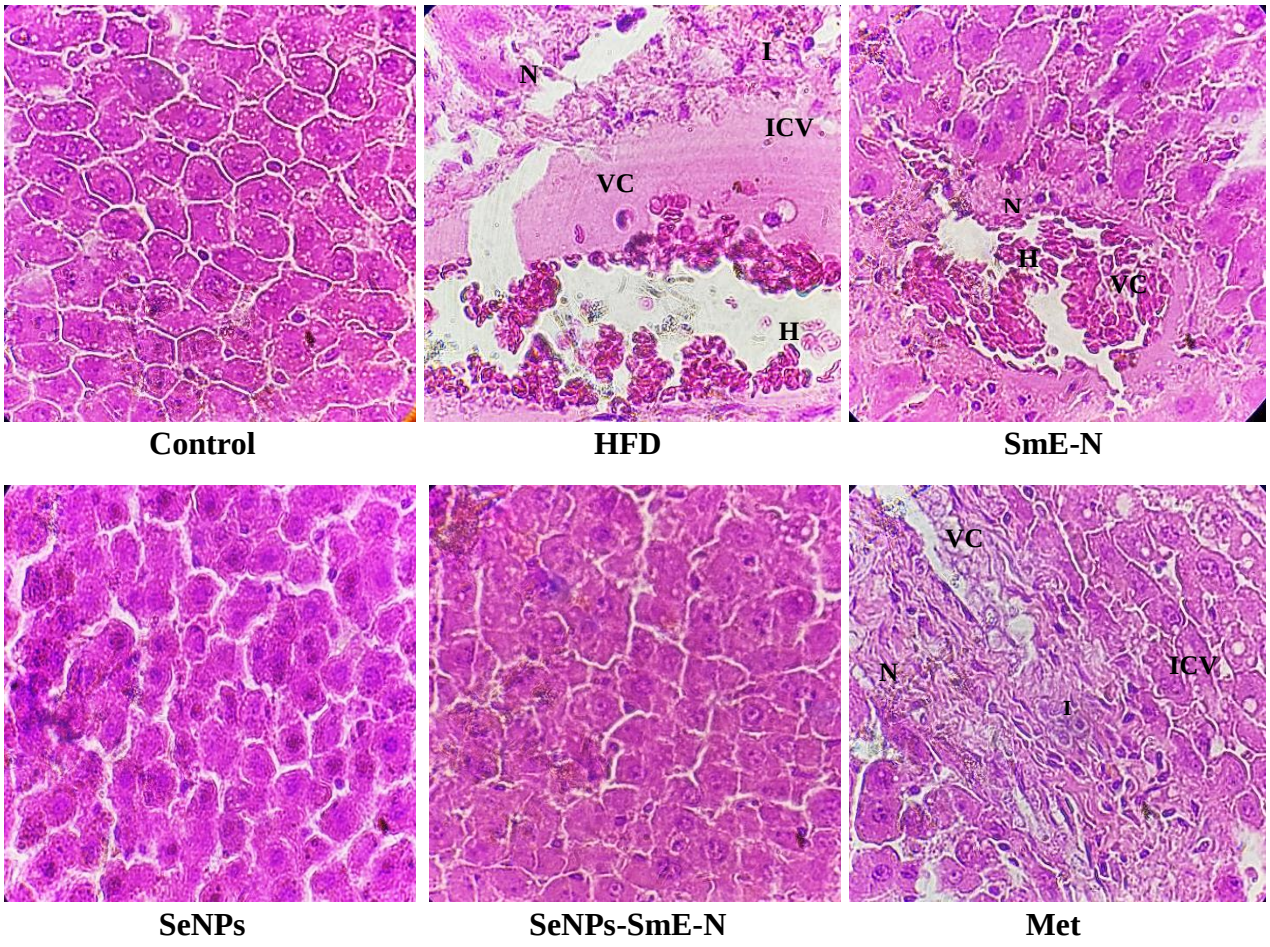

Figure 45: Histological micrographs of liver section in control, HFD and treated groups with hematoxylin and eosin (H&E) at magnification ×400.

Necrosis (N); Inflammation (I); Hemorrhage (H); Vacuolar cytoplasm (VC); Intracytoplasmic vacuoles (ICV)

Table 15: Grading of histological modifications in liver section in control, HFD and treated groups

Parameters	Control	HFD	SmE-N	SeNPs	SeNPs-SmE-N	Met
Inflammation	-	+++	+	-	-	++
Hemorrhage	-	+++	+	-	+	++
Necrosis	-	++	+	-	-	++
Cytoplasm vacuolization	-	+++	+	-	-	++
Intracytoplasmic vacuoles	-	++	+	-	+	+++

none (-); moderate (+); severe (++); very severe (+++)

11.2. Histology of brain tissue section

Figure 46 and table 16 presented microscopic analysis and grading of histological alterations of brain section, control group showed a normal histological cells structure, whereas brain section of HFD group demonstrated modifications from degeneration of cells, hemorrhage to infiltration of inflammatory cells in the section but treatment using nanosized material of SmE-N, SeNPs and SeNPs-SmE-N improved totally these changes and presented a normal histological cells structure better than showed in Met group.

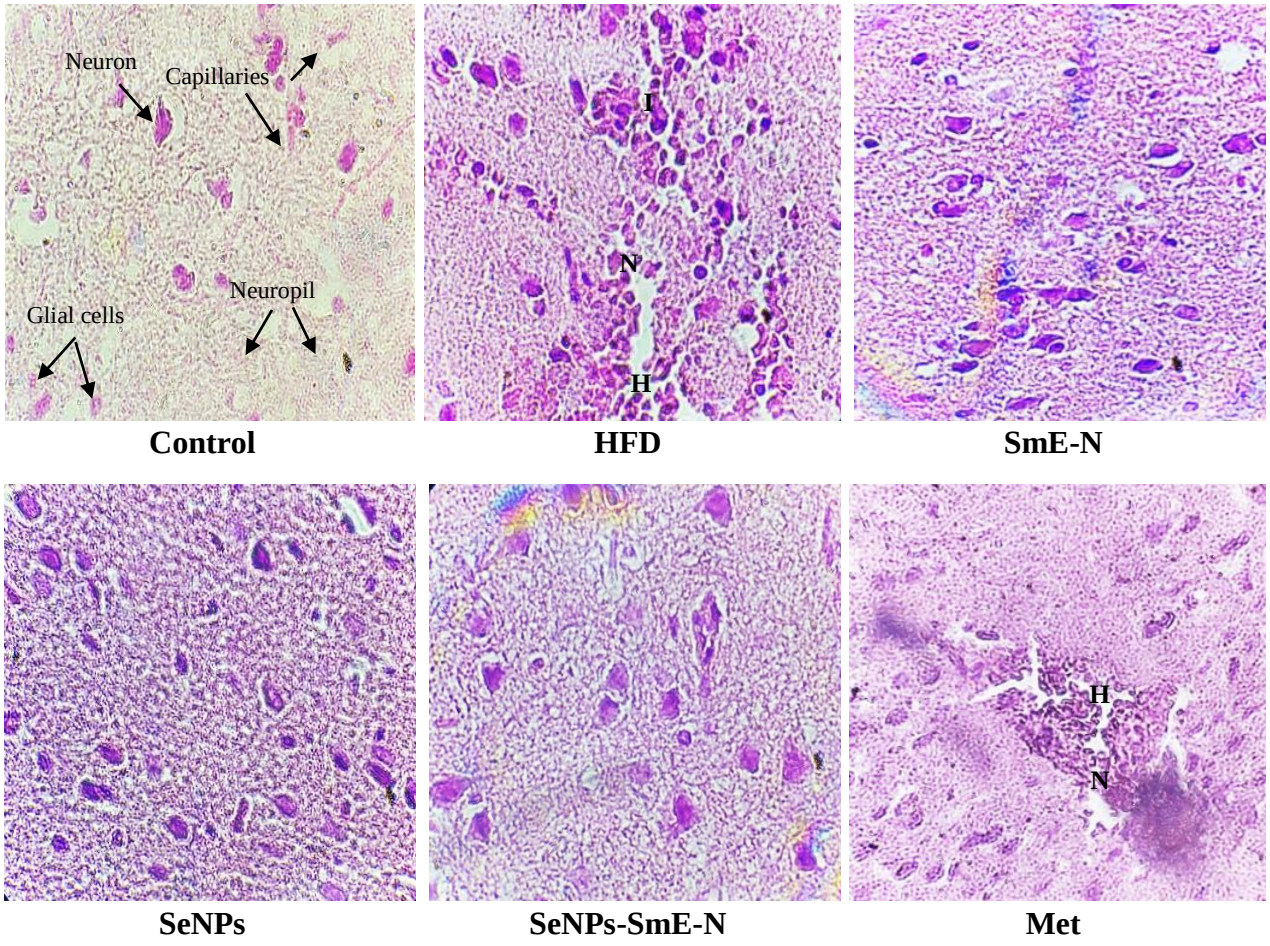

Figure 46: Histological micrographs of brain section in control, HFD and treated groups with hematoxylin and eosin (H&E) at magnification ×400.

Necrosis (N); Inflammation (I); Hemorrhage (H)

Table 16: Grading of histological modifications in brain section in control, HFD and treated groups

Parameters	Control	HFD	SmE-N	SeNPs	SeNPs-SmE-N	Met
Inflammation	-	+++	-	-	-	+
Hemorrhage	-	+++	-	-	-	+
Necrosis	-	+++	-	-	-	+
Cytoplasm vacuolization	-	-	-	-	-	-

none (-); moderate (+); severe (++); very severe (+++)

11.3. Histology of heart section

Histologic photomicrograph of the control group's heart tissue showed normal cells and myofibrillar structure with striations and branches (A) with appearance of a few collagen profiles (B). However, HFD group demonstrated alterations of heart tissue including necrosis, inflammatory cells infiltrations, hemorrhage and vacuolization of cytoplasm in addition to accumulation of large bundles of collagen in the tissue. Heart section of treated group presented improvement in tissue structure in SmE-N, SeNPs and Met groups while treatment using SeNPs-SmE-N showed few degenerated cardia-myocyte with appearance of normal heart cells in tissue. Also, a significant amelioration in collage distribution as shown in part (B) of treated groups, where the reduction of collagen deposition degree (Figure 47 & Table 17).

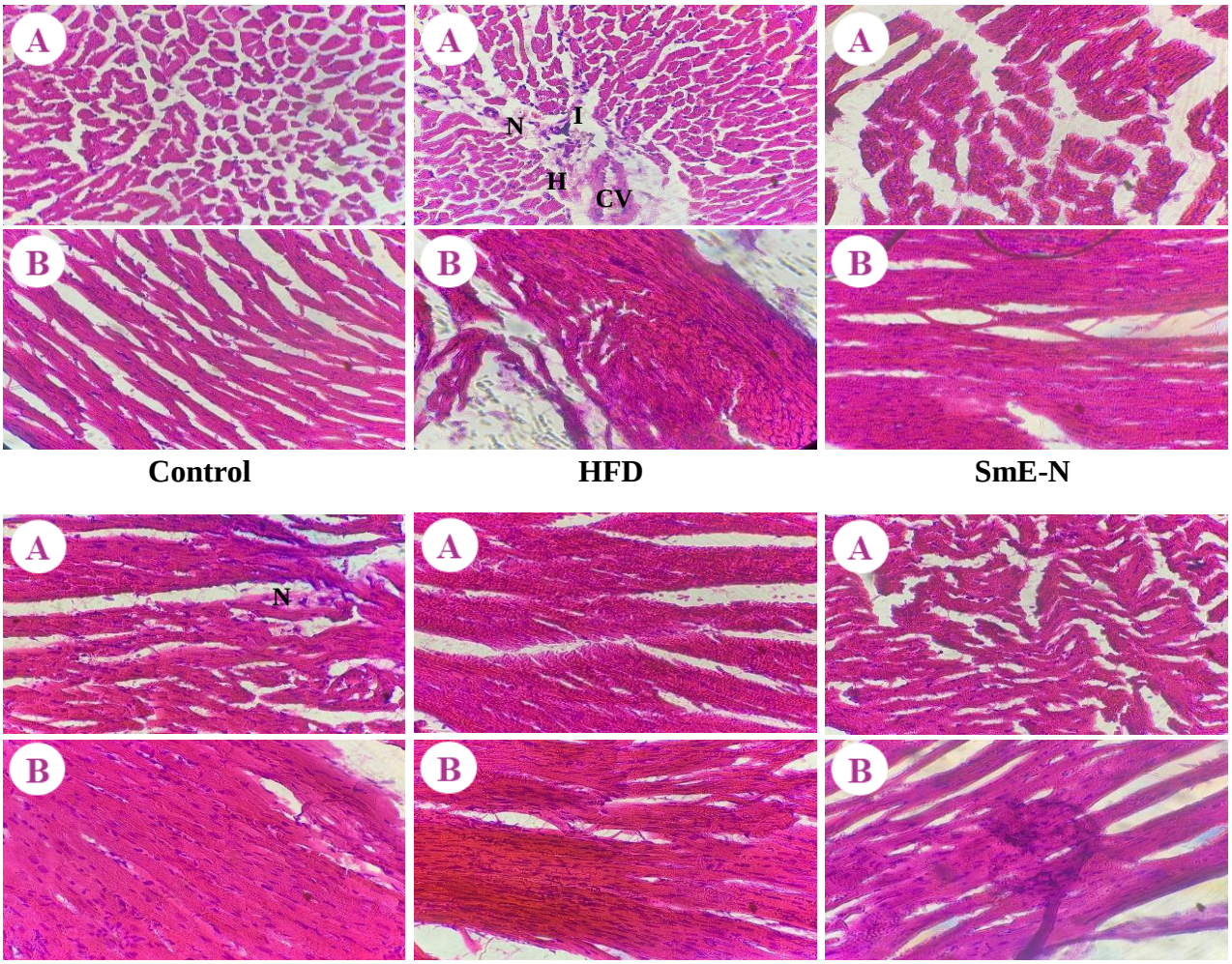

Figure 47: Histological micrographs of heart tissue (A) and collagen (B) in control, HFD and treated groups with hematoxylin and eosin (H&E) at magnification ×400.

Inflammation (I); Necrosis (N); Hemorrhage (H); Cytoplasm vacuolization (CV)

Table 17: Grading of histological modifications in heart section of control, HFD and treated groups

Parameters	Control	HFD	SmE-N	SeNPs	SeNPs-SmE-N	Met
Inflammation	-	++	-	-	-	-
Hemorrhage	-	++	-	-	-	-
Necrosis	-	+++	-	-	+	-
Cytoplasm vacuolization	-	+++	-	-	-	-
Collagen Accumulation	-	+++	+	+	+	+

none (-); moderate (+); severe (++); very severe (+++)

11.4. Histology of kidney tissue section

Histological examination of kidney tissue section showed normal morphological tissue structure, similar sizes of glomerulus, Bowmen's space and circular renal tubules in control group. While histological changes appeared in the tissue of HFD group, including necrosis, inflammation and hemorrhage with expansion of Bowmen's space, a glomerulus atrophy and tubules dilatation. Treatment by niosomes of SmE-N and SeNPs-SmE-N with nanosized SeNPs demonstrated better correction of most morphological alterations of renal section than metformin treatment which provided slight corrections with survival of Bowmen's space expansion and glomerulus atrophy (Figure 48 & Table 18).

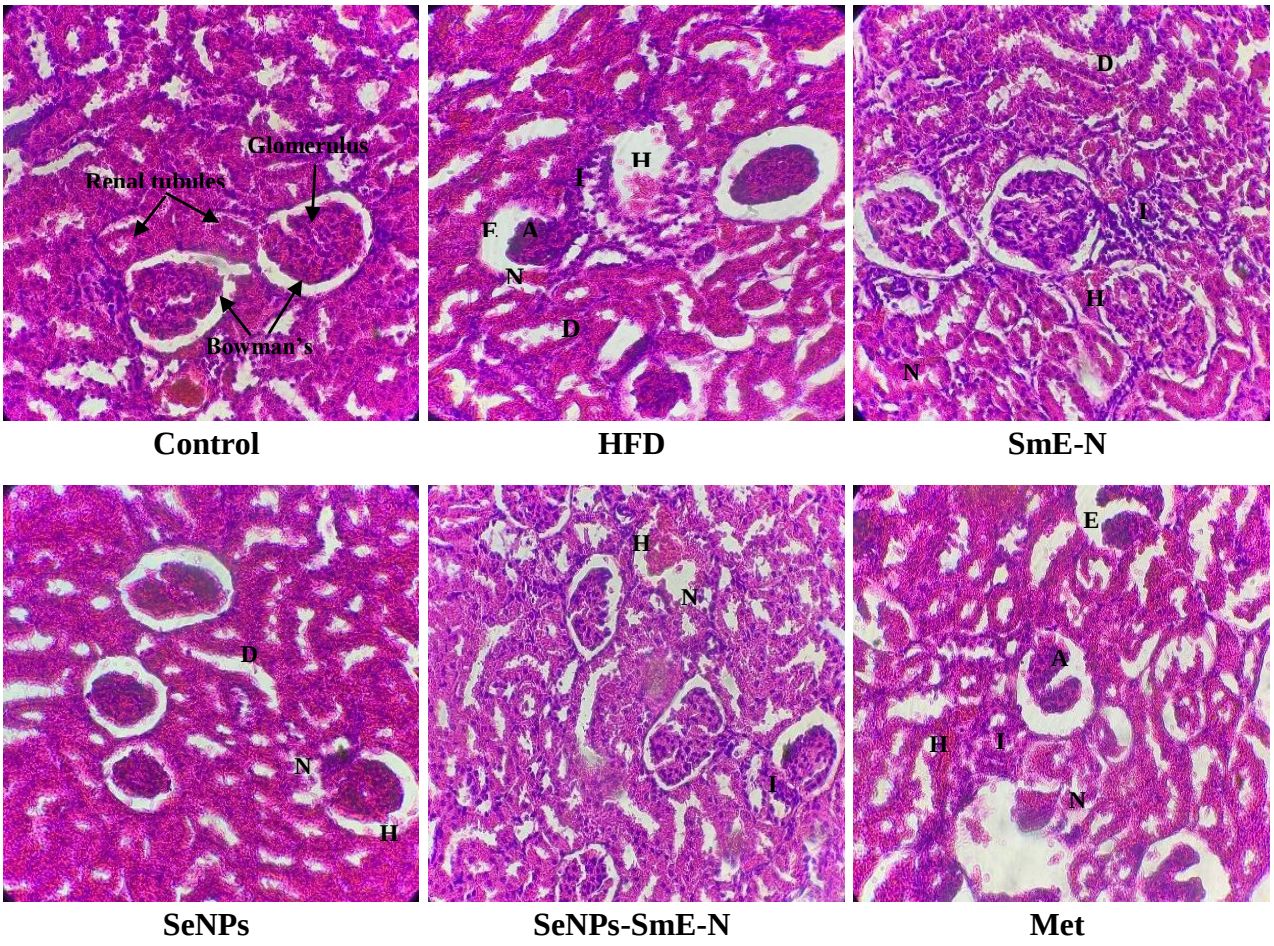

Figure 48: Histological micrographs of kidney section in control, HFD and treated groups with hematoxylin and eosin (H&E) at magnification ×400.

Necrosis (N); Inflammation (I); Hemorrhage (H); Bowman's space expansion (E); Glomerulus atrophy (A); Renal tubule dilatation (D)

Table 18: Grading of histological modifications in kidney section in control, HFD and treated groups

Parameters	Control	HFD	SmE-N	SeNPs	SeNPs-SmE-N	Met
Hemorrhage	-	+++	+	+	+	++
Inflammation	-	+++	+	+	+	++
Necrosis	-	+++	+	+	+	++
Bowman's space expansion	-	+++	-	-	-	+++
Glomerulus atrophy	-	+++	-	-	-	+++
Renal tubule dilatation	-	+++	+	+	++	+++

none (-); moderate (+); severe (++); very severe (+++)

11.5. Histology of testicle tissue section

Photomicrograph of testiculs tissue section demonstrated in figure 49 and table 19, control group showed normal structure of tissue, typical distribution of leydig cells and seminiferous tubes in the histological section in addition to appearance of spermatogenesis phases inside of the seminiferous tubes, involved Sertoli cells and spermatogonia on the periphery, spermatocytes, smaller spermatids and spermatozoons, while the entire tube lumen nearly filled with flagella. HFD group showed necrosis of cells, deformation of seminiferous tube walls structure and appearance of irregular boundaries, deterioration of spermatogenic cells including reduction of sperm condensation, which induced to increase of intercellular space (void between the cells). The testicular sections of treated rats by SeNPs and metformin presented better improvement than that presented by SmE-N and SeNPs-SmE-N treatment, where the morphological structure amelioration of testiculs tissue was partially noticed but the reduction of sperm condensation and increase of void between the cells were also remarked very well in the groups.

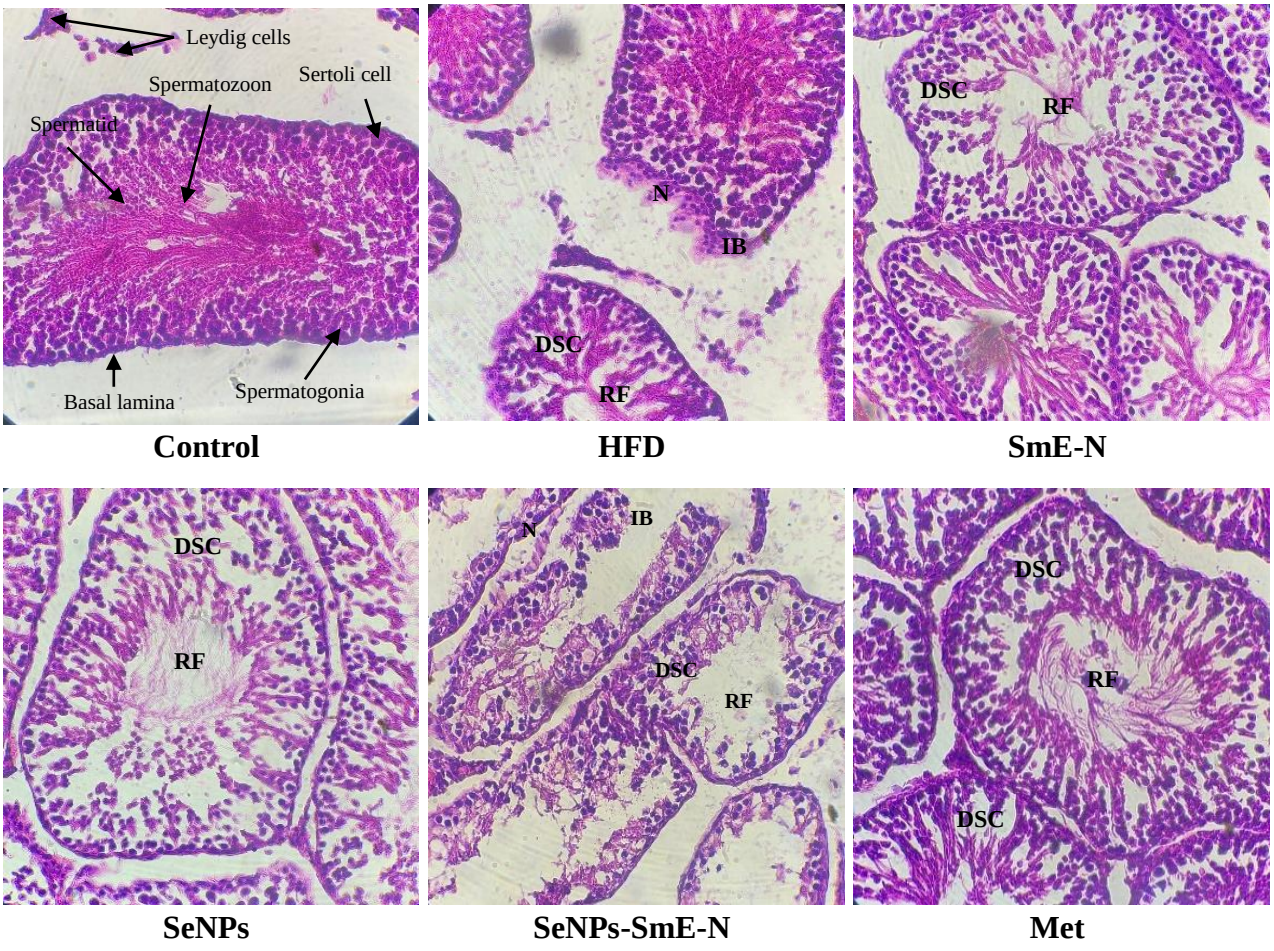

Figure 49: Histological micrographs of testiculs section in control, HFD and treated groups with hematoxylin and eosin (H&E) at magnification ×400.

Necrosis (N); Irregular boundaries (IB); Reduction of flagella condensation (RF); Degeneration of spermatogenic cells (DSC)

Table 19: Grading of histological modifications in testiculs section in control, HFD and treated groups

Parameters	Control	HFD	SmE-N	SeNPs	SeNPs-SmE-N	Met
Necrosis	-	+++	-	-	+	-
Irregular boundaries	-	+++	-	-	+	-
Reduction of flagella condensation	-	+	++	++	+++	++
Degeneration of spermatogenic cells (spermatocytes and spermatogonia)	-	++	+	++	++	++

none (-); moderate (+); severe (++); very severe (+++)

Discussion

I. *In vitro* study

1. Qualitative and quantitative phytochemical analysis of *Sonchus maritimus*

In plants, leaves are the largest part that accumulates the bioactive substances like secondary metabolites, according to numerous research, leaf extracts obtained from various plants have different phytochemical profiles and biological properties. Therefore, despite being regarded as agricultural waste, plant leaves are an excellent source of high-value nutra-pharmaceutical compounds (Kumar et al., 2021). The phytochemical analysis of *Sonchus maritimus* aqueous extract revealed presence of diverse phyto-compounds, including phenols, flavonoids, terpenoids, tannins, unsaturated steroids, derived steroids and saponins,

The phytochemical screening proves useful for determining the different elements of plant extracts for discovering bioactive substances that may be utilized in producing effective pharmaceuticals (Pant et al., 2017). There is evidence from numerous research that medicinal plants include phenols, flavonoids, terpenoids, and tannins. These bioactive components are now used as therapeutic agents due to the expansion of scientific knowledge of herbal treatments as significant alternatives or complementary therapies for the treatment of disease (Kebede et al., 2021). These phyto-constituents are present in *S. maritimus* and have a number of pharmacological effects, including hepatoprotective, anti-hyperglycemic, anti-hyperlipidimic and neuroprotective effects (Iranshahy et al., 2017). Phenols, flavonoids, and terpenoids have been shown to have the most beneficial effects (Prabu et al., 2019). Saponins also have a relaxing effects on the nervous system, along to their ability to regulate the immune system, regulate blood sugarand lower blood pressure (Ya-Zheng et al., 2018). Regarding phytosterols, it performs a hypolipidemic function (Tarish et al., 2019).

The amount of total phenols present could be used as the basis for an extensive evaluation of antioxidant activity, the ability of phenolic compounds to serve as antioxidants and free radical scavengers is enhanced by the hydroxyl groups (-OH) present in these compounds (Kaouachi & Derouiche, 2018). Flavonoids are an ubiquitous group of polyphenolic compounds found in most plants, they are thought to be responsible for repairing the oxidative damage that is linked to the majority of diseases due to their important antioxidant activity, also, they have been shown to have antibacterial, vasodilator, antithrombotic, anti-inflammatory and antineoplastic properties (Ayoola et al., 2019). Condensed tannins ,a secondary metabolite in the plant, are well-known for their positive impacts on animal health and they have a nutritional value through their ability to act as antioxidants (Soldado et al., 2021).

The existence of dietary minerals in the dry leaves of *S.maritimus,* including, sodium (Na), potassium (K), calcium (Ca), magnesium (Mg), copper (Cu), zinc (Zn), iron (Fe) and manganese (Mn) are supported by other study that found some of this meniral in *S.maritimus* (Hameed et al., 2021). These phytomineral contribute to increase the nutritional value profile of this plant (Petropoulos et al., 2016).

HPLC technique has become a sensitive, rapid and precise method to analyze the chemical compounds such as phenols, flavonoids, alkaloids ...ect, which have been extracted from the plant (Jiao et al., 2014). The Presence of quercetin, naringin and rutin, in addition to gallic acid, chlorogenic acid, vanilic acid, and caffiec acid in the aqueous extract of *S.maritimus* is reported in previous research paper which detect these bioactive compounds in various species of *Sonchus* genus, this illustrates significance of *S.maritimus* extract as an antioxidant and its ability to combat harmful microorganisms and other metabolic disorders (AL Juhaimi et al., 2017; Bashir et al., 2018; Fouad et al., 2020).

Polyphenols, which are widely recognized for their antioxidant and anti-carcinogenic properties, are a major focus of medical research. It has been previously demonstrated that the discovered metabolites have a significant role in both preventing and managing the progression of various diseases (Elhady et al., 2022). The o-coumaric acid (hydroxycinnamic acids), ferulic acid, protocatechuic acid (hydroxybenzoic acids) and quercetin (flavonols) are detected in species belong to Asteraceae (AL Juhaimi et al., 2017; Bessada et al., 2015; Sareedenchai & Zidorn, 2010), which confirms the validity of LC-MS results in the current study. Furthermore, there content especially in the plant aqueous extracts can explain their antioxidant actions (Bessada et al., 2015). Significant and powerful bioactive compounds were found in the cured extract, including luteolin and apigenin-7-o-glucoside (flavones), that exhibit a range of biological properties and have an anti-inflammatory action which is explained by the inhibition of cyclooxygenase-2 (Sareedenchai & Zidorn, 2010; Ziyan et al., 2007).

Several studies have documented the beneficial therapeutic effects of volatile chemicals in different plants; yet, other publications have verified that numerous volatile components in the plant have exhibited potent cytotoxic properties (Neethu & Yathiender, 2023). GC analysis were performed in a prior work to identify the phytochemical compounds of the aerial portion extract of Sonchus oleraceus; GC chromatogram represent a plant's fingerprint based on the chemical substances it contains (Ahmad et al., 2021). 2-ethyl-1-hexanol is considered a strong volatile substance, has antifungal properties similar to Fusarium (Cruz et al., 2012). An excellent antioxidant and antifungal properties were demonstrated by cyclotrisiloxane, hexamethyl- against mycoses, which are known to cause a high death rate in patients with weakened immune

systems (Helal et al., 2019). Gaafar *et al.* (2020) report that cyclopentasiloxane, decamethyl-, has been identified using GC analysis in other plant extract and may play a role in the cytotoxic effect on breast cancer cells (MCF-7) and colon cancer cells (HCT116). Moreover, it might show antiviral action against the H5N1 influenza virus by obstructing its viral adsorption, replication, and propagation processes.

2. Characterization of SmE-loaded niosomes

Niosomes are characterized as vesicular systems and have the capacity to encapsulate both hydrophilic and hydrophobic substances (Colorado et al., 2020). The electronic and optical microscopes are employed to determine the niosomes' size and shape after they had been synthesized (Hajizadeh et al., 2019). The current study, optical microscopy assessment of SmE-loaded niosomes, as a novel approach of bioactive drug delivery system, revealed a round and spherical shape. Another study utilizing optical microscopy demonstrate that the produced clarithromycin-loaded niosomes were sphere in shape as well (Shilakari Asthana et al., 2016). According to scanning electron microscopy results, the niosomes had a great average size and spherule structure. Baranei *et al.* (2020), demonstrated the same morphological results, and the size of their formulations of niosomes loaded with green tea extract ranged from 100 to 200 nm.

Most recent research indicates that niosomes are formulations that are utilized to encapsulate bioactive substances and to deliver them as therapeutic system (García-Manrique et al., 2020). Niosomes' encapsulation efficiency of up to 61.4% suggests that a significant amount of bioactive molecules of *S. maritimus* extract are entrapped within, which supporting the evidence of niosomes formulation. An earlier investigation revealed that about 60% of the curcumin is encapsulated in the niosomes formulation that prepared by use of Tween 85 (Obeid et al., 2019).

Our obtained results showed that *Sonchus maritimus*-loaded niosomes had an important encapsulation efficiency reach up 66.4 % after 7 days and demonstrated a great stability over 60 successive days of sample storage at 4°C, which show that there wasn’t leakage of our plant extract from formulated vesicles. Stability of encapsulation efficiency of the synthesized niosomes is in accordance with results of another investigation, which found that the quercetin-loaded niosomes was stable and did not change significantly after 30 days of cold storage under the same conditions (Javani et al., 2021).

3. Characterization of selenium nanoparticles

The ability of plant extract to synthesize nanoparticles is verified firstly by the ability to visually identify color changes (Rajeshkumar et al., 2018). In this current study, the use of *S. maritimus* aqueous extract for eco-friendly synthesis of SeNPs were successful an according to transitions of color from yellow to ruby red which was a clear indication that SeNPs had been synthesized (Cittrarasu et al., 2021). Extraction is a necessary step to isolate and identify the phenolic compounds (Boukada et al., 2022). The broad shoulder at 360 nm in UV-visible spectrum may be appeared by phytochemicals like flavonoids and phenols that present in plant extract (Maheo et al., 2022). A notable plasmon resonance peak at 300 nm was also observed during the various stages of the synthesis of SeNPs on the UV-visible spectra, this finding confirmed the existence of SeNPs in the samples according to earlier investigation found Se-NPs are absorbing the light between 250 and 400 nm (Ghaderi et al., 2021). Others demonstrated SeNPs produced from sodium selenite employing the ascorbic acid reduction ability, exhibit a significant absorbance peak at 370 nm (Ananth et al., 2019). Additionally, the wet chemical method yielded the highest absorption of SeNPs at 390 nm in the work of (Malhotra et al., 2014).

The FT-IR technique measures the vibrational frequencies of chemical bonds to identify the functional groups existing on the surface of SeNP, allowing for the detection of various reducing and stabilizing functional groups of compounds to confirm that they participate in the synthesis of SeNPs (Alipour et al., 2021). the emergence of peaks in the *S. maritimus* extract and SeNPs spectra; a significant absorption band that showed up at approximately 3400 cm^{-1} indicated the plant extract's extended hydrogen-bonded O-H alcohol and phenols. Moreover, additional peaks, such as those at about 1600 cm^{-1} that show the existence of the -N-H group (bending vibrations), were shown also in the both spectrums. The secondary-OH bending vibrations are of around 1200 cm^{-1}, and the intense peak, which are measure approximately 1400 cm^{-1}, indicates the C-H group. The stretching vibration of the two functional groups C=O and C-O expressed by appearance of peaks around 1050 cm^{-1} and 1100 cm^{-1}, respectively. Strong C-H bending vibrations have been detected in relation to the peaks observed at 824 cm^{-1}. The various wave numbers determined here are consistent with the findings of Rajagopal *et al.* (2021) and Nagalingam et al. (2022). According to results and in agreement with a previous study, the surface of produced SeNPs is capped with proteins, polyphenols, and flavonoids which found in the leaves aqueous extract, the same study was confirmed that the distinct signal at 588 cm^{-1}, indicating Se-O interaction (Mulla et al., 2020).

The distribution and surface morphology of the synthesized nanoparticles were assessed using scanning electron microscopy (SEM) (Abu-Elghait et al., 2021). Our results were in accordance with finding of Pandey *et al.* (2021), who informed that selenium was produced biogenically, taking on a spherical form. The elemental content of particular areas inside SEM slices was examined using energy dispersive X-ray (EDX) microanalysis apparatus, which was also utilized to assess the qualitative and quantitative status of elements that might be implicated in the formulation of nanoparticles (Shahbaz et al., 2022). EDX spectrum of our prepared SeNPs showed that Se and O are main elemental compositions, which designates the purity of the samples. Due to surface plasmon resonance (SPR), metallic nanoparticles in the EDX spectrum produce a characteristic absorption signal of the metal; O peaks are observed as a result of biomolecules attaching to the surface of the SeNPs; and carbon peaks reveal that the nanoparticles created by biosynthesis are coated in a thin layer of some capping organic component, in addition to the carbon tape that is used in the spectrum analysis (Singla et al., 2022).

Our obtained results of TEM analysis revealed clearly that our synthesized SmE-SeNPs was spherical and monodispersed with extremely small size reach less than 7.154 nm. The small size and monodisperse SeNPs are very important features for medical applications since these properties facilitate the entry of SeNPs into the cells easily (Baran et al., 2023). A study used sea buckthorn leaves extract to greenly produce SeNPs showed a pseudo-spherical shape (Dima et al., 2024). According to a recent investigation, TEM images demonstrated that the mean diameter of the selenium nanoparticles created using *Allium paradoxum* extract was 37.5 nm (Alizadeh et al., 2023).

3. Biological activities

Two methods were used in this investigation to assess the antioxidant properties of SeNPs green produced using *S. maritimus* leaves aqueous extract. DPPH scavenging property estimates when DPPH molecules is a stable through taking of hydrogen or electrons from the antioxidant agents (Vyas & Rana, 2018). FRAP assay, in which the ability of the agents in the sample to reduce ferric iron to ferrous iron indicates their antioxidant activity (Perera et al., 2016). Our results demonstrated that *S. maritimus* extract and SmE-SeNPs had an antioxidant activity compared to ascorbic acid. According to Hernández-Díaz *et al.* (2021), antioxidant compounds work via a variety of mechanisms, based on the substance's makeup and capacity to interact with the substrate in which it dissolves. A plant extract antioxidant capacity is influenced by the quantity of phenols it contains because the phenolic compounds represent the more bioactive substances that have a therapeutic biological effect (Adhikari et al., 2020). An

investigation used DPPH and FRAP assays to demonstrate the antioxidant efficacy of selenium nanoparticles green produced by *Geobacillus* cell-free extract (Kumar et al., 2020). It was also established that SeNPs possess the capacity to scavenge free radicals and regulate their production, which makes them useful in biomedical applications (Hernández-Díaz et al., 2021).

The effectiveness of *S. maritimus* extract to inhibit protein denaturation can be due to presence of secondary metabolites in our plant extract, such as phenols and flavonoids, which have shown through several studies to have potent anti-inflammatory activities (Truong et al., 2019). Furthermore, Hilton-Simpson discovered that *Sonchus maritimus* had previously been utilized in Algeria during the 20th century for the treatment of inflammation of the eyes (Helmstadter, 2016). Previous study informed that nanoparticles of Se, which biosynthesized with extract of *Clitoria ternatea,* had a potential anti-inflammatory properties (Barma et al., 2022). Recent research on the synthesis of SeNPs by an aqueous extract of different plant parts, including leaves, fruits and flowers, demonstrated that biochemicals including phenols, carboxylic acids, amines, terpenoids, sugar, and alcohols, may be involved in the stabilizing of SeNPs and the reducing of selenium ions, in addition to their role as a mediator of the anti-inflammatory activity of SeNPs through their presence in surface of the bioproduced nanoparticles (Pandiyan et al., 2022).

In this study, the anti-hemolytic properties of *S. maritimus* leaves extract and SmE-SeNPs were assessed for their ability to protect and stabilize RBC membranes. Because the membrane of an erythrocyte is thought to be similar to the membrane of a lysosome, the stabilization of the membrane by plant extract or nanoparticles signifies the stabilization of the membrane of the lysosome (Patil et al., 2023). The primary mechanism for the RBC membrane protection by *S. maritimus* leaves aqueous extract is related to the bioactive chemicals found in the extract, which reduce inflammation and cell damage by decreasing lipid peroxidation (Oruka & Achuba, 2023). The results showed that SmE-SeNPs suppressed hemolysis as a form of anti-inflammatory treatment, which was supported by previous research conducted by (Dhabian & Jasim, 2023) in which they synthesized SeNPs using an extract from *Elettaria Cardamomum*, and showed that the plant extracts and its nanoparticle-solutions were not harmful for human erythrocytes. Our findings suggest that the greenly produced SeNPs from *S. maritimus* leaf extract could be a useful and interesting anti-inflammatory product.

The results of the α-amylase inhibitory experiments indicate that *Sonchus maritimus* extract and SmE-SeNPs exhibited a potential ability for inhibition compared to acarbose. The test samples showed that the aqueous extract had the highest potential for suppression the enzyme. The components of the extract were revealed by the analysis may be related to the

higher level of activity that the extract exhibited. Various studies proved that the extract has been discovered to include essential phytochemicals such phytosterols, aromatic compounds, terpenes and their derivatives...etc that have the ability to inhibit α-amylase *in vitro* (Chike-Ekwughe et al., 2023; Jelenković et al., 2014). Our research finding supported by recent investigation that used SeNPs phytofabricated by *Moringa oleifera* to inhibit α-amylase *in vitro*, and confirmed that the capped agents which is phytocompounds and the size of SeNPs may have a role in inhibiting the activity of carbohydrate enzyme (Ahamad Tarmizi et al., 2023).

Leaves extract of *Sonchus maritimus* demonstrated excellent activity to increase the uptake of glucose by yeast cells and enhanced absorption of glucose more than metformin which is typical medication and widely recognized for its ability to cause hypoglycemia (Khan et al., 2023), suggesting that the extract may be able to discharge glucose into the cells, this is consistent with a prior study on hypoglycemia (Abdulrasheed-Adeleke et al., 2023). Selenium has been demonstrated in previous research to improve cell absorption and transport of glucose (Varlamova et al., 2021). The antidiabetic capability of biosynthesized metal NPs is expected to be enhanced by biomolecules, indicating that these particles may have the potential to be effective antidiabetic agents for the treatment of diabetes (Shwetha et al., 2020).

In our study, the adsorption capacity of SmE-SeNPs and *S. maritimus* leaf aqueous extract with glucose molecules was much better than standard which is metformin at all experienced concentrations. The adsorption activity of the extract might be due to the existence of phytochemicals. Whereas in intestinal lumen, the glucose adsorption by extract may help in decreasing the postprandial increase of blood glucose level. These biomolecules may enhance the viscosity of the fluids contained in the small intestine and give a barrier in the passage of glucose from the luminal into the circulation. Or may bind with glucose, which would reduce their concentration in the small intestinal lumen (Rehman et al., 2018). Research demonstrated that metal nanoparticles had a greater capacity to bind glucose than did plant extracts, suggesting that these NPs may function as a possible barrier to reducing blood glucose levels by preventing the transit and absorption of glucose in the intestinal tract (Sharma et al., 2023).

SmE-SeNPs demonstrated a significant antibacterial activity, however *S. maritimus* aqueous extract exhibited negligible action against both Gram-negative and Gram-positive bacteria. An earlier study confirmed the antibacterial activity of selenium nanoparticles against Gram-positive bacteria including *Escherichia coli* and *Staphylococcus aureus* through the inhibitory zone (Milovanović et al., 2021). Our findings are consistent with previous research showing that the antibacterial activity of SeNPs remains unclear and that variations in the synthesis conditions of SeNPs themselves influence on their action mechanism (Shoeibi &

Mashreghi, 2017). Just now, numerous studies have been carried out to demonstrate the anti-microbial capabilities of nanoparticles against Gram positive and Gram negative bacteria, while the concept's underlying molecular insights have not been fully investigated (Vinu et al., 2020). However, there are some theories about their antibacterial activity. Menon et al. suggested that SeNPs can induce oxidative stress due to the production of reactive oxygen species that lead to protein denaturation by interacting with thiol and sulfhydryl groups of transmembrane proteins or interacting with intracellular proteins, thus inhibiting the food and respiratory metabolic pathway, leading to DNA damage by deteriorating DNA replication and leading to cell death (Menon et al., 2020). Sarkar *et al.* (2022) informed that bacterial cells were probably killed by the SeNPs with bioactive molecules that coat their surface, which increases the importance of SeNPs for use in the biomedical field.

Evaluating the ability of SmE-SeNPs to reduce or stop the proliferation of cancer cells allows the detection of anti-cancer activity. In other study, the exposition of MCF-7 cells to biosynthetic SeNPs made using Acinetobacter sp. sW30, showed the same morphological alterations as we had discovered in our experiment (Wadhwani et al., 2017). These changes result in early apoptosis during the intracellular ROS generation pathway. Apoptosis, or programmed cell death, is the result of various elements of the cell being destroyed by such an oxidative stress situation, including DNA, proteins and other organelles (Benithaj et al., 2023). Based on the findings of Ahmad et al. (2015), SeNPs' potential to reduce Cu (II) to Cu (I) by binding is one mechanism that might be responsible for its anticancer action. Reactive oxygen species are subsequently produced by the regeneration of Cu (II), and since malignant cells have elevated copper levels, they more frequently destroy cancer cells. Thus, MCF-7 cells may be more susceptible to ROS generation due to electron transfer between copper ions and Se nanoparticles in cancer cells (Ahmad et al., 2015).

II. *In vivo* study

Metabolic syndrome (MetS) defines as a combination of metabolic disorders that co-occur, among them dyslipidemia, insulin resistance, hyperglycemia, oxidative stress and pro-inflammation state, it further relates to a pathophysiological state that includes an increased risk of developing type 2 diabetes (T2DM), cardiovascular disease (CVD), gout, non-alcoholic fatty liver disease (NAFLD), chronic kidney disease, gout, neuroinflammation disease and hypogonadism disease (Gorbachinsky et al., 2022; Rodríguez-Correa et al., 2020). Fructose is a widely used glucose isomer in modern industry, and it has been shown in epidemiological investigations that high fructose intake has been an etiological factor for MetS in the last few decades (Semnani-Azad et al., 2020). Fructose is a simple ketose mono-saccharide that enters

enterocytes through the brush surface of the small intestine and is absorbed directly by glucose transporter (GLUT 5). It is afterwards transported out of enterocytes to the blood by GLUT2, which positioned at the basolateral pole of the enterocytes (Jones et al., 2011). It is hypothesized that after fructose enters the bloodstream, the majority of it gets absorbed and metabolized in the liver through the portal circulation. Accordingly, at least a part of burden of the fructose metabolism on extrahepatic tissues due to direct or indirect metabolites resulting from the metabolism of fructose in the liver (Pan & Kong, 2018). In fructolysis pathway, fructokinase and aldolase B catalyze the synthesis of dihydroxyacetone phosphate, that is utilized to generate glycerol, which is necessary for lipogenesis activities, and glyceraldehyde, which enters the glycolytic or gluconeogenic pathway (Tappy & Rosset, 2017). Triose kinase is also essential for the metabolism of fructose due to the fact that it increases the storage of fat in the liver (Liu et al., 2020). In contrast to glucose, its metabolism is precisely controlled by phosphofructokinase, metabolism of fructose is not susceptible to this limitation, thus fructolysis has infinite potential. Due to a lack of regulation, a significant amount of substrate is produced and used in several metabolic pathways (glycolysis, gluconeogenesis, glycogenesis, and oxidative phosphorylation) in accordance with cellular needs (Hannou et al., 2018). A high fructose levels stimulates the synthesis of malonyl CoA, which prevents the oxidation of fatty acids and causes an accumulation of triglycerides in hypatocyts, consequently, increases the synthesis and secretion of very light density lipoproteins (Coronati et al., 2022). Additionally, fructose stimulates insulin resistance which alters lipid profiles, involving change of triglycerides, free fatty acids, total cholesterol and increase of diacylglycerol in liver and plasma (Pan & Kong, 2018). Furthermore, the limitless of fructolysis needs more ATP production for fructose phosphorylation by phosphofructokinase, which increases generation of reactive species through extra activation of oxidative phosphorylation. These can disrupt insulin signaling pathway in hepatic and extrahepatic tissues (Pan & Kong, 2018). It is well recognized that oxidative stress promotes inflammation and is crucial to the IR process. The electron transport chain's process leads mitochondria to produce a substantial amount of reactive oxygen species (ROS). This increases the risk of DNA damage by raising the degree of oxidative stress adjacent to the mitochondrial DNA. Stress levels could increase if the mechanisms for DNA repair were disrupted, which could cause IR (Ziolkowska et al., 2021). Oxidative stress stimulate several kinds of stress pathways, alters transcription factors, and promotes the production of proinflammatory cytokines, it also leads to metabolic problems like decreased glucose tolerance and lipid disorders which in turn lead to MetS (Lee & Jose, 2021).

1. Acute toxicity study

Depending on particular behaviors and factors in toxicological control, including eye health, mobility, sleep patterns, diarrhea and mortality (Derouiche et al., 2020). The results distinctly demonstrated that the administration of *S. maritimus* extract and SeNPs did not lead to any mortality or proof of toxicity. It has been confirmed that *Sonchus maritimus* extract is not considered toxic due to its pharmacological properties (Fouad et al., 2020), and it has been proven for use in traditional medicine (Helmstadter, 2016). Furthermore, acute and subacute toxicity tests were performed in mice confirmed the establish safety of extract of *Sonchus oleraceus* L. aerial parts which is belong to Sonchus genus of Asteraceae family (Aissani et al., 2022). The safe and beneficial uses of eco-friendly produced selenium nanoparticles have been reported by Ranjitha & Rai (2021). Moreover, an acute toxicity research study on selenium nanoparticles in rats showed that there was no selenium toxicity specific to nanoparticles (Hadrup et al., 2019). Green synthesis of SeNPs has advantages over the chemical and physical approach owing to their biocompatibility and in vivo actions, whereas it has been proven that uncoated and chemically synthesized NPs have a higher genotoxic and cytotoxic effect than coated and green synthesized NPs, which makes their biocompatibility typically due to phytocompounds in plant extract (Derouiche et al., 2022). According to our results, SmE-loaded niosomes may be considered non-toxic and safe for *in vivo* studies because our formulated niosomes encapsulated safe bioactive substances, either S. maritumus extract or SmE-SeNPs, and were constructed using safe components. Tween 80, also known as Polysorbate 80, is a synthetic nonionic surfactant frequently used in drug formulations, cosmetics, and food as a stabilizer or emulsifier due to its safety *in vivo*. It is composed of esterified fatty acids of polyoxyethylene sorbitan. The fatty acid construction is primarily oleic acid, while other fatty acids, like linoleic or palmitic acid, may be included. Tween 80 is quickly removed from systemic circulation in each of clinical or animal studies. In addition, in vitro studies have proposed that tween 80 is metabolized by rapid carboxylesterase-mediated hydrolysis (Schwartzberg & Navari, 2018). Cholesterol is an important molecule, able to control a variety of biological functions, including the fluidity of membranes. As the building block of all steroid hormones and vitamin D analogs, cholesterol also functions as a regulatory molecule in and of itself (Schade et al., 2020). There has been a great deal of interest in the use of natural compounds as medications, particularly polyunsaturated fatty acids like linoleic acid, which are useful as functional dietary "bioactive lipids" (Hegazy et al., 2019). It targets the liver to control energy metabolism as well as maintain metabolic balance (Yustisia et al., 2022).

2. Growth parameters

Rusults of previous investigation shown that giving mice a high-fructose diet in drinking water for ten weeks caused the loss of mice's terminal body weight, and it also decreased the amount of food and liquids they consumed each day (Akar et al., 2012). Maintaining of a stable body weight is countered by an increase in metabolic demands, whereas changes in cellular utilization of energy are associated with the maintenance of a reduced or increased body weight (Olajide et al., 2017). It confirmed that HFD induced insulin resistance without obesity in rats (Bugga et al., 2022). Furthermore, it has been previously reported that fructose supplementation lowers food intake (Gancheva et al., 2015). All of these variables were improved by the niosomes of *S. maritimus* aqueous extract and SeNPs, particularly the body weight, which was correlated with an increase in food and water intake due to phyto chemicals in the extract. Previous work has found that a plant's aqueous extract may regain the total body weight (Ahmad & Zeb, 2019), and linoleic acid in SmE-N is a polyunsaturated fatty acid that enhances body composition and increases muscle mass, which explains its widespread use in body configuration (Hegazy et al., 2019). SeNPs inhibit weight loss of mice, which may be explained by their ability to decrease glycogenolysis and proteolysis. Food intake is associated with energy intake as well as complicated neurological and hormonal pathways that affect appetite and satiety modulations. SeNPs additionally regulate the amount of water consumed (Gutiérrez et al., 2022).

Our results indicated that fructose increased the relative liver, heart, kidneys and testiculs weight. Similar results of relative liver and heart weight have been showed in previous experiences on animal model due to augmentation of tissue mass of the liver and heart (Andrade et al., 2020; Li & Lu, 2018), as result of necrosis and inflammation of the tissues (Derouiche et al., 2022) as proved in histological study. The increased triglyceride content in the kidneys may have contributed to the considerable increase in the relative kidney weight of the HFD rats compared to the control group (Bier et al., 2022). The change of relative testiculs weight in HFD group due to reproductive alterations in the testicles (Tkachenko et al., 2020). The beneficial effect of our niosomal therapeutic system containing *sonchus maritimus* extract to reduce and improve relative organs weight reflects the importance of our formulated drug delivery system in delivering the phytochemicals in the plant extract which have the ability to limit the pathogenesis of disease and reduce free radicals in tissues which in turn lowering lipid peroxidation, inflammation, and serum triglycerides (Al-Megrin et al., 2020; Alkreathy et al., 2014). Biosynthesized selenium nanoparticles revealed their potential effects against oxidative stress

and inflammation in HFD-fed mice, enhancing the results of treated group with SmE-SeNPs (Martínez-Esquivias et al., 2024).

Additionally, SeNPs-SmE-N treatment which provided positive results for growth parameters similar to each alone treatment, demonstrating the therapeutic efficiency of the combination of both niosomal and nanometric systems, which may be through the combined effects of SeNPs and *S. maritimus* leaves extract to improve functioning of organs that have altered due to exposure to high fructose diet.

3. Liver glycogen level

The decline of hepatic glycogen level in rats fed high fructose diet is associated to resistance to insulin and glucose tolerance, This information could be used to demonstrate how fructose cannot increase the production of insulin from pancreatic β-cells because the fructose transporter, GLUT 5, is not highly concentrated in the described cells (Chenni et al., 2022). It has been demonstrated in prior studies that the Sonchus genus increases the production of liver glycogen by activating phosphoenolpyruvate carboxykinase, an essential enzyme that controls hepatic gluconeogenesis (Yuan et al., 2019). Additionally, linoleic acid, which is included in niosomes, can be increased the amount of glycogen in the liver (Sukanya et al., 2020). According to previous investigations have suggested that selenium can be responsible to activate kinases that control the signaling pathway of insulin and metabolism of glucose (Abo-zalam et al., 2023). The elevated hepatic glycogen levels by the biosynthesized SeNPs could be explained by the combined action of selenium element and bioactive substances that cover their surface, to stimulate the release of insulin hormone from cells of the pancreas and activate the enzyme glycogen synthase which is key to glycogen synthesis (Gutiérrez et al., 2022). The combination of selenium nanoparticles and *S. maritimus* extract in niosomes appeared similar results of each alone therapeutic systems may be related to the metabolic effect of this formulation on the restoration of glycogen regulation through amelioration of signaling pathway of insulin and glucose metabolism.

4. Biochemical parameters and lipid profile

The high-fructose diet's rise of blood glucose levels and alteration of lipid profile in this study are supported by other investigations (Feyisa et al., 2019; Said et al., 2021). The increase in the amount of glycosylated hemoglobin in blood have resulted from the elevation of glucose levels in the blood that observed in animals fed fructose diet (Mahesh et al., 2021) as consequence of the insulin resistance (Hadzhibozheva et al., 2023). Gallic and vanillic acids in

Sonchus maritimus extract which contained in niosomes may be responsible for the hypoglycemic impact of SmE-N. In fact, it was discovered that they improved the metabolism of carbohydrates in the liver and caused a considerable drop in fasting glucose levels (Benkhaled et al., 2022). Further, the integrated linoleic acid into niosomes formulation may be implicated in lowering blood glucose levels (Sukanya et al., 2020). The reduced blood glucose level resulting from the biosynthesized SeNPs might have been related to the paired action of Selenium and the phytosubstances of surface through promoting insulin synthesis and secretion from pancreatic cells β (Gutiérrez et al., 2022). The results of other experiment demonstrated that SeNPs have an antioxidant action that inhibits lipid peroxidation, which may be caused the decrease in glycosylated hemoglobin in SeNPs group (Gutiérrez et al., 2022).

The consumption of fructose induces insulin resistance, which is defined as a specific condition in which the cells fail to respond normally to insulin, whereas insulin is an effective lipoprotein lipase activator that promotes the catabolism of triglycerides in lipoproteins (VLDL, chylomicrons) and enhances LDL clearance through the LDL-receptor way. For that, The majority of lipid abnormalities are related to the insulin resistance condition (Kuefner, 2021; Shang & Rodrigues, 2021). HMG-CoA reductase is an enzyme found in hepatocytes, responsible to regulate the rate of cholesterol synthesis (Hasimun et al., 2019). According to research work, the consuming 20% fructose in water used for drinking over a 12-week period by rats, enhanced HMG-CoA reductase production and activity, which causes an excessive amount of endogenous cholesterol to be synthesized (Kumar et al., 2021). There is a lack of knowledge regarding the basic mechanisms by which excessive fructose causes dyslipidemia (Ichigo et al., 2019). The effect of SmE-loaded niosomes didn't clearly appeared improving the lipid profile in general but their effect clearly appeared in HDL-C and LDL-C levels, which may be due to the polyphenols molecules as informed in preceding studies that caffiec and chlorogenic acid and have confirmed their useful consequence on lipid metabolism when they inhibit the activity of HMG-coA reductase, lower levels of total cholesterol, LDL-C and rise HDL-C level, with reduce the amount of circulating triglycerides and their accumulation in hepatocytes (Nwafor et al., 2022; Y. Wang et al., 2022). Niosomal linoleic acid may contribute to lowering the level of plasma lipids since it has a notable hypolipidemic effect as report in study of to Mokhtari *et al.* (2022). SeNPs enhanced capacity to transform cholesterol to bile acid compounds, coupled with their decreased synthesis of cholesterol and LDL receptor activation. Furthermore, it was observed that Se supplementation enhanced the gene expression levels of the cholesterol esterification enzyme while lowering the expression of HMGR

(Abdallah et al., 2023). These mechanisms might be responsible for the hypolipidemic impact of SeNPs.

Glutamyl-oxaloacetate transferase (GOT) and glutamyl-pyruvate-transaminase (GPT) are among the most critical hepatic enzymes that pass into the circulation if the liver gets injured or impaired, which making them essential biomarkers enzymes for assessing hepatic dysfunction (Campos et al., 2020). Our results indicated that a high-fructose diet increases the rate of transaminase enzymes activities in blood of animals, these findings agree with a study of Alemán *et al.* (2022) that found that a 10% fructose liquid raises the activities of GOT and GPT. The potential hepatoprotective impact of *S. maritimus* extract -loaded niosomes has been shown through a considerable reduction in the level of these enzymes in plasma; a prior investigation shows that flavonoids, including quercetin and rutin, effectively lower the hepatic aminotransferase activities in HepG2 cells and prevent them from hepatotoxicity (Lee et al., 2019), in addition to incorporated linoleic acid in SmE-N for reducing significantly the ASAT and ALAT enzymes levels in blood (Azemi et al., 2023). An earlier study showed that SeNPs reduce the ALAT and ASAT activities to their usual levels; this finding could be connected to selenium's ability to neutralize free radicals and its involvement in maintaining the functional and structural unity of tissues (Al-quraishy et al., 2023).

Metabolic syndrome increases kidney function parameters, including high level of creatinine, blood urea and uric acid (Lin et al., 2022). Since it has been suggested that uric acid concentration increases caused by a metabolic syndrome, may play a role in the development of whole-body insulin resistance (Debray et al., 2021). It is well known that elevated uric acid synthesis decreases endothelial nitric oxide (NO), which in turn causes endothelial dysfunction and decreased skeletal muscle insulin utilization (Bratoeva et al., 2017). Excessive consumption of fructose lead to oxidative stress state that affect the renal system and induced its dysfunction, which cause the increase of mention biomarkers (Qiao et al., 2018). In this study, *S. maritimus* extract proven its effect to improve levels of urea and uric acid in blood, it may be due to its phytochemicals that ameliorate the biomarkers level through their antioxidant effect in the body (Salehi et al., 2019). The potential therapeutic effect of single and combined administration of SeNPs is by the ultra- small size and surface of nanoparticles playing an important role in their bioavailability, as well as their antioxidant effect, thus improving kidney function (Hassan et al., 2021).

Lower serum testosterone is due to primary hypogonadism and alteration of testicular cells in rats compared to controls, which induced by high-fructose feeding due to the oxidative stress, as confirmed previously (Tkachenko et al., 2020). In our study, testosterone level was

increased by our therapeutic system (SeNPs) but not significantly which may be due to the severity of testicular destruction but the restoration effect was demonstrated in the histological section of testes in the current study.

The therapeutic system (SeNPs-SmE-N) showed hypoglycemic and hypolipidimic effects with amelioration of renal and hepatic markers may be due to metabolic contribution through hepatoprotective, nephroprotective proprieties either by stabilizing the membrane to prevent malfunctions or by combating inflammatory or oxidative stress pathways.

5. Acetyl cholinesterase activity and clinical grading scores of rat's behaviors

Our findings showed that excessive fructose consumption inhibits the activity of AChE, as evidenced by a notable decline in activity in all rats fed a high-fat diet. This last causes an accumulation of acetylcholine induces hyper-stimulation of muscarinic and nicotinic receptors, disrupting neurotransmission in cholinergic synapses (Lazarevic-Pasti et al., 2017). According to other study, the inclusion of chlorogenic acid in the extract of *Sonchus maritimus* promotes the activity of AChE and exhibits a neuroprotective effect to the brain of rats, which explains the return of AChE activity by *S. maritimus* extract-loaded niosomes treatment (Metwally et al., 2020). According to a prior study, selenium (Se) may influence the cholinergic system by preventing the activity of acetylcholinesterase (AChE) in the rat brain (Tarmizi et al., 2023). It has been confirmed that a diet high in fructose causes neuroinflammation and metabolic malfunction, which in turn causes neurological and behavioral problems (Harrell et al., 2018). The clinical score grade improved by alone treatment of niosomal (SmE-N) and nanoparticles (SeNPs) systems and their combination treatment (SeNPs-SmE-N) which may be related to amelioration of acetylcholine esterase activity and oxidative stress situation in brain.

6. Protein levels

Excessive fructose consumption has been linked to the accumulation of fat in the liver, which can lead to non-alcoholic fatty liver disease (NAFLD), which damages the liver and causes oxidative stress and hypatocytes irritation (Li et al., 2022). The process of oxidative stress may lead to cell destruction and alter the structure of macromolecules, including proteins, through a variety of mechanisms. Among them, it can add a carbonyl group to protein molecules via a reaction with lipid peroxidation or an interaction with pro-oxidants (Bachi et al., 2013; Muñoz et al., 2018). Large aggregates formed in hepatocytes by carbonylated proteins are usually resistant to degradation mechanisms by proteases (Nair et al., 2021). The raise of protein in brain of HFD rats can be explained by direct effect of fructose consumption to upregulate

beta-secretase-1 enzyme, to accumulate Aβ plaques and to phosphorylate tau protein, in addition to enhance the production of pro-inflammatory mediators (such as IL-6 and TNF-α) as what reported in previous research papers (Khan et al., 2021; Mohamed et al., 2021). It proven that metabolic syndrome can be responsible to enhance also the transcription and production of pro-inflammatory proteins that contribute to induce oxidative stress in renal tissue, thus increase the percentage of protein in kidneys (Flisiński et al., 2022). The high protein in the heart of our experimental rat may be caused by elevation of the collagen accumulation in the heart of the metabolic syndrome model animal by fructose consumption as mentioned previously (Yeşil & Özer, 2023). It has been theorized that a rise in matrix metalloproteinases, which cause tissue fibrosis, may be the cause of cardiac fibrosis. when the production of ROS promotes their release (Ahmed et al., 2020). Study of Akar *et al.* (2022) showed the opposite of the results we obtained regarding the protein level in testicular tissue.

The protein level decreased by SmE-loaded niosomes may be recovered using flavonoids, such as quercetin, rutin, and naringin, as well as linoleic acid in SmE-N, which also inhibit pro-inflammatory cytokines and prevent unusual Aβ accumulation and tau protein hyper-phosphorylation (Agwa et al., 2020; Meng-zhen et al., 2022). It shown that inhibiting NF-κB, one of the primary inflammatory mediators, in renal endothelial cells halts the signaling cascade, which lowers kidney inflammation. Since flavonoids are secondary metabolite substances found in plants that have a crucial impact on kidney physiology, including nephro-protective effects, numerous research have been conducted to scientifically verify that plants can be utilized to treat kidney illness (Sujana et al., 2021). Medicinal plants proven also its efficiency for reducing collagen accumulation and decline their expression in the cardiac tissue (Shabab et al., 2021). The high content of phenolic substances in the leaves extract of *S. maritimus* and its antioxidant activity helps to normalize the structure and function of the testicles, which contributed to restore protein level in testiculs (Mekki et al., 2023). Treatment with nanoparticles of selenium can attenuate oxidative damage in the liver and kidneys of rats due to its bioavailability in the tissues due to their small size (Qiu et al., 2022).

Selenium (Se) is an important trace element for brain function, works to reduce and inhibit the aggregation progression of amyloid b in brain through preventing oxidative stress (Luo et al., 2023). Selenium nanoparticle demonstrated its effect against cardiac fibrosis and confirmed by the histological assessment as described in study of (Moghaddam et al., 2022). Findings from previous investigation showed the synergistic impact of SeNPs to attenuate testicular oxidative damage and to regulate their functionality pathways in rats (Ebokaiwe et al., 2020).

Co-treatment of SeNPs and extract of *S. maritimus* using niosomes as drug delivery system of these materials demonstrated also its efficiency to restore protein levels in different tissues including brain, heart, kidneys and testiculs, may be by the various therapeutic approach against pathogenesis agents that mention above.

7. Hematological parameters

Hematological analysis is crucial to assess the health status, it provides image about erythrogram and leukogram, since any variation in these parameters suggests that there is evidence of a particular disease (Bojarski et al., 2021). According to our data, MetS induce a significant decrease on erythrogram results, including red blood cells, hemoglobin and hematocrit, which is agrees with previous study that suggest that MetS in rats stimulates erythrocyte hemolysis and a decrease of erythrocyte number in blood, which referred to as high lipid profile markers that elevate production of peroxides species and oxidative stress which could destroy plasma membrane and cytosolic constituents, leading to oxidative hemolysis of red blood cells and dropped survival of oxidized RBCs in the circulation (Arafa et al., 2023). A similar findings in a MetS rodent model revealed a decline in cellular immunity, whereas, the main probable cause of decreased leukocytes may be related to the increase of corticosteroid and IL-6 secretion in MetS, resulting in decrease of peripheral lymphocytes number and enhance bone marrow-derived neutrophil mobilization (Kilany et al., 2020). The inflammatory mediators typically increase with stress which leads to inflammatory injury of cellular components, including DNA, lipid and protein, inducing by the overproduction of reactive oxygen and nitrogen species, which is exacerbated by mitochondrial damage, and contributes to decline in physiological functions particularly immune, neural and endocrine systems that control homeostasis (Cardinali & Hardeland, 2017). Platelets have the ability to repair the endothelium through stimulation of hemostatic responses , the occurrence of metabolic disorders, such as impaired glucose homeostasis, insulin resistance and dyslipidemia, alter platelet function and increases the tendency towards thrombus formation and arterial occlusion, may be due to hyperactivation ad platelet hyperaggregability (Barale & Russo, 2020).

The antioxidant activity of *S. maritimus* extract may contribute to provide hematoprotective potential due to phytoconstituents like phenolic compounds, steroids, flavonoids and tannin via their anti-free radicals power activities, in addition to elemental contents like iron, zinc, calcium, phosphorus and potassium, which are critical substances to assure the restore RBC, hemoglobin and hematocrit levels in blood (Kamble et al., 2019). Niosomes administration restored the HFD-induced changes in the leukogram of MetS group

through the inhibitory effect of flavonoids include more particularly the apigenin and kaempfero, against inflammatory cytokines expression via repressing the transcription of genes encoding to the cytokines (Lim et al., 2015). This reflect the immunomodulatory effect of Sonchus plants as reported in current study (Wahyuni et al., 2023). Our results showed that the platelet count is decreased in SmE-N due to flavones in the extract as reported in recent investigation (Ren et al., 2023).

The potent antioxidant property of selenium nanoparticles (SeNPs) may help maintain the stability and integrity of cells whereas protecting them from hemolysis, numerous studies have demonstrated the role of selenium in enhancing the hematological indices including hematocrit, hemoglobin, and the number of red blood cells (Khan et al., 2016; Saffari et al., 2018). The incorporation of selenium in the tridimensional structure of selenoproteins, which plays a significant role in immunomodulation and redox balance, may be the cause of the immunomodulatory effect of SmE-NPs in this study, while, the primary role of selenium is to enhance immune responses through its positive effects on immune cell differentiation and proliferation as well as immune cytokine secretion (Jin et al., 2021). SeNPs play an essential role for preventing cardiovascular diseases by decreasing platelet hyperactivation and aggregation and strengthening the antioxidant defense mechanism against oxidative modification of lipid (Amini & Mahabadi, 2018).

The hematological and immunological regulation effects shown by niosomal approach of co-treatment by SeNPs-SmE-N, which may be due to protective activity either through the antioxidant power to protect elements of blood or by modulation of immune system.

8. Oxidative stress markers

Excessive intake of fructose leads to an imbalance in antioxidant defense system and an increase in the production of free radicals in various tissues (Gubur et al., 2022; Shi et al., 2018). A high consumption of fructose (MetS) causes an increase in reactive species formation, which alters the antioxidant balance and allows greater amounts of reactive species to be retained in the cells (Mehta et al., 2021). The neutralization of reactive oxygen species (ROS), reactive nitrogen species (RNS), and other free radicals is enhanced by glutathione (GSH) which named "master antioxidant" (Cazzola et al., 2021). Glutathione represent the active thiol group found in cells. The amount of cellular thiols is regulated by processes related to their fundamental antioxidant activity, as well as by their synthesis and elimination from cells through glutathione redox cycles and conjugation with xenobiotic (Kütük et al., 2023). GSH is among the most favored co-factor reducing reagent for mammalian GPx enzyme (Weaver & Skouta, 2022). For these reason, the

high-fructose diet in this study caused the decreasing of total thiol levels and altered the total antioxidant activity in different organs of rats' body. Our research study showed that rats' liver MDA levels were markedly elevated by excess fructose intake, while the SOD and GPx activities were inhibited. These findings have been confirmed by other studies which revealed that elevated liver MDA are a crucial sign of oxidative impairment of liver cells (Wang et al., 2020). Deficits in the activities of the enzymatic antioxidant system, such as superoxide dismutase (SOD) and glutathione peroxidase (GPx), with lowering of total glutathione cause increasing of lipid susceptibility to peroxidation and oxidative damage. These alterations may occur as a precursor to the development of oxidative stress (Chenni et al., 2022). Montesano *et al.* (2020) state that the accumulation of fat in the liver causes a decrease in SOD, which is a primary and significant antioxidant defense line. The present study revealed a notable decline in brain antioxidant markers after 15-week of high-fructose diet intake. These findings correspond to previous research, which indicated that long-term fructose consumption causes oxidative stress, lowering reduced glutathione levels and inhibiting cerebral enzymatic antioxidant activities, as SOD and GPx. (Ekici et al., 2022; Spagnuolo et al., 2021). One characteristic of metabolic syndrome (MetS) that has been significantly linked to the development of several cardiovascular diseases is the imbalance between the high generation of ROS and the failure of endogenous antioxidant activity in individuals with MetS (Arias-Chávez et al., 2022). In a study, the rats with MetS proves the presence of oxidative stress in kidney tissue by increase of MDA levels, and decrease of antioxidants markers that inversely correlated with MDA levels. Where, the antioxidant activity decreases in MetS due to activation of inflammation process which causes an increase in free radical production due to pro-inflammatory mediators (Şener et al., 2020). Furthermore, metabolic disorders may enhance endogenous oxidants by elevation of MDA levels and downregulating of SOD, GPx and GSH, which in turn can cause excessive oxidative stress in the testes (Ebrahimi et al., 2023).

Due to flavonoids as well as phenolic compounds' ability to successfully prevent lipid peroxidation, neutralize peroxyl radicals ($ROO^{\cdot}$), and eliminate oxidizing free radicals like superoxide ($O_2^{\cdot-}$) and hydroxyl radicals ($OH^{\cdot}$), SmE-loaded niosomes was able to reduce the oxidative stress which was caused by a diet rich in fructose in each of liver and brain (Ahmed et al., 2022; Mondal et al., 2021). Due to the potent antioxidant properties, which reduce tissue damage through reduction of oxidative stress, several prior studies have shown the hepatopotective and neuroprotective effects of both rutin and quercetin (Wang et al., 2021; Wu et al., 2021). Furthermore, metallic elements like manganese (Mn) which exist in *Sonchus maritimus* (Hameed et al., 2021) can act as co-factors and increase the activity of enzymes that

inhibit free radicals (Abdel-Magied et al., 2020). According to earlier researches, linoleic acid has the ability to enhance the liver's and brain's antioxidant defenses by suppressing ROS's interaction with proteins and lipids (Cigliano et al., 2019; Hao et al., 2021). It has been suggested that the antioxidant efficacy of polyphenols in the heart reduced the production of reactive oxygen species (ROS) by scavenging ROS and stimulating the expression of protecting antioxidant defending enzymes (SOD and GSH-Px) in the model of Mets rats. Moreover, flavonoids' potential to reduce lipid peroxidation was in the following order: quercetin, kaempferol, luteolin then apigenin (Liu et al., 2019). According to Salehi *et al*. (2019) Sonchus genus extract showed significant reduction in oxidative stress markers and high antioxidant potential in the kidneys, the beneficial effects might be attributed by their notable capability to scavenge free radicals, their hypoglycemic activity, and their ability to avoid oxidative stress, which may be responsible for the positive consequences in treated rats by the SmE-N. Previous results demonstrated that antioxidants enzymes activities as well as glutathione levels in the testiculs homogenate were significantly increased, while malondialdehyde and protein carbonyl levels were significantly lowered by riche extract with polyphenols, which are agree with our obtained finding in this study (Budin et al., 2018). Thus, it explains restoring of the antioxidants agents' levels and antioxidant activity in tissues due to efficiency of our formulated drug delivery system to deliver the bioactive substances in *S. maritimus* to affected sites.

Since selenium (Se) is an essential element for numerous biological processes, SeNPs effectively mitigated the oxidative stress in the liver caused by a high-fructose diet by inhibiting lipid peroxidation and increasing GSH levels, GPx, and SOD activity. Iodothyronine deiodinases, thioredoxin reductases, and glutathione peroxidases (GPx) are examples of seleniproteins which showed redox system homeostatic action in the context of oxidative stress and inflammation responses, in addition to biochemical and cellular survival (Abo-zalam et al., 2023). The increase levels of oxidative stress are resulting in the destruction of nerves and neurobehavioral problems. SeNP reduced MDA levels, increased SOD and GPX activities, and protected neurons from oxidative stress. SeNPs can therefore be employed as a potential therapeutic drug to prevent behavioral changes related to neurological changes due to their extremely small size and availability to physiological systems thanks to the nanoparticle biosynthesis pathway via plant extracts (Varlamova et al., 2021). There are two possible explanations for the antioxidant action of SeNPs in the kidneys and heart of the rat that exposed to excessive fructose diet in this investigation. Firstly, the antioxidant selenoenzymes such GPx which inhibit the production of reactive oxygen species (ROS) may be effectively overexpressed

and activated by SeNPs. Secondly, SeNPs may also be converted into H_2Se after being absorbed into the body and then integrate into different selenoproteins because H_2Se is a precursor for the production of selenoproteins (Guo et al., 2020). The higher antioxidant activity of coated SeNPs may have contributed to the considerable restoration of the deficient antioxidant enzymes, including total SOD and GPx activities, and the suppression of the elevated MDA concentration in testicular tissue (El-hakim et al., 2021).

Moreover, in treated group by SeNPs-SmE-N approach, it noticed a significant amelioration of oxidative stress markers by reducing the lipid peroxidation and increasing the antioxidants system, which provided impression that this new niosomal nanotechnology approach has a great effect as power antioxidant, either by the superior capacity to avoid the generation and spread of free radicals or by up-regulation the enzymatic antioxidants, this combination treatment could also possess beneficial effect to stimulate tissues cells to increase the synthesis of non-enzymatic antioxidants like glutathione which translated by amelioration of total thiol levels in tissues.

9. Histological analysis

Histopathological examination of the present study revealed the deleterious effects of long-term exposure to a high-fructose diet on the liver, brain, heart, kidney, and testiculs structure sections of rats. Mirzaei *et al.* (2022) proved the histopathological changes in the hepatocytes and cerebral cells because of the harmful effects resulting from a high-fructose diet, which contributes to the generation of damaging free radicals in the tissues that cause inflammation and the appearance of vacuolar degeneration of cytoplasm in the liver's cells. Six weeks of drinking a liquid containing 30% fructose caused hepatic tissue inflammation, cell degradation, and hemorrhage (Yeşilot et al., 2022). Consumption of a high-carbohydrate diet by rats promotes hepatocytes to generate a significant number of intracytoplasmic vacuoles that called cytoplasmic lipid droplets which accumulate in excess as a result of fructose-induced lipid dysfunction (Agoun et al., 2021). These histologic alterations in the structure of liver cells have been linked to increased steatosis and damage, as well as to the infiltration of inflammatory cells and the activation of macrophage marker expressions (Schmidt et al., 2021; Virgen-Carrillo et al., 2021). In the fact, a high lipid inflow into the liver increases mitochondrial oxidative action, which advances the generation of ROS and stimulates the release of inflammatory cytokines that induce cell necrosis (Iskender et al., 2022). An inflammatory reaction in the brain initiated by fructose accelerating the extracellular formation of amyloid beta (Aβ) and the intracellular formation of phosphorylated tau protein (p-tau) which affect the neural protective antioxidant

system (Gomaa et al., 2022; Shandilya et al., 2022). The study's findings indicate a potential role for MetS in the advancement of cardiac disease in rats, which manifests as heart tissue deterioration resulted due to the presence of fibrotic cells and hypertrophic cardiac cells as well as the presence of inflammatory cells in heart tissue. The change in the histology is evidence of chronic inflammation, which begins as an adaptive response in the myocardium and progresses to activate free radicals and cell hypertrophy through increased protein synthesis and alterations in the configuration of the sarcomeric structure. Prolonged inflammation raises TNF-α production, which triggers IL-6 release, which causes cell hypertrophy and inflammatory cells infiltration (Handayani et al., 2021; Vashishth et al., 2022). Additional research revealed that rats given fructose had histological impairment of the kidneys, including glomerulosclerosis, Bowman's space dilatation, necrosis and infiltration of mononuclear cells in the interstitium. Further, the experimental group's kidneys showed an increased tubulus proximalis area, it was suggested that this increase might have been brought on by the proliferation of tubular cells caused by the rats' high fructose diet, in addition to inflammation and oxidative stress, which are considered important factors to induce and to progress the kidney damage (Elsisy et al., 2021; Güleş & Tatar, 2020). In the current investigation, high-fructose intake lead to a rise in the percentage of irregular seminiferous tubules, which is supported by the findings of Medaglia *et al.* (2022) who found intratubular deterioration in the testicles of Wistar rats administered fructose. They also revealed the degeneration and loss of seminiferous tubules through a decrease in flagella condensation with spermatogonia and sertoli cell degeneration.

The efficiency of our niosomes to deliver the bioactive compounds of leaves aqueous extract of *S. maritimus* to deteriorated tissue due to MetS appeared through histological ameliorations in brain, heart, liver, kidney and testiculs sections. It suggests that these structural reparations are caused by bioactive substances in the plant extract found in niosomes. It confirmed that chlorogenic acid increases the activity of antioxidant enzymes, has an anti-apoptotic pathway and possess an anti-hemorrhagic effect in the liver (Koriem et al., 2018; Silva et al., 2022). Gallic acid, quercetin, vanillic acid and caffeic acid demonstrated their hepatoprotective proprieties through inhibition of infiltration of the inflammatory cells and reduction the number of intracytoplasmic vacuoles. (Golabi-habashi et al., 2021; Saleem et al., 2019). Many results regarding the neuroprotective benefits of phenolic acids and flavonoids such as quercetin, naringin, caffeic acid and rutin have been widely showed in several *in vivo* studies; these findings involve the anti-inflammatory properties of the compounds by inhibiting proinflammatory cytokine release and the antioxidant effect by strengthening the antioxidant

defense mechanism in the brain (Islam et al., 2022; Kadar et al., 2022). Furthermore, it has been demonstrated that linoleic acid supplementation is useful in reducing the severity of hepatic and cerebral destructions by lowering inflammatory cytokine levels and controlling the oxidative stress that is linked to the MetS condition (Alam et al., 2021; Han et al., 2019). Numerous studies have demonstrated a connection between the natural bioactive substances in food and the advancement of health and the prevention of disease. Bioactive substances such as triterpenoids, unsaturated fatty acids, flavonoids, phenolic compounds and their derivatives, phytosterols, and saponins are naturally found in medicinal plants, in addition to significant amounts of potassium, phosphorus, magnesium, and other minor minerals like copper, zinc, iron, calcium and manganese. The montioned minerals and bioactives have the ability to function at the same or separate target locations at the same time, providing physiological benefits, enhancing wellbeing, and lowering oxidative stress linked to heart disease, testiculs disorder, and problems of kidneys (Bagetta et al., 2020; Dotto & Chacha, 2020).

Treatment of experimental MetS rats by SeNPs provided a partial histological improvement in brain, heart, liver, kidney and testiculs tissues sections. Khiralla (2019) declares that significant liver protection has been achieved by the SeNPs therapy, as demonstrated in histological analysis, where SeNPs preserve liver cell membranes and provide protection against oxidative damage. On the other hand, therapy with SeNPs reduced neurohistological changes due to their antioxidant capacity in tissue through the down-regulation of ROS species (Bashir et al., 2021). Applications of nanotechnology include the delivery of antiamyloid therapies and neuroprotections against oxidative damage, which may be enhanced by distribution across the blood-brain barrier (Krol et al., 2013). The biosynthesis SeNPs restore cardioprotective metabolites by reducing MDA generation and restore the activities of antioxidant enzymes in order to improve cytoarchitectures of altered cardiac tissue, as shown in histopathological studies, because bio-SeNPs are more biocompatible and have less toxicity with potontial biological effects (Khan et al., 2022). Little impairment was detected in the kidneys of rats in research study of Martínez-Esquivias *et al.* (2024) due to the controlling impact of SeNPs against oxidative stress, which translated by the preservation of cell organelles and regulation of metabolic pathways in order to avoid the side effects of diet rich in fructose in treated rats. Other investigation confirmed also SeNPs through its antioxidant ability may be useful to avoid the testicular impairment in rat by dropping the oxidative stress pathways (Keshta et al., 2023).

The protective capacity of combined treatment by SeNPs and *S. maritimus* extract in the niosomal system (SeNPs-SmE-N) in different tissues including brain, liver, heart, kidneys and testiculs, may be provided using many biochemical ways and factors that contribute in the

alteration of mentioned organs, either associated with different molecules and mechanisms involved in the oxidative and inflammatory system.

Conclusion & Perspective

Conclusion

Metabolic syndrome (MetS) is one of the most prevalent syndromes worldwide that can lead to death due to its complications. The "one-compound-one-target" treatment approach has proved unsuccessful in this time, fortunately, new research has shown that multi-target medications may inhibit several factors that have been suggested to involved in MetS. According to our findings, we are able to reach the following conclusions:

- ✓ The phytochemical results showed that *Sonchus maritimus* is source of flavonoids, phenols, saponins, terpenoids and steroids. Chomatographic analysis identify several important phenolic acids, flavonoids and volatile compounds. It is also source of important phytominerals such as sodium, potassium, calcium, magnesium, copper, zinc, iron and manganese, which qualifies the plant to play a major nutritional and pharmaceutical role against many diseases.
- ✓ The green synthesis of SeNPs using *S. maritimus* leaves aqueous extract related to the reducing potential of plant that considered as natural stabilizers of NPs, which characterized by spherical shape and very small size.
- ✓ SmE-SeNPs may be classify as one of the important bioactive molecules that can use in medical field due to *in vitro* antioxidant, anti-inflammatory, cell membrane stabilization, hypoglycemic, antibacterial and anticancer activities.
- ✓ Successful encapsulation of *S. maritimus* into linoleic acid-conjugated niosomes, which were of appropriate size and physical stability, enhancing their medical application as drug delivery system and contributing to target specifically the liver.
- ✓ *In vivo* acute toxicity investigation gives permission for the safe use of *S. maritimus* extract and SeNPs as therapeutic agents.
- ✓ Our treatment using *S. maritimus* extract-loaded niosomes, SeNPs and SeNPs-SmE-N ameliorate the physiological parameters in our study, through enhancing the body weight, food and water intake with reducing the relative liver, heart, kidneys and testiculs weight that clearly backing the therapeutic efficacy against alteration of tissues.
- ✓ The positive impact of *S. maritimus*, SeNPs and SeNPs-SmE-N on restoring some of biochemical markers and lipid profile through the beneficial effect against the metabolic and physiologic alteration in various biological systems that linked to our studying data.
- ✓ The observed changing of acetyl cholinesterase activity and behaviors of rats corrected by our treatments that contribute to improve the cellular cholinergic signalization.

- ✓ Overall, we demonstrate that nano-phytotherapy and nanotherapy ameliorate the erytrogram profile, including red blood cells number, hemoglobin content and hematocrit level, and enhance the immune system via a remarkable immunomodulatory effect.
- ✓ All therapeutic systems decreasing protein levels in each of liver, brain, heart, kidneys that show a protective effect against the carbonylic protein that induced by oxidative stress.
- ✓ Oxidative stress is the critical factor in MetS attenuated by *S. maritimus* extract-loaded niosomes, SeNPs and SeNPs-SmE-N treatments that neutralize the free radical and inhibit their propagation through the reducing lipid peroxidation in the different systems and stimulating the antioxidant defense by promoting the expression of each of enzymatic or non-enzymatic antioxidants.
- ✓ The high protection capability of our treatments extended to microscopic level, which demonstrate their protection and reparation effects of cells against damage induced by the oxidative stress. These allows us to considered that these therapies have the potential effect for limiting the damage which related to metabolic syndrome.

At the end, taking in consideration everything indicated above, we can say that the novel combination -loaded niosomes (SeNPs-SmE-N) that is based on nanotechnology has demonstrated remarkable efficacy against metabolic syndrome factors related to biochemical, oxidative stress, hematological, immunological and histological aspects., which offered a new optimism about the possibility to treat the MetS complications.

Perspective

Regarding the significance of these findings, they provide new avenues for experimentation and further comprehensive research that ought to enable us to precisely determine:

- ➢ The utilization of nano-phytotherapy as an approach to treat chronic diseases.
- ➢ The extraction of *S. maritimus* flavonoids and their application in order to inhibit the factors widely known to be involved in MetS.
- ➢ *In vivo* evaluation study of anti-cancer and anti-diabetic activity of green synthesized selenium nanoparticles uings *S. maritimus* extract (SmE-SeNPs).
- ➢ Try making a particular medication form using the niosomal system include SeNPs-SmE-N.
- ➢ Improve the SeNPs-SmE-N efficiency and assessing the long-termconsequence of its use.

Bibliographical references

Abdallah, A. B. E., El-Ghannam, M. A., Hasan, A. A., Mohammad, L. G., Mesalam, N. M., & Alsayed, R. M. (2023). Selenium Nanoparticles Modulate Steroidogenesis-Related Genes and Improve Ovarian Functions via Regulating Androgen Receptors Expression in Polycystic Ovary Syndrome Rat Model. *Biological Trace Element Research*, *1*, 1–13. https://doi.org/10.1007/s12011-023-03616-0

Abdel-Magied, N., Elkady, A. A., & Abdel Fattah, S. M. (2020). Effect of Low-Level Laser on Some Metals Related to Redox State and Histological Alterations in the Liver and Kidney of Irradiated Rats. *Biological Trace Element Research*, *194*(2), 410–422. https://doi.org/10.1007/s12011-019-01779-3

Abdulrasheed-Adeleke, T., Lawal, B., Agwupuye, E. I., Kuo, Y., Eni, A. M., Ekoh, O. F., Lukman, H. Y., Onikanni, A. S., Olawale, F., Saidu, S., Ibrahim, Y. O., Al Ghamdi, M. A. S., Aggad, S. S., Alsayegh, A. A., Aljarba, N. H., Batiha, G. E. S., Wu, A. T. H., & Huang, H. S. (2023). Apigetrin-enriched Pulmeria alba extract prevents assault of STZ on pancreatic β-cells and neuronal oxidative stress with concomitant attenuation of tissue damage and suppression of inflammation in the brain of diabetic rats. *Biomedicine and Pharmacotherapy*, *162*, 1–14. https://doi.org/10.1016/j.biopha.2023.114582

Abo-zalam, H. B., El Denshary, E. E. D., Abdalsalam, R. A., Khalil, I. A., Khattab, M. M., & Hamzawy, M. (2023). Alleviation of hyperlipidemia , insulin resistance , and myopathy by nano selenium / nano CoQ10 platform with simvastatin in hyperlipidemic rats ; comprehensive outlook. *Research Square*, *1*, 1–37. https://doi.org/10.21203/rs.3.rs-2385794/v1

Aboonabi, A., Meyer, R. R., & Singh, I. (2019). The association between metabolic syndrome components and the development of atherosclerosis. *Journal of Human Hypertension*, *33*(12), 844–855. https://doi.org/10.1038/s41371-019-0273-0

Abu-Elghait, M., Hasanin, M., Hashem, A. H., & Salem, S. S. (2021). Ecofriendly novel synthesis of tertiary composite based on cellulose and myco-synthesized selenium nanoparticles: Characterization, antibiofilm and biocompatibility. *International Journal of Biological Macromolecules*, *175*, 294–303. https://doi.org/10.1016/j.ijbiomac.2021.02.040

Adhikari, P., Joshi, K., Singh, M., & Pandey, A. (2020). Influence of altitude on secondary metabolites, antioxidants, and antimicrobial activities of Himalayan yew (Taxus wallichiana). *Plant Biosystems - An International Journal Dealing with All Aspects of Plant Biology*, *156*(1), 187–195. https://doi.org/10.1080/11263504.2020.1845845

Agoun, H., Semiane, N., Mallek, A., Bellahreche, Z., Hammadi, S., Madjerab, M., Abdlalli, M., Khalkhal, A., & Dahmani, Y. (2021). High-carbohydrate diet-induced metabolic disorders in Gerbillus tarabuli (a new model of non-alcoholic fatty-liver disease). Protective effects of

20-hydroxyecdysone. *Archives of Physiology and Biochemistry*, *127*(2), 127–135. https://doi.org/10.1080/13813455.2019.1621350

Aguilar-Salinas, C. A., & Viveros-Ruiz, T. (2019). Recent advances in managing/understanding the metabolic syndrome. *F1000Research*, *8*, 1–9. https://doi.org/10.12688/F1000RESEARCH.17122.1

Agwa, M. M., Abdelmonsif, D. A., Khattab, S. N., & Sabra, S. (2020). Self- assembled lactoferrin-conjugated linoleic acid micelles as an orally active targeted nanoplatform for Alzheimer's disease. *International Journal of Biological Macromolecules*, *162*, 246–261. https://doi.org/10.1016/j.ijbiomac.2020.06.058

Ahamad Tarmizi, A. A., Nik Ramli, N. N., Adam, S. H., Abdul Mutalib, M., Mokhtar, M. H., & Tang, S. G. H. (2023). Phytofabrication of Selenium Nanoparticles with Moringa oleifera (MO-SeNPs) and Exploring Its Antioxidant and Antidiabetic Potential. *Molecules*, *28*(14), 1–19. https://doi.org/10.3390/molecules28145322

Ahmad, F., Abdallah, E. T., & Kamil, M. (2021). Scientific studies on aerial parts of sonchus oleraceus linn. *Arabian Journal of Medicinal and Aromatic Plants*, *7*(2), 196–214. https://doi.org/10.48347/IMIST.PRSM/ajmap-v7i2.26287

Ahmad, M. S., Yasser, M. M., Sholkamy, E. N., Ali, A. M., & Mehanni, M. M. (2015). Anticancer activity of biostabilized selenium nanorods synthesized by Streptomyces bikiniensis strain Ess_amA-1. *International Journal of Nanomedicine*, *10*, 3389–3401. https://doi.org/10.2147/IJN.S82707

Ahmad, S., & Zeb, A. (2019). Effects of phenolic compounds from aqueous extract of Trifolium repens against acetaminophen-induced hepatotoxicity in mice. *Journal of Food Biochemistry*, *43*(9), 1–11. https://doi.org/10.1111/jfbc.12963

Ahmed, H. M., Roy, A., Wahab, M., Ahmed, M., Othman-qadir, G., Elesawy, B. H., Khandaker, M. U., Islam, M. N., & Emran, T. Bin. (2021). Applications of Nanomaterials in Agrifood and Pharmaceutical Industry. *Journal of Nanomaterials*, *2021*, 1–10. https://doi.org/10.1155/2021/1472096

Ahmed, O. M., Elkomy, M. H., Fahim, H. I., Ashour, M. B., Naguib, I. A., Alghamdi, B. S., Mahmoud, H. U. R., & Ahmed, N. A. (2022). Rutin and Quercetin Counter Doxorubicin-Induced Liver Toxicity in Wistar Rats via Their Modulatory Effects on Inflammation, Oxidative Stress, Apoptosis, and Nrf2. *Oxidative Medicine and Cellular Longevity*, *2022*, 1–19. https://doi.org/10.1155/2022/2710607

Ahmed, R. M., Abdel-Latif, S. L. A., Abdelwahed, M. Y., Hussein, M., Elmahdi, A. M. H., & Rohym, H. H. (2020). Therapeutic effect of selenium and vitamin E on arsenic induced cardiac damage in adult male albino rat: Histological, biochemical and pharmacological

study. *Life Science Journal*, *17*(9), 71–83. https://doi.org/:10.7537/marslsj170920.09.

Ahn, M. R., Kumazawa, S., Usui, Y., Nakamura, J., Matsuka, M., Zhu, F., & Nakayama, T. (2007). Antioxidant activity and constituents of propolis collected in various areas of China. *Food Chemistry*, *101*(4), 1383–1392. https://doi.org/10.1016/j.foodchem.2006.03.045

Aissani, F., Grara, N., & Guelmamene, R. (2022). Phytochemical screening and toxicity investigation of hydro-methanolic and aqueous extracts from aerial parts of Sonchus oleraceus L. in Swiss albino mice. *Comparative Clinical Pathology*, *31*(3), 509–528. https://doi.org/10.1007/s00580-022-03349-x

Akar, F., Uludağ, O., Aydin, A., Aytekin, Y. A., Elbeg, S., Tuzcu, M., & Sahin, K. (2012). High-fructose corn syrup causes vascular dysfunction associated with metabolic disturbance in rats: Protective effect of resveratrol. *Food and Chemical Toxicology*, *50*(6), 2135–2141. https://doi.org/10.1016/j.fct.2012.03.061

Akar, F., Yildirim, O. G., Yucel Tenekeci, G., Tunc, A. S., Demirel, M. A., & Sadi, G. (2022). Dietary high-fructose reduces barrier proteins and activates mitogenic signalling in the testis of a rat model: Regulatory effects of kefir supplementation. *Andrologia*, *54*(3), e14342. https://doi.org/10.1111/and.14342

Al-Megrin, W. A., El-Khadragy, M. F., El-Khadragy, M. F., Hussein, M. H., Mahgoub, S., Abdel-Mohsen, D. M., Taha, H., Bakkar, A. A. A., Abdel Moneim, A. E., & Amin, H. K. (2020). Green Coffea arabica Extract Ameliorates Testicular Injury in High-Fat Diet/Streptozotocin-Induced Diabetes in Rats. *Journal of Diabetes Research*, *2020*, 1–13. https://doi.org/10.1155/2020/6762709

Al-quraishy, S., Dkhil, M. A., & Moneim, A. E. A. (2023). Anti-hyperglycemic activity of selenium nanoparticles in streptozotocin-induced diabetic rats. *International Journal of Nanomedicine*, *1*, 1–17. https://doi.org/10.2147/IJN.S91377

AL Juhaimi, F., Ghafoor, K., Ahmed, I. A. M., Babiker, E. E., & Özcan, M. M. (2017). Comparative study of mineral and oxidative status of Sonchus oleraceus, Moringa oleifera and Moringa peregrina leaves. *Journal of Food Measurement and Characterization*, *11*(4), 1745–1751. https://doi.org/10.1007/s11694-017-9555-9

Alam, S. I., Kim, M. W., Shah, F. A., Saeed, K., Ullah, R., & Kim, M. O. (2021). Alpha-linolenic acid impedes cadmium-induced oxidative stress, neuroinflammation, and neurodegeneration in mouse brain. *Cells*, *10*(9), 1–14. https://doi.org/10.3390/cells10092274

AlAmri, O. D., Albeltagy, R. S., M. A. Akabawy, A., Mahgoub, S., Abdel-Mohsen, D. M., Abdel Moneim, A. E., & Amin, H. K. (2020). Investigation of antioxidant and anti-inflammatory activities as well as the renal protective potential of green coffee extract in

high fat-diet/streptozotocin-induced diabetes in male albino rats. *Journal of Functional Foods*, *71*(May), 103996. https://doi.org/10.1016/j.jff.2020.103996

Alemán, M. N., Sánchez, S. S., & Honoré, S. M. (2022). Daily Intake of Smallanthus sonchifolius (Yacon) Roots Reduces the Progression of Non-alcoholic Fatty Liver in Rats Fed a High Fructose Diet. *Plant Foods for Human Nutrition*, *77*(4), 521–528. https://doi.org/10.1007/s11130-022-01009-7

Alhazza, I. M., Ebaid, H., Omar, M. S., & Hassan, I. (2022). Supplementation with selenium nanoparticles alleviates diabetic nephropathy during pregnancy in the diabetic female rats Supplementation with selenium nanoparticles alleviates diabetic nephropathy during pregnancy in the diabetic female rats. *Environmental Science and Pollution Research*, *29*, 5517–5525. https://doi.org/10.1007/s11356-021-15905-z

Alipour, S., Kalari, S., Morowvat, M. H., Sabahi, Z., & Dehshahri, A. (2021). Green Synthesis of Selenium Nanoparticles by Cyanobacterium *Spirulina platensis* (abdf2224): Cultivation Condition Quality Controls. *BioMed Research International*, *2021*, 6635297. https://doi.org/10.1155/2021/6635297

Alizadeh, S. R., Seyedabadi, M., Montazeri, M., Khan, B. A., & Ebrahimzadeh, M. A. (2023). Allium paradoxum extract mediated green synthesis of SeNPs: Assessment of their anticancer, antioxidant, iron chelating activities, and antimicrobial activities against fungi, ATCC bacterial strains, Leishmania parasite, and catalytic reduction of methyle. *Materials Chemistry and Physics*, *296*, 127240. https://doi.org/10.1016/j.matchemphys.2022.127240

Alkreathy, M. M., Khan, A. A., Khan, R. R., & Sahreen, S. (2014). CCl4 induced genotoxicity and DNA oxidative damages in rats: Hepatoprotective effect of Sonchus arvensis. *BMC Complementary and Alternative Medicine*, *14*(1), 2–8. https://doi.org/10.1186/1472-6882-14-452

Amini, S. M., & Mahabadi, V. P. (2018). Selenium nanoparticles role in organ systems functionality and disorder. *Nanomedicine Research Journal*, *3*(3), 117–124. https://doi.org/10.22034/NMRJ.2018.03.001

Ananth, A., Keerthika, V., & Rajan, M. R. (2019). Synthesis and characterization of nano-selenium and its antibacterial response on some important human pathogens. *Current Science*, *116*(2), 285–290. https://doi.org/10.18520/cs/v116/i2/285-290

Andrade, N., Andrade, S., Silva, C., Rodrigues, I., Guardão, L., Guimarães, J. T., Keating, E., & Martel, F. (2020). Chronic consumption of the dietary polyphenol chrysin attenuates metabolic disease in fructose-fed rats. *European Journal of Nutrition*, *59*(1), 151–165. https://doi.org/10.1007/s00394-019-01895-9

Annamalai, J., Ummalyma, S. B., Pandey, A., & Bhaskar, T. (2021). Recent trends in microbial

nanoparticle synthesis and potential application in environmental technology: a comprehensive review. *Environmental Science and Pollution Research*, *28*(36), 49362–49382. https://doi.org/10.1007/s11356-021-15680-x

Arafa, D., Elshobaky, G., Risha, E., & Abdelhamid, F. (2023). Potential Effects of Vitamin D and Resveratrol on Hematological and Renal Indicators Associated with Metabolic Syndrome in Rats. *Mansoura Veterinary Medical Journal*, *24*(3), 19–26. https://doi.org/10.21608/mvmj.2022.142976.1114

Arias-Chávez, D. J., Mailloux-Salinas, P., Altamirano, J., Huang, F., Gómez-Viquez, N. L., & Bravo, G. (2022). Consumption of combined fructose and sucrose diet exacerbates oxidative stress, hypertrophy and CaMKIIδ oxidation in hearts from rats with metabolic syndrome. *Molecular and Cellular Biochemistry*, *477*(4), 1309–1320. https://doi.org/10.1007/s11010-022-04364-w

Ashraf, H., Cossu, D., Ruberto, S., Noli, M., Jasemi, S., Simula, E. R., & Sechi, L. A. (2023). Latent Potential of Multifunctional Selenium Nanoparticles in Neurological Diseases and Altered Gut Microbiota. *Materials*, *16*(2), 1–19. https://doi.org/10.3390/ma16020699

Asif, A., & Saeed, M. A. (2020). Exploring Irritant Activity of Some of the Phytochemical Components from Wild Sonchus arvensis (L.) ssp arvensis (D.C.) Kirp herb. *ACTA Pharmaceutica Sciencia*, *58*(3), 305–319. https://doi.org/10.23893/1307-2080.APS.05817

Ayoola, G. A., Folawewo, A. D., Adesegun, S. A., & Abioro, O. O. (2019). Phytochemical and antioxidant screening of some plants of apocynaceae from South West Nigeria. *International Journal of Plant Breeding and Genetics*, *6*(4), 1–5.

Azemi, N. A., Azemi, A. K., Abu-bakar, L., Sevakumaran, V., Sifzizul, T., Muhammad, T., & Ismail, N. (2023). Effect of Linoleic Acid on Cholesterol Levels in a High-Fat Diet-Induced Hypercholesterolemia Rat Model. *Metabolites*, *13*, 1–15. https://doi.org/10.3390/metabo13010053

Bachi, A., Dalle-donne, I., & Scaloni, A. (2013). Redox Proteomics : Chemical Principles , Methodological Approaches and Biological / Biomedical Promises. *Chemical Reviews*, *113*(1), 596–698. https://doi.org/10.1021/cr300073p

Bagetta, D., Maruca, A., Lupia, A., Mesiti, F., Catalano, R., Romeo, I., Moraca, F., Ambrosio, F. A., Costa, G., & Artese, A. (2020). Mediterranean products as promising source of multi-target agents in the treatment of metabolic syndrome. *European Journal of Medicinal Chemistry*, *186*, 111903. https://doi.org/10.1016/j.ejmech.2019.111903

Bagheri, A., Chu, B., & Yaakob, H. (2014). Niosomal Drug Delivery Systems : Formulation , Preparation and Applications. *World Applied Sciences Journal*, *32*(8), 1671–1685. https://doi.org/10.5829/idosi.wasj.2014.32.08.848

Ballester, M. P., Gallego, J. J., Fiorillo, A., Casanova-Ferrer, F., Giménez-Garzó, C., Escudero-García, D., Tosca, J., Ríos, M. P., Montón, C., Durbán, L., Ballester, J., Benlloch, S., Urios, A., San-Miguel, T., Kosenko, E., Serra, M. Á., Felipo, V., & Montoliu, C. (2022). Metabolic syndrome is associated with poor response to rifaximin in minimal hepatic encephalopathy. *Scientific Reports*, *12*(1), 1–12. https://doi.org/10.1038/s41598-022-06416-z

Barale, C., & Russo, I. (2020). Influence of cardiometabolic risk factors on platelet function. *International Journal of Molecular Sciences*, *21*(2), 1–27. https://doi.org/10.3390/ijms21020623

Baran, M. F., Keskin, C., Baran, A., Kurt, K., İpek, P., Eftekhari, A., Khalilov, R., Fridunbayov, I., & Cho, W. C. (2023). Green synthesis and characterization of selenium nanoparticles (Se NPs) from the skin (testa) of Pistacia vera L. (Siirt pistachio) and investigation of antimicrobial and anticancer potentials. *Biomass Conversion and Biorefinery*, *1*, 1–11. https://doi.org/10.1007/s13399-023-04366-8

Baranei, M., Taheri, R. A., Tirgar, M., Saeidi, A., Oroojalian, F., Uzun, L., Asefnejad, A., Wurm, F. R., & Goodarzi, V. (2020). Anticancer Effect of Green Tea Extract (GTE)-Loaded pH-responsive Niosome Coated with PEG against Different Cell Lines. *Materials Today Communications*, *June*, 101751. https://doi.org/10.1016/j.mtcomm.2020.101751

Barma, M. D., Indiran, M. A., Rathinavelu, P. K., & Srisakthi, D. (2022). Anti-inflammatory and antioxidant activity of Clitoria ternatea extract mediated selenium nanoparticles. *International Journal of Health Sciences*, *6*, 2605–2613. https://doi.org/10.53730/ijhs.v6ns1.5329

Bashir, D. W., Rashad, M. M., Ahmed, Y. H., Drweesh, E. A., Elzahany, E. A. M., Abou-El-Sherbini, K. S., & EL-Leithy, E. M. M. (2021). The ameliorative effect of nanoselenium on histopathological and biochemical alterations induced by melamine toxicity on the brain of adult male albino rats. *NeuroToxicology*, *86*, 37–51. https://doi.org/10.1016/j.neuro.2021.06.006

Bashir, T., Anum, W., Ali, I., Ghaffar, A., Ali, L., Raza, M. U., Javed, Z., Zafar, A., Mahmood, N., & Shabir, A. (2018). Allelopathic effects of perennial sow thistle (Sonchus arvensis L.) on germination and seedling growth of maize (zea mays L.). *Allelopathy Journal*, *43*(1), 105–116. https://doi.org/10.26651/allelo.j./2018-43-1-1134

Bauer, I., Rimbach, G., Nevermann, S., Neuhauser, C., Schwarzinger, B., Schwarzinger, C., Weghuber, J., & Luersen, K. (2023). in-Vitro Antidiabetic Activity of a Bistorta Officinalis Delarbre Root Extract Can Not Be Confirmed in the in-Vivo Models Hen'S Egg Test and Drosophila Melanogaster. *Journal of Physiology and Pharmacology*, *74*(1), 31–42.

https://doi.org/10.26402/jpp.2023.1.04

Bayda, S., Adeel, M., Tuccinardi, T., Cordani, M., & Rizzolio, F. (2020). The history of nanoscience and nanotechnology: From chemical-physical applications to nanomedicine. *Molecules*, *25*(1), 1–15. https://doi.org/10.3390/molecules25010112

Beauchamp, C., & Fridovich, I. (1971). Superoxide dismutase: Improved assays and an assay applicable to acrylamide gels. *Analytical Biochemistry*, *44*(1), 276–287. https://doi.org/10.1016/0003-2697(71)90370-8

Belhayara, M. I., Mellouk, Z., Hamdaoui, M. S., Bachaoui, M., Kheroua, O., & Malaisse, W. J. (2020). The metabolic syndrome: Emerging novel insights regarding the relationship between the homeostasis model assessment of insulin resistance and other key predictive markers in young adults of western Algeria. *Nutrients*, *12*(3), 1–14. https://doi.org/10.3390/nu12030727

Benithaj, G., Ramani, P., Ramalingam, K., & Ramasubramaniam, A. (2023). Anticancer activity of Green synthesized selenium nanoparticles from Garcinia Mangostana Crude extract against MCF-7 Breast cancer cells. *Journal of Population Therapeutics and Clinical Pharmacology*, *30*(6), 74–82. https://doi.org/10.47750/jptcp.2023.30.06.011

Benkhaled, A., Réggami, Y., Boudjelal, A., Senator, A., Bouriche, H., Demirtaş, I., Kheniche, A., Benyettou, H., Larabi, N., & Ruberto, G. (2022). Chemical characterisation, hypoglycaemic and renoprotective effects of aqueous leaf extract of Limoniastrum guyonianum on fructose-induced metabolic syndrome in rats. *Archives of Physiology and Biochemistry*, *128*(4), 914–923. https://doi.org/10.1080/13813455.2020.1739715

Bessada, S. M. F., Barreira, J. C. M., & Oliveira, M. B. P. P. (2015). Asteraceae species with most prominent bioactivity and their potential applications: A review. *Industrial Crops and Products*, *76*, 604–615. https://doi.org/10.1016/j.indcrop.2015.07.073

Bier, A., Shapira, E., Khasbab, R., Sharabi, Y., Grossman, E., & Leibowitz, A. (2022). High-Fructose Diet Increases Renal ChREBPβ Expression, Leading to Intrarenal Fat Accumulation in a Rat Model with Metabolic Syndrome. *Biology*, *11*(4), 1–12. https://doi.org/10.3390/biology11040618

Bojarski, B., Sowi, N., Strus, M., & Chmurska-g, M. (2021). Changes in Leukogram and Erythrogram Results in Bitches with Vaginitis. *Animals*, *11*(5), 1–7. https://doi.org/10.3390/ani11051403

Boukada, F., Sitayeb, S., & Khadem, H. (2022). CHEMICAL COMPOSITION , ANTIOXIDANT AND ANTIBACTERIAL ACTIVITY OF Adiantum capillus-veneris L . EXTRACT FROM ALGERIA. *Kragujevac Journal of Science*, *44*, 91–101. https://doi.org/10.5937/KgJSci2244091B

Bovolini, A., Garcia, J., Andrade, M. A., & Duarte, J. A. (2021). Metabolic Syndrome Pathophysiology and Predisposing Factors. *International Journal of Sports Medicine*, *42*(3), 199–214. https://doi.org/10.1055/a-1263-0898

Bradford, M. M. (1976). A rapid and sensitive method for the quantitation of microgram quantities of protein utilizing the principle of protein-dye binding. *Analytical Biochemistry*, *72*(1), 248–254. https://doi.org/10.1016/0003-2697(76)90527-3

Bratoeva, K., Stoyanov, G. S., Merdzhanova, A., & Radanova, M. (2017). Manifestations of Renal Impairment in Fructose-induced Metabolic Syndrome. *Cureus*, *9*(11), 1–8. https://doi.org/10.7759/cureus.1826

Broadhurst, R. B., & Jones, W. T. (1978). Analysis of condensed tannins using acidified vanillin. *Journal of the Science of Food and Agriculture*, *29*(9), 788–794. https://doi.org/10.1002/jsfa.2740290908

Buchmann, N., Fielitz, J., Spira, D., König, M., Norman, K., Pawelec, G., Goldeck, D., Demuth, I., & Steinhagen-Thiessen, E. (2022). Muscle Mass and Inflammation in Older Adults: Impact of the Metabolic Syndrome. *Gerontology*, *68*(9), 989–998. https://doi.org/10.1159/000520096

Budin, S. B., Zafirah, W., Rahman, A., Jubaidi, F. F., Liyana, N., Yusof, M., & Taib, I. S. (2018). Roselle (Hibiscus sabdiriffa) Polyphenol-Rich Extract Prevents Testicular Damage of Diabetic Rats. *Journal of Applied Pharmaceutical Science*, *8*(02), 65–70. https://doi.org/10.7324/JAPS.2018.8210

Bugga, P., Mohammed, S. A., Alam, M. J., Katare, P., Meghwani, H., Maulik, S. K., Arava, S., & Banerjee, S. K. (2022). Empagliflozin prohibits high-fructose diet-induced cardiac dysfunction in rats via attenuation of mitochondria-driven oxidative stress. *Life Sciences*, *307*, 120862. https://doi.org/https://doi.org/10.1016/j.lfs.2022.120862

Campos, O. C. De, Osaigbovo, D. I., Bisi-adeniyi, T. I., Iheagwam, F. N., Rotimi, S. O., & Chinedu, S. N. (2020). Protective Role of Picralima nitida Seed Extract in High-Fat High-Fructose-Fed Rats. *Advances in Pharmacological and Pharmaceutical Sciences*, *2020*, 1–11. https://doi.org/10.1155/2020/5206204

Cardinali, D. P., & Hardeland, R. (2017). Inflammaging, Metabolic Syndrome and Melatonin: A Call for Treatment Studies. *Neuroendocrinology*, *104*(4), 382–397. https://doi.org/10.1159/000446543

Cazzola, M., Rogliani, P., Santosh, S., Josuel, S., Maria, O., & Matera, G. (2021). Use of Thiols in the Treatment of COVID - 19 : Current Evidence. *Lung*, *199*(4), 335–343. https://doi.org/10.1007/s00408-021-00465-3

Chenni, A., Cherif, F. Z. H., Chenni, K., Elius, E. E., Pucci, L., & Yahia, D. A. (2022). Effects of

Pumpkin (Cucurbita pepo L.) Seed Protein on Blood Pressure, Plasma Lipids, Leptin, Adiponectin, and Oxidative Stress in Rats with Fructose-Induced Metabolic Syndrome. *Preventive Nutrition and Food Science*, *27*(1), 78–88. https://doi.org/10.3746/pnf.2022.27.1.78

Chetehouna, S., Derouiche, S., Atoussi, O., & Guemari, I. (2022). Physico-chemical Analysis , Phytochemical content and Antioxidant properties of honey dates " Robe " of some Algeria date variety from Oued Righ and Oued Souf regions. *Asian Journal of Research in Chemistry*, *15*(6), 399–403. https://doi.org/10.52711/0974-4150.2022.00070

Chike-Ekwughe, A., Adegboyega, A. E., Johnson, T. O., Adebayo, A. H., & Ogunlana, O. O. (2023). In vitro and in-silico inhibitory validation of Tapinanthus cordifolius leaf extract on alpha-amylase in the management of type 2 diabetes. *Informatics in Medicine Unlocked*, *36*, 1–11. https://doi.org/10.1016/j.imu.2022.101148

Cigliano, L., Spagnuolo, M. S., Boscaino, F., Ferrandino, I., Capriello, T., Cocca, E., Iannotta, L., Treppiccione, L., Luongo, D., Maurano, F., Rossi, M., & Bergamo, P. (2019). Dietary Supplementation with Fish Oil or Conjugated Linoleic Acid Relieves Depression Markers in Mice by Modulation of the Nrf2 Pathway. *Molecular Nutrition & Food Research*, *63*(21), 1–11. https://doi.org/10.1002/mnfr.201900243

Cirillo, V. P., Wilkins, P. O., & Anton, J. (1963). Sugar Transport in a Psychrophilic Yeast. *Journal of Bacteriology*, *86*, 1259–1264. https://doi.org/10.1128/jb.86.6.1259-1264.1963

Cittrarasu, V., Kaliannan, D., Dharman, K., Maluventhen, V., Easwaran, M., Liu, W. C., Balasubramanian, B., & Arumugam, M. (2021). Green synthesis of selenium nanoparticles mediated from Ceropegia bulbosa Roxb extract and its cytotoxicity, antimicrobial, mosquitocidal and photocatalytic activities. *Scientific Reports*, *11*(1), 1032. https://doi.org/10.1038/s41598-020-80327-9

Colorado, D., Fernandez, M., Orozco, J., Lopera, Y., Muñoz, D. L., Acín, S., & Balcazar, N. (2020). Metabolic Activity of Anthocyanin Extracts Loaded into Non-ionic Niosomes in Diet-Induced Obese Mice. *Pharmaceutical Research*, *37*(8), 1–11. https://doi.org/10.1007/s11095-020-02883-z

Coronati, M., Baratta, F., Pastori, D., Ferro, D., Angelico, F., & Ben, M. Del. (2022). Added Fructose in Non-Alcoholic Fatty Liver Disease and in Metabolic Syndrome : A Narrative Review. *Nutrients*, *14*(6), 1–10. https://doi.org/10.3390/ nu14061127 Academic

Cruz, A. F., Hamel, C., Yang, C., Matsubara, T., Gan, Y., Singh, A. K., Kuwada, K., & Ishii, T. (2012). Phytochemicals to suppress Fusarium head blight in wheat-chickpea rotation. *Phytochemistry*, *78*, 72–80. https://doi.org/10.1016/j.phytochem.2012.03.003

Debray, F. G., Seyssel, K., Fadeur, M., Tappy, L., Paquot, N., & Tran, C. (2021). Effect of a

high fructose diet on metabolic parameters in carriers for hereditary fructose intolerance. *Clinical Nutrition*, *40*(6), 4246–4254. https://doi.org/10.1016/j.clnu.2021.01.026

Deepasree, K., & Venugopal, S. (2022). Therapeutic potential of selenium nanoparticles. *Frontiers in Nanotechnology*, *4*, 1–12. https://doi.org/10.3389/fnano.2022.1042338

Derouiche, S., Abbas, K., & Djermoune, M. (2017). Polysaccharides and Ascorbic Acid Content and the Effect of Aqueous Extract of Portulaca Oleracea in High-Fat Diet-Induced Obesity, Dyslipidemia and Liver Damage in Albino Wistar Rats = Contenu des Polysaccharides et Acide Ascorbique et Effet de l'Extrait. *Algerian Journal of Arid Environment*, *7*(2), 16–26. https://doi.org/10.12816/0046095

Derouiche, S., Chetehouna, S., & Atoussi, W. (2022). The effects of aqueous leaf extract of Portulaca oleracea on haemato-biochemical and histopathological changes induced by sub-chronic aluminium toxicity in male wistar rats. *Pharmacological Research - Modern Chinese Medicine*, *4*, 100101. https://doi.org/10.1016/j.prmcm.2022.100101

Derouiche, S., Chetehouna, S., Djouadi, A., Boulaares, I., & Guemari, I. Y. (2022). The Possible Mechanisms of Silver Nanoparticles against Sars-Cov 2. *Frontiers in Biomedical Technologies*, *9*(2), 149–158. https://doi.org/10.18502/fbt.v9i2.8854

Derouiche, S., Degachi, O., & Gharbi, K. (2019). Phytochemistry analysis and modulatory activity of Portulaca oleracea and Aquilaria malaccensis extracts against High fructose and high-fat high diet induced immune cells alteration and heart lipid peroxidation in Rats. *International Research Journal of Biological Sciences*, *8*(4), 6–11.

Derouiche, S., Guemari, I. Y., & Boulaares, I. (2020). Characterization and acute toxicity evaluation of the MgO Nanoparticles Synthesized from Aqueous Leaf Extract of Ocimum basilicum L. *Algerian Journal of Biosciences*, *1*(1), 1–6. https://doi.org/10.57056/ajb.v1i1.18

Dhabian, S. Z., & Jasim, R. S. (2023). Antioxidant , Cytotoxic , and Antihemolytic Activity of Greenly Synthesized Selenium Nanoparticles Using Elettaria Cardamomum Extract. *Journal of Nanostructures*, *13*(1), 76–85. https://doi.org/10.22052/JNS.2023.01.009

Dikshit, P. K., Kumar, J., Das, A. K., Sadhu, S., Sharma, S., Singh, S., Gupta, P. K., & Kim, B. S. (2021). Green synthesis of metallic nanoparticles: Applications and limitations. *Catalysts*, *11*(8), 259–281. https://doi.org/10.1016/b978-0-12-822401-4.00022-2

Dima, S., Tric, B., Tritean, N., Cimpean, A., Oancea, F., & Ghiurea, M. (2024). Cytocompatibility , Antimicrobial and Antioxidant Activity of a Mucoadhesive Biopolymeric Hydrogel Embedding Selenium Nanoparticles Phytosynthesized by Sea Buckthorn Leaf Extract. *Pharmaceuticals*, *17*(1), 1–35. https://doi.org/10.3390/ph17010023

Djouadi, A., & Derouiche, S. (2021). Current Research in Green and Sustainable Chemistry

Spinach mediated synthesis of zinc oxide nanoparticles : Characterization , In vitro biological activities study and in vivo acute toxicity evaluation. *Current Research in Green and Sustainable Chemistry*, *4*, 100214. https://doi.org/10.1016/j.crgsc.2021.100214

Dotto, J. M., & Chacha, J. S. (2020). The potential of pumpkin seeds as a functional food ingredient: A review. *Scientific African*, *10*, e00575.

Dutta, K. N., Lahkar, M., Sarma, D., & Sharma, R. K. (2020). A Comparative Study on the antidiabetic activity of Sonchus asper and Sonchus arvensis in Alloxan Induced Diabetic Rats. *International Journal of Scientific Development and Research*, *5*(5), 1–6.

Duvhåteau, G., & Florkin, M. (1959). Sur La Tréhalosémie Des Insectes Et Sa Signification. *Archives Internationales de Physiologie et de Biochimie*, *67*(2), 306–314. https://doi.org/10.3109/13813455909074435

Ebokaiwe, A. P., Obeten, K. E., Okori, S. O., David, E. E., Olusanya, O., Chukwu, C. J., Okoro, N., & Ehiri, R. C. (2020). Co-administration of Selenium Nanoparticles and Metformin Abrogate Testicular Oxidative Injury by Suppressing Redox Imbalance, Augmenting Sperm Quality and Nrf2 Protein Expression in Streptozotocin-Induced Diabetic Rats. *Biological Trace Element Research*, *198*(2), 544–556. https://doi.org/10.1007/s12011-020-02082-2

Ebrahimi, N. D., Sadeghi, A., & Ala, M. (2023). Protective effects of melatonin against oxidative stress induced by metabolic disorders in the male reproductive system : a systematic review and meta- analysis of rodent models. *Frontiers in Endocrinology*, *14*, 1–16. https://doi.org/10.3389/fendo.2023.1202560

Ekici, Ö., Aslan, E., Aladağ, T., Güzel, H., Korkmaz, Ö. A., Bostancı, A., Sadi, G., & Pektaş, M. B. (2022). Masseter muscle and gingival tissue inflammatory response following treatment with high-fructose corn syrup in rats: Anti-inflammatory and antioxidant effects of kefir. *Journal of Food Biochemistry*, *46*(3), 1–12. https://doi.org/10.1111/jfbc.13732

El-hakim, Y. M. A., Mohamed, A. A., Khater, S. I., Arisha, A. H., Metwally, M. M. M., Nassan, M. A., & Hassan, M. E. (2021). Chitosan-Stabilized Selenium Nanoparticles and Metformin Synergistically Rescue Testicular Oxidative Damage and Steroidogenesis-Related Genes Dysregulation in High-Fat Diet / Streptozotocin-Induced Diabetic Rats. *Antioxidants*, *10*, 1–17. https://doi.org/10.3390/ antiox10010017

El Shafey, A. M. (2020). Green synthesis of metal and metal oxide nanoparticles from plant leaf extracts and their applications : A review. *Green Processing and Synthesis*, *9*(1), 304–339. https://doi.org/10.1515/gps-2020-0031

Elhady, S. S., Abdelhameed, R. F. A., Mehanna, E. T., Wahba, A. S., Elfaky, M. A., Koshak, A. E., Noor, A. O., Bogari, H. A., Malatani, R. T., & Goda, M. S. (2022). Metabolic Profiling, Chemical Composition, Antioxidant Capacity, and In Vivo Hepato- and Nephroprotective

Effects of Sonchus cornutus in Mice Exposed to Cisplatin. *Antioxidants*, *11*(5). https://doi.org/10.3390/antiox11050819

Ellman, G. L. (1959). Tissue Sulfhydryl Groups. *Archives of Biochemistry and Biophysics*, *82*(1), 70–77. https://doi.org/10.1016/j.abb.2022.109245

Ellman, G. L., Courtney, K. D., Andres, V., & Featherstone, R. M. (1961). A new and rapid colorimetric determination of acetylcholinesterase activity. *Biochemical Pharmacology*, *7*(2), 88–95. https://doi.org/10.1016/0006-2952(61)90145-9

Elsisy, R. A., El-Magd, M. A., & Abdelkarim, M. A. (2021). High-fructose diet induces earlier and more severe kidney damage than high-fat diet on rats. *Egyptian Journal of Histology*, *44*(2), 535–544. https://doi.org/10.21608/ejh.2020.31508.1304

Evans, W. C. (2009). *Trease and Evans' pharmacognosy* (16th ed.). Elsevier Health Sciences, London.

Fahed, G., Aoun, L., Zerdan, M. B., Allam, S., Zerdan, M. B., Bouferraa, Y., & Assi, H. I. (2022). Metabolic Syndrome: Updates on Pathophysiology and Management in 2021. *International Journal of Molecular Sciences*, *23*(2), 2–38. https://doi.org/10.3390/ijms23020786

Faijer-Westerink, H. J., Kengne, A. P., Meeks, K. A. C., & Agyemang, C. (2020). Prevalence of metabolic syndrome in sub-Saharan Africa: A systematic review and meta-analysis. *Nutrition, Metabolism and Cardiovascular Diseases*, *30*(4), 547–565. https://doi.org/10.1016/j.numecd.2019.12.012

Fan, D., Li, L., Li, Z., Zhang, Y., Ma, X., Wu, L., & Zhang, H. (2020). Biosynthesis of selenium nanoparticles and their protective , antioxidative effects in streptozotocin induced diabetic rats. *Science and Technology of Advanced Materials*, *21*(1), 505–514. https://doi.org/10.1080/14686996.2020.1788907

Farjam, M., Dehdab, P., Abbassnia, F., Mehrabani, D., Tanideh, N., Pakbaz, S., & Imanieh, M. (2012). Thioacetamide-induced acute hepatic encephalopathy in rat: Behavioral, biochemical and histological changes. *Iranian Red Crescent Medical Journal*, *14*(3), 164–170.

Feyisa, T. O., Melka, D. S., Menon, M., Labisso, W. L., & Habte, M. L. (2019). Investigation of the effect of coffee on body weight, serum glucose, uric acid and lipid profile levels in male albino Wistar rats feeding on high-fructose diet. *Laboratory Animal Research*, *35*(1), 1–8. https://doi.org/10.1186/s42826-019-0024-y

Flisiński, M., Brymora, A., Skoczylas-Makowska, N., Stefańska, A., & Manitius, J. (2022). Fructose-rich diet is a risk factor for metabolic syndrome, proximal tubule injury and urolithiasis in rats. *International Journal of Molecular Sciences*, *23*(1), 1–17.

https://doi.org/10.3390/ijms23010203

Flohé, L., & Günzler, W. A. (1984). Assays of glutathione peroxidase. *Methods in Enzymology*, *105*, 114–120. https://doi.org/10.1016/S0076-6879(84)05015-1

Fouad, H., Habib, E. S., & Ahmed, S. A. (2020). Phytochemistry and Pharmacological Effects of Plants in Genus Sonchus (Asteraceae). *Records of Pharmaceutical and Biomedical Sciences*, *4*(1), 40–50. https://doi.org/10.21608/RPBS.2019.18952.1046

Friedewald, W. T., Levy, R. I., & Fredrickson, D. S. (1972). Estimation of the concentration of low-density lipoprotein cholesterol in plasma, without use of the preparative ultracentrifuge. *Clinical Chemistry*, *18*(6), 499–502. https://doi.org/10.1093/clinchem/18.6.499

Fritea, L., Laslo, V., Cavalu, S., Costea, T., & Vicas, S. I. (2017). Green biosynthesis of selenium nanoparticles using parsley (Petroselinum crispum) leaves extract. *Studia Universitatis Vasile Goldis Arad, Seria Stiintele Vietii*, *27*(3), 203–208.

Gaafar, A. A., Ali, S. I., Kutkat, O., Kandeil, A. M., & El-Hallouty, S. M. (2020). Bioactive Ingredients and Anti-influenza (H5N1), Anticancer, and Antioxidant Properties of Urtica urens L. *Jordan Journal of Biological Sciences*, *13*, 647–657.

Gancheva, S., Zhelyazkova-Savova, M., Galunska, B., & Chervenkov, T. (2015). Experimental models of metabolic syndrome in rats. *Scripta Scientifica Medica*, *47*(2), 14–21. https://doi.org/10.14748/ssm.v47i2.1145

García-Manrique, P., Machado, N. D., Fernández, M. A., Blanco-López, M. C., Matos, M., & Gutiérrez, G. (2020). Effect of drug molecular weight on niosomes size and encapsulation efficiency. *Colloids and Surfaces B: Biointerfaces*, *186*, 110711. https://doi.org/10.1016/j.colsurfb.2019.110711

Ghaderi, R. S., Adibian, F., Sabouri, Z., Davoodi, J., Kazemi, M., Jamehdar, S. A., Meshkat, Z., & Daroudi, M. (2021). Green synthesis of selenium nanoparticle by Abelmoschus esculentus extract and assessment of its antibacterial activity. *Materials Technology*, *37*(10), 1289–1297. https://doi.org/10.1080/10667857.2021.1935602

Ghosh, S., Dhar, S., Bhattacharjee, S., & Bhattacharjee, P. (2023). Contribution of environmental, genetic and epigenetic factors to obesity-related metabolic syndrome. *Nucleus*, *66*(2), 215–237. https://doi.org/10.1007/s13237-023-00420-y

Giner, R. M., Ubeda, A., Just, M. J., Serrano, A., Manez, S., & Rios, J. (1993). A Chemotaxonomic Survey of Sonchus Subgenus Sonchus. *Biochemical Systemadcs and Ecology*, *21*(5), 617–620. https://doi.org/10.1016/0305-1978(93)90062-V

Golabi-habashi, N., Salimi, A., & Malekinejad, H. (2021). Quercetin attenuated the Benzene-induced hemato- and hepatotoxicity in mice. *Toxicology Reports*, *8*, 1569–1575. https://doi.org/10.1016/j.toxrep.2021.08.001

Gomaa, A. A., Farghaly, H. S. M., Ahmed, A. M., El-Mokhtar, M. A., & Hemida, F. K. (2022). Advancing combination treatment with cilostazol and caffeine for Alzheimer's disease in high fat-high fructose-STZ induced model of amnesia. *European Journal of Pharmacology*, *921*, 174873. https://doi.org/10.1016/j.ejphar.2022.174873

Gorbachinsky, I., Akpinar, H., & Assimos, D. G. (2022). Metabolic syndrome and urological diseases. *Reviews in Urology*, *12*(4), 157–180. https://doi.org/10.23736/S0031-0808.21.04638-3

Gour, A., & Jain, N. K. (2019). Advances in green synthesis of nanoparticles. *Artificial Cells, Nanomedicine and Biotechnology*, *47*(1), 844–851. https://doi.org/10.1080/21691401.2019.1577878

Guan, B., Yan, R., Li, R., & Zhang, X. (2018). Selenium as a pleiotropic agent for medical discovery and drug delivery. *International Journal of Nanomedicine*, 7473–7490. https://doi.org/10.2147/IJN.S181343

Gubur, S., Ercan, A., & Coskun Yazici, Z. M. (2022). Protective effects of green tea on blood and liver of rats fed with high fructose diet. *Acta Alimentaria*, *51*(3), 437–447. https://doi.org/10.1556/066.2022.00081

Güleş, Ö., & Tatar, M. (2020). Effects of Fructose-Induced Metabolic Syndrome on Kidney Histology in Rats. *Kocatepe Veterinary Journal*, *13*(2), 203–209. https://doi.org/10.30607/kvj.715053

Guo, L., Xiao, J., Liu, H., & Liu, H. (2020). Selenium nanoparticles alleviate hyperlipidemia and vascular injury in ApoE-deficient mice by regulating cholesterol metabolism and reducing oxidative stress. *Metallomics*, *12*, 204–217. https://doi.org/10.1039/C9MT00215D

Gutiérrez, R. M. P., Gómez, J. T., Urby, R. B., Soto, J. G. C., & Parra, H. R. (2022). Evaluation of Diabetes Effects of Selenium Nanoparticles Synthesized from a Mixture of Luteolin and Diosmin on Streptozotocin-Induced Type 2 Diabetes in Mice. *Molecules*, *27*(17), 1–19. https://doi.org/10.3390/molecules27175642

Hadjihambi, A., Konstantinou, C., Klohs, J., Monsorno, K., Guennec, A. Le, Donnelly, C., Cox, I. J., Kusumbe, A., Hosford, P. S., Soffientini, U., Lecca, S., Mameli, M., Jalan, R., Paolicelli, R. C., & Pellerin, L. (2022). Partial MCT1 invalidation protects against diet-induced non-alcoholic fatty liver disease and the associated brain dysfunction. *Journal of Hepatology*, *78*, 180–190. https://doi.org/10.1016/j.jhep.2022.08.008

Hadrup, N., Loeschner, K., Mandrup, K., Ravn-Haren, G., Frandsen, H. L., Larsen, E. H., Lam, H. R., & Mortensen, A. (2019). Subacute oral toxicity investigation of selenium nanoparticles and selenite in rats. *Drug and Chemical Toxicology*, *42*(1), 76–83. https://doi.org/10.1080/01480545.2018.1491589

Hadzhibozheva, P., Pashova-stoyanova, L., Tsokeva, Z., Ganeva, M., Nancheva, K., Ilieva, G., Nanchev, V., Tolekova, A., & Georgiev, T. (2023). Appetite – regulating hormones in rats with fructose-induced metabolic changes. *Pharmacia*, *70*(1), 1–7. https://doi.org/10.3897/pharmacia.70.e87712

Hajizadeh, M. R., Parvaz, N., Barani, M., Khoshdel, A., Fahmidehkar, M. A., Mahmoodi, M., & Torkzadeh-Mahani, M. (2019). Diosgenin-loaded niosome as an effective phytochemical nanocarrier: physicochemical characterization, loading efficiency, and cytotoxicity assay. *DARU, Journal of Pharmaceutical Sciences*, *27*(1), 329–339. https://doi.org/10.1007/s40199-019-00277-0

Hameed, A. T., Al-alh, N. M. A., & Jumaa, A. W. (2021). Antioxidant Activity and Phytominerals Study of Some Asteraceae Species Growth in Western of Lraq. *Indian Journal of Forensic Medicine & Toxicology*, *15*(1), 2239–2245. https://doi.org/10.37506/ijfmt.v15i1.13736

Han, H., Guo, Y., Li, X., Shi, D., Xue, T., Wang, L., Li, Y., & Zheng, M. (2019). Plant Sterol Ester of α -Linolenic Acid Attenuates Nonalcoholic Fatty Liver Disease by Rescuing the Adaption to Endoplasmic Reticulum Stress and Enhancing Mitochondrial Biogenesis. *Oxidative Medicine and Cellular Longevity*, *2019*, 1–14. https://doi.org/10.1155/2019/8294141

Handayani, D., Febrianingsih, E., Kurniawati, A. D., Kusumastuty, I., Nurmalitasari, S., Widyanto, R. M., Oktaviani, D. N., Innayah, A. M., & Sulistyowati, E. (2021). High-fructose diet initially promotes increased aortic wall thickness, liver steatosis, and cardiac histopathology deterioration, but does not increase body fat index. *Journal of Public Health Research*, *10*(2), 1–7. https://doi.org/10.4081/jphr.2021.2181

Hannou, S. A., Haslam, D. E., McKeown, N. M., & Herman, M. A. (2018). Fructose metabolism and metabolic disease. *Journal of Clinical Investigation*, *128*(2), 545–555. https://doi.org/10.1172/JCI96702

Hao, H., Li, X., Guo, Y., Zheng, M., Xue, T., & Wang, L. (2021). Plant sterol ester of α-linolenic acid ameliorates high-fat diet-induced nonalcoholic fatty liver disease in mice association with regulating mitochondrial dysfunction and oxidative stress via activating AMPK signaling. *Food & Function*, *12*(5), 2171–2188.

Harborne, A. J. (1998). *Phytochemical methods a guide to modern techniques of plant analysis*. springer science & business media.

Harborne, J. B. (1973). Phytochemical methods. In *A guide to modern techniques of plant analysis 2* (pp. 5–11). London. chapman and hall, Ltd.

Harrell, C. S., Zainaldin, C., McFarlane, D., Hyer, M. M., Stein, D., Sayeed, I., & Neigh, G. N.

(2018). High-fructose diet during adolescent development increases neuroinflammation and depressive-like behavior without exacerbating outcomes after stroke. *Brain, Behavior, and Immunity*, *73*, 340–351. https://doi.org/10.1016/j.bbi.2018.05.018

Hasimun, P., Sulaeman, A., Mulyani, Y., Islami, W. N., & Lubis, F. A. T. (2019). Antihyperlipidemic Activity and HMG CoA Reductase Inhibition of Ethanolic Extract of Zingiber Cassumunar Roxb in Fructose-Induced Hyperlipidemic Wistar Rats. *Journal of Pharmaceutical Sciences and Research*, *11*(5), 1897–1901. https://search.proquest.com/openview/ecf7f9e5fba20bc7cedb41febf3f38f9/1?pq-origsite=gscholar&cbl=54977

Hassan, R. M., Elsayed, M., Kholief, T. E., Hassanen, N. H. M., Gafer, J. A., & Attia, Y. A. (2021). Mitigating effect of single or combined administration of nanoparticles of zinc oxide, chromium oxide, and selenium on genotoxicity and metabolic insult in fructose/streptozotocin diabetic rat model. *Environmental Science and Pollution Research*, *28*(35), 48517–48534. https://doi.org/10.1007/s11356-021-14089-w

Hassan, S., Moustafa, A. A., Kabil, S. L., & Mahmoud, N. M. (2020). Alagebrium mitigates metabolic insults in high carbohydrate and high fat diet fed Wistar rats. *Pharmaceutical Sciences*, *26*(1), 13–24. https://doi.org/10.34172/PS.2019.66

Hegazy, M., Elsayed, N. M., Ali, H. M., Hassan, H. G., & Rashed, L. (2019). Diabetes mellitus, nonalcoholic fatty liver disease, and conjugated linoleic acid (OMEGA 6): What is the link? *Journal of Diabetes Research*, *2019*, 1–7. https://doi.org/10.1155/2019/5267025

Helal, N. M., Ibrahim, N. A., & Khattab, H. (2019). Phytochemical analysis and antifungal bioactivity of Pulicaria undulata (L.) methanolic extract and essential oil. *Egyptian Journal of Botany*, *59*(3), 827–844. https://doi.org/10.21608/ejbo.2019.12259.1308

Helmstadter, A. (2016). Ethnopharmacology in the work of Melville William Hilton-Simpson (1881-1938) - Historical analysis and current research opportunities. *Pharmazie*, *71*(6), 352–360. https://doi.org/10.1691/ph.2016.6533

Hernández-Díaz, J. A., Garza-García, J. J., León-Morales, J. M., Zamudio-Ojeda, A., Arratia-Quijada, J., Velázquez-Juárez, G., López-Velázquez, J. C., & García-Morales, S. (2021). Antibacterial Activity of Biosynthesized Selenium Nanoparticles Using Extracts of Calendula officinalis against Potentially Clinical Bacterial Strains. *Molecules*, *26*, 1–29. https://doi.org/10.3390/molecules26195929

Hu, Z., Ren, L., Wang, C., Liu, B., & Song, G. (2012). Effect of chenodeoxycholic acid on fibrosis, inflammation and oxidative stress in kidney in high-fructose-fed wistar rats. *Kidney and Blood Pressure Research*, *36*(1), 85–97. https://doi.org/10.1159/000341485

Hudish, L. I., Reusch, J. E. B., & Sussel, L. (2019). β Cell dysfunction during progression of

metabolic syndrome to type 2 diabetes. In *Journal of Clinical Investigation* (Vol. 129, Issue 10, pp. 4001–4008). https://doi.org/10.1172/JCI129188

Ichigo, Y., Takeshita, A., Hibino, M., Nakagawa, T., Hayakawa, T., Patel, D., Field, C. J., & Shimada, M. (2019). High-fructose diet-induced hypertriglyceridemia is associated with enhanced hepatic expression of ACAT2 in Rats. *Physiological Research*, *68*(6), 1021–1026. https://doi.org/10.33549/physiolres.934226

Ikram, M., Javed, B., Raja, N. I., & Mashwani, Z.-R. (2021). Biomedical Potential of Plant-Based Selenium Nanoparticles : A Comprehensive Review on Therapeutic and Mechanistic Aspects. *International Journal of Nanomedicine*, *16*, 249–268. https://doi.org/10.2147/IJN.S295053

Iranshahy, M., Javadi, B., Iranshahi, M., Jahanbakhsh, S. P., Mahyari, S., Hassani, F. V., & Karimi, G. (2017). A review of traditional uses, phytochemistry and pharmacology of Portulaca oleracea L. *Journal of Ethnopharmacology*, *205*, 158–172. https://doi.org/10.1016/j.jep.2017.05.004

Iskender, H., Yenice, G., Terim Kapakin, K. A., Dokumacioglu, E., Sevim, C., Hayirli, A., & Altun, S. (2022). Effects of high fructose diet on lipid metabolism and the hepatic NF-κB/ SIRT-1 pathway. *Biotechnic and Histochemistry*, *97*(1), 30–38. https://doi.org/10.1080/10520295.2021.1890214

Islam, F., Bepary, S., Nafady, M. H., Islam, R., Emran, T. Bin, Sultana, S., Huq, A., Mitra, S., Chopra, H., Sharma, R., & Sweilam, S. H. (2022). Polyphenols Targeting Oxidative Stress in Spinal Cord Injury : Current Status and Future Vision. *Oxidative Medicine and Cellular Longevity*, *2022*, 1–21.

Ivanova, N., Liu, Q., Agca, C., Agca, Y., Noble, E. G., Whitehead, S. N., & Cechetto, D. F. (2020). White matter inflammation and cognitive function in a co-morbid metabolic syndrome and prodromal Alzheimer's disease rat model. *Journal of Neuroinflammation*, *17*(1), 1–18. https://doi.org/10.1186/s12974-020-1698-7

Javani, R., Sadat, F., & Ghanbarzadeh, B. (2021). Quercetin-loaded niosomal nanoparticles prepared by the thin-layer hydration method : Formulation development , colloidal stability , and structural properties. *LWT - Food Science and Technology*, *141*, 110865. https://doi.org/10.1016/j.lwt.2021.110865

Jelenković, L., Jovanović, V. S., Palić, I., Mitić, V., & Radulović, M. (2014). In vitro screening of α-amylase inhibition by selected terpenes from essential oils. In *Tropical Journal of Pharmaceutical Research* (Vol. 13, Issue 9, pp. 1421–1428). https://doi.org/10.4314/tjpr.v13i9.7

Jha, N., Esakkiraj, P., Annamalai, A., Lakra, A. K., Naik, S., & Arul, V. (2022). Synthesis,

optimization, and physicochemical characterization of selenium nanoparticles from polysaccharide of mangrove Rhizophora mucronata with potential bioactivities potential bioactivities. *Journal of Trace Elements and Minerals*, *2*, 100019. https://doi.org/10.1016/j.jtemin.2022.100019

Jin, Y., He, Y., Liu, L., Tao, W., Wang, G., Sun, W., Pei, X., Xiao, Z., Wang, H., & Wang, M. (2021). Effects of Supranutritional Selenium Nanoparticles on Immune and Antioxidant Capacity in Sprague-Dawley Rats. *Biological Trace Element Research*, *199*(12), 4666–4674. https://doi.org/10.1007/s12011-021-02601-9

Jones, H. F., Butler, R. N., & Brooks, D. A. (2011). Intestinal fructose transport and malabsorption in humans. *American Journal of Physiology - Gastrointestinal and Liver Physiology*, *300*(2), 202–206. https://doi.org/10.1152/ajpgi.00457.2010

Kadar, N. N. M. A., Ahmad, F., Teoh, S. L., & Yahaya, M. F. (2022). Comparable Benefits of Stingless Bee Honey and Caffeic Acid in Mitigating the Negative Effects of Metabolic Syndrome on the Brain. *Antioxidants*, *11*, 1–16. https://doi.org/10.3390/antiox11112154

Kamble, S. S., Killedar, S. G., Jarag, R. J., & Dol, H. S. (2019). Screening and evaluation of Sonchus asper n-hexane extract against Phenylhydrazine induced anemia. *International Journal of Advance Research and Development*, *4*(1), 68–74. www.IJARND.com

Kamenova, P. (2020). Therapeutic potential of metformin in normal glucose tolerant persons with metabolic syndrome. *Biotechnology and Biotechnological Equipment*, *34*(1), 30–37. https://doi.org/10.1080/13102818.2019.1711184

Kaouachi, A., & Derouiche, S. (2018). Phytochemical analysis, DPPH antioxidant activity and Acute toxicity of bark aqueous extracts of Pinus halepensis. *Research Journal of Chemical and Environmental Sciences*, *6*, 86–91.

Kebede, T., Gadisa, E., & Tufa, A. (2021). Antimicrobial activities evaluation and phytochemical screening of some selected medicinal plants: A possible alternative in the treatment of multidrug-resistant microbes. *PLoS ONE*, *16*, 1–16. https://doi.org/10.1371/journal.pone.0249253

Keshta, A. T., Fathallah, A. M., Attia, Y. A., Salem, E. A., & Watad, S. H. (2023). Ameliorative effect of selenium nanoparticles on testicular toxicity induced by cisplatin in adult male rats. *Food and Chemical Toxicology*, *179*, 113979. https://doi.org/10.1016/j.fct.2023.113979

Khan, K. U., Zuberi, A., Nazir, S., Fernandes, J. B. K., Jamil, Z., & Sarwar, H. (2016). Effects of dietary selenium nanoparticles on physiological and biochemical aspects of juvenile Tor putitora. *Turkish Journal of Zoology*, *40*(5), 704–712. https://doi.org/10.3906/zoo-1510-5

Khan, M. A., Singh, D., Arif, A., Sodhi, K. K., Singh, D. K., Islam, S. N., Ahmad, A., Akhtar,

K., & Siddique, H. R. (2022). Protective effect of green synthesized Selenium Nanoparticles against Doxorubicin induced multiple adverse effects in Swiss albino mice. *Life Sciences*, *305*, 120792. https://doi.org/10.1016/j.lfs.2022.120792

Khan, M., Sohail, Raja, N. I., Asad, M. J., & Mashwani, Z. ur R. (2023). Antioxidant and hypoglycemic potential of phytogenic cerium oxide nanoparticles. *Scientific Reports*, *13*(1), 1–13. https://doi.org/10.1038/s41598-023-31498-8

Khan, T., Khan, S., Akhtar, M., Ali, J., & Najmi, A. K. (2021). Empagliflozin nanoparticles attenuates type2 diabetes induced cognitive impairment via oxidative stress and inflammatory pathway in high fructose diet induced hyperglycemic mice. *Neurochemistry International*, *150*, 105158. https://doi.org/10.1016/j.neuint.2021.105158

Khandsuren, B., & Prokisch, J. (2021). The production methods of selenium nanoparticles. *Acta Universitatis Sapientiae, Alimentaria*, *14*(1), 14–43. https://doi.org/10.2478/ausal-2021-0002

Khiralla, G. (2019). Protective Effect of Selenium Nanoparticles against Acrylamide-Induced Hepatotoxicity in Albino Rats. *Journal of Food and Dairy Sciences*, *10*(10), 359–363. https://doi.org/10.21608/jfds.2019.60768

Khodabakhsh, F., Bourbour, M., Yaraki, M. T., Bazzazan, S., Bakhshandeh, H., Cohan, R. A., & Tan, Y. N. (2022). pH-Responsive PEGylated Niosomal Nanoparticles as an Active-Targeting Cyclophosphamide Delivery System for Gastric Cancer Therapy. *Molecules*, *27*(17), 1–25. https://doi.org/10.3390/ molecules27175418

Khurana, A., Tekula, S., Aslam, M., Venkatesh, P., & Godugu, C. (2019). Biomedicine & Pharmacotherapy Therapeutic applications of selenium nanoparticles. *Biomedicine & Pharmacotherapy Journal*, *111*, 802–812. https://doi.org/10.1016/j.biopha.2018.12.146

Kilany, O. E., Abdelrazek, H. M. A., Aldayel, T. S., Abdo, S., & Mahmoud, M. M. A. (2020). Anti-obesity potential of Moringa olifera seed extract and lycopene on high fat diet induced obesity in male Sprauge Dawely rats. *Saudi Journal of Biological Sciences*, *27*(10), 2733–2746. https://doi.org/10.1016/j.sjbs.2020.06.026

Kim, S., & Chunghee, L. (2007). Phylogenetic analysis of chloroplast DNA mat K gene and ITS of nrDNA sequences reveals polyphyly of the genus Sonchus and new relationships among the subtribe Sonchinae (Asteraceae : Cichorieae). *Molecular Phylogenetics and Evolution*, *44*, 578–597. https://doi.org/10.1016/j.ympev.2007.03.014

Kojouri, G., Arbabi, F., & Mohebbi, A. (2020). The effects of selenium nanoparticles (SeNPs) on oxidant and antioxidant activities and neonatal lamb weight gain pattern. *Comparative Clinical Pathology*, *29*(2), 369–374. https://doi.org/10.1007/s00580-019-03061-3

Korde, P., Ghotekar, S., Pagar, T., Pansambal, S., Oza, R., & Mane, D. (2020). Plant Extract

Assisted Eco-benevolent Synthesis of Selenium Nanoparticles-A Review on Plant Parts Involved , Characterization and Their Recent Applications. *Journal of Chemical Reviews*, *2*(3), 157–168. https://doi.org/10.33945/SAMI/JCR.2020.3.3

Koriem, K. M. M., Arbid, M. S. S., & Gomaa, N. E. (2018). The Role of Chlorogenic Acid Supplementation in Anemia and Mineral Disturbances Induced by 4- Tert-Octylphenol Toxicity. *Journal of Dietary Supplements*, *15*(1), 55–71. https://doi.org/10.1080/19390211.2017.1321079

Krol, S., Macrez, R., Docagne, F., Defer, G., Laurent, S., Rahman, M., Hajipour, M. J., Kehoe, P. G., & Mahmoudi, M. (2013). Therapeutic benefits from nanoparticles: the potential significance of nanoscience in diseases with compromise to the blood brain barrier. *Chemical Reviews*, *113*(3), 1877–1903. https://doi.org/10.1021/cr200472g

Kuefner, M. S. (2021). Secretory Phospholipase A2s in Insulin Resistance and Metabolism. *Frontiers in Endocrinology*, *12*(August), 1–8. https://doi.org/10.3389/fendo.2021.732726

Kumar, A., Prasad, B., Manjhi, J., & Prasad, K. S. (2020). Antioxidant activity of selenium nanoparticles biosynthesized using a cell-free extract of Geobacillus. *Toxicological & Environmental Chemistry*, *102*(10), 556–567. https://doi.org/10.1080/02772248.2020.1829623

Kumar, M., Tomar, M., Amarowicz, R., Saurabh, V., Nair, M. S., Maheshwari, C., Sasi, M., Prajapati, U., Hasan, M., Singh, S., Changan, S., Prajapat, R. K., Berwal, M. K., & Satankar, V. (2021). Guava (Psidium guajava L .) Leaves : Nutritional Composition, Phytochemical Profile, and Health-Promoting Bioactivities. *Foods*, *10*(4), 1–20. https://doi.org/10.3390/foods10040752

Kumar, S. R., Ramli, E. S. M., Nasir, N. A. A., Ismail, N. M., & Fahami, N. A. M. (2021). Methanolic extract of piper sarmentosum attenuates obesity and hyperlipidemia in fructose-induced metabolic syndrome rats. *Molecules*, *26*(13), 1–14. https://doi.org/10.3390/molecules26133985

Kütük, A., Akar, F., & Sadi, G. (2023). Changes in hepatic thiol contents and regulation of glutathione S-transferase by high-fructose diet : Effects of kefir and some probiotic bacteria. *HEALTH SCIENCES QUARTERLY*, *3*(2), 127–137.

Lasker, S., Rahman, M. M., Parvez, F., Zamila, M., Miah, P., Nahar, K., Kabir, F., Sharmin, S. B., Subhan, N., Ahsan, G. U., & Alam, M. A. (2019). High-fat diet-induced metabolic syndrome and oxidative stress in obese rats are ameliorated by yogurt supplementation. *Scientific Reports*, *9*(1), 1–15. https://doi.org/10.1038/s41598-019-56538-0

Lazarevic-Pasti, T., Leskovac, A., Momic, T., Petrovic, S., & Vasic, V. (2017). Modulators of Acetylcholinesterase Activity: From Alzheimer's Disease to Anti-Cancer Drugs. *Current*

Medicinal Chemistry, *24*(30), 1–27. https://doi.org/10.2174/0929867324666170705123509

Lee, H., & Jose, P. A. (2021). Coordinated Contribution of NADPH Oxidase- and Mitochondria-Derived Reactive Oxygen Species in Metabolic Syndrome and Its Implication in Renal Dysfunction. *Frontiers in Pharmacology*, *12*, 1–18. https://doi.org/10.3389/fphar.2021.670076

Lee, S., Lee, J., Lee, H., & Sung, J. (2019). Relative protective activities of quercetin, quercetin-3-glucoside, and rutin in alcohol-induced liver injury. *Journal of Food Biochemistry*, *43*(11), 1–9. https://doi.org/10.1111/jfbc.13002

Li, L., Fang, B., Zhang, Y., Yan, L., He, Y., Hu, L., Xu, Q., Li, Q., Dai, X., Kuang, Q., Xu, M., Tan, J., & Ge, C. (2022). Carminic acid mitigates fructose-triggered hepatic steatosis by inhibition of oxidative stress and inflammatory reaction. *Biomedicine & Pharmacotherapy*, *145*, 112404. https://doi.org/10.1016/j.biopha.2021.112404

Li, Q., Dong, D.-D., Huang, Q.-P., Li, J., Du, Y.-Y., Li, B., Li, H.-Q., & Huyan, T. (2017). The anti-inflammatory effect of Sonchus oleraceus aqueous extract on lipopolysaccharide stimulated RAW 264 . 7 cells and mice. *Pharmaceutical Biology*, *55*(1), 799–809. https://doi.org/10.1080/13880209.2017.1280514

Li, W., & Lu, Y. (2018). Hepatoprotective Effects of Sophoricoside against Fructose-Induced Liver Injury via Regulating Lipid Metabolism, Oxidation, and Inflammation in Mice. *Journal of Food Science*, *83*(2), 552–558. https://doi.org/10.1111/1750-3841.14047

Lim, H., Park, H., & Kim, H. P. (2015). Effects of flavonoids on senescence-associated secretory phenotype formation from bleomycin-induced senescence in BJ fibroblasts. *Biochemical Pharmacology*, *96*(4), 337–348. https://doi.org/10.1016/j.bcp.2015.06.013

Lim, S., Kim, J. W., & Targher, G. (2021). Links between metabolic syndrome and metabolic dysfunction-associated fatty liver disease. *Trends in Endocrinology and Metabolism*, *32*(7), 500–514. https://doi.org/10.1016/j.tem.2021.04.008

Lin, L., Tan, W., Pan, X., Tian, E., Wu, Z., & Yang, J. (2022). Metabolic Syndrome-Related Kidney Injury : A Review and Update. *Frontiers in Endocrinology*, *13*, 1–12. https://doi.org/10.3389/fendo.2022.904001

Lin, X., Ali, A., Xiao, X., Deng, H., Lin, X., Sameir, A., Ali, M., & Viscardi, A. (2023). Selenium nanoparticles : Properties , preparation methods , and therapeutic applications. *Chemico-Biological Interactions*, *378*, 110483. https://doi.org/10.1016/j.cbi.2023.110483

Liu, K., Luo, M., & Wei, S. (2019). The Bioprotective Effects of Polyphenols on Metabolic Syndrome against Oxidative Stress : Evidences and Perspectives. *Oxidative Medicine and Cellular Longevity*, *2019*, 1–17. https://doi.org/10.1155/2019/6713194 Review

Liu, L., Li, T., Liao, Y., Wang, Y., Gao, Y., Hu, H., Huang, H., Wu, F., Chen, Y. G., Xu, S., &

Fu, S. (2020). Triose Kinase Controls the Lipogenic Potential of Fructose and Dietary Tolerance. *Cell Metabolism*, *32*(4), 605–618. https://doi.org/10.1016/j.cmet.2020.07.018

Liu, Z., Kiessling, F., & Jessica, G. (2010). Advanced Nanomaterials in Multimodal Imaging : Design , Functionalization, and Biomedical Applications. *Journal of Nanomaterials*, *2010*, 1–15. https://doi.org/10.1155/2010/894303

Lombardo, D., Kiselev, M. A., & Caccamo, M. T. (2019). Smart Nanoparticles for Drug Delivery Application : Development of Versatile Nanocarrier Platforms in Biotechnology and Nanomedicine. *Journal of Nanomaterials*, *2019*, 1–27. https://doi.org/10.1155/2019/3702518

Lopez-candales, A., Burgos, P. M. H., Hernandez-suarez, D. F., & Harris, D. (2017). Linking Chronic Inflammation with Cardiovascular Disease: From Normal Aging to the Metabolic Syndrome. *Journal of Natural Sciences*, *3*(4), 1–22. https://www.ncbi.nlm.nih.gov/pmc/articles/PMC5488800/pdf/nihms868857.pdf

Lorke, D. (1983). A new approach to practical acute toxicity testing. *Archives of Toxicology*, *54*(4), 275–287. https://doi.org/10.1007/BF01234480

Luo, J., Su, L., He, X., Du, Y., Xu, N., Wu, R., Zhu, Y., Wang, T., Shao, R., & Unverzagt, F. W. (2023). Blood Selenium and Serum Glutathione Peroxidase Levels Were Associated with Serum β-Amyloid in Older Adults. *Biological Trace Element Research*, *201*(8), 3679–3687.

Maheo, A. R., B., S. M. V., & T., A. A. P. (2022). Biosynthesis and characterization of Eupatorium adenophorum and chitosan mediated Copper oxide nanoparticles and their antibacterial activity. *Results in Surfaces and Interfaces*, *6*, 100048. https://doi.org/10.1016/j.rsurfi.2022.100048

Mahesh, M., Pandey, H., Raja Gopal Reddy, M., Prabhakaran Sobhana, P., Korrapati, D., Uday Kumar, P., Vajreswari, A., & Jeyakumar, S. M. (2021). Carrot Juice Consumption Reduces High Fructose-Induced Adiposity in Rats and Body Weight and BMI in Type 2 Diabetic Subjects. *Nutrition and Metabolic Insights*, *14*, 11786388211014916. https://doi.org/10.1177/11786388211014917

Mahmood, R. I., Kadhim, A. A., Ibraheem, S., Albukhaty, S., Salih, H. S. M., Abbas, R. H., Jabir, M. S., Mohammed, M. K. A., Nayef, U. M., Almalki, F. A., & Sulaiman, G. M. (2022). Biosynthesis of copper oxide nanoparticles mediated Annona muricata as cytotoxic and apoptosis inducer factor in breast cancer cell lines. *Scientific Reports*, *12*(1), 1–10. https://doi.org/10.1038/s41598-022-20360-y

Malhotra, S., Jha, N., & Desai, K. (2014). A SUPERFICIAL SYNTHESIS OF SELENIUM NANOSPHERES USING WET CHEMICAL APPROACH Enhancement of Biofuel production from microalgae View project A SUPERFICIAL SYNTHESIS OF SELENIUM

NANOSPHERES USING WET CHEMICAL APPROACH. *International Journal of Nanotechnology and Application (IJNA) ISSN(P*, *3*(2), 7–14. www.tjprc.org

Martínez-Esquivias, F., Guzmán-Flores, J. M., Párez-Larios, A., Rico, J. L., & Becerra-Ruiz, J. S. (2021). A review of the effects of gold, silver, selenium, and zinc nanoparticles on diabetes mellitus in murine models. *Mini Reviews in Medicinal Chemistry*, *21*(14), 1798–1812. https://doi.org/10.2174/1389557521666210203154024

Martínez-Esquivias, F., Perez-Larios, A., & Guzmán-Flores, J. M. (2024). Effect of Administration of Selenium Nanoparticles Synthesized Using Onion Extract on Biochemical and Inflammatory Parameters in Mice Fed with High-Fructose Diet: In Vivo and In Silico Analysis. *Biological Trace Element Research*, *202*(2), 558–568. https://doi.org/10.1007/s12011-023-03685-1

Masenga, S. K., Kabwe, L. S., Chakulya, M., & Kirabo, A. (2023). Mechanisms of Oxidative Stress in Metabolic Syndrome. *International Journal of Molecular Sciences*, *24*(9), 1–28. https://doi.org/10.3390/ijms24097898

Medaglia, D. S. A., Vieira, H. R., Silveira, S. da S., Siervo, G. E. M. de L., Marcon, M. S. da S., Mathias, P. C. de F., & Fernandes, G. S. A. (2022). High-fructose diet during puberty alters the sperm parameters, testosterone concentration, and histopathology of testes and epididymis in adult Wistar rats. *Journal of Developmental Origins of Health and Disease*, *13*(1), 20–27. https://doi.org/10.1017/S2040174420001385

Mehta, R., Sonavane, M., Migaud, M. E., & Gassman, N. R. (2021). Exogenous exposure to dihydroxyacetone mimics high fructose induced oxidative stress and mitochondrial dysfunction. *Environmental and Molecular Mutagenesis*, *62*(3), 185–202. https://doi.org/10.1002/em.22425

Mekki, S., Belhocine, M., Bouzouina, M., Chaouad, B., & Mostari, A. (2023). Therapeutic effects of Salvia balansae on metabolic disorders and testicular dysfunction mediated by a high-fat diet in Wistar rats. *Mediterranean Journal of Nutrition and Metabolism*, *16*(2), 21–39. https://doi.org/10.3233/MNM-220094

Mendrick, D. L., Diehl, A. M., Topor, L. S., Dietert, R. R., Will, Y., La Merrill, M. A., Bouret, S., Varma, V., Hastings, K. L., Schug, T. T., Hart, S. G. E., & Burleson, F. G. (2018). Metabolic syndrome and associated diseases: From the bench to the clinic. *Toxicological Sciences*, *162*(1), 36–42. https://doi.org/10.1093/toxsci/kfx233

Meng-zhen, S., Ju, L., Lan-chun, Z., Cai-feng, D., Shu-da, Y., Hao-fei, Y., & Wei-yan, H. (2022). Potential therapeutic use of plant flavonoids in AD and PD. *Heliyon*, *8*(11), e11440. https://doi.org/10.1016/j.heliyon.2022.e11440

Menon, S., Agarwal, H., Rajeshkumar, S., Jacquline Rosy, P., & Shanmugam, V. K. (2020).

Investigating the Antimicrobial Activities of the Biosynthesized Selenium Nanoparticles and Its Statistical Analysis. *BioNanoScience*, *10*(1), 122–135. https://doi.org/10.1007/s12668-019-00710-3

Metwally, D. M., Alajmi, R. A., El-khadragy, M. F., Yehia, H. M., Al-megrin, W. A., Akabawy, A. M. A., Amin, H. K., & Abdel, A. E. (2020). Chlorogenic acid confers robust neuroprotection against arsenite toxicity in mice by reversing oxidative stress , inflammation , and apoptosis. *Journal of Functional Foods*, *75*, 104202. https://doi.org/10.1016/j.jff.2020.104202

Mikkelsen, A. C. D., Thomsen, K. L., Mookerjee, R. P., & Hadjihambi, A. (2022). The role of brain inflammation and abnormal brain oxygen homeostasis in the development of hepatic encephalopathy. *Metabolic Brain Disease*, *38*(5), 1707–1716. https://doi.org/10.1007/s11011-022-01105-2

Milovanovic, T., Pantic, I., Dragasevic, S., Lugonja, S., Dumic, I., & Rajilic-Stojanovic, M. (2021). The interrelationship among non-alcoholic fatty liver disease, colonic diverticulosis and metabolic syndrome. *Journal of Gastrointestinal and Liver Diseases*, *30*(2), 1–9. https://doi.org/10.15403/jgld-3308

Milovanović, V., Petrović, Z., Petrović, V., Simijonović, D., Mladenović, M., Tomašević, N., Čomić, L., & Radojević, I. (2021). In vitro and in silico lipoxygenase inhibition studies and antimicrobial activity of pyrazolyl-phthalazine-diones. *Kragujevac Journal of Science*, *43*(43), 35–52. https://doi.org/10.5937/kgjsci2143035m

Mirzaei, R., Bidgoli, S. A., Khosrokhavar, R., Shoeibi, S., & Ashtiani, H. A. (2022). Consumption of High-Fructose Corn Syrup Compared with Sucrose in Female Wistar Rat Promotes Concomitant Cerebral and Hepatic Injuries in Comparable clinical responses . *Research Square*, *1*, 1–22. https://doi.org/10.21203/rs.3.rs-1568213/v1

Moghaddam, R., Hamidreza, S., Hosseini, M., Sabzi, F., Fard, F. H., Marefati, N., Beheshti, F., Darroudi, M., Bideskan, A. E., & Anaeigoudari, A. (2022). Cardiovascular protective effect of nano selenium in hypothyroid rats: protection against oxidative stress and cardiac fibrosis. *Clinical and Experimental Hypertension*, *44*(3), 268–279. https://doi.org/10.1080/10641963.2022.2036994

Mohamad, E. A., & Fahmy, H. M. (2020). Niosomes and liposomes as promising carriers for dermal delivery of annona squamosa extract. *Brazilian Journal of Pharmaceutical Sciences*, *56*, 1–8. https://doi.org/10.1590/s2175-97902019000318096

Mohamed, H. E., Asker, M. E., Shaheen, M. A., Eissa, R. G., & Younis, N. N. (2021). Alleviation of fructose-induced Alzheimer's disease in rats by pioglitazone and decaffeinated green coffee bean extract. *Journal of Food Biochemistry*, *45*(5), 1–12.

https://doi.org/10.1111/jfbc.13715

Mohasib, R. M. M., Nagib, A., Samad, A. A., Salama, Z. A., & Gaafar, A. A. (2020). IDENTIFICATION OF BIOACTIVE INGREDIENTS IN SONCHUS OLERACEUS BY HPLC AND GC / MS. *Plant Archives*, *20*(2), 9714–9720.

Mokhtari, I., Taaifi, Y., Harnafi, M., Belhaj, K., Mansouri, F., Melhaoui, R., Addi, M., Hano, C., Amrani, S., Harnafi, H., & Amrani, A. El. (2022). Hypolipidemic Effect of Hemp Seed Oil from the Northern Morocco Endemic Beldiya Ecotype in a Mice Model : Comparison with Fenofibrate Hypolipidemic Drugs. *Journal of Food Quality*, *2022*, 1–7. https://doi.org/10.1155/2022/9142395

Mondal, M., Kundu, S. K., Islam, M. T., Reiner, Ž., Martorell, M., & Sharifi-Rad, J. (2021). Protective effect of Bridelia tomentosa due to its phenolic acids and flavonoids against oxidative stress-mediated hepatic toxicity induced by carbofuran. *South African Journal of Botany*, *141*, 447–456. https://doi.org/10.1016/j.sajb.2021.06.006

Montesano, A., Senesi, P., Vacante, F., Mollica, G., Benedini, S., Mariotti, M., Luzi, L., & Terruzzi, I. (2020). l-Carnitine counteracts in vitro fructose-induced hepatic steatosis through targeting oxidative stress markers. *Journal of Endocrinological Investigation*, *43*(4), 493–503. https://doi.org/10.1007/s40618-019-01134-2

Mottillo, S., Filion, K. B., Genest, J., Joseph, L., Pilote, L., Poirier, P., Rinfret, S., Schiffrin, E. L., & Eisenberg, M. J. (2010). The metabolic syndrome and cardiovascular risk a systematic review and meta-analysis. *Journal of the American College of Cardiology*, *56*(14), 1113–1132. https://doi.org/10.1016/j.jacc.2010.05.034

Mulè, G., Calcaterra, I., Nardi, E., Cerasola, G., & Cottone, S. (2014). Metabolic syndrome in hypertensive patients: An unholy alliance. *World Journal of Cardiology*, *6*(9), 890–907. https://doi.org/10.4330/wjc.v6.i9.890

Mulla, N. A., Otari, S. V., Bohara, R. A., Yadav, H. M., & Pawar, S. H. (2020). Rapid and size-controlled biosynthesis of cytocompatible selenium nanoparticles by Azadirachta indica leaves extract for antibacterial activity. *Materials Letters*, *264*, 127353. https://doi.org/10.1016/j.matlet.2020.127353

Muñoz, S., Méndez, L., Dasilva, G., Torres, J. L., Ramos-Romero, S., Romeu, M., Nogués, M. R., & Medina, I. (2018). Targeting Hepatic Protein Carbonylation and Oxidative Stress Occurring on Diet-Induced Metabolic Diseases through the Supplementation with Fish Oils. *Marine Drugs*, *16*, 1–23. https://doi.org/10.3390/md16100353

Murugesan, G., Nagaraj, K., Sunmathi, D., & Subramani, K. (2019). Methods involved in the synthesis of selenium nanoparticles and their different applications-a review. *European Journal of Biomedical and Pharmaceutical Sciences*, *6*(4), 189–194.

Mwitari, P. G., Ayeka, P. A., Ondicho, J., Matu, E. N., & Bii, C. C. (2013). Antimicrobial Activity and Probable Mechanisms of Action of Medicinal Plants of Kenya: Withania somnifera, Warbugia ugandensis, Prunus africana and Plectrunthus barbatus. *PLoS ONE*, *8*(6), 4–12. https://doi.org/10.1371/journal.pone.0065619

Nagalingam, M., Rajeshkumar, S., Balu, S. K., Tharani, M., & Arunachalam, K. (2022). Anticancer and Antioxidant Activity of Morinda Citrifolia Leaf Mediated Selenium Nanoparticles. *Journal of Nanomaterials*, *2022*, 1–7. https://doi.org/10.1155/2022/2155772

Nair, D., Nedungadi, D., Mishra, N., Nair, B. G., & Nair, S. S. (2021). Identification of carbonylated proteins from monocytic cells under diabetes-induced stress conditions. *Biomedical Chromatography*, *35*, 1–12. https://doi.org/10.1002/bmc.5065

Nakhaei, H., Mogharnasi, M., & Fanaei, H. (2019). Effect of swimming training on levels of asprosin, lipid profile, glucose and insulin resistance in rats with metabolic syndrome. *Obesity Medicine*, *15*, 1–7. https://doi.org/10.1016/j.obmed.2019.100111

Ndwandwe, B. K., Malinga, S. P., Kayitesi, E., & Dlamini, B. C. (2021). Advances in green synthesis of selenium nanoparticles and their application in food packaging. *International Journal of Food Science and Technology*, *56*(6), 2640–2650. https://doi.org/10.1111/ijfs.14916

Neethu, B. K., & Yathiender, S. (2023). Phytochemical Screening and GC- MS Analysis of Three Indian Traditional Medicinal Plants. *Current Trends in Biotechnology and Pharmacy*, *17*, 1097–1105. https://doi.org/10.5530/ctbp.2023.3s.48

Ngwasiri, C., Kinoré, M., Samadoulougou, S., & Kirakoya-Samadoulougou, F. (2023). Sex-specific-evaluation of metabolic syndrome prevalence in Algeria : insights from the 2016 – 2017 non-communicable diseases risk factors survey. *Research Square*, 1–15.

Nilsson, P. M., Tuomilehto, J., & Rydén, L. (2019). The metabolic syndrome – What is it and how should it be managed? *European Journal of Preventive Cardiology*, *26*(2S), 33–46. https://doi.org/10.1177/2047487319886404

Nwafor, E. O., Lu, P., Zhang, Y., Liu, R., Peng, H., Xing, B., Liu, Y., Li, Z., Zhang, K., Zhang, Y., & Liu, Z. (2022). Chlorogenic acid: Potential source of natural drugs for the therapeutics of fibrosis and cancer. *Translational Oncology*, *15*(1), 101294. https://doi.org/10.1016/j.tranon.2021.101294

Nwidu, L. L., Elmorsy, E., Thornton, J., Wijamunige, B., Wijesekara, A., Tarbox, R., Warren, A., & Carter, W. G. (2017). Anti-acetylcholinesterase activity and antioxidant properties of extracts and fractions of carpolobia lutea. *Pharmaceutical Biology*, *55*(1), 1875–1883. https://doi.org/10.1080/13880209.2017.1339283

Nylén, E. S., Gandhi, S. M., & Lakshman, R. (2019). Cardiorespiratory Fitness, Physical

Activity, and the Metabolic Syndrome. *Nutrients*, *11*(7), 1–18. https://doi.org/10.1007/978-3-030-04816-7_12

Obeid, M. A., Khadra, I., Albaloushi, A., Mullin, M., Alyamani, H., & Ferro, V. A. (2019). Microfluidic manufacturing of different niosomes nanoparticles for curcumin encapsulation : Physical characteristics , encapsulation efficacy , and drug release. *Beilstein Journal of Nanotechnology*, *10*, 1826–1832. https://doi.org/10.3762/bjnano.10.177

Olajide, O. J., Yawson, E. O., Gbadamosi, I. T., Arogundade, T. T., Lambe, E., Obasi, K., Lawal, I. T., Ibrahim, A., & Ogunrinola, K. Y. (2017). Ascorbic acid ameliorates behavioural deficits and neuropathological alterations in rat model of Alzheimer's disease. *Environmental Toxicology and Pharmacology*, *50*, 200–211. https://doi.org/10.1016/j.etap.2017.02.010

Oruka, O., & Achuba, F. I. (2023). In vitro Antioxidant and Anti-Inflammatory Activities of Aqueous Leaf Extract of Alchornea cordifolia. *Journal of Applied Sciences and Environmental Management*, *27*(2), 299–304. https://doi.org/10.4314/jasem.v27i2.16

Othman, M. S., Obeidat, S. T., Al-Bagawi, A. H., Fareid, M. A., Fehaid, A., & Moneim, A. E. A. (2022). Green-synthetized selenium nanoparticles using berberine as a promising anticancer agent. *Journal of Integrative Medicine*, *20*(1), 65–72. https://doi.org/10.1016/j.joim.2021.11.002

Oyaizu, M. (1986). Studies on products of browning reaction. Antioxidative activities of products of browning reaction prepared from glucosamine. *The Japanese Journal of Nutrition and Dietetics*, *44*(6), 307–315. https://doi.org/10.5264/eiyogakuzashi.44.307

Pan, Y., & Kong, L. D. (2018). High fructose diet-induced metabolic syndrome: Pathophysiological mechanism and treatment by traditional Chinese medicine. *Pharmacological Research*, *130*, 438–450. https://doi.org/10.1016/j.phrs.2018.02.020

Pandey, S., Awasthee, N., Shekher, A., Rai, L. C., Gupta, S. C., & Dubey, S. K. (2021). Biogenic synthesis and characterization of selenium nanoparticles and their applications with special reference to antibacterial, antioxidant, anticancer and photocatalytic activity. *Bioprocess and Biosystems Engineering*, *44*(12), 2679–2696. https://doi.org/10.1007/s00449-021-02637-0

Pandiyan, I., Sri, S. D., Indiran, M. A., Rathinavelu, P. K., Prabakar, J., & Rajeshkumar, S. (2022). Antioxidant, anti-inflammatory activity of Thymus vulgaris-mediated selenium nanoparticles: An in vitro study. *Journal of Conservative Dentistry : JCD*, *25*(3), 241–245. https://doi.org/10.4103/JCD.JCD_369_21

Pant, D. R., Pant, N. D., Saru, D. B., Yadav, U. N., & Khanal, D. P. (2017). Phytochemical screening and study of antioxidant, antimicrobial, antidiabetic, anti-inflammatory and

analgesic activities of extracts from stem wood of pterocarpus marsupium roxburgh. *Journal of Intercultural Ethnopharmacology*, *6*(2), 170–176. https://doi.org/10.5455/jice.20170403094055

Patil, T. P., Vibhute, A. A., Patil, S. L., Dongale, T. D., & Tiwari, A. P. (2023). Green synthesis of gold nanoparticles via Capsicum annum fruit extract: Characterization, antiangiogenic, antioxidant and anti-inflammatory activities. In *Applied Surface Science Advances* (Vol. 13, p. 100372). https://doi.org/10.1016/j.apsadv.2023.100372

Perera, H. D. S. M., Samarasekera, J. K. R. R., Handunnetti, S. M., & Weerasena, O. V. D. S. J. (2016). In vitro anti-inflammatory and anti-oxidant activities of Sri Lankan medicinal plants. *Industrial Crops & Products*, *94*, 610–620. https://doi.org/10.1016/j.indcrop.2016.09.009

Petropoulos, S., Karkanis, A., Martins, N., & Ferreira, I. C. F. R. (2016). Phytochemical composition and bioactive compounds of common purslane (Portulaca oleracea L.) as affected by crop management practices. *Trends in Food Science & Technology*, *55*, 1–10. https://doi.org/10.1016/j.tifs.2016.06.010

Prabu, K., Rajasekaran, A., Bharathi, D., & Ramalakshmi, S. (2019). Anti-oxidant activity, phytochemical screening and HPLC profile of rare endemic Cordia diffusa. *Journal of King Saud University - Science*, *31*(4), 724–727. https://doi.org/10.1016/j.jksus.2018.04.025

Qiao, L., Dou, X., Yan, S., Zhang, B., & Xu, C. (2020). Biogenic selenium nanoparticles synthesized by: Lactobacillus casei ATCC 393 alleviate diquat-induced intestinal barrier dysfunction in C57BL/6 mice through their antioxidant activity. *Food and Function*, *11*(4), 3020–3031. https://doi.org/10.1039/d0fo00132e

Qiao, Y., Xu, L., Tao, X., Yin, L., Qi, Y., Xu, Y., Han, X., Tang, Z., Ma, X., Liu, K., & Peng, J. (2018). Protective effects of dioscin against fructose-induced renal damage via adjusting Sirt3-mediated oxidative stress, fibrosis, lipid metabolism and inflammation. *Toxicology Letters*, *284*, 37–45. https://doi.org/10.1016/j.toxlet.2017.11.031

Qiu, Y., Chen, X., Chen, Z., Zeng, X., Yue, T., & Yuan, Y. (2022). Effects of Selenium Nanoparticles on Preventing Patulin-Induced Liver, Kidney and Gastrointestinal Damage. *Foods*, *11*(5), 1–15. https://doi.org/10.3390/foods11050749

Qureshi, S. J., Awan, A. G., Khan, M. A., & Bano, S. (2002). Taxonomic Study of the Genus Sonchus L . from Pakistan. *Online Journal of Biological Sciences*, *2*(5), 309–314. https://doi.org/10.3923/jbs.2002.309.314

Raeiszadeh, M., Pardakhty, A., Sharififar, F., Mehrabani, M., Nejatmehrab-Kermani, H., & Mehrabani, M. (2018). Phytoniosome: A novel drug delivery for myrtle extract. *Iranian Journal of Pharmaceutical Research*, *17*(3), 804–817.

Rajagopal, G., Nivetha, A., Ilango, S., Muthudevi, G. P., Prabha, I., & Arthimanju, R. (2021). Phytofabrication of selenium nanoparticles using Azolla pinnata: Evaluation of catalytic properties in oxidation, antioxidant and antimicrobial activities. *Journal of Environmental Chemical Engineering*, *9*(4), 105483. https://doi.org/10.1016/j.jece.2021.105483

Rajeshkumar, S., Veena, P., & Santhiyaa, R. V. (2018). Synthesis and Characterization of Selenium Nanoparticles Using Natural Resources and Its Applications. In *Exploring the Realms of Nature for Nanosynthesis* (pp. 63–79). Springer International Publishing. https://doi.org/10.1007/978-3-319-99570-0_4

Ranchoux, B., Nadeau, V., Bourgeois, A., Provencher, S., Tremblay, É., Omura, J., Coté, N., Abu-Alhayja'a, R., Dumais, V., & Nachbar, R. T. (2019). Metabolic syndrome exacerbates pulmonary hypertension due to left heart disease. *Circulation Research*, *125*(4), 449–466. https://doi.org/10.1161/CIRCRESAHA.118.314555

Ranjitha, V. R., & Rai, V. R. (2021a). Selenium nanostructure: Progress towards green synthesis and functionalization for biomedicine. *Journal of Pharmaceutical Investigation*, *51*(2), 117–135. https://doi.org/10.1007/s40005-020-00510-y

Ranjitha, V. R., & Rai, V. R. (2021b). Selenium nanostructure: Progress towards green synthesis and functionalization for biomedicine. *Journal of Pharmaceutical Investigation*, *51*, 117–135. https://doi.org/10.1007/s40005-020-00510-y

Reaven, G. M. (1992). Role of insulin resistance in human disease. *America Diabetes Association*, 91–97. https://doi.org/10.1007/978-94-011-2700-4_10

Réggami, Y., Benkhaled, A., Boudjelal, A., Berredjem, H., Amamra, A., Benyettou, H., Larabi, N., Senator, A., Siracusa, L., & Ruberto, G. (2021). Artemisia herba-alba aqueous extract improves insulin sensitivity and hepatic steatosis in rodent model of fructose-induced metabolic syndrome. *Archives of Physiology and Biochemistry*, *127*(6), 541–550. https://doi.org/10.1080/13813455.2019.1659825

Regufe, V. M. G., Pinto, C. M. C. B., & Perez, P. M. V. H. C. (2020). Metabolic syndrome in type 2 diabetic patients : a review of current evidence. *Porto Biomedical Journal*, *5*(6), 1–6. https://doi.org/10.1097/j.pbj.0000000000000101

Rehman, G., Hamayun, M., Iqbal, A., Ul Islam, S., Arshad, S., Zaman, K., Ahmad, A., Shehzad, A., Hussain, A., & Lee, I. (2018a). In vitro antidiabetic effects and antioxidant potential of cassia nemophila pods. *BioMed Research International*, *2018*, 1–6. https://doi.org/10.1155/2018/1824790

Rehman, G., Hamayun, M., Iqbal, A., Ul Islam, S., Arshad, S., Zaman, K., Ahmad, A., Shehzad, A., Hussain, A., & Lee, I. (2018b). In vitro antidiabetic effects and antioxidant potential of cassia nemophila pods. *BioMed Research International*, *2018*, 1–6.

https://doi.org/10.1155/2018/1824790

Reilly, M. P., & Rader, D. J. (2003). The Metabolic Syndrome More Than the Sum of Its Parts? *Circulation*, *108*(13), 1546–1551. https://doi.org/10.1161/01.CIR.0000088846.10655.E0

Ren, Y., Hou, S., He, J., Chang, N., Zhang, Z., & Zhou, Y. (2023). Total flavones from Sonchus arvensis L. ameliorate colitis by adjusting the gut microbiota. *Annals of Medicine*, *55*(2), 1–11. https://doi.org/10.1080/07853890.2023.2292246

Rodríguez-Correa, E., González-Pérez, I., Clavel-Pérez, P. I., Contreras-Vargas, Y., & Carvajal, K. (2020). Biochemical and nutritional overview of diet-induced metabolic syndrome models in rats: what is the best choice? *Nutrition and Diabetes*, *10*(1), 1–15. https://doi.org/10.1038/s41387-020-0127-4

Russa, D. La, Giordano, F., Marrone, A., Parafati, M., Janda, E., & Pellegrino, D. (2019). Oxidative imbalance and kidney damage in cafeteria diet-induced rat model of metabolic syndrome: Effect of bergamot polyphenolic fraction. *Antioxidants*, *8*(3), 1–15. https://doi.org/10.3390/antiox8030066

Sabarathinam, S., Kumar, R. C. S., & Vijayakumar, T. M. (2022). Necessity of Herbal Medicine in the Management of Metabolic Syndrome. In N. Shiomi (Ed.), *Lifestyle-Related Diseases and Metabolic Syndrome* (p. 160). IntechOpen. https://doi.org/10.5772/intechopen.105199

Saed, Z. H., Abohbell, H. A., & Mahklouf, M. H. (2019). Floristic Analysis of the Family Asteraceae in Sabratha city- Libya. *American Journal of Life Science Researches*, *7*(1), 18–25.

Saffari, S., Keyvanshokooh, S., Zakeri, M., Johari, S. A., Pasha-Zanoosi, H., & Mozanzadeh, M. T. (2018). Effects of dietary organic, inorganic, and nanoparticulate selenium sources on growth, hemato-immunological, and serum biochemical parameters of common carp (Cyprinus carpio). *Fish Physiology and Biochemistry*, *44*(4), 1087–1097. https://doi.org/10.1007/s10695-018-0496-y

Safi-Stibler, S., & Gabory, A. (2020). Epigenetics and the Developmental Origins of Health and Disease: Parental environment signalling to the epigenome, critical time windows and sculpting the adult phenotype. *Seminars in Cell & Developmental Biology*, *97*, 172–180. https://doi.org/10.1016/j.semcdb.2019.09.008

Said, M. A., Nafeh, N. Y., & Abdallah, H. A. (2021). Spexin alleviates hypertension, hyperuricaemia, dyslipidemia and insulin resistance in high fructose diet induced metabolic syndrome in rats via enhancing PPAR-ɣ and AMPK and inhibiting IL-6 and TNF-α. *Archives of Physiology and Biochemistry*, *1*, 1–7. https://doi.org/10.1080/13813455.2021.1899242

Saleem, M., Ali, H. A., Akhtar, M. F., Saleem, U., Saleem, A., & Irshad, I. (2019). Chemical

characterisation and hepatoprotective potential of Cosmos sulphureus Cav. and Cosmos bipinnatus Cav. *Natural Product Research*, *33*(6), 897–900. https://doi.org/10.1080/14786419.2017.1413557

Salehi, B., Ata, A., Nanjangud, A. K., Sharopov, F., Ramirez Alarcón, K., Ruiz Ortega, A., Addbulmajid, S., Valere Tsouch, P., Kobarfard, F., & Amiruddin, Z. (2019). Antidiabetic Potential of Medicinal Plants and Their Active Components. *Biomolecules*, *9*, 1–121. https://doi.org/10.3390/biom9100551

Salem, S. S., & Fouda, A. (2021). Green Synthesis of Metallic Nanoparticles and Their Prospective Biotechnological Applications : an Overview. *Biological Trace Element Research*, *199*, 344–370. https://doi.org/10.1007/s12011-020-02138-3

Saravanan, A., Kumar, P. S., Karishma, S., Vo, D. V. N., Jeevanantham, S., Yaashikaa, P. R., & George, C. S. (2021). A review on biosynthesis of metal nanoparticles and its environmental applications. *Chemosphere*, *264*, 128580. https://doi.org/10.1016/j.chemosphere.2020.128580

Sareedenchai, V., & Zidorn, C. (2010). Flavonoids as chemosystematic markers in the tribe Cichorieae of the Asteraceae. *Biochemical Systematics and Ecology*, *38*(5), 935–957. https://doi.org/10.1016/j.bse.2009.09.006

Sarkar, R. D., Lahkar, P., & Kalita, M. C. (2022). Bioresource Technology Reports Glycosmis pentaphylla (Retz .) DC leaf extract mediated synthesis of selenium nanoparticle and investigation of its antibacterial activity against urinary tract pathogens. *Bioresource Technology Reports*, *17*, 1–6. https://doi.org/10.1016/j.biteb.2021.100894

Schade, D. S., Shey, L., & Eaton, R. P. (2020). Cholesterol review: A metabolically important molecule. *Endocrine Practice*, *26*(12), 1514–1523. https://doi.org/10.4158/EP-2020-0347

Schmidt, N. H., Svendsen, P., Albarrán-Juárez, J., Moestrup, S. K., & Bentzon, J. F. (2021). High-fructose feeding does not induce steatosis or non-alcoholic fatty liver disease in pigs. *Scientific Reports*, *11*(1), 1–10. https://doi.org/10.1038/s41598-021-82208-1

Schwartzberg, L. S., & Navari, R. M. (2018). Safety of Polysorbate 80 in the Oncology Setting. *Advances in Therapy*, *35*(6), 754–767. https://doi.org/10.1007/s12325-018-0707-z

Semnani-Azad, Z., Khan, T. A., Blanco Mejia, S., De Souza, R. J., Leiter, L. A., Kendall, C. W. C., Hanley, A. J., & Sievenpiper, J. L. (2020). Association of Major Food Sources of Fructose-Containing Sugars with Incident Metabolic Syndrome: A Systematic Review and Meta-analysis. *JAMA Network Open*, *3*(7), 1–15. https://doi.org/10.1001/jamanetworkopen.2020.9993

Şener, T. E., Çevik, Ö., Çetinel, Ş., & Şener, G. (2020). Oxidative stress and urinary system damage in fructose-induced rat model of metabolic syndrome: Effect of calorie restriction

and exercise. *Journal of Research in Pharmacy*, *24*(3), 318–325. https://doi.org/10.35333/jrp.2020.153

Shabab, S., Gholamnezhad, Z., & Mahmoudabady, M. (2021). Protective effects of medicinal plant against diabetes induced cardiac disorder: A review. *Journal of Ethnopharmacology*, *265*, 113328. https://doi.org/10.1016/j.jep.2020.113328

Shahbaz, M., Akram, A., Raja, N. I., Mukhtar, T., Mashwani, Z.-R., Mehak, A., Fatima, N., Sarwar, S., Haq, E. U., & Yousaf, T. (2022). GREEN SYNTHESIS AND CHARACTERIZATION OF SELENIUM NANOPARTICLES AND ITS APPLICATION IN PLANT DISEASE MANAGEMENT: A REVIEW. *Pakistan Journal of Phytopathology*, *34*(01), 189–202. https://doi.org/10.33866/phytopathol.034.01.0739

Shandilya, S., Kumar, S., Kumar, N., Kumar, K., & Ruokolainen, J. (2022). Interplay of gut microbiota and oxidative stress : Perspective on neurodegeneration and neuroprotection. *Journal of Advanced Research*, *38*, 223–244. https://doi.org/10.1016/j.jare.2021.09.005

Shang, R., & Rodrigues, B. (2021). Lipoprotein lipase and its delivery of fatty acids to the heart. *Biomolecules*, *11*(7), 1–11. https://doi.org/10.3390/biom11071016

Sharma, A., Nagraik, R., Venkidasamy, B., Khan, A., Dulta, K., Kumar Chauhan, P., Kumar, D., & Shin, D. (2023). In vitro antidiabetic, antioxidant, antimicrobial, and cytotoxic activity of Murraya koenigii leaf extract intercedes ZnO nanoparticles. *Luminescence*, *38*(7), 1139–1148. https://doi.org/10.1002/bio.4244

Shen, W. C., Sun, Z. J., Chou, C. Y., Chou, Y. T., Lu, F. H., Yang, Y. C., Chang, C. J., & Wu, J. S. (2022). Association of simple renal cysts with metabolic syndrome in adults. *Frontiers in Public Health*, *10*, 1–8. https://doi.org/10.3389/fpubh.2022.951638

Shi, Y. S., Li, C. Bin, Li, X. Y., Wu, J., Li, Y., Fu, X., Zhang, Y., & Hu, W. Z. (2018). Fisetin Attenuates Metabolic Dysfunction in Mice Challenged with a High-Fructose Diet. *Journal of Agricultural and Food Chemistry*, *66*(31), 8291–8298. https://doi.org/10.1021/acs.jafc.8b02140

Shilakari Asthana, G., Sharma, P. K., & Asthana, A. (2016). In Vitro and In Vivo Evaluation of Niosomal Formulation for Controlled Delivery of Clarithromycin. *Scientifica*, *2016*, 6492953. https://doi.org/10.1155/2016/6492953

Shoeibi, S., & Mashreghi, M. (2017). Biosynthesis of selenium nanoparticles using Enterococcus faecalis and evaluation of their antibacterial activities. *Journal of Trace Elements in Medicine and Biology*, *39*, 135–139. https://doi.org/10.1016/j.jtemb.2016.09.003

Shwetha, U. R., Latha, M. S., Rajith Kumar, C. R., Kiran, M. S., & Betageri, V. S. (2020). Facile Synthesis of Zinc Oxide Nanoparticles Using Novel Areca catechu Leaves Extract and Their In Vitro Antidiabetic and Anticancer Studies. *Journal of Inorganic and*

Organometallic Polymers and Materials, *30*(12), 4876–4883. https://doi.org/10.1007/s10904-020-01575-w

Silva, D. P. da, Ferreira, S. de S., Torres-Rˆego, M., Furtado, A. A., Yamashita, F. de O., Diniz, E. A. da S., Vieira, D. S., Ururahy, M. A. G., Silva-Júnior, A. A. da, Luna, K. P. de O., & Fernandes-Pedrosa, M. de F. (2022). Antiophidic potential of chlorogenic acid and rosmarinic acid against Bothrops leucurus snake venom. *Biomedicine & Pharmacotherapy*, *148*, 112766. https://doi.org/10.1016/j.biopha.2022.112766

Sim, S., & Wong, N. K. (2021). Nanotechnology and its use in imaging and drug delivery (Review). *Biomedical Reports*, *14*(5), 1–9. https://doi.org/10.3892/br.2021.1418

Simeoni, M., Borrelli, S., Garofalo, C., Fuiano, G., Esposito, C., Comi, A., & Provenzano, M. (2021). Atherosclerotic-nephropathy: an updated narrative review. *Journal of Nephrology*, *34*, 125–136.

Singh, A., & Dhaliwal, H. (2015). GREEN SYNTHESIS OF SILVER NANOPARTICLES USING PHYLLANTHUS NIRURI LEAF EXTRACT AND EVALUATION OF THEIR ANTIMICROBIAL ACTIVITIES. *European Journal of Environmental Ecology*, *2*(1), 9–13.

Singla, S., Jana, A., Thakur, R., Kumari, C., Goyal, S., & Pradhan, J. (2022). Green synthesis of silver nanoparticles using Oxalis griffithii extract and assessing their antimicrobial activity. *OpenNano*, *7*, 100047. https://doi.org/10.1016/j.onano.2022.100047

Slinkard K., Singleton V. L.: Total phenol analysis: Automation and comparison with manual methods. Am J Enol Viticult 1977;28:49-55. (1977). 1977.

Slinkard, K., & Singleton, V. L. (1977). Total phenol analysis: automation and comparison with manual methods. *American Journal of Enology and Viticulture*, *28*(1), 49–55. https://doi.org/10.5344/ajev.1977.28.1.49

Soldado, D., Bessa, R. J. B., & Jerónimo, E. (2021). Condensed tannins as antioxidants in ruminants—effective-ness and action mechanisms to improve animal antioxidant status and oxidative stability of products. *Animals*, *11*(11), 1–25. https://doi.org/10.3390/ani11113243

Southon, S., Gee, J. M., & Johnson, I. T. (1984). Hexose transport and mucosal morphology in the small intestine of the zinc-deficient rat. *British Journal of Nutrition*, *52*(2), 371–380. https://doi.org/10.1079/bjn19840103

Spagnuolo, M. S., Iossa, S., & Cigliano, L. (2021). Sweet but bitter: Focus on fructose impact on brain function in rodent models. *Nutrients*, *13*(1), 1–18. https://doi.org/10.3390/nu13010001

Sujana, D., Saptarini, N. M., Sumiwi, S. A., & Levita, J. (2021). Nephroprotective activity of medicinal plants: A review on in silico-, in vitro-, and in vivo- based studies. *Journal of Applied Pharmaceutical Science*, *11*(9), 113–127.

https://doi.org/10.7324/JAPS.2021.1101016

Sukanya, V., Pandiyan, V., Vijayarani, K., & Padmanath, K. (2020). A Study on Insulin Levels and the Expression of Glut 4 in Streptozotocin (STZ) Induced Diabetic Rats Treated with Mustard Oil Diet. *Indian Journal of Clinical Biochemistry*, *35*, 488–496. https://doi.org/10.1007/s12291-019-00852-x

Tain, Y. L., & Hsu, C. N. (2022). Metabolic Syndrome Programming and Reprogramming: Mechanistic Aspects of Oxidative Stress. *Antioxidants*, *11*(11), 1–23. https://doi.org/10.3390/antiox11112108

Tappy, L., & Rosset, R. (2017). Fructose Metabolism from a Functional Perspective: Implications for Athletes. *Sports Medicine*, *47*, 23–32. https://doi.org/10.1007/s40279-017-0692-4

Tarish, R. J., Ghazi, A. M., & Abd-Alhassen, J. K. (2019). Hypolipidemic effect of portulaca oleracea and salvia officinalis comparing to atorvastatin in rats. *International Journal of Pharmaceutical Quality Assurance*, *10*(4), 613–618. https://doi.org/10.25258/ijpqa.10.4.9

Tarmizi, A. A. A., Adam, S. H., Ramli, N. N. N., Hadi, N. A. A., Maisarah, A. M., Tang, S. G. H., & Mokhtar, M. H. (2023). The Ameliorative Effects of Selenium Nanoparticles (SeNPs) on Diabetic Rat Model: A Narrative Review. *Sains Malaysiana*, *52*(7), 2037–2053. https://doi.org/10.17576/jsm-2023-5207-12

Tkachenko, O. Y., Shayakhmetova, G. M., Matvienko, A. V., & Kovalenko, V. M. (2020). Reproductive disorders in male rats induced by high-fructose consumption from juvenile age to puberty. *Arhiv Za Higijenu Rada i Toksikologiju*, *71*(1), 78–86. https://doi.org/10.2478/aiht-2020-71-3303

Truong, D. H., Nguyen, D. H., Ta, N. T. A., Bui, A. V., Do, T. H., & Nguyen, H. C. (2019). Evaluation of the use of different solvents for phytochemical constituents, antioxidants, and in vitro anti-inflammatory activities of severinia buxifolia. *Journal of Food Quality*, *2019*, 1–9. https://doi.org/10.1155/2019/8178294

Varlamova, E. G., Turovsky, E. A., & Blinova, E. V. (2021). Therapeutic potential and main methods of obtaining selenium nanoparticles. *International Journal of Molecular Sciences*, *22*(19), 1–25. https://doi.org/10.3390/ijms221910808

Vashishth, K., Singh, S. K., Jain, A., Bhatia, A., & Sharma, Y. P. (2022). Pathological involvement of apoptotic and inflammatory molecules in cardiovascular remodeling in rats on high fructose diet-induced metabolic syndrome. *Journal of Food Biochemistry*, *46*(7), e14107. https://doi.org/10.1111/jfbc.14107

Vennila, K., Chitra, L., Balagurunathan, R., & Palvannan, T. (2018). Comparison of biological activities of selenium and silver nanoparticles attached with bioactive phytoconstituents:

Green synthesized using Spermacoce hispida extract. *Advances in Natural Sciences: Nanoscience and Nanotechnology*, *9*(1), 1–10. https://doi.org/10.1088/2043-6254/aa9f4d

Vinjamuri, S., Afshan, S., Shekar, S., & Saraswathi, V. J. (2015). Evaluation of hemolytic activity, atpase inhibitory activity and antitumor activity of TLC extract of lemon grass (Cymbpogon citratus). *International Journal of Pharmacognosy and Phytochemical Research*, *7*(4), 785–788.

Vinu, D., Govindaraju, K., Vasantharaja, R., Nisa, S. A., Kannan, M., & Anand, K. V. (2020). Biogenic zinc oxide , copper oxide and selenium nanoparticles : preparation , characterization and their anti - bacterial activity against Vibrio parahaemolyticus. *Journal of Nanostructure in Chemistry*, *11*(0123456789), 271–286. https://doi.org/10.1007/s40097-020-00365-7

Virgen-Carrillo, C. A., Moreno, A. G. M., Rodríguez-Gudiño, J. J., & Pineda-Lozano, J. E. (2021). Feeding pattern, biochemical, anthropometric and histological effects of prolonged ad libitum access to sucrose, honey and glucose-fructose solutions in wistar rats. *Nutrition Research and Practice*, *15*(2), 187–202. https://doi.org/10.4162/nrp.2021.15.2.187

Vona, R., Gambardella, L., Cittadini, C., Straface, E., & Pietraforte, D. (2019). Biomarkers of oxidative stress in metabolic syndrome and associated diseases. *Oxidative Medicine and Cellular Longevity*, *2019*, 1–19. https://doi.org/10.1155/2019/8267234

Vyas, J. A. Y., & Rana, S. (2018). A COMPARATIVE STUDY ON THE GREEN SYNTHESIS OF SELENIUM NANOPARTICLES AND EVALUATION OF THEIR ANTIOXIDANT POTENTIAL USING ALLIUM. *The Journal of Indian Botanical Society*, *97*(3&4), 119–128. https://doi.org/10.5958/2455-7218.2018.00004.9

Vyletelová, V., Nováková, M., & Pašková, L. (2022). Alterations of HDL ’ s to piHDL ’ s Proteome in Patients with Chronic Inflammatory Diseases , and HDL-Targeted Therapies. *Pharmaceuticals*, *15*, 1–63. https://doi.org/10.3390/ ph15101278

Wadhwani, S. A., Gorain, M., Banerjee, P., Shedbalkar, U. U., Singh, R., Kundu, G. C., & Chopade, B. A. (2017). Green synthesis of selenium nanoparticles using Acinetobacter sp. SW30: Optimization, characterization and its anticancer activity in breast cancer cells. *International Journal of Nanomedicine*, *12*, 6841–6855. https://doi.org/10.2147/IJN.S139212

Wadood, A., Ghufran, M., Jamal, S. B., Naeem, M., Khan, A., & Ghaffar, R. (2013). Phytochemical analysis of medicinal plants occurring in local area of Mardan. *Biochemistry and Analytical Biochemistry*, *2*(4), 1–4. https://doi.org/10.4172/2161-1009.1000144

Wahyuni, D. K., Wacharasindhu, S., Bankeeree, W., Wahyuningsih, S. P. A., Ekasari, W., Purnobasuki, H., Punnapayak, H., & Prasongsuk, S. (2023). In vitro and in vivo

antiplasmodial activities of leaf extracts from Sonchus arvensis L. *BMC Complementary Medicine and Therapies*, *23*(1), 1–12. https://doi.org/10.1186/s12906-023-03871-7

Wang, G., Zhang, Y., Zhang, R., Pan, J., Qi, D., Wang, J., & Yang, X. (2020). The protective effects of walnut green husk polysaccharide on liver injury, vascular endothelial dysfunction and disorder of gut microbiota in high fructose-induced mice. *International Journal of Biological Macromolecules*, *162*, 92–106. https://doi.org/10.1016/j.ijbiomac.2020.06.055

Wang, H. H., Lee, D. K., Liu, M., Portincasa, P., & Wang, D. Q. H. (2020). Novel insights into the pathogenesis and management of the metabolic syndrome. In *Pediatric Gastroenterology, Hepatology and Nutrition* (Vol. 23, Issue 3). https://doi.org/10.5223/PGHN.2020.23.3.189

Wang, J., Zhai, Y., Ou, M., Bian, Y., Tang, C., Zhang, W., Cheng, Y., & Li, G. (2021). Protective effect of lemon peel extract on oxidative stress in h9c2 rat heart cell injury. *Drug Design, Development and Therapy*, *15*, 2047–2058. https://doi.org/10.2147/DDDT.S304624

Wang, Y., Kaur, G., Kumar, M., Kushwah, A. S., Kabra, A., & Kainth, R. (2022). Caffeic Acid Prevents Vascular Oxidative Stress and Atherosclerosis against Atherosclerogenic Diet in Rats. *Evidence-Based Complementary and Alternative Medicine*, *2022*, 1–8. https://doi.org/10.1155/2022/8913926

Weaver, K., & Skouta, R. (2022). The Selenoprotein Glutathione Peroxidase 4 : From Molecular Mechanisms to Novel Therapeutic Opportunities. *Biomedicines*, *10*, 1–20. https://doi.org/10.3390/biomedicines10040891

Weckbecker, G., & Cory, J. G. (1988). Ribonucleotide reductase activity and growth of glutathione-depleted mouse leukemia L1210 cells in vitro. *Cancer Letters*, *40*(3), 257–264. https://doi.org/10.1016/0304-3835(88)90084-5

Werner, M., Auth, T., Beales, P. A., Fleury, J. B., Höök, F., Kress, H., Van Lehn, R. C., Müller, M., Petrov, E. P., & Sarkisov, L. (2018). Nanomaterial interactions with biomembranes: Bridging the gap between soft matter models and biological context. *Biointerphases*, *13*(2), 028501. https://doi.org/10.1116/1.5022145

Witika, B. A., Bassey, K. E., Demana, P. H., Siwe-Noundou, X., & Poka, M. S. (2022). Current Advances in Specialised Niosomal Drug Delivery: Manufacture, Characterization and Drug Delivery Applications. *International Journal of Molecular Sciences*, *23*(17), 1–26. https://doi.org/10.3390/ijms23179668

Wu, M., Luo, Q., Nie, R., Yang, X., Tang, Z., & Chen, H. (2021). Potential implications of polyphenols on aging considering oxidative stress, inflammation, autophagy, and gut microbiota. *Critical Reviews in Food Science and Nutrition*, *61*(13), 2175–2193.

https://doi.org/10.1080/10408398.2020.1773390

Xia, I. F., Kong, H.-K., Wu, M. M. H., Lu, Y., Wong, K.-H., & Kwok, K. W. H. (2022). Selenium Nanoparticles (SeNPs) Immunomodulation Is More Than Redox Improvement: Serum Proteomics and Transcriptomic Analyses. *Antioxidants (Basel, Switzerland)*, *11*(5), 964. https://doi.org/10.3390/antiox11050964

Ya-Zheng, Z., Yuan-Yuan, Z., Han, H., Rui-Ping, F., Yang, H., Liang, Z., Jun-Ping, K., & Bo-Yang, Y. (2018). Advances in the antitumor activities and mechanisms of action of steroidal saponins. *Chinese Journal of Natural Medicines*, *16*(10), 732–748. https://doi.org/10.1016/S1875-5364(18)30113-4

Yagi, K. (1976). A simple fluorometric assay for lipoperoxide in blood plasma. *Biochemical Medicine*, *15*(2), 212–216. https://doi.org/10.1016/0006-2944(76)90049-1

Yahya, A. Z., Taqa, G. A., & Alkataan, M. A. (2023). Evaluation of the Effects of N-Acetylcysteine on Serum Glucose, Lipid Profile, and Body Weight in Rats With Fructose-Induced Metabolic Syndrome. *Military Medical Science Letters*, *92*, 1–14. https://doi.org/10.31482/mmsl.2022.039

Yanai, H., Adachi, H., Hakoshima, M., & Katsuyama, H. (2021). Molecular Biological and Clinical Understanding of the Pathophysiology and Treatments of Hyperuricemia and Its Association with Metabolic Syndrome , Cardiovascular Diseases and Chronic Kidney Disease. *International Journal of Molecular Sciences*, *22*(17), 1–20. https://doi.org/10.3390/ijms22179221

Yang, J., Zhou, W., Shi, D., Pan, F., Sun, W., Yang, P., & Li, X. (2023). The Interaction between Oxidative Stress Biomarkers and Gut Microbiota in the Antioxidant Effects of Extracts from Sonchus brachyotus DC . in Oxazolone-Induced Intestinal Oxidative Stress in Adult Zebrafish. *Antioxidants*, *12*(1), 1–15. https://doi.org/10.3390/antiox12010192

Yang, M., Liu, C., Jiang, N., Liu, Y., Chen, W., Li, L., Xiao, L., & Sun, L. (2023). Myostatin : a potential therapeutic target for metabolic syndrome. *Frontiers in EndocrinologyEndocrinol*, *14*, 1–9. https://doi.org/10.3389/fendo.2023.1181913

Yao, Y., Zang, Y., Qu, J., Tang, M., & Zhang, T. (2019). The toxicity of metallic nanoparticles on liver: The subcellular damages, mechanisms, and outcomes. *International Journal of Nanomedicine*, *14*, 8787–8804. https://doi.org/10.2147/IJN.S212907

Yazdani, E., Talebi, M., Zarshenas, M. M., & Moein, M. (2019). Evaluation of possible antioxidant activities of barberry solid formulation, a selected formulation from Traditional Persian Medicine (TPM) via various procedures. *Biointerface Research in Applied Chemistry*, *9*(6), 4517–4521. https://doi.org/10.33263/BRIAC96.517521

Yeşil, A. H., & Özer, Ç. (2023). Metabolic Syndrome and Cardiovascular Problems Associated

with Different Types of Diet. *Gazi Medical Journal*, *34*(1), 106–109. https://doi.org/10.12996/gmj.2023.22

Yeşilot, Ş., Özerc, M. K., Gultekind, F., Öncüe, M., Candanf, İ. A., Dağdevireng, B. H., & Çiçekh, E. (2022). An experimental study to investigate the impact of Aspirin and Vitamin C therapy on fructose induced hepatic and pancreatic damage. *Turkish Journal of Health Science and Life*, *5*(2), 121–131. https://doi.org/10.56150/tjhsl.1143635

Ying, S., Guan, Z., Ofoegbu, P. C., Clubb, P., Rico, C., He, F., & Hong, J. (2022). Green synthesis of nanoparticles: Current developments and limitations. *Environmental Technology and Innovation*, *26*, 102336. https://doi.org/10.1016/j.eti.2022.102336

Yuan, T., Wu, D., Sun, K., Tan, X., Wang, J., Zhao, T., Ren, B., Zhao, B., Liu, Z., & Liu, X. (2019). Anti-fatigue activity of aqueous extracts of sonchus arvensis L. In exercise trained mice. *Molecules*, *24*(6), 1–13. https://doi.org/10.3390/molecules24061168

Yustisia, I., Tandiari, D., Cangara, M. H., Hamid, F., & Daud, N. A. (2022). A high-fat, high-fructose diet induced hepatic steatosis, renal lesions, dyslipidemia, and hyperuricemia in non-obese rats. *Heliyon*, *8*(10), e10896. https://doi.org/10.1016/j.heliyon.2022.e10896

Z. Jiao, H. Wang, P. Wang, H. Sun, S. Yue, L. X. (2014). Detection and quantification of cyclo-dopa amides in Portulaca oleracea L. by HPLC-DAD and HPLC-ESI-MS/MS. *Journal of Chinese Pharmaceutical Sciences*, *23*(8), 533–542. https://doi.org/10.5246/jcps.2014.08.069

Zafar, U., Khaliq, S., Ahmad, H. U., Manzoor, S., & Lone, K. P. (2018). Metabolic syndrome: an update on diagnostic criteria, pathogenesis, and genetic links. *Hormones*, *17*(3), 299–313. https://doi.org/10.1007/s42000-018-0051-3

Zamani-Garmsiri, F., Emamgholipour, S., Rahmani Fard, S., Ghasempour, G., Jahangard Ahvazi, R., & Meshkani, R. (2022). Polyphenols: Potential anti-inflammatory agents for treatment of metabolic disorders. *Phytotherapy Research : PTR*, *36*(1), 415–432. https://doi.org/10.1002/ptr.7329

Zambonino, M. C., Quizhpe, E. M., Jaramillo, F. E., Rahman, A., Vispo, N. S., Jeffryes, C., & Dahoumane, S. A. (2021). Green synthesis of selenium and tellurium nanoparticles: Current trends, biological properties and biomedical applications. *International Journal of Molecular Sciences*, *22*(3), 1–34. https://doi.org/10.3390/ijms22030989

Zhu, C., Zhang, S., Song, C., Zhang, Y., Ling, Q., Hoffmann, P. R., Li, J., Chen, T., Zheng, W., & Huang, Z. (2017). Selenium nanoparticles decorated with Ulva lactuca polysaccharide potentially attenuate colitis by inhibiting NF-KB mediated hyper inflammation. *Journal of Nanobiotechnology*, *15*(1), 1–15. https://doi.org/10.1186/s12951-017-0252-y

Ziolkowska, S., Binienda, A., Jablkowski, M., Szemraj, J., & Czarny, P. (2021). The interplay

between insulin resistance, inflammation, oxidative stress, base excision repair and metabolic syndrome in nonalcoholic fatty liver disease. *International Journal of Molecular Sciences*, *22*(20), 1–27. https://doi.org/10.3390/ijms222011128

Ziyan, L., Yongmei, Z., Nan, Z., Ning, T., & Baolin, L. (2007). Evaluation of the anti-inflammatory activity of luteolin in experimental animal models. *Planta Medica*, *73*(3), 221–226. https://doi.org/10.1055/s-2007-967122

Annex

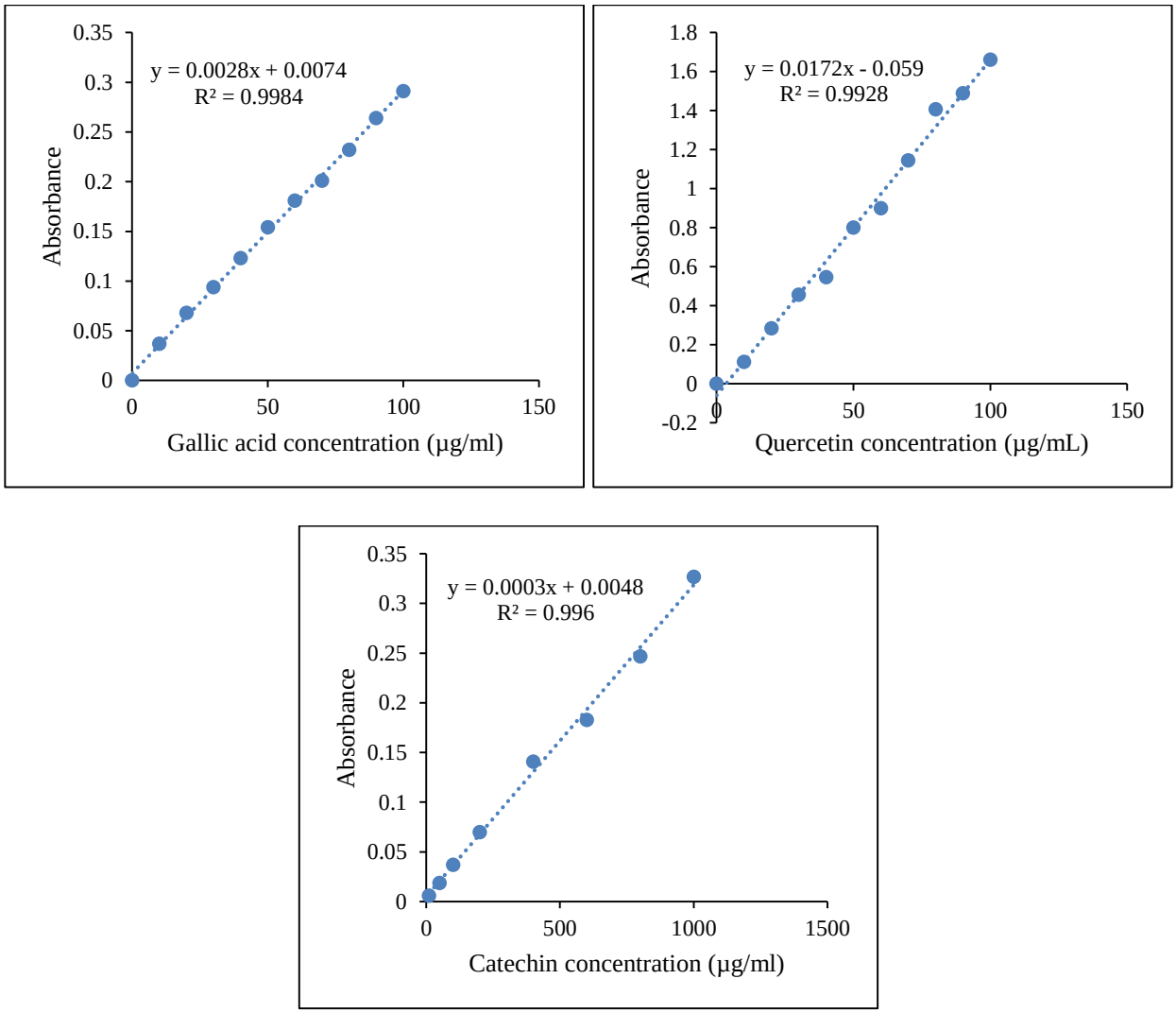

Annex 01: Calibration curves of Gallic acid, Quercetin and Catechin for estimation of total phenols, flavonoids and condensed tannins respectively

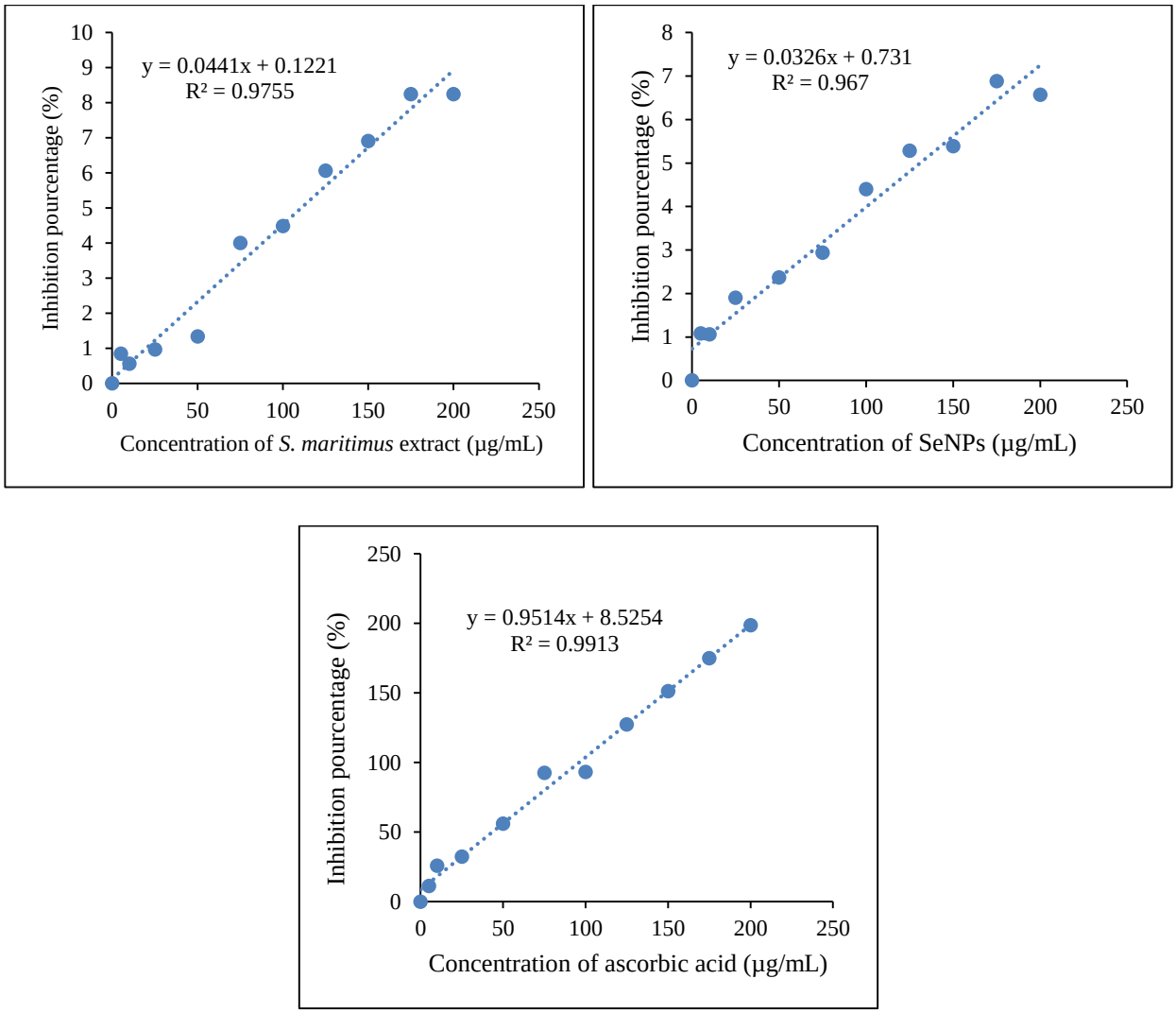

Annex 02: Inhibition percentage of *S. maritimus* extrat, SeNPs and ascorbic acid for IC_{50} determination of DPPH scavenging activity

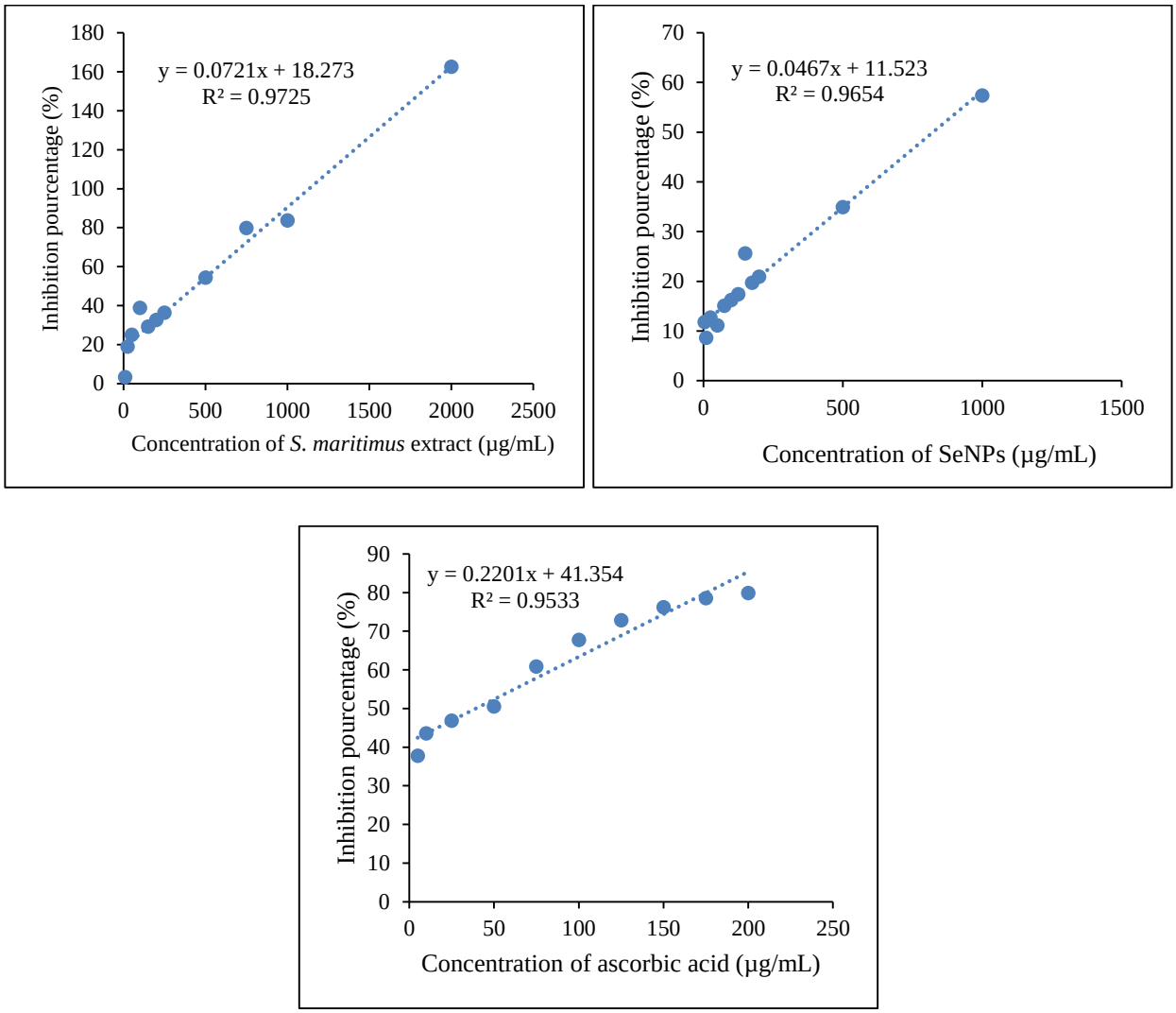

Annex 03: Inhibition percentage of *S. maritimus* extrat, SeNPs and ascorbic acid for IC_{50} determination of FRAP activity

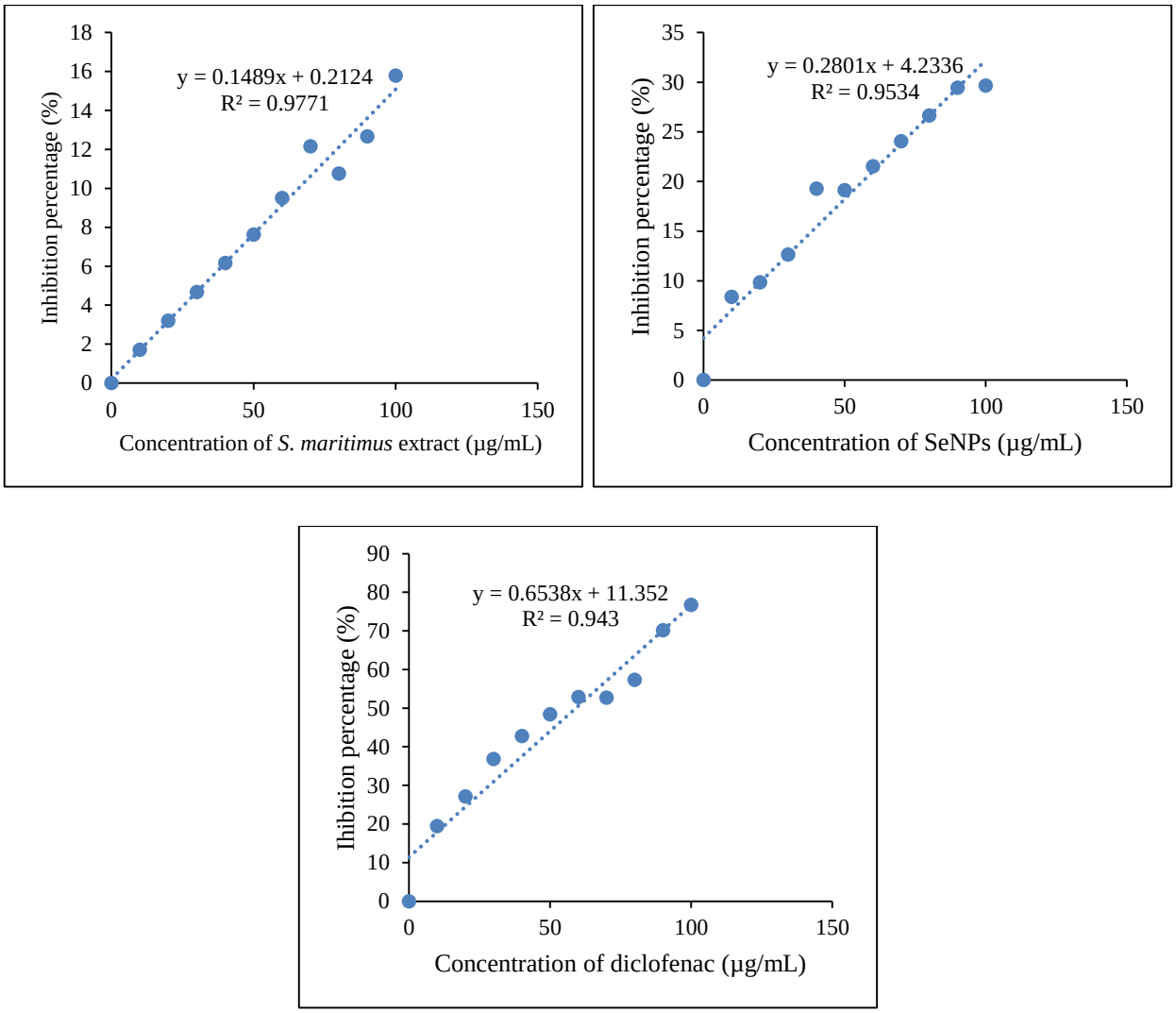

Annex 04: Inhibition percentage of *S. maritimus* extrat, SeNPs and diclofenac for IC_{50} determination of anti-inflammatory activity

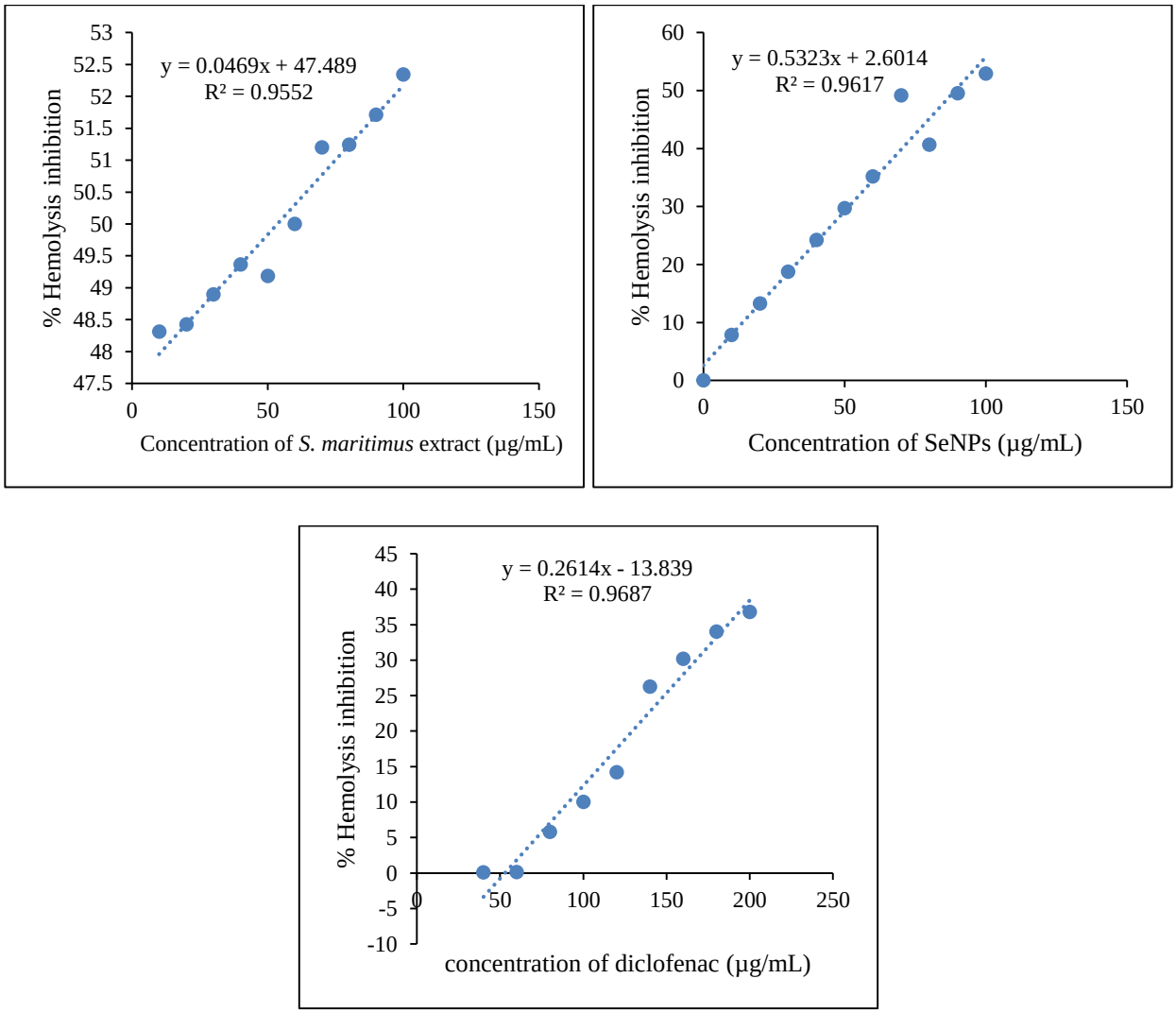

Annex 05: Inhibition percentage of *S. maritimus* extrat, SeNPs and diclofenac for IC_{50} determination of anti-hemolysis activity

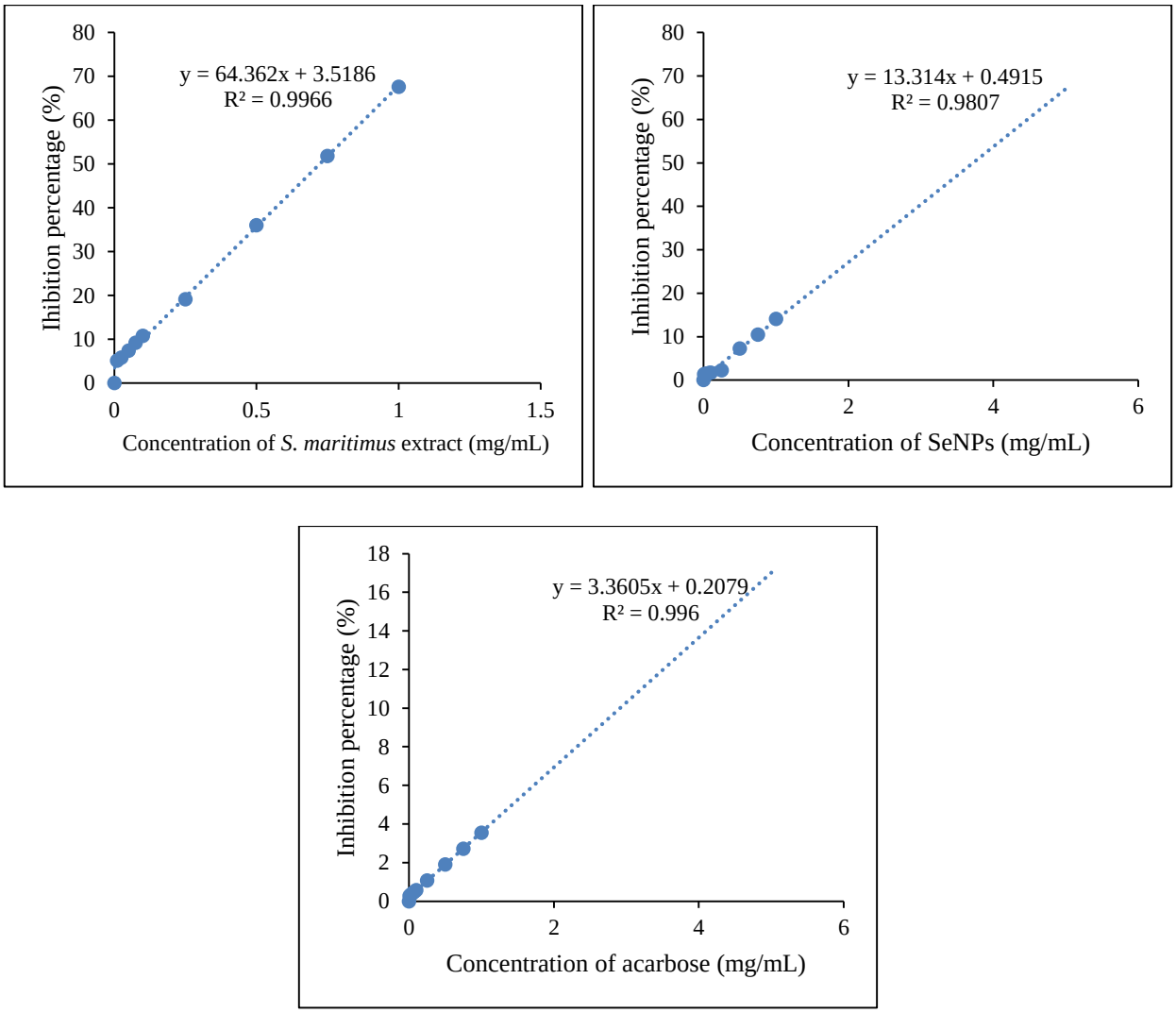

Annex 06: Inhibition percentage of *S. maritimus* extrat, SeNPs and acarbose for IC_{50} determination of anti-α-amylase activity

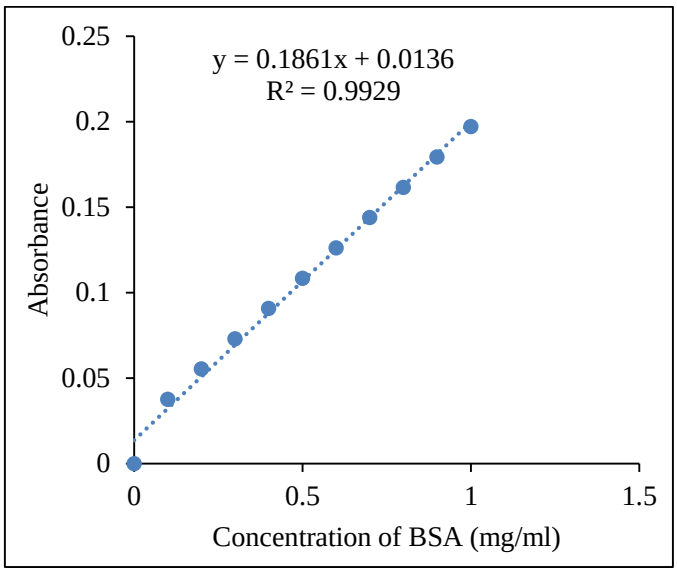

Annex 07: Calibration curve of BSA for determination protein levels